A Study of Pathogenesis of West Nile Virus Encephalitis in the Adult Murine Model

Bimmi Shrestha (M.Sc., M.Sc.)

A thesis submitted in fulfilment of the requirements for the degree of Doctor of Philosophy

Faculty of Medicine
Department of Pathology
The University of Sydney
Sydney, Australia
March 2002

JAYA GURUDEV

SHREE GURU CHARAN KAMALEBHYO NAMAH:

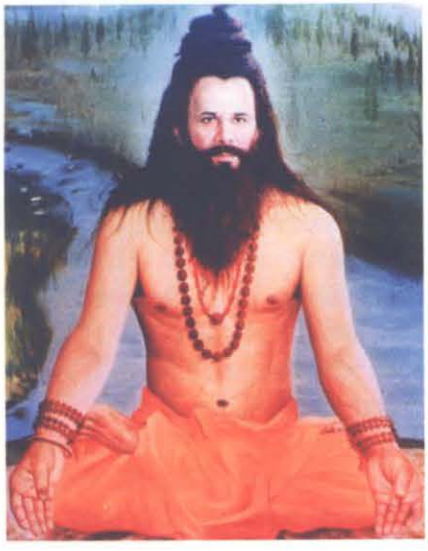

Shree paramhanswa Swami Nikhileshwarananda Maharaj

Shree Shree Mahayogi Goraksha Gurudev

This thesis is dedicated to the holy feet of my Gurudevs

Table of contents

Chapter 2

Chapter 3

Chapter 4

Chapter 5

Chapter 6

Chapter 7

Chapter 8

Declaration

I hereby declare that this thesis is my own work and to the best of my knowledge the material presented herein contains no material previously published or written by another person. Unless state below, all work presented in this thesis was performed by the author.

TUNEL assay of paraffin brain sections in chapter 4 was performed by Jane Radford, a senior Technical Officer from histology laboratory, Department of Pathology, University of Sydney.

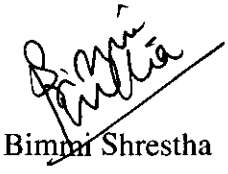

Bimmi Shrestha

Acknowledgements

First and foremost, I would like to express my deep gratitude to my Gurudevs (spiritual masters) Shree Shree Mahayogi Goraksha Gurudev and Shree Paramhanswa Swami Nikhileshwarananda Maharaj for giving me the opportunity to undertake this project, for their support, continuous guidance in invisible form and providing many other opportunities throughout my Ph.D. course.

I would like to thank my supervisor, Associate Professor Nicholas J.C. King for having faith in my abilities, for his valuable suggestions, encouragements sometimes when experiments were not working according to plan and for sharing my excitement and happiness when experiments were working. I still remember that I used to disturb you in the middle of your work to discuss about my experiments and results. I am extremely thankful to you Nick for making a time when I needed it. I would like to thank Dr. G. Chaudhri and Dr. G. Karupiah, viral immunologists of John Curtin School of Medical Research (JCMR), Australian National University, for their valuable time and helpful suggestions, as well as providing B cell-deficient mice during the course. I would like to thank Dr. J. Kril and Dr. R. Pamphlett, a neuropathologist in the Department of Pathology, for their valuable time and suggestions in the histopathological studies of the brain and spinal cord. I am extremely greatful to Virginia Turner, Jane Radford and Van Tran, members at the histology laboratory in the Department of Pathology for teaching me the skills involved with all aspects of the histology and immunohistochemistry techniques, providing the facilities and access to materials in their laboratory. All the friends of my lab: Ying Cheng, Wei Wu, Loubhnah Slitini, Shanon Burke, Sabita Rana and Virginia Breen, I am very thankful to your friendship and understanding. I would like to thank Anna Hansen, senior Ph.D. student in the Department of Pathology for helping me to set up some of the preliminary experiments and techniques used for these experiments and Vijaya Panchanathan, a Ph.D. student at JCMR for teaching me ELISA technique. I am indebted to Mrs. Uma Kumar, Account Officer in the Department of Pathology for her help and friendship during my course.

Finally, I would like to give my special thanks to my sister Saroj Shrestha and brother Ashish Man Shrestha for their moral and financial support, understanding, friendship and faith in my abilities. Above all, this thesis is totally dedicated to the feet of my beloved Gurudevs Shree Shree Mahayogi Goraksha gurudev and Shree Paramhanswa Swami Nikhileshwarananda Maharaj.

"O' My Dearest Gurudevs This Work Is Just For You"

Publications arising from this work

Shrestha B., Chaudhri G., Karupiah G., Kril J. and King NJC. IFN-γ Exacerbates Disease in Murine Model of West Nile Virus Encephalitis (Submitted *to American Journal of Pathology*).

King NJC., **Shrestha B**. and Kesson A. Immune Modulation in Flaviviruses. In The flaviviruses ED Monath T and Chambers TJ. Academic Press (In press).

Shrestha B., Kril J. and King N J.C. Role of Microglia in West Nile Virus Encephalitis (in preparation).

Shrestha B., Karupiah G. and King NJC. Route of Infection Determines Disease Profile in West Nile Virus Encephalitis (in preparation).

Posters and Presentations arising from this work

Shrestha B., Chaudhri G., Karupiah G., Kril J. and King NJC. The immunokinetics of West Nile Virus Encephalitis in C57BL/6 IFN–gamma +/+ and -/- mice (Poster Presentation). XIth International Congress of Virology, Sydney Convention Center, Sydney, 9-13 August 1999.

Shrestha B., Chaudhri G., Karupiah G., Kril J. and King NJC. The immunokinetics of West Nile Virus Encephalitis (oral Presentation). Australian Society for Immunology, New South Wales meeting, Quarantine Station, Manly, Australia,13-14 September 1999.

Shrestha B., Chaudhri G., Karupiah G., Kril J. and King NJC.. The immunokinetics of West Nile Virus Encephalitis in IFN–γ deficient mice (oral Presentation). 29th Annual Conference of the Australian Society for Immunology Dunedin, Newzeland, 5-8 December 1999.

Shrestha B., Chaudhri G., Karupiah G., Kril J. and King NJC. West Nile Virus Encephalitis (oral Presentation). Australian Society for Medical Research Scientific Meeting, Sydney, Australia, 5 June 2000.

Shrestha B., Chaudhri G., Karupiah G., Kril J. and King NJC. West Nile Virus Encephalitis- Pathogenesis of Disease (oral Presentation). Second Research Conference 2000 "From Cell to Society 2" The Medical Foundation and The College of Health Sciences, University of Sydney, Australia,1-2 November 2000.

Shrestha B., Chaudhri G., Karupiah G., Kril J. and King NJC. Immunopathology in West Nile Virus Encephalitis (oral Presentation). 30th Annual Conference of the Australian Society for Immunology, Sydney, Australia,11-14 December 2000.

Shrestha B., Chaudhri G., Karupiah G., Kril J. and King NJC. West Nile Virus Encephalitis, 21st Annual Meeting, Australian Neuroscience Society, Brisbane Convention Center, Brisbane, Australia, 28-31 January 2001.

Shrestha B., Chaudhri G., Karupiah G., Kril J. and King NJC. Interferon γ: A cause of Immunopathology in West Nile Virus Encephalitis (Poster Presentation). 6th International Symposium on Positive strand RNA Viruses, Institute Pasteur, Paris, 28 May-2 June 2001.

Shrestha B., Kril J. and King NJC. Role of Microglia in WNV Encephalitis (Poster Presentation). 6th International Symposium on Positive strand RNA Viruses, Institute Pasteur, Paris, 28 May-2 June 2001.

Shrestha B., Karupiah G. and King NJC. Route of Infection Determines Disease Profile in West Nile Virus Encephalitis (Poster Presentation). 6th International Symposium on Positive strand RNA Viruses, Institute Pasteur, Paris, 28 May-2 June 2001.

Shrestha B., Chaudhri G., Karupiah J. and King NJC. Pathogenesis of WNV Encephalitis. Washington University School of Medicine, Saint Louis, USA, 29th October, 2001.

Shrestha B., Chaudhri, G. Karupiah J. and King NJC. Pathogenesis of WNV Encephalitis. New York State Health Department, Albany, USA, 30th October, 2001.

Abstract

West Nile virus (WNV) is one of the most widely spread emerging neurotropic flaviviruses. It is found in Asia, Africa and Europe and is closely related to Japanese encephalitis (JE), Murray Valley encephalitis (MVE) and Saint Louis encephalitis (SLE) viruses. Recently, this virus received world attention due to epidemic outbreaks in the new world, including USA, Europe and Russia associated with some 10% mortality on each occasion. Although pathogenesis of WNV encephalitis has been studied to some extent, still very little is known. Such studies have used neonatal or young mice as a model. These do not accurately reflect the pathogenesis of disease in adult mice due to immaturity of the immune system which facilitates severe encephalitis. Therefore, an adult model using a systemic route of WNV inoculation was developed in this project to understand better the mechanisms of pathogenesis of WNV encephalitis. This model exhibits similar histopathological and clinical features of human disease. Since IFN-γ is critical for resolution of many viral infections, its role in WNV encephalitis was investigated using IFN-γ-deficient (B6.IFN-γ-/-) mice compared to the corresponding wildtype (B6.WT) mice.

Survival studies after intraperitoneal (i.p.) inoculation (i.p. model) showed that more than twice the number of B6.IFN-γ-/- mice survived compared to B6.WT mice. Upon rechallenged with a 50-fold higher dose of WNV surviving mice were completely protected. Using immunoperoxidase labelling and plaque assay techniques, WNV antigen (Ag) was detected from day 6 post infection (p.i.) in the brain but was undetectable after day 11 p.i. Replicating WNV was only detectable between day 6 and 10 p.i. in both groups. The maximum virus titres were 2.23 $\log_{10}$ pfu/gm in B6.WT and 2.22 $\log_{10}$ pfu/gm in B6.IFN-γ-/- mice on day 8 p.i. WNV Ag was confined to the neurones and their dendrites. The kinetics of infection of WNV was similar in both groups, however, twice the number of B6.IFN-γ-/- brains showed neuronal infection from day 6-11 (p.i.). There was no significant difference in the number of infected neurones and the virus titres between the groups.

Leukocyte migration into the CNS is a hallmark feature of viral encephalitis. Using hematoxylin and eosin (H and E) staining in paraffin sections, infiltration of leukocytes

into the brain parenchyma was determined and quantitated. In both groups, leukocyte infiltration was evident from day 5 p.i. consisting of both mononuclear and polymorphonuclear leukocytes with perivascular cuffing. In B6.WT, leukocyte infiltration was significantly ($p=<0.001$) increased from day 7 p.i., compared to day 5 and 6 and significantly decreased by day 9 p.i. ($p=<0.001$) compared to day 7 p.i. In B6.IFN-γ-/- mice, leukocyte infiltration peaked on day 8, decreased by day 9 p.i. However, in both groups of mice, the number of infiltrating leukocytes returned nearly to baseline values by day 15 p.i and leukocytes were undetectable by day 30 p.i. Although the kinetics of leukocyte infiltration were similar between the groups, approximately 4-fold higher numbers of leukocytes were observed in the brain parenchyma of B6.WT compared to B6.IFN-γ-/- mice on day 7 p.i.

Expression of intercellular cell adhesion molecule-1 (ICAM-1) and vascular cell adhesion molecule-1 (VCAM-1) in the neurovascular endothelial cells is required to facilitate the transmigration of leukocytes into the CNS. Using immunoperoxidase labelling, expression of these adhesion molecules in the neurovascular endothelium was determined and the number of blood vessels positive for these molecules was quantitated. There was no constitutive expression of ICAM-1 in the neurovascular vessels in B6.WT mice. It was expressed at low levels initially at day 3 p.i., increased by day 6 p.i., and was maximal on day 9 p.i. In B6.IFN-γ-/- mice, ICAM-1 was constitutively expressed in the vessels, upregulated by day 3 p.i., numbers peaking on days 8 and 10 p.i. The number of ICAM-1 positive vessels was significantly higher ($p=<0.001$ on each day) in B6.IFN-γ-/- mice from day 6 onwards compared to B6.WT mice. In both groups of mice, the number of vessels expressing ICAM-1 returned to nearly baseline values by day 15 p.i. In addition to this, ICAM-1 was also expressed on the microglia in B6.IFN-γ-/- mice from day 6 p.i., but not on those from B6.WT mice at any timepoint. More than 85% mice were postive for microglial ICAM-1 expression. The number of microglia expressing ICAM-1 was quantitated. The number of ICAM-1-positive vessels increased at least 24h before ICAM-1-positive microglia. Microglia and vessels thus expressed increased ICAM-1 with different kinetics in B6.IFN-γ-/- mice. Microglia expressed ICAM-1 earlier than activation detected by GS-lectin. Significantly higher numbers of microglia were expressing ICAM-1 ($p=<0.05$) on day 6-8 compared to activated microglia, however on day 9-10 p.i. the numbers of cells positive for both were nearly equal and both returned to nearly baseline levels on day 15 p.i.

Unlike ICAM-1, VCAM-1 was not constitutively expressed in either group and increased significantly after infection with similar kinetics. In B6.WT mice, VCAM-1 was expressed from day 5 p.i., and was maximal on day 9, whereas in B6.IFN-γ-/- mice, VCAM-1 was expressed from day 3 p.i., peaking on day 9 p.i. approximately 3-fold higher ($p=<0.001$) than in B6.WT. However, in both groups, the number of vessels positive for VCAM-1 declined nearly to baseline values from day 15 p.i. Despite significantly increased CAM levels, significantly less leukocyte infiltration was observed in the brain parenchyma of B6.IFN-γ-/- mice.

Microglia and astrocytes are immunocompetent cells of the CNS. Expression of glial fibrillary acidic protein (GFAP) and isolectin-B4 derived from *Griffonia simplicifolia* (GS-lectin) were used as markers of astrocyte and microglial activation, respectively, and the number of activated glial cells were quantitated. In both groups of mice, astrocytes were extremely rarely activated. Thus the presence or absence of IFN-γ did not influence astrocyte activation. In contrast, microglia were highly activated in both groups of mice, independently of IFN-γ, from day 7 p.i. onwards. Microglial activation was associated with various altered morphologies as well as nodule formation. Microglial activation was observed after 24h of neuronal infection in both groups. In B6.WT mice, activation of microglia was significantly increased on days 7-11 ($p=<0.001$), peaking on day 10 p.i. whereas in B6.IFN-γ-/- mice, the number of activated microglia was significantly increased on days 8-11 ($p=<0.001$), peaking on day 9 p.i. However, in both groups of mice, the number of activated microglia and their activated morphology, returned to nearly baseline values and their normal state, respectively, from day 15 p.i., after WNV Ag was undetectable. These values returned completely to baseline values at day 30 p.i. Although the kinetics of activation was similar between the groups, significantly higher ($p=<0.001$) numbers of microglia were activated in B6.IFN-γ-/- compared to B6.WT mice on day 9 p.i. Microglial nodules were observed from day 7 p.i. in both groups. In B6.WT, the number of nodules peaked on day 10 and 11 p.i. whereas in B6.IFN-γ-/- mice they were maximal on day 9 p.i. However, in both groups, the number of nodules had decreased by day 15 p.i., concurrent with the return to normal resting microglial morphology. Despite the significant numbers of nodules formed, neuronal death occurred in <1% infected neurones that had microglial nodules around them. Since microglia are regarded as antigen presenting cells (APC) of the CNS, immunoperoxidase labelling was also used to detect MHC-II expression in activated microglia. Microglia expressed

increased levels of MHC-II from day 7 p.i., independently of IFN-γ in WNV encephalitis. Despite a high degree of activation, as detected by lectin histochemistry, significantly fewer ($p=<0.001$) microglia expressed MHC-II at any timepoint from day 7-10 p.i. from either group.

The pathogenesis and outcome of disease is often linked to the route of virus inoculation in the host. Therefore, the pathogenesis and role of IFN-γ was also evaluated in WNV encephalitis using intranasal (i.n.) WNV inoculation (i.n. model) in both B6.WT and B6.IFN-γ-/- mice. Both groups of mice were highly susceptible to i.n. inoculation with 100% mortality by day 7 p.i. with nearly 5-fold higher virus titres in the brain at the time of death, compared to the peak virus titres detected in both groups of mice in the i.p. model. At the time of death, extremely high neuronal infection was observed throughout the brain, although not in the cerebellum. Leukocyte infiltration was observed from day 5 p.i. It was maximal at the time of death but concentrated only in the olfactory bulb (OB) in the i.n. model. Although microglial activation was observed concurrently with neuronal infection from day 3 p.i., significantly fewer numbers of microglia were activated compared to numbers of infected neurones at the time of death in the i.n. model.

The portal of CNS invasion by neurotropic viruses also depends upon the route of inoculation. In the i.p. model, WNV Ag was first detected in the cervical spinal cord motor neurones 24h before it was detectable in the brain. After 24h WNV Ag was detected in the brainstem for the first time and was then detectable in other parts of the brain, however, at no point was the OB found to be infected. Extremely rare neurovascular endothelium infection and blood brain barrier damage suggests that WNV gains access to the CNS via retrograde axonal migration along the spinal cord in the i.p. model. In contrast, in the i.n. model, WNV Ag was first detected in the outermost layer of the OB on day 3 p.i. and nowhere else in the brain. After day 3 p.i. WNV Ag was detected in other parts of the OB and brain proper, spreading rostral-to-caudal, indicating that WNV gains access to the brain via the olfactory route in i.n. infection.

Antibody is important in controlling many neurotropic viral infections. Therefore, preliminary experiments were undertaken to evaluate its role in WNV using passive transfer of HI serum both in the i.p. and i.n. model in B6.WT mice. Passive transfer of HI serum i.p. 24h before and 48h after infection completely abrogated encephalitis in the i.p.

model. Moreover, the preliminary studies on B cell-deficient (B6.μMT-/-) mice showed 100% mortality by day 9 p.i. with extensive brain and cervical spinal cord infection, compared to the corresponding B6.WT mice in the i.p. model, further confirming the importance of Ab in controlling WNV. However, the passive transfer of the same dose of HI seum was unable to protect mice from lethal WNV encephalitis in the i.n. model. Although passive transfer of 750-fold higher dose of HI serum than the original dose extended the survival time of mice in the i.n. model, only 13% of mice survived until day 14 p.i. Moreover, adoptive transfer of splenocytes ($5x10^7$ splenocytes per mouse) from HI mice 24h before i.n. infection to naïve mice also failed to protect mice in this model. Interestingly, surviving mice from low-dose i.n. WNV infection were completely protected when rechallenged i.n. with a 600-fold higher dose of WNV than the original dose.

This thesis presents the significant results of a study of the pathogenesis of WNV encephalitis in adult mice. In short, IFN-γ does not play an important role in survival against WNV infection or development of secondary anti-WNV immunity. Leukocyte recruitment is significantly reduced in the absence of IFN-γ. The induction of ICAM-1 and VCAM-1 in the CNS is IFN-γ-independent and is not sufficient to facilitate transmigration of a compensatory number of leukocytes into the brain parenchyma during infection. WNV clearance is also independent of IFN-γ. Microglia are activated in response to neuronal infection and activation is independent of IFN-γ. These cells may be involved in WNV clearance. The route of inoculation of WNV determines the disease profile and severity of disease. Passive protection against WNV infection occurs reliably only in the i.p. model, but not in the i.n. model.

Finally, these results clearly indicate that effective WNV clearance and generation of immunological memory can occur in the absence of IFN-γ. However, most importantly, it suggests that IFN-γ is involved in exacerbating disease. The mechanism by which it exerts this action within the CNS is unresolved.

Abbreviations

WNV	West Nile Virus
MVE	Murray Valley encephalitis
JE	Japanese encephalitis virus
YF	Yellow fever
SLE	Saint Louis encephalitis
TBE	Tick borne encephalitis
HIV	Human immunodeficiency virus
HSV	Herpes simplex virus
SBV	Sindbis virus
SFV	Semliki Forest virus
VEE	Venezuelan equine virus
VSV	Vesicular stomatitis virus
LCMV	Lymphocyte choriomeningitis virus
MHV	Mouse hepatitis virus
NS	Non structural protein
MS	Multiple sclerosis
EAE	Experimentalauotoimmune/allergic encephalomyelitis
CNS	Central nervous system
PNS	Peripheral nervous system
CSF	Cerebrospinal fluid
BBB	Blood-brain barrier
OB	Olfactory bulb
GFAP	Glial fibrillary acidic protein
T lymphocyte	Thumus-dependent lymphocyte
B lymphocyte	Bursal, thymic-independent lymphocyte
T_H	T helper
T_C	T cytotoxic
CTL	Cytotoxic T lymphocyte
Ab	Antibody
Ag	Antigen
FcR	Fc receptor
HI	Hyper-immune
CR3	Complement receptor type 3
NK	Natural killer
APC	Ag-presenting cells
MHC-I	Major histocompatibility complex-I
MHC-II	Major histocompatibility complex-II
RBC	Red blood cells
IFN	Interferons
IFN-α/β	Interferon-α/β

IFN-γ	Interferon-γ
IFN-γR	Interferon-γR
TNF	Tumor necrosis factor
TNFR	TNF receptor
IL	Interleukin
TGF-β	Tumor growth factor-β
CSF-1	Colony stimulating factor-1
M-CSF	Macrophage-colony stimulating factor
IDO	Indoleamine-2-3-dioxygenase
NO	Nitric oxide
NOS	Nitric oxide synthase
QA	Quinolinic acid
NMDA	N-methyl-D-aspartate
MIP-1α	Inflammatory protein-1α
RANTES	Regulated upon activation normal T expressed and secreted
MIP-1β	Macrophage inflammatory protein-1β
MCP-1	Monocyte chemotactic protein-1
Mig	Monokine induced by interferon-gamma
IP-10	Interferon-γ inducible protein-10
CAM	Cellular adhesion molecules
ICAM-1	Intercellular adhesion molecule-1
VCAM-1	Vascular cellular adhesion molecule-1
L-selectin	Leukocyte-selectin
P-selectin	Platelet-selectin
E-selectin	Endothelial- selectin
LFA-1	Leukocyte function-related antigen
VLA-4	Very late antigen-4
MAdCAM-1	Mucosal addresin cell adhesion molecule-1
PECAM-1	Platelet-endothelial cell adhesion molecule-1
i.p.	Intraperitoneal
i.n.	Intranasal
p.i.	Post infection
FCS	Fetal calf serum
CM	Complete medium
RT	Room temperature
h	Hour
mins	Minutes
pfu	Plaque forming unit
H.P.F.	High power field
L-NAME	Nω-nitro-L-arginine methyl ester

Chapter-1

General introduction

1.1. Viral Encephalitis: one of the severe and devastating human diseases

Encephalitis is an inflammation of the brain parenchyma and is almost always accompanied by inflammation of the adjacent meninges. It can occur at any age in any part of the world and has a high mortality rate. The reported incidence of encephalitis is 7.4/100,000 per year across the total population (Encephalitis Support Group 2001). Many aetiological agents may cause encephalitis, including viruses, bacteria, parasites, fungi, rickettsia, etc.,. However, viruses are the most common cause. Indeed, encephalitis may be caused by more than 100 different neurotrophic viruses (Gutierrez & Prober 1998).

Viral infections are the major cause of human morbidity and mortality throughout the world (Whitton & Oldstone 1996). Viral infections of the central nervous system (CNS) are one of the most severe and devastating human diseases. They can produce a wide range of neurological diseases including encephalitis, meningitis, myelitis and several demyelinating and degenerative syndromes (Griffin *et al.* 1992). The severity and the nature of clinical disease depends upon the virulence of the infecting virus and the quality of the host immune response to the infecting viruses (Weiner & Fleming 1999). In order to cause encephalitis, virus should have both neurovirulence and neuroinvasive properties. Neurovirulence is defined as the ability of neurotropic virus to infect CNS tissue, to replicate in some of its cells and injure them. Neuroinvasiveness is defined as ability of virus to invade the CNS by a peripheral route. Therefore, a neurovirulent virus necessarily does not cause encephalitis unless it is also neuroinvasive and absence of neuroinvasiveness makes a highly neurovirulent virus non-encephalitic (Halevy *et al.* 1994). Similarly, host responses also vary from one virus to another, depending upon the route of virus entry and spread within the CNS as well as tropism of the virus for specific CNS cells (Weiner & Fleming 1999). In most viral infections, neurones are the primary cells infected in the CNS (Griffin & Hardwick 1999).

Experimental studies on animal models show that invasion of CNS generally follows initial viral replication in various peripheral sites and a period of viremia (Albrecht 1968). Different neurotropic viruses use different anatomical sites and different mechanisms to invade the CNS (Johnson 1982). Some viruses use the neural route, where they replicate within nerves and are moved towards the brain parenchyma via the axonal transport system of neurones (Tang *et al.* 1999; Nathanson *et al.* 1961; Carbone *et al.* 1987). Virus movement rates have been estimated 2.4 and 3 mm/hour for rabies and poliovirus respectively (Nathanson and Cole, 1970). Other viruses use the haematogenous route (Johnson 1964; Dallasta *et al.* 1999). In this manner, they can infect brain capillary endothelial cells (Soilu-Hanninen *et al.* 1994), or use the transport system through brain endothelial cells without replication (Coffin *et al.* 1957; Liou & Hsu 1998), cross the choroid plexus with subsequent infection of the ependymal lining of the ventricles (Nathanson & Cole 1970) or use the olfactory route (Andrews *et al.* 1999; Monath *et al.* 1983). Independent of the routes of neuroinvasion, disease can occur only if virus spreads within the CNS, replicates extensively within the susceptible resident cells and induces changes in those cells. Within the CNS, viral spread may take place either from cell to cell, often along dendritic or axonal processes, or extracellularly (Johnson 1987). Viruses that enter into the brain via the haematogenous route cause widely scattered pathology throughout the brain whereas those using the neural pathway tend to cause more localized and contiguous pathology (Albrecht 1968).

Viral encephalitis manifests as either acute encephalitis or postinfectious encephalomyelitis (also known as acute disseminated encephalomyelitis) depending on cause and pathogenesis. Acute viral encephalitis is caused by direct viral infection of neural cells with associated perivascular inflammation and destruction of brain tissue, including grey matter. In contrast, postinfectious encephalomyelitis occurs a few days or weeks after the appearance of systemic symptoms of viral infection with perivenular inflammation and demyelination of brain tissue, including white matter (Gutierrez & Prober 1998; Johnson 1987). Although acute encephalitis may be caused by many different groups of viruses, fatal cases are reported predominantly due to either arthropod-borne viruses or herpes simplex virus (HSV) (Johnson 1987).

1.1.1. Arboviral encephalitis: a global health problem

Arthropod-borne viruses, hence the name arboviruses, are one of the commonest causes of viral encephalitis. They have been reported to cause 10% of all cases of sporadic encephalitis and up to 50% of all cases in epidemic years (Gutierrez & Prober 1998). Arboviral infections occur worldwide. The highest incidence of arboviral disease occurs in tropical and subtropical regions (Halley *et al.* 2000). As the name arbovirus implies, these viruses are transmitted by arthropods but they replicate in both the arthropods and vertebrate host. Therefore, these viruses are usually maintained in a reservoir cycle that consists of both arthropods and vertebrate hosts, both being needed to maintain the virus in nature. Groups of arthropods involved in the transmission of arbovirus include mosquitoes, ticks, sandflies and midges (Shope & Meegan 1993). Arboviruses that cause human encephalitis are members of three families, the Togaviridiae, Flaviviridiae and Bunyaviridae.

1.1.2. Flaviviral encephalitis: the most common arboviral encephalitis

Flaviviruses are enveloped, single-stranded plus sense, positive stranded RNA viruses, the genome of which consists of approximately 11, 000 bases. They are genetically quite stable compared to other RNA viruses. The name flavivirus derived from the latin word *flavus*, meaning yellow from the jaundice associated with yellow fever, caused by yellow fever virus (Rice 1996).

Japanese encephalitis (JE), dengue, yellow fever (YF), tick borne encephalitis (TBE), Murray Valley encephalitis (MVE), Saint Louis encephalitis (SLE) and West Nile viruses are the most important flaviviruses to cause regional endemic and epidemic disease throughout the world (Rice 1996). The large majority of incidents of flaviviral encephalitis are inferred from case reports, hospital case lists and reports of presumed outbreaks of the infectious disease. Thorough investigation of the aetiology and risk factors of encephalitis in well-defined populations is still lacking. The epidemiology of some of the flaviviral infections throughout the world is summarised in table 1.1. Flaviviruses produce a wide spectrum of infection and disease depending upon the virus dose, age and other factors which affect the host response. Usually, one of 3 different patterns of disease occur in

Table 1.1 Summary of important flaviviruses causing disease in humans

Viruses	Geographic region(s)	Vectors	Mortality rate	Disease pattern
Dengue	Southeast Asia	Mosquito – *Aedes aegypti*	10-40%	Endemic and epidemic
Japanese encephalitis	Orient, China, Japan, India, Korea, Australia	Mosquito - *Culex tritaeniorhynchus* other culicines	30-40%	Endemic and epidemic
Murray Valley encephalitis	Australia	Mosquito – *Culex annulirostris*	10%	Epidemic, sporadic over wide areas
Saint Louis encephalitis	Southern, central and western states of America	Mosquito – *Culex pipens* and others	5-15%	Endemic and epidemic
Tick borne encephalitis	Russia and Northern Europe	Ticks - *Ixodos ricinus* and others	5-20%	Endemic in forested regions
Yellow fever	New world and Africa	Mosquito – *Aedes aegypti*	3-20%	Endemic and epidemic
West Nile	Asia, Africa, Europe, Middle East	Mosquito – *Culex pipens* and others	5-10%	Endemic and epidemic

Derived from Centre for Disease Control 2000; Morbidity and Mortality Weekly Report 1999; Dumpis *et al.* 1999; Monath 1994; Shope & Meegan 1993; Russell & Dwyer 2000.

infected individuals. These viruses may thus cause fatal encephalitis, subclinical encephalitis or there may be clinically inapparent infection (Monath 1986).

1.1.3. West Nile Virus: one of the deadly flavivirus

1.1.3.1. History and Epidemiology

West Nile virus (WNV) belongs to the family flaviviridae which comprises approximately 70 viruses, nearly 40 of which cause human disease (Monath & Heinz 1996; Leyssen *et al.* 2000). Serologically, WNV is a member of Japanese encephalitis virus complex that includes JE, SLE, Kunjin and MVE viruses (Calisher *et al.* 1989). WNV was first isolated from the blood of a febrile woman in the West Nile province of Uganda in 1937 (Smithburn *et al.* 1940) and since then has been found subsequently in west and central Asia, Africa, Middle East, Europe and America. It causes serious epidemics outside these areas and can infect a wide range of vertebrates such as humans, animals and birds with significant morbidity and mortality (Sampson *et al.* 2000; Steele *et al.* 2000; Ben-Nathan *et al.* 1996; Smithburn *et al.* 1940). The reported WNV outbreaks throughout the world are presented in table 1.2.

Table 1.2. Summary of WNV outbreaks throughout the world

Country	Year outbreaks
Israel	1951-1954, 1957
France	1962
South Africa	1974
Western Ukraine	1985
Algeria	1994
Romania	1996
Italy	1998
Democratic Republic of the Congo	1998
Russia	1999
United State	1999
France	2000
Israel	2000

Derived from Hubalek 2000; Roehrig 2001; Tsai *et al.* 1998

In humans, WNV infection is usually asymptomatic or presents with mild febrile disease, but during epidemics, 10% or more of reported cases show severe or fatal encephalitic infection (MMWR 1999; Briese *et al.* 1999, Ceausu *et al.* 1997). Typically, the disease is characterized by high fever, severe headache, lymphadenopathy and maculopopular rash, (George *et al.* 1984; Flatau *et al.* 1981), variably associated with other manifestations, such as diffuse muscular pain, nausea, vomiting and conjunctivitis (Sampson *et al.* 2000). Encephalitis is a common complication of WNV infection (Katz *et al.* 1989), other complications occur rarely but include myocarditis, hepatitis and pancreatitis (Georges *et al.* 1987; Perelman & Stern 1974; Albagalic 1959). Recently, WNV has been isolated from a patient with human immunodeficiency virus (HIV) (Szilak & Minamoto 2000).

1.1.3.2. Mode of WNV transmission

Wild birds, especially wetland and terrestrial avian species, are the principal hosts of WNV (Hubalek & Halouzka 1999). Mosquitoes, largely bird-feeding species, especially Culex species (43 species), are the principal vector for WNV (Hubalek & Halouzka 1999). Mosquitoes become infected after feeding on infected birds. WNV then replicates in the cells of the midgut epithelium, circulates in their blood and is transferred to the salivary gland via haemocytes. This cycle takes approximately 10 to 14 days and once complete, mosquitoes can transmit WNV to human or animal hosts, secreting virus in the saliva during a blood meal (Kettle 1995). Mosquitoes may remain infected and able to transmit virus for many weeks or months (Shope & Meegan 1993).

Humans and domestic animals are usually regarded as incidental or "dead-end" hosts. They are generally thought not to participate in the WNV transmission cycle due to the low levels of viremia (Halley *et al.* 2000). The transmission cycle of WNV in the ecosystem is presented in figure 1.1. Although the natural foci of WNV infections mainly occur in wetland ecosystems and are characterized by repeated bird-mosquito cycles, sometimes ticks may serve as a substitute vector (bird-tick cycle) in some warm and dry habitats in the absence of mosquitoes (Hubalek & Halouzka 1999).

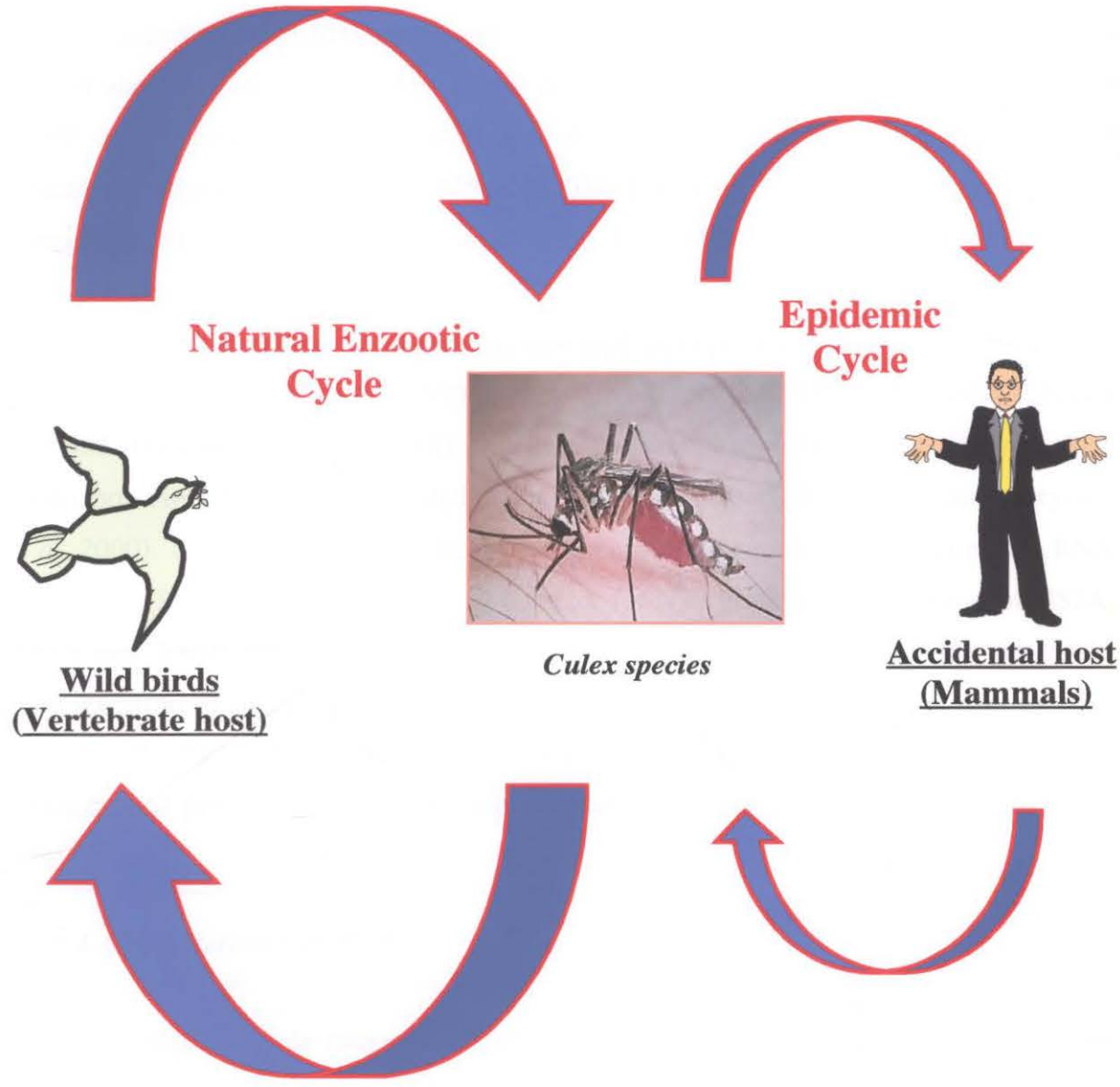

Figure: 1.1 Transmission cycle of WNV.

1.1.3.3. Organization of WNV genome

All flaviviruses, including WNV share a common size of 40-60nm, and can be readily visualized under the electron microscope. WNV consists of an isometric ribonucleoprotein core of about 35 nm surrounded by a lipid envelope. Transmission electron micrograph of WNV on a vero cell monolayer is shown in figure 1.2. The viral genome consists of infectious positive, single-stranded 42S RNA. This functions, via a long open reading frame containing 10,290 nucleotides, as mRNA for the synthesis of all structural and non-structural viral proteins *in vivo* (Castle *et al.* 1985). In the flaviviral genome, the structural proteins consist of nucleocapsid protein, envelope glycoprotein and precursor membrane glycoprotein. The non structural (NS) proteins are NS1, NS2A, NS2B, NS3, NS4A, NS4B and NS5. The exact functions of NS1 protein in virus replication has not been defined (Rice 1996), however, it has been suggested that it plays a role in early RNA replication (Leyssen *et al.* 2000). NS3 and NS5 are believed to be enzymatic components required for RNA replication (Rice 1996). NS2B acts as a cofactor for NS3 protein. The functions of NS2A, NS4A and NS4B are still unknown (Leyssen *et al.* 2000; Rice 1996). The schematic representation of organization of flaviviral genome is presented in figure 1.3. *In vitro* experiments have shown the presence of large amounts of WNV structural and nonstructural proteins incorporated into cellular membranes in vero cells (Castle *et al.* 1986).

1.1.3.4. Characteristics of WNV

WNV can infect a wide range of vertebrates (Sampson *et al.* 2000; Steele *et al.* 2000; Ben-Nathan *et al.* 1996; Pogodina *et al.* 1983). The requirement to replicate alternately in both mosquitoes and vertebrate hosts under very different cellular conditions may explain the highly conserved genome of WNV, relatively unusual in an RNA virus. Genetic drift and/or recombination, thought to be an immune evasion survival strategy in other viruses, is thus not an option for WNV. Therefore this makes mechanistic interaction with the vertebrate host immune system more likely as a possible survival strategy. WNV infection of a wide variety of vertebrate cells from different species results variously in the increased expression of the critical immune recognition molecules, class I and II major histocompatibility complex (MHC-I and MHC-II) antigens (Bao *et al.* 1992; Argall *et al.* 1991; King *et al.* 1989; Liu *et al.* 1989; King & Kesson 1988) intercellular adhesion

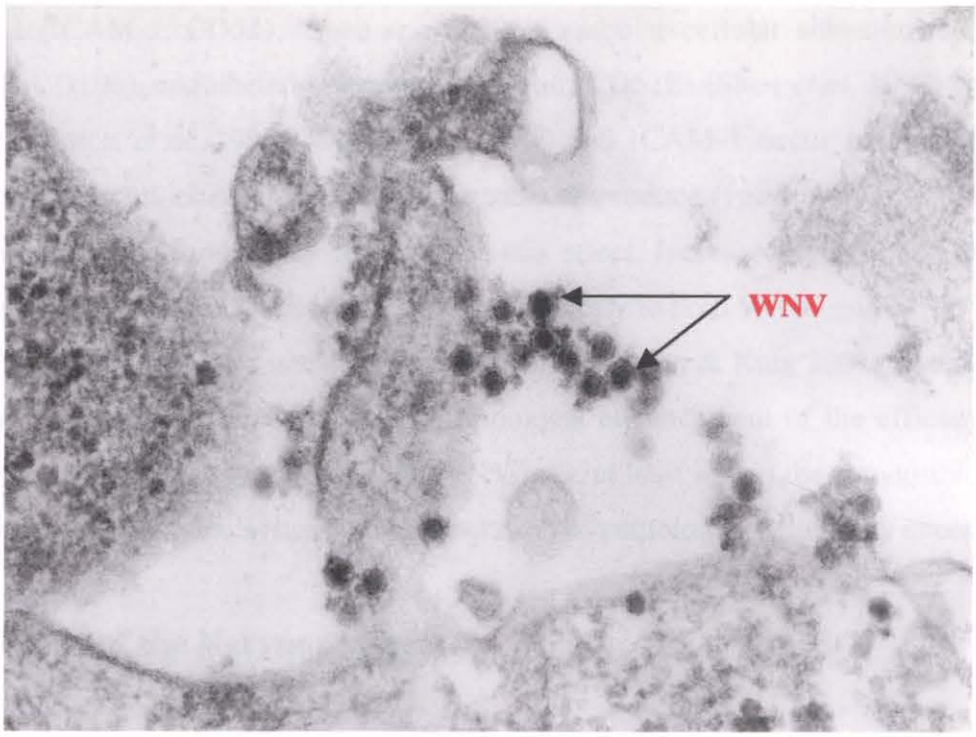

Figure: 1.2 Electron micrograph of WNV in vero cell culture infected with WNV. Adapted from Centre for Disease Control 2001.

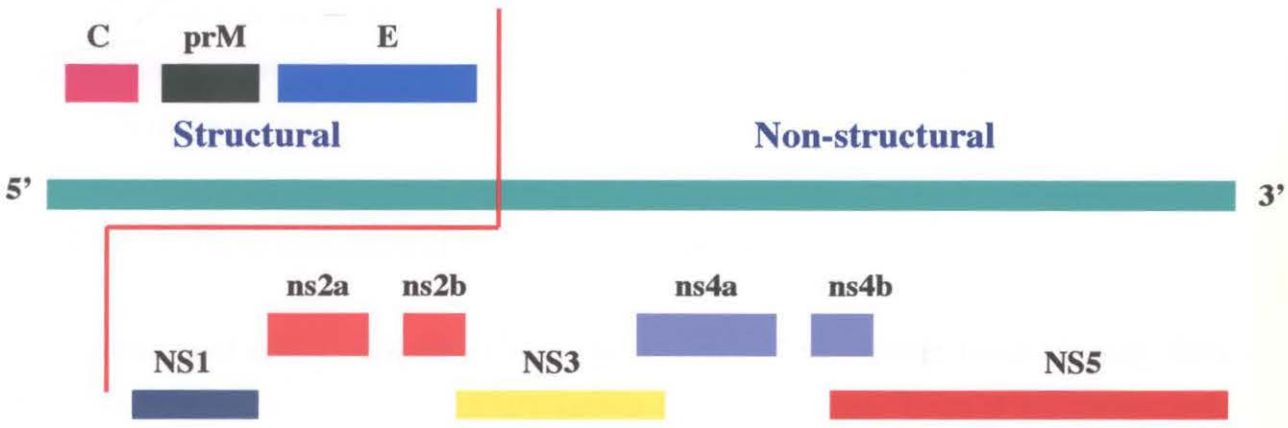

Figure: 1.3 Schematic diagram of organization of flaviviral genome. Abbreviation: C, core or nucleocapsid protein, E, envelope glycoprotein, NS, non-structural protein, prM, precursor membrane glycoprotein. Drawings taken from Roehrig *et al.* 2000.

molecule-1 (ICAM-1; CD54), (Shen *et al.* 1995), vascular cellular adhesion molecule-1 (VCAM-1; CD106), endothelial-selectin, (E-selectin; CD62E) (Shen *et al.* 1997) and B7-1 (CD80) (Johnston *et al.* 1996). Changes in MHC and ICAM-1 occur independently of interferons, since this effect is seen in cells unable to produce type I interferon and type I interferon-specific antibody does not abrogate this effect. Increased cell surface molecule expression is also functional; thus increased susceptibility to both WNV- and MHC-specific cytotoxic T lymphocyte lysis is clearly demonstrable (Kesson & King 2001; Douglas *et al.* 1994; King *et al.* 1993). This apparently paradoxical enhancement of the efficacy of the host antiviral cellular immune response by WNV may, at least in part, be responsible for the involvement of the immune system in the generation of pathology, particularly encephalitis.

1.2. Divisions of the Nervous system

The nervous system is an internal communication network that enables animals to adjust minutely to changes in the environment. It is divided into the CNS and the peripheral nervous system (PNS). The CNS consists of the brain and spinal cord, located in the cranial cavity and spinal cavity, respectively. The PNS consists of cranial and spinal nerves (both motor and sensory), various ganglia (collections of nerve cells outside the CNS) and receptors such as motor nerve and sensory nerve endings (Burkitt 1993). The cranial and spinal nerves serve as "telephone wires" that carry messages to and from every receptor and effector in the body.

1.2.1. Cellular organization of the central nervous system

The brain and spinal cord are covered by 3 layers of supporting tissue namely: dura, arachnoid and pia mater, collectively known as the meninges. There is no conventional lymphatic drainage in the CNS, however, it has been shown that blood fluids pass out from the capillaries and seep through the neural tissue towards the brain surface and ventricles (Albrecht 1968). As well, various proteins, such as ovalbumin, drain from the brain into the deep cervical lymph nodes (reviewed in Matyszak 1998).

The brain is an extremely complicated organ, consisting of 3 principal parts, the cerebellum, brainstem and cerebrum. The cerebrum directs and coordinates hearing, sight, touch,

thinking, use of language, emotions and learning. The brainstem is connected to the spinal cord. It relays information from the sense organs and regulates autonomic functions, such as balance, blood pressure, breathing and heart rate. The cerebellum helps to maintain gravitational balance while coordinating muscular movements with sensory information (Stevens 2001).

The spinal cord is a long cylindrical structure that is directly continuous with the brain, essentially serving as a neuronal cable. Near the muscle cells, the axons of spinal cord motor neurones divide into numerous branches that form the neuromuscular junctions with the muscle cell (Carpenter 1991). The function of the spinal cord is critical. It contains afferent pathways that carry sensory information from most parts of the body to the brain and descending efferent pathways that relay commands from the brain to the motor neurones. It also contains fibre systems and neurones that mediate segmental reflexes and provide autonomic innervation (Carpenter 1991; Stevens 2001).

Despite extensive protection, the CNS can be invaded and damaged by variety of microorganisms. Resident cells of the CNS, such as microglia and astrocytes, and haematogenous cells that can invade the CNS from the vasculature are involved in the defence against such infections (Marten *et al.* 2001; Kreutzberg 1996; Mucke & Eddleston 1993). In order to illustrate how these components are integrated, it is first necessary to review the normal cellular components of the CNS and the immune response.

1.2.1.1. Neurone: the functional unit of the nervous system

The CNS controls and coordinates the activities of the entire nervous system by means of two principle types of cells, neurones and glial cells. Schematic diagrams of the CNS resident cells are presented in figure 1.4. The neurones are specialized to receive stimuli and conduct electrical impulses to other parts of the system and are arranged as an integrated communication network. The glial cells are nonconducting. They are in intimate physical contact with the neurones, providing physical and metabolic support to these cells as well as electrical insulation for neuronal cell bodies and processes. The neurone consists of a nucleus surrounded by cytoplasm and processes such as axons and dendrites. Axons are the neuronal processes that transmit stimuli to other neurones or to effector cells; dendrites

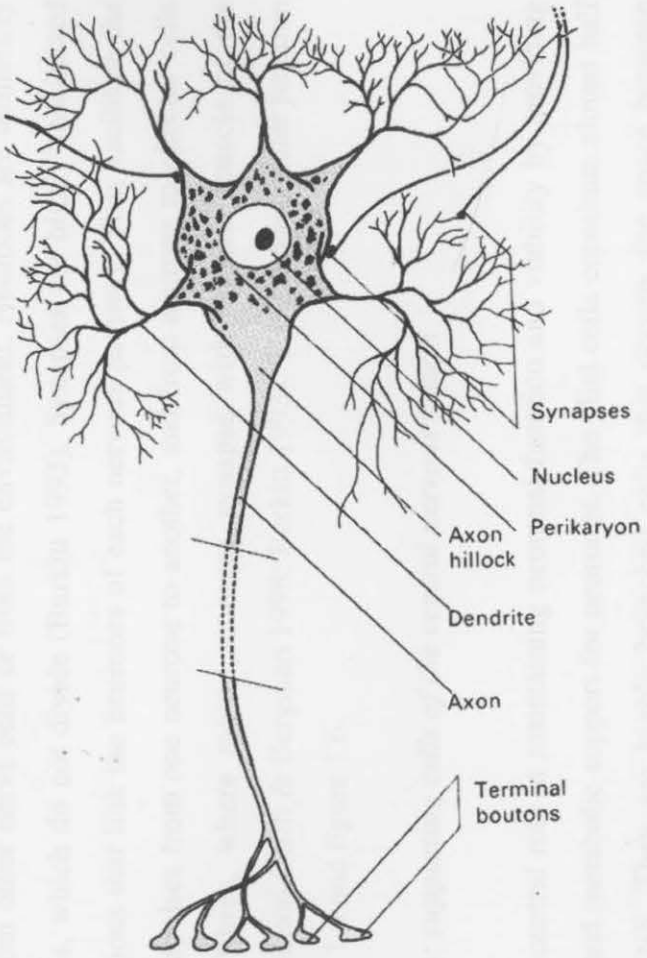

Neurone

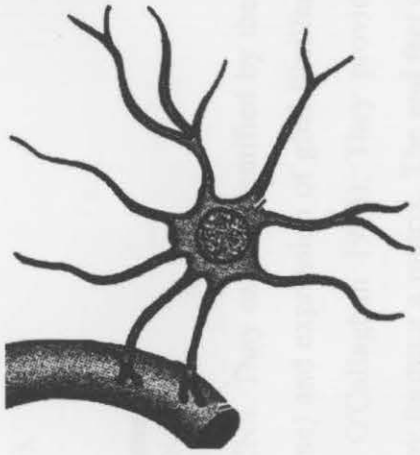

Astrocyte

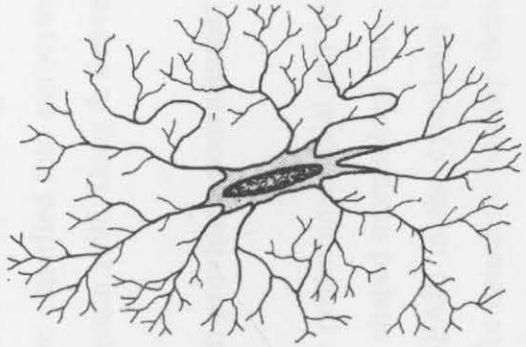

Microglia

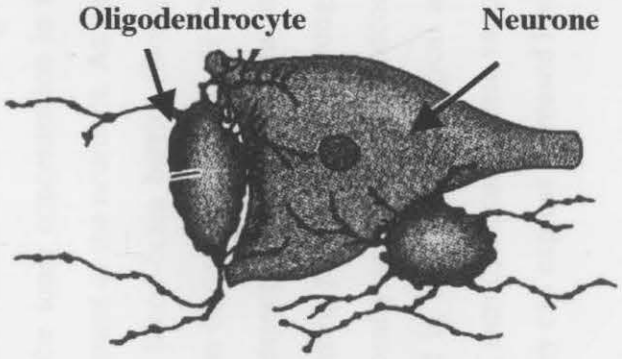

Oligodendrocyte

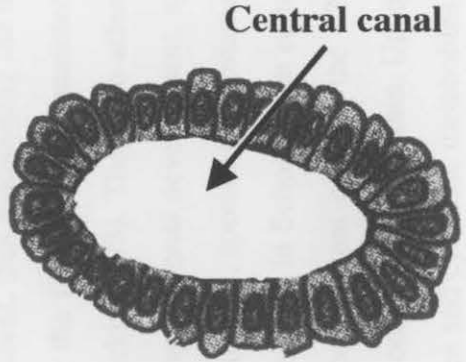

Ependymal cells

Figure: 1.4 Schematic diagram of CNS resident cells. Adapted from Afifi & Bergman 1998; Burkitt *et al.* 1993.

receive stimuli from other nerve cells or from the environment. Neurones are terminally differentiated cells, which do not divide (Burkitt 1993). Synapses are highly specialized intercellular junctions that link the neurones of each nervous pathway. They facilitate the transmission of impulses from one neurone to another, and from neurone to effector cells such as muscle fibres, where motor neurones synapse with skeletal muscle at the neuromuscular junction (Afifi & Bergman 1998; Burkitt 1993). The neuromuscular junction is shown in figure 1.5 and figure 1.6.

1.2.1.2. Glial cells: supporting cells of the central nervous system

Glial cells play a central role in maintaining neuronal function and viability by providing both mechanical and metabolic support for neurones. The glial cells constitute almost half the volume of CNS. They are highly branched cells that occupy the space between neurones. They are classified into astrocytes, microglia, oligodendrocytes and ependymal cells (Afifi & Bergman 1998; Dong & Benveniste 2001).

- **Astrocytes: providing nourishment for neurones**

Astrocytes are the predominant glial cell type in the CNS. They can be identified by their characteristic star shaped morphology (hence their name) and expression of glial fibrillary acidic protein (GFAP) in the cytoplasm (Martin & O'Callaghan 1995). They provide physical support for neurones, holding them in place by forming a matrix. The *end feet* of astrocytes are in close proximity to the microvessels. These facilitate the exchange of metabolites and waste to and from neurones and regulate the ionic concentration in the intercellular compartment, thus maintaining the microenvironment of the neurones. As well, they are involved in the formation and maintenance of the blood-brain barrier (Dong & Benveniste 2001; Burkitt 1993). They also affect the function of neurones in normal CNS physiology by guiding neuronal development, synthesizing essential neurotrophic factors, removing neurotransmitters, specifically glutamate, and buffering potassium ions (Dong & Benveniste 2001; reviewed in Schoneboom *et al.* 1999). Recently astrocytes have become recognised as imunocompetent cells of the CNS, involved in both immunological and inflammatory events occurring in the brain. Upon stimulation, astrocytes can secrete various cytokines, chemokines and cytotoxic metabolites. As well, they can express increased levels

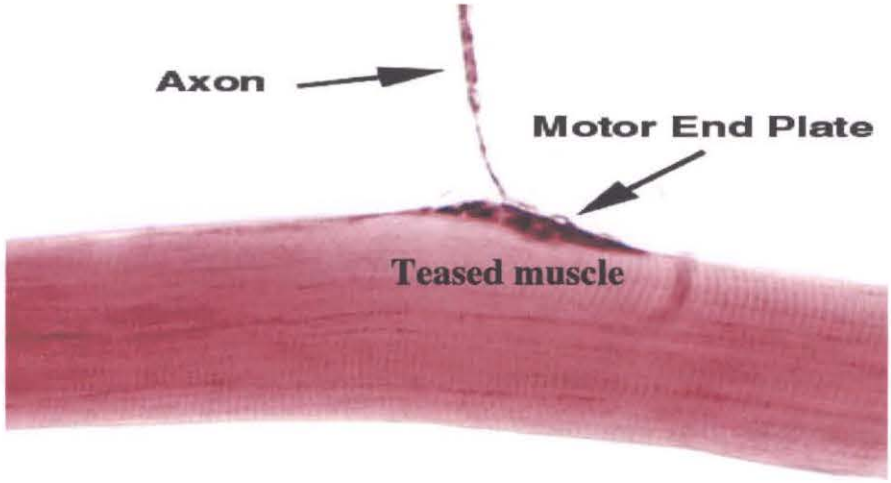

Figure: 1.5 Whole mount preparation of "teased" skeletal muscle fibre stained with iron hematoxylin stain showing the neuromuscular junction or motor end plate. Adapted from Caeci 2001.

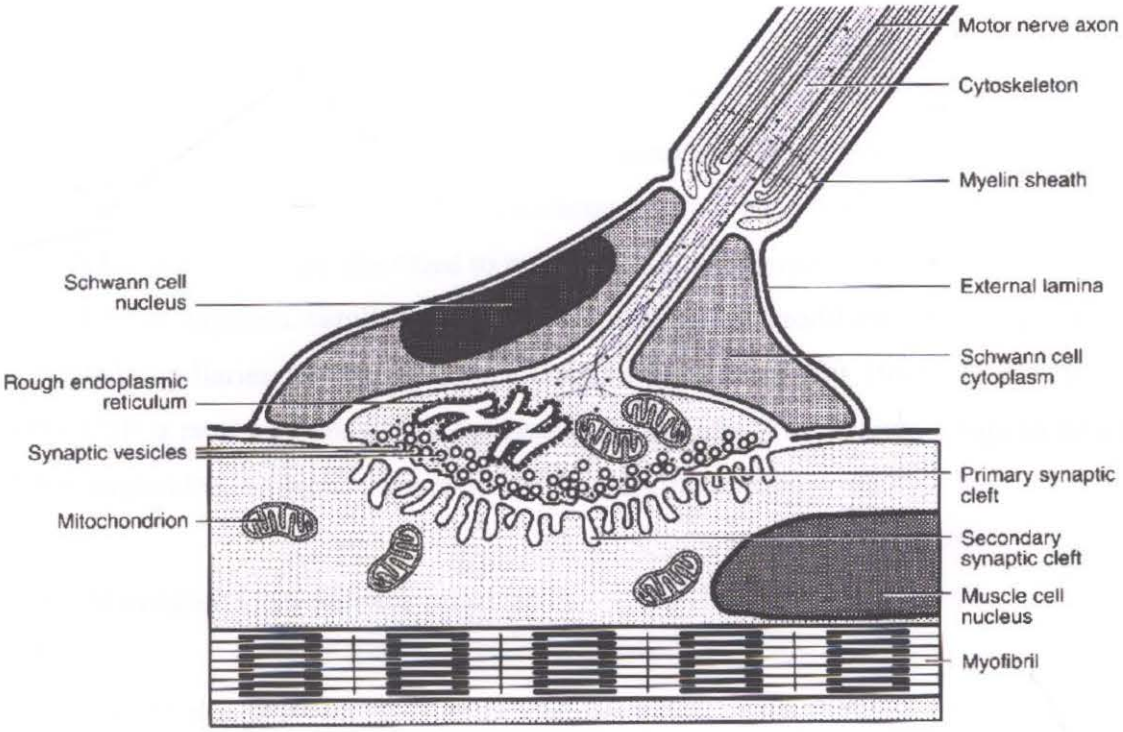

Figure: 1.6 Schematic ultrastructural diagram of the neuromuscular junction (NMJ). NMJ is 40-60μm in diameter and is typically located near the midpoint of the muscle fibre. The synaptic gap between the nerve and muscle is 50μm. when a motor neuron is activated, the nerve impulses reache the axon terminal and communicate with the muscle fibre by discharging acetylcholine, present in the axon terminal, into the gap between pre and postsynaptic membranes. Adapted from Burkitt *et al.* 1993.

of various molecules critically involved in cellular immune recognition interactions, including ICAM-1, MHC-I and MHC-II molecules (Dallasta *et al.* 2000; Glabinski *et al.* 1999; Brodie *et al.* 1997; Grzybicki *et al.* 1997; Benveniste 1992). This will be discussed in more detail in section 1.5.

- **Oligodendocytes: myelin synthesizing cells**

Oligodendrocytes can be identified by the characteristic expression of myelin specific protein such as myelin basic protein and myelin glycolipid such as galactocerebroside (Benveniste 1992). They provide support for neurones by producing the myelin sheath that electrically insulates axons (Adams *et al.* 1994). In the grey matter, oligodendrocytes closely aggregate around neuronal cell bodies and are also known as perineuronal satellite cells. In the white matter, they are lined up between myelinated fibres and referred to as interfascicular glia (Adams *et al.* 1994).

- **Ependyma: CSF synthesizing cells**

Ependymal cells are the epithelial lining of the ventricles of the brain and spinal cord, and have morphologic and physiological characteristics of fluid-transporting cells. In many areas of the brain, they are modified to produce CSF by transport and secretion of materials derived from adjacent capillary loops in the CNS. The modified ependymal cells and associated capillaries are known as the choroid plexus (Burkitt 1993; Afifi & Bergman 1998). CSF is produced constantly by these cells and effectively forms a bath in which the CNS is suspended, acting as a shock absorber (Burkitt 1993).

- **Microglia: CNS defence cells**

Microglia are the smallest glial cells and comprise up to 20% of the total glial cell population in the brain (Lawson *et al.* 1990), belonging to the mononuclear phagocyte system (Davis *et al.* 1994; Ling & Wong, 1993). They are present in nearly equal numbers in the grey and white matter (Kreutzberg 1996; Dickson *et al.* 1991). The cellular form of microglia present in the normal adult brain displays a ramified morphology with small somata and long thin branched processes. Expression of immune molecules, such as MHC,

ICAM-1, cytokines and chemokines, is low or absent (Sudo *et al.* 1998; Banati *et al.* 1993). They respond to the slightest alteration in their microenvironment (Greenfield 1997; Matyszak 1998). Once activated, they can produce several different kinds of secretory products as well as other immune molecules. These include cytokines, chemokines, cytotoxic metabolites, neurotrophic growth factors as well as increased expression of cell surface receptors like Fc receptor (FcR), complement receptor type 3 (CR3), α-D-galactoside residues and other marker molecules such as ICAM-1, MHC-I and MHC-II (Nakajima & Kohsaka 1998; Banati *et al.* 1993; Benveniste, 1992). Microglial activation is critical in the defence of the neural parenchyma against infectious diseases, inflammation, trauma, ischaemia, brain tumors and neurodegeneration (Kreutzberg 1996). This will be discussed in more detail in section 1.5 and chapter 4.

1.2.2. Olfactory system

The olfactory system, which senses and processes odors, is one of the oldest and most vital parts of the brain and plays an important role in the survival of many animals. Lower vertebrates and many mammals rely heavily on the sense of smell for information about their environment. Olfaction is a basic or even primary mode of communication and is fundamental to vital functions such as detection and location of food sources and/or predators, as well as social and sexual behaviour (Carpenter 1991; Switzer *et al.* 1985). The olfactory system consists of the olfactory epithelium, bulb and tracts, together with the cerebral olfactory areas and their projections to other centres. The relationship between the nasal cavity and the olfactory bulb (OB) is shown in figure 1.7. In the olfactory system, the axons of the olfactory receptor neurones (also known as olfactory neuroepithelial cells) in the epithelium lining the nasal cavity, project to the OB, located at the anterior or rostral end of the cerebrum, where they synapse on the dendrites of second-order neurones within glomeruli (Barr & Kiernan 1983) as shown in figure 1.8.

1.2.3. Blood-brain barrier; a specialized vessel wall in the central nervous system

The proper function of all neurones of the CNS is dependent on the maintenance of a physical and chemical milieu within certain narrow limits. The system that regulates the exchange of water and solutes between the blood, the CSF, and the brain involves

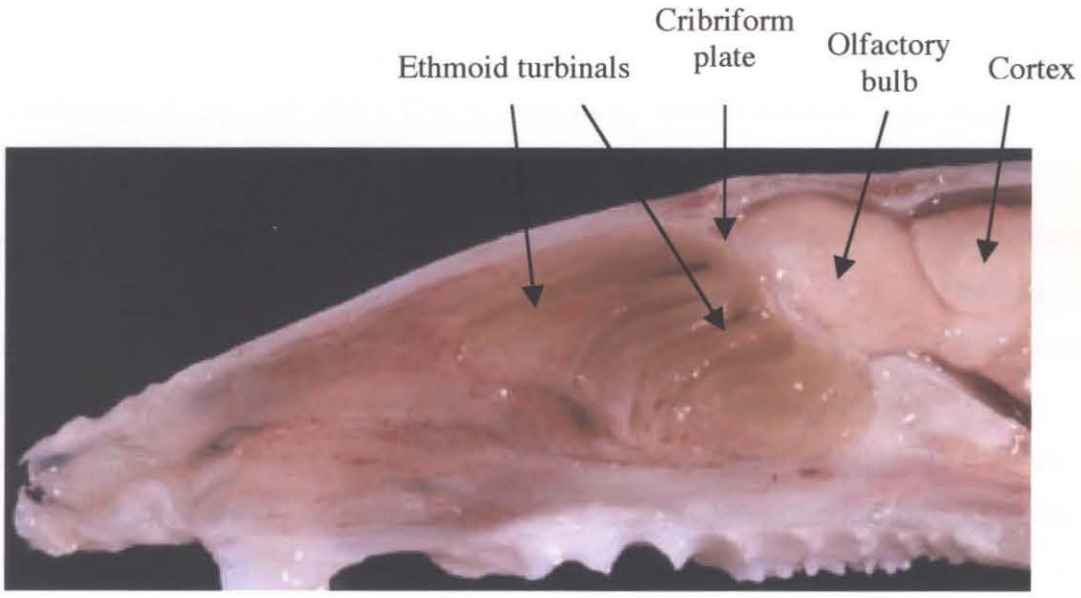

Figure: 1.7 Sagittal section through the skull of a rodent shows the relationship of the nasal cavity with the olfactory bulb and the cortex (cerebrum). Adapted from Puche 2001.

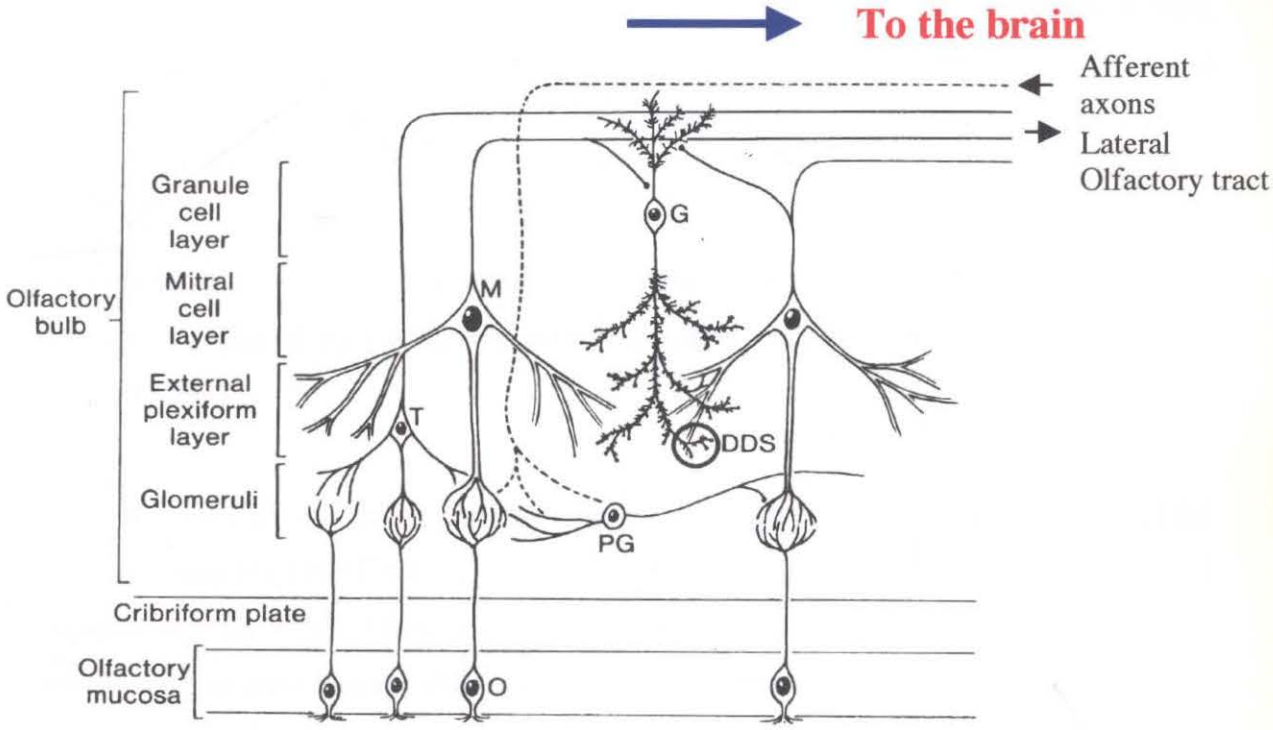

Figure: 1.8 Schematic diagram of the major olfactory bulb and their relationships. Olfactory receptor neurons (*O*) are in the olfactory mucosa. They project axons to the OB and synapse with dendrites of mitral cells (*M*) forming complexes known as glomeruli. Axons of *M* projecting centrally form the lateral olfactory tract. Granule cells (*G*) have no axons, but dendritic spines on external dendrites form dendrodendritic synapses (*DDS*) with M dendrites. Periglomerular cells (*PG*) provide a linkage between glomeruli. Tufted cells (*T*) are similar to M, but their cell bodies are dispersed throughout the external plexiform layer. Adapted from Carpenter 1991.

membranes with selective permeability and specific carrier-mediated transport systems which form barriers (Carpenter 1991). This is collectively known as blood-brain barrier.

The blood-brain barrier (BBB) is a series of interfaces between blood, CSF and neural tissue, formed mainly by microvascular capillary endothelial cells, a continuous homogeneous basement membrane and numerous astrocytic processes (de Boer & Breimer 1998; Carpenter 1991). Capillaries within the CNS contain a continuous inner layer of unfenestrated endothelial cells connected by a high density of continuous, high-resistance tight junctions, derived totally or partially from the neuroectoderm (Andjelkovic & Pachter 1998; Carpenter, 1991). The basement membrane surrounding the endothelial cells has approximately 85% of its surface covered by astrocytic *end feet* (Hurwitz *et al.* 1994; Carpenter 1991), which thus contribute to the maintenance of structural integrity of the BBB (Benveniste 1992). Besides astrocytes, microglia also extend their processes into the perivascular basement membrane where they may be in direct contact with endothelial cells. In addition to these, perivascular macrophages and pericytes are also present in tight apposition to endothelial cells (Andjelkovic & Pachter 1998). All these structural and cytologic properties of cells contribute to maintain BBB integrity, which is a critical regulator of CNS homeostasis and function. However, the BBB in the CNS is not complete everywhere. The circumventricular organs, including the postrema, median eminence, pineal gland, and choroid plexus are devoid of BBB. Here capillary endothelium with tight junctions is replaced by capillaries with fenestrated endothelium (Banks *et al.* 1995; Carpenter 1991).

The BBB is critically important not only to maintain the physiochemical composition of the microenvironment of the CNS, but also to prevent the entry of circulating leukocytes and pathogens into the CNS (Hurwitz *et al.* 1994). Excepting activated T cells, immune cells normally do not pass through the intact BBB, unless there is an enhanced expression of endothelial adhesion molecules (Hickey *et al.* 1991). However, during inflammatory diseases of the CNS, the disruption of BBB can occur facilitating the entry of inflammatory cells as well as infectious pathogens (Petito & Cash 1992; Andersen *et al.* 1991). Thus, breakdown of the BBB can facilitate infection of the brain parenchyma and has been reported in many viral encephalitides (Dallasta *et al.* 1999; Eralinna *et al.* 1996; Andersen *et al.* 1991).

1.3. Cross talk between the central nervous system and the immune system

The nervous system and the immune system are both designed to receive and respond to minute changes in physical or chemical stimuli generated within or outside of the body. Traditionally, it was thought that there was no communication between the CNS and the immune system, with both acting separately (Neumann & Wekerle 1998). However, recent studies have demonstrated that the immune system can interfere with CNS function and the CNS can also influence the activity of the immune system (Aarali 1983; Becher *et al.* 2000). The communication between the CNS and the immune system occurs via the coordinate use of surface molecules, as ligands and receptors in cell adhesion, and soluble mediators such as cytokines, chemokines, nitric oxide (NO), neuropeptides, neurohormones, synaptic transmitters and neurotrophic factors (Neumann & Wekerle 1998; Black 1994; Benveniste 1998). The occurrence of neurotransmitter receptors on lymphocytes, as well as cytokine receptors on neurones and glial cells (Gebicke-Haerter *et al.* 2001; Zhao & Schwartz 1998; Yamada & Yamanaka 1995), further support the notion that a bi-directional communication exists between the CNS and the immune system (Black 1994).

Previously, the CNS was thought to be an "immune privileged" site due to the presence of the BBB, which prevented the entry of leukocytes, plasma proteins and cytokines. The evident lack of professional antigen presenting cells (APC), such as B cells, dendritic cells, and macrophages, and low expression or absence of MHC-I and II molecules (Benveniste 1992; Neumann 2001) in the CNS cells further promoted this idea. Although access of immune cells to the CNS is restricted (Fontana 1987; Cserr *et al.* 1992) a small number of activated T lymphocytes, irrespective of their antigen receptor specificity, do pass through the BBB (Hickey *et al.* 1991), but do not seem to interact much with the cells of the CNS (Neumann & Wekerle 1998), presumably due to the absence or low expression of MHC molecules which are required for the initiation and propagation of antigen-specific immune responses (Neumann 2001). However, several recent studies have demonstrated that in response to invasion by microorganisms, resident cells of the CNS such as astrocytes and microglia can mount a significant response, with the production of many different kinds of cytokines and chemokines, as well as the upregulation of MHC-I and II molecules (Renno

et al. 1995; Acarin *et al.* 2000; Cross & Woodroofe 2001; Banati *et al.* 1993). These cells can also actively participate in integrative communication pathways between resident immune cells of the CNS and those of the periphery (Aarali 1983). In addition to this, the influx of massive number of inflammatory leukocytes also occurs in the CNS parenchyma during infection or injury (Chan *et al.* 1989; Nansen *et al.* 1998; Ferber *et al.* 1996). Thus, despite important differences between the CNS and periphery, they can no longer be regarded as independent or isolated from one another, either anatomically or functionally.

1.4. Immunity: a host defence mechanism

The outcome of viral infection is determined by a race between the replicating agent and the host defences. Several experiments on immune-deficient mice or mice treated with immunosuppressive drugs have proven the crucial role of the immune response in controlling viral infections (Camenga & Nathanson 1974; Nathanson & Cole 1970; Beland *et al.* 1999; Pasparakis *et al.* 1996; Ben-Nathan *et al.* 1996; Ferber *et al.* 1996; Liu & Chamber 2001; Planz *et al.* 1997). In neurotropic viral infections, significant depression of immune reactivity is associated with enhanced virus-mediated morbidity and mortality from encephalitis, characterized by prolonged viremia, elevated virus levels in the CNS and other peripheral tissues, and a reduced or undetectable antibody response (Nathanson & Cole 1970; Ben-Nathan *et al.* 1996; Liu & Chambers 2001).

Immunity, the state of protection from infectious disease and injury results from the ability to generate an enormous variety of effector cells and molecules that are capable of specifically recognizing and eliminating many different types of microorganisms. The immune response consists of innate and adaptive immune components (Kuby 1994). The innate immune system allows recognition of foreign substance (antigen) via germ-line encoded pattern recognition receptors, and thus, are responsible for immediate action against antigen (Ag). In contrast to innate immunity, adaptive or acquired immunity enables Ag recognition via specific Ag-receptors generated by somatic recombination, and demonstrate plasticity and memory (De Leo & Yezierski 2001; Becher *et al.* 2000). The mechanism of host defence against infections or injury is a symphony of many innate and adaptive immunologic components, both working together to effectively eliminate foreign invaders (Janeway *et al.* 2001).

1.4.1. Innate immunity: the vanguard of host defence

Innate (non-specific) immunity is regarded as a pre-existing or rapidly inducible host effector system for the control of infection, against which the host has not been previously immunized (Welsh *et al.* 1997). Innate resistance mechanisms are important barriers to pathogens, particularly in controlling virus multiplication at the onset of infections, prior to the development of an adaptive immune response. They enable the host to "knock down" the immediate accumulation of viruses that could otherwise be lethal prior to the generation of the specific immune response (Baron *et al.* 2000). Innate immunity includes a series of anatomical and physiological barriers, as well as non-specific cellular responses with antimicrobial activity. Besides these, apoptosis, *i.e.*, programmed cell death is also considered to be part of the innate immune reponse, induced to counteract viral infection (Everett & Mcfadden 1999).

1.4.1.1. Anatomic and physiological barriers

Anatomic barriers that tend to prevent the entry of pathogens are regarded as the first line of defence of the host. Skin and mucous membranes are included in this category. When intact, the skin is impermeable to most pathogens and the low pH also inhibits their growth (Kuby 1994). The mucous membranes, lining the inner surfaces of the body, also act as a protective barrier. They block the adherence of pathogens by means of various secretions such as mucus, tears, saliva, etc., that contain antimicrobial compounds, *eg.*, lysozyme in tears. Physiological barriers further include temperature, pH, oxygen tension, and various soluble factors (Janeway *et al.* 2001). Body fluids such as gastric juice contain acid that prevents microbial colonization in the intestine, since very few ingested microorganisms can survive the low pH of the stomach. Basic responses of the body to infection such as hyperthermia also have an inhibitory effect on virus replication and may alter the outcome of infection (Nathanson & Cole 1970). Elevated body temperature reduces the replication or increases the inactivation of some flaviviruses and may convert a lethal infection into a sublethal one (Monath 1986).

1.4.1.2. Cells of the innate immune system: role in antiviral defence

Cellular components of innate immunity include natural killer (NK) cells, macrophages, and granulocytes. These cells act directly to reduce the impact of infection in the earliest stages. However, these cells also play a key role in the initiation and subsequent direction of the adaptive immune response, as well as participating in the removal of pathogens that have been targeted by the adaptive immune response.

- **Granulocytes**

Granulocytes are phagocytic cells. They include neutrophils, eosinophils and basophils. Neutrophils are predominant among the leukocyte population in the blood and are a major cell type that plays an important role in early host defence. The ability of neutrophils to restrict bacterial and fungal infections has long been recognised, however, its role in antiviral defence has been little studied. Recent studies have shown the role of neutrophils in controlling the viral infections (Milligan *et al.* 2001; Watanabe *et al.* 1999; Srivastava *et al.* 1999; Van Strijp *et al.* 1990; Tsuru *et al.* 1987). It has been proposed that neutrophils produce antiviral cytokines such as tumor necrosis factor (TNF) (Maatta *et al.* 1998) and NO (Andrews *et al.* 1999) which may contribute to the control of viral infection (Rossol-Voth *et al.* 1991, Guidotti *et al.* 2000). They can degrade the phagocytosed virion proteins by generating reactive oxygen species, as has been seen in JE virus (Srivastava *et al.* 1999) and HSV (Van Strijp *et al.* 1990) infections. Reactive oxygen species play an important role in antiviral defence (Skulachev 1998). The role of basophils and eosinophils in antiviral immunity is also poorly understood. Recently, it has been shown that eosinophils may be directly involved in controlling viral infection by secreting an antiviral component, ribonuclease (Domachowske *et al.* 2000).

- **Macrophages**

Macrophages are professional phagocytes that reside in many different organs and tissues. They mature continuously from circulating monocytes and migrate into the tissues throughout the body, and are widely distributed within the host organs. Their ability to phagocytose and destroy pathogens, including virus particles, allows them to act in the front

line of host defence against initiation and dissemination of viral infections (Janeway *et al.* 2001). Besides phagocytosis, macrophages are also involved in controlling viral infections directly, by producing antiviral cytokines such as interferon-α/β (IFN-α/β), TNF and NO (MacMicking *et al.* 1997; Abbas *et al.* 1997) or indirectly, by modulating several immunoregulatory functions (Guidotti & Chisari 2001). Activated macrophages also produce chemokines that not only facilitate the recruitment of inflammatory cells to the site of infection, but also exert antiviral function by themselves (Alkhatib *et al.* 1996; Deng *et al.* 1996; Yang *et al.* 1997). Several animal models of viral encephalitis have demonstrated the crucial role of macrophages in early antiviral defence (Ben-Nathan *et al.* 1996; Zisman *et al.* 1971). In a study by Ben-Nathan *et al.* (1996), depletion of macrophages by dichloromethylene diphosphonate in WNV infection resulted in an extended viraemia with higher blood virus levels which was associated with accelerated development of encephalitis and death. Moreover, depletion of macrophages also enhanced the neuroinvasion of noninvasive (attenuated) virus and increased mortality by 70-75%, compared to control mice.

- **Natural killer cells**

NK cells are large granular lymphocytes that make up 5-10% of the recirculating lymphocytes (Kuby 1994). NK cells play an important role in eliminating virus-infected cells via cytolysis and are a critical component of the innate immune system (Biron *et al.* 1999). NK cells recognise virus-infected cells before the upregulation of MHC-I expression, suggesting that the NK cell response is important especially for those viral infections, in which downregulated MHC-I expression is a dominant feature as a strategy to escape the adaptive immune response (Ghiasi *et al.* 2000; Guidotti & Chisari 2001). In addition to the cytolytic function, NK cells are also involved in noncytolytic antiviral effector functions, producing antiviral cytokines like IFN-γ and chemokines (Ghiasi *et al.* 2000; Karupiah *et al.* 1990; Fehniger *et al.* 1998). Adler *et al.* (1999) have demonstrated that in the absence of T cells, NK cells can protect mice from HSV-1 encephalitis.

- **Soluble factors**

In addition to the cellular components, various soluble molecules secreted by leukocytes are involved in innate immunity. These include the type I interferons, complement and natural antibodies.

Interferons (IFN) are potent antiviral cytokines. They are classified into type I and type II IFN. Type I IFN includes IFN-α and IFN-β, produced by virus-infected cells and thus involved in the first line of antiviral defence. Type II IFN includes IFN-γ, which is produced by T cells recognizing cognate Ag and is thus not directly induced on infected cells by viral infection. IFN-α/β makes several contributions to host defence against viral infection. Both inhibit viral replication directly (Kurane *et al.* 1990; Schijns *et al.* 1991; Grieder & Vogel 1999), inducing resistance to viral replication in uninfected cells. They also activate NK cells which can kill virus-infected cells selectively and which also produce IFN-γ. Rokutanda (1969) has demonstrated that circulating IFN-α/β reduced viraemia in JE virus infection. Several studies on IFN-α/β or IFN-α/β receptor gene knock out mice have shown the importance of these cytokines in early antiviral defence (Muller *et al.* 1994; Durbin *et al.* 2000). Type I IFN may also markedly influence the adaptive immune response (Janeway *et al.* 2001; Tilg & Kaser 1999).

Complement is another first line of host defence against viral infections. Complement functions as a modulator of the humoral immune response and can control viral infection in several ways: by neutralizing virus infectivity, by contributing to the inflammatory response, by opsonization of viral Ag and by lysis of virus-infected cells via the membrane attack complex (Lachmann *et al.* 1997; Kuby 1994). Ochsenbein *et al.* (1999) have shown the important role of complement in antiviral immunity, using an animal model of vesicular stomatitis virus (VSV) infection.

Like complement, natural antibodies (Ab) are also an essential part of the innate immunity. Indeed, these two components effectively work together. Spontaneously occurring immunoglobulins in the normal host in the absence of apparent Ag stimulation are known as natural Ab. They belong to the immunoglobulin M class of Ab produced by peritoneal B-1

cells (Ochsenbein *et al.* 1999). Natural Ab is involved in early viral defence by facilitating Ag uptake, processing, and presentation to B lymphocytes via complement and Fc receptors (Ochsenbein *et al.* 1999). Recently, it has been shown that natural Ab plays a key role in preventing the spread of viruses, such as VSV, lymphocyte choriomeningitis virus (LCMV) and vaccinia virus, to vital organs. It also improves immunogenicity through enhanced Ag-trapping in the secondary lymphoid organs (Ochsenbein *et al.* 1999).

1.4.1.3. Apoptosis: an innate host defence strategy against viral infection

Apoptosis is thought to play an important role in viral infection for the elimination of virus-infected cells, prior to the development of adaptive immunity. Thus, apoptosis may be considered as part of the innate immune response to viral infection (Everett & McFadden 1999; Griffin & Hardwick 1997). Apoptosis may result via a default mechanism, where the cell commits suicide to prevent viral replication and spread to adjacent cells (Razvi & Welsh 1995). This view is further supported by findings that many viruses encode genes which can inhibit apoptosis (Griffin & Hardwick 1997). However, although it is an important host defence strategy, apoptosis of crucial and nonreplaceble cells, like neurones, result in long term functional defects of CNS or death (Griffin *et al.* 1994, Griffin & Hardwick 1999).

Apoptosis is a normal cell response required for the tissue remodeling that occurs during development and metamorphosis, as well as in healing in all multicellular animals. A hallmark of apoptosis is the fragmentation of nuclear DNA into 200 base pair pieces through the activation of endogeneous nucleases (Janeway *et al.* 2001). Apoptosis is different from that of necrotic cell death. Many different stimuli can induce apoptosis. These include cytokines, steroids, growth factor withdrawal and DNA-damaging agents. In the case of B and T cells, Ag-receptor engagement can also induced apoptosis. In contrast to apoptosis, necrosis is induced by those agents which affect membrane integrity, generalized protein synthesis or energy metabolism (Razvi & Welsh 1995).

Some viruses induce apoptosis of infected cells (Despres *et al.* 1998; Lewis *et al.* 1996) by triggering cellular sensors that initiate cell death, presumably to assist virus dissemination (Everett & McFadden 1999). Alternatively, some viruses actively prevent the apoptosis of

infected cells (Aleman *et al.* 2001) by inducing *bcl-2* gene expression or by using homologs of the *bcl-2* gene contained in the viral genome (Akbar *et al.* 1994). The bcl-2 molecule is an anti-apoptotic transmembrane cellular protein that inhibits the apoptosis normally induced by a variety of insults. Increased levels of bcl-2 can significantly decrease apoptosis (Akbar *et al.*1994). Geiger *et al.* (1995) observed that upregulation of bcl-2 expression in the brains of transgenic mice was correlated with markedly decreased neuronal apoptosis and increased survival in HSV infection. Moreover, Levine *et al.* (1996) observed an antiviral property of bcl-2 involved in preventing viral replication as well as apoptosis in the CNS. This protected mice from lethal Sindbis virus (SBV) encephalitis. However, Liao *et al.* (1997) showed that enforced expression of bcl-2 was unable to protect many cell types from JE virus-induced apoptosis *in vitro*. Moreover, CTL, NK cells and cytotoxic cytokines all can eliminate virus-infected target cells via apoptosis (Razvi & Welsh 1995, DeLuca *et al.* 1999), regardless of bcl-2 levels in these cells.

Apoptosis can also occur in non-infected cells in the CNS during viral encephalitis (McQuaid *et al.* 1997) as an indirect consequence of viral infection (DeLuca *et al.* 1999). Just as recruitment of inflammatory cells are important for the control of infection, termination of inflammatory reactions are also equally important to protect the CNS from continuing immune-mediated damage such as that seen in lymphocytic choriomeningitis and MS (Pender & Rist 2001; Bauer *et al.* 1998; Zinkernagel 1992). Thus, all infiltrating inflammatory cells, including T cells, B cells and macrophages may undergo apoptosis in the CNS and are cleared by microglia through phagocytosis (Magnus *et al.* 2001).

1.4.1.4. Inflammatory cells in viral infections

Disease occurs when an infectious pathogen succeeds in invading or overwhelming the innate host defences to establish a local site of infection and replication that allows its further dissemination. Virus spread is often countered by an inflammatory response that results in the influx of more effector molecules from local blood vessels. The hallmark of the inflammatory response is the infiltration and/or migration of cells to the sites of injury *(De Leo & Yeziersk 2001).*

Inflammation is a physiological response to stimuli such as microbial infection and tissue injury. It is characterized by redness, heat, swelling and pain at the local site. Inflammation is thus classically associated with localized increased vascular permeability, accompanied by an infiltration of 'inflammatory' leukocytes. It is usually initiated within minutes at the site of infection or injury (Janeway *et al.* 2001). Local tissue macrophages respond immediately to counter infecting pathogens and help to set up a state of inflammation in the tissue at the site of infection (Matyszak 1998). Local blood vessels increase in diameter to increase local blood flow. They activate endothelial cells lining the blood vessels to express adhesion molecules which then arrest leukocytes attracted by soluble mediators. Blood flow is then reduced and this facilitates the transmigration of inflammatory cells into the site of infection (Janeway *et al.* 2001; Kuby 1994). Neutrophils are the first cells that migrate to the inflammatory site, followed by monocytes, which differentiate into tissue macrophages, and then NK cells. In the later stages of inflammation, lymphocytes (T lymphocytes and B lymphocytes) and eosinophils enter into the inflammatory sites, where they participate in resolution of infections and tissue repair (Janeway *et al.* 2001). Besides these, increased vascular permeability leads to leakage of fluid and proteins from the blood into the tissue. This results in tissue swelling, oedema and pain. The accumulation of plasma proteins, including those of complement and natural Ab in the tissue further act in host defence and trigger a continuing inflammatory cascade. All these changes are initiated by proinflammatory cytokines such as TNF, interlukin-1 (IL-1) and chemokines produced by macrophages, in response to the infectious pathogens (Janeway *et al.* 2001; Kuby 1994) and are aimed at preventing infection from becoming established. If they fail to control the infection, activated macrophages and other cells from the early innate response help to initiate the development of an adaptive immune response.

1.4.1.5. Cellular adhesion molecules: role in inflammatory response

Leukocyte recruitment to the sites of inflammation is central to the normal progression of the inflammatory response, which is mediated by chemokines produced by activated macrophages. However, other mechanisms are involved in arresting circulating leukocytes and supporting their transmigration from the blood into adjacent inflammatory sites. This is mediated through the interaction between leukocytes and endothelium (Imhof & Dunon 1995; Janeway *et al.* 2001). This interaction is enabled via a number of different cell surface glycoproteins known as cellular adhesion molecules (CAM). In the absence of CAM

expression, the adhesive forces between leukocytes and the vascular endothelium are very weak. This effectively disables leukocyte tethering and extravasation and prevents development of inflammatory responses in these tissues resulting in more severe infection (Dallasta *et al.* 2000; Meager 1999). Thus adhesion molecules are pivotal to leukocyte/endothelial interactions in the inflammatory response, and hence, in host defence mechanisms (Andjelkovic & Pachter 1998). A stepwise schematic diagram of leukocyte extravasation during inflammation is presented in figure 1.9.

CAM were initially discovered as cell surface structures mediating cell-cell and cell-extracellular matrix interactions (Lee & Benveniste 1999). CAM involved in the immune response have been classified into 3 families on the basis of different molecular structure. These are the selectins, which are prominent in initial leukocyte interactions with vascular endothelium, the integrins, which regulate adhesion and migration, and the immunoglobulin superfamily, whose many members also include the Ag-specific receptors of T and B cells (Springer 1990).

- **Selectins**

Selectins are a family of adhesive receptors found on leukocytes, platelets and endothelial cells. They are involved in the initial attachment and rolling of leukocytes on the vascular endothelium (Ley & Tedder 1995) before extravasation (Meager 1999). The selectin family is comprised of three proteins, namely leukocyte-selectin (L-selectin, CD62L), platelet-selectin (P-selectin, CD62P) and endothelial-selectin (E-selectin, CD62E) (Carlos & Harlan 1994). L-selectin is constitutively expressed by all circulating leukocytes, whereas P-selectin serves as a receptor found on endothelial cells and platelets for molecules expressed by both neutrophils and macrophages. Expression of P-selectin on the endothelium initiates the earliest phase of leukocyte migration into the inflammatory site whereas its expression on platelets initiates recruitment of leukocytes to thrombi to induce production of fibrin during haemostasis (Imhof & Dunon 1995). E-selectin is present exclusively in endothelial cells and is expressed only upon stimulation by cytokines such as TNF and IL-1 (Bernardes-Silva *et al.* 2001; Meager 1999). E-selectin is responsible for the initial capture of leukocytes by the endothelium, including neutrophils, monocytes and T cell subsets from the circulation by setting them rolling on a path towards interaction with

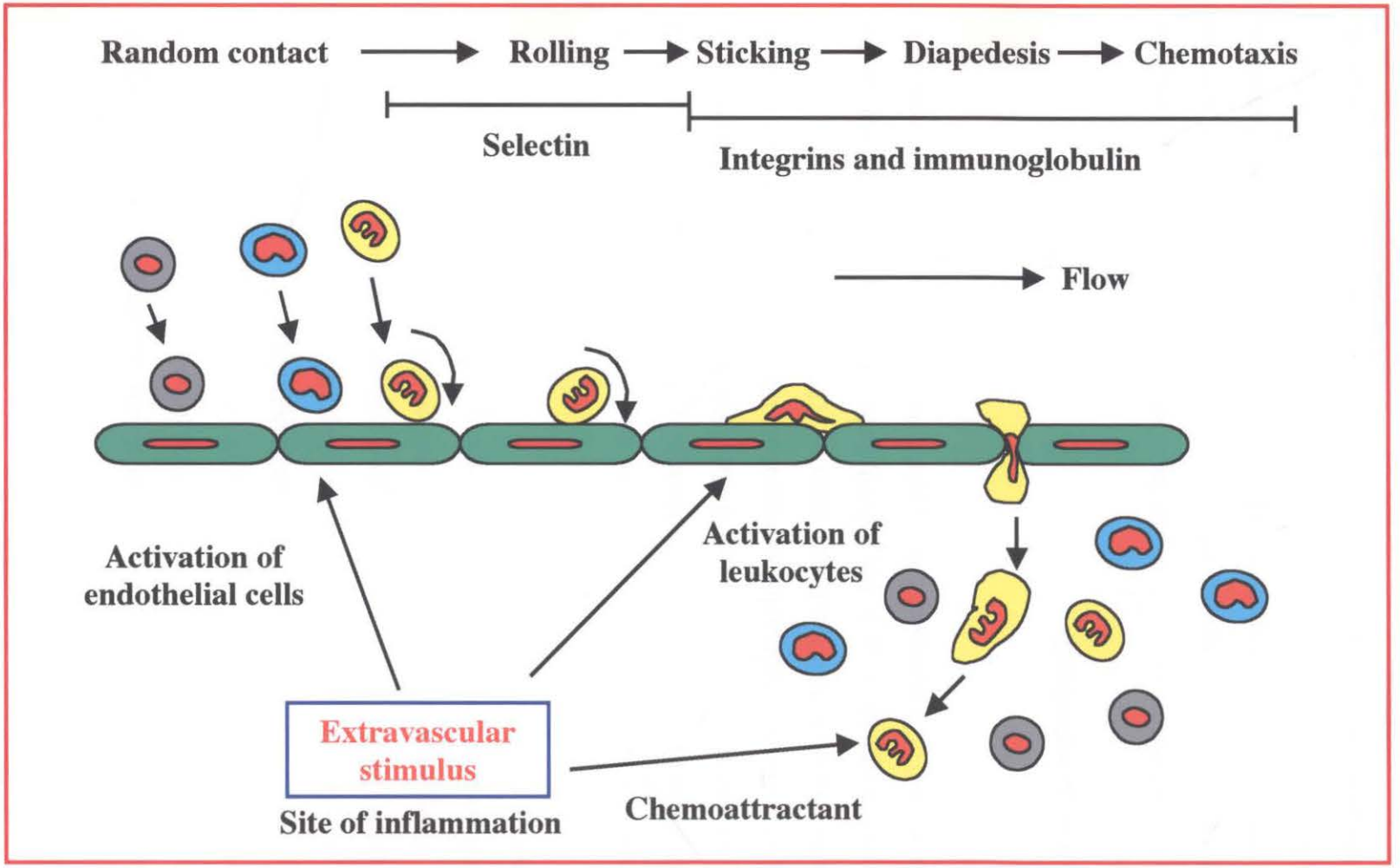

Figure: 1.9 Diagrammatic representation of adhesive interactions during leukocyte emigration to the site of inflammation. During the process of blood flow, leukocytes first roll along endothelium adjacent to the extravascular site of inflammation. Subsequently, some of the rolling leukocytes adhere firmly and diapedese between endothelial cells with the help of different cell adhesion molecules that are expressed by activated vascular endothelium, and then migrate into subendothelial tissue. Modified from Carlos & Harlan 1994.

Neutrophil , Macrophages- , Lymphocytes and natural killer cells , Endothelial cells

ICAM-1 and VCAM-1 before diapedesis into the site of inflammation (Andjelkovic & Pachter 1998).

- **Integrins**

Integrins are adhesion molecules expressed constitutively on the surface of leukocytes. They serve as receptors for members of the immunoglobulin superfamily expressed on activated vascular endothelium. Integrins provide a versatile mechanism for the arrest and tight adhesion of circulating leukocytes on vascular endothelium. This is rapidly followed by intermediate adhesion during transendothelial migration and finally deadhesion at extravasation (Imhof & Dunon 1995). Different populations of leukocytes express different integrins, among them leukocyte function-related antigen (LFA-1, CD11a/CD18), Mac-1 (CD11b/CD18) and very late antigen-4 (VLA-4/CD49d) are the most important integrins as regards cell adhesion.

LFA-1 is expressed on the surface of all leukocytes that interact with ICAM-1, Mac-1 is expressed on macrophages, granulocytes, and dendritic cells whereas VLA-4 is expressed only on lymphocytes and monocytes (Carlos & Harlan 1994; Fischer and Reichmann 2001). Besides their role in leukocyte endothelial interactions, integrins also participate in other cell-cell interactions. These include T cell activation by APC, killing of virus-infected cells by cytotoxic T lymphocytes (Albelda & Buck 1990; Imhof & Dunon 1995), as well as the modulation of growth and differention of many connective tissues and nervous system cells (Springer 1990).

- **Immunoglobulin superfamily**

CAM of the immunoglobulin superfamily are involved in cell-cell adhesion and are especially important during inflammatory responses, wound healing and embryogenesis (Albelda & Buck 1990). Five members of this family are involved in leukocyte/endothelium interactions: ICAM-1, ICAM-2, VCAM-1, platelet-endothelial cell adhesion molecule-1 (PECAM-1) and the mucosal addresin cell adhesion molecule-1 (MAdCAM-1) (Carlos & Harlan 1994). Among them, ICAM-1 and VCAM-1 have been extensively studied in viral encephalitis (Dallasta *et al.* 2000; Lewandowski & Hobbs 1998; Sasseville *et al.* 1992;

Nansen *et al.* 1998; Sobel *et al.* 1990; Irani & Griffin 1996). This will be discussed in more detail in chapter 5.

In the process of cell adhesion, ICAM-1 binds to LFA-1 as a prelude to leukocyte adhesion and migration (Wong & Dorovini-Zis 1995). ICAM-1 is present at very low levels on many cell types, including all haematopoietic cells, epithelial cells and endothelial cells. These cells can be induced to express high levels of ICAM-1 by the proinflammatory cytokines, TNF, IL-1 and IFN-γ (Dobbie *et al.* 1999; Lee *et al.* 1999; Fabry *et al.* 1992). This upregulation of ICAM-1 enables both leukocyte-leukocyte and leukocyte-endothelial cell interactions. ICAM-1 also serves as an accessory protein for Ag receptor activation on B and T cells (Lee & Benveniste 1999), as well as being the major receptor for rhinoviruses (Sethi *et al.*1997). VCAM-1 is a ligand for VLA-4 and plays an important role in leukocyte extravasation. Since VLA-4 is not expressed on the surface of granulocytes, VCAM-1 is involved only in the extravasation of mononuclear cells *i.e.*, lymphocytes and monocytes. VCAM-1 is not expressed constitutively, but can be induced by TNF, IL-1 and IFN-γ stimulator (Barten & Ruddle 1994; De Jong *et al.* 1996). Therefore, VCAM-1 was originally identified as a cytokine-inducible adhesion molecule (Imhof & Dunon 1995). In addition to this, VCAM-1 is also involved in the initiation of T cell activation and proliferation (Lee & Benveniste 1999).

1.4.2. Adaptive immunity: the second line of defence

As previously mentioned, the host defence against viral infections is prosecuted by a symphony of many innate and adaptive immunologic components. These may act alone or in cooperation, depending upon the nature of infecting viral Ag. Adaptive (specific) immunity reflects the presence of a functional immune system capable of specifically recognizing and selectively eliminating Ags. Unlike innate immunity, adaptive immunity displays specificity, diversity, memory, and self/nonself recognition. Humoral and cell-mediated (cellular) immunity represents the two principal arms of adaptive immunity.

1.4.2.1. Humoral immunity: a long term defensive strategy against viral infections

The humoral branch of immunity involves the interaction of B cells with Ag and their subsequent proliferation and differentiation into Ab-secreting plasma cells. Body fluids were once known as humors, therefore, immunity mediated by Ab is known as humoral immunity (Janeway *et al.* 2001). Ab is produced either in a membrane-bound form by B (bursal, thymic-independent) lymphocytes or in a secreted form by plasma cells that represent the terminal differentiation of B cells upon antigenic stimulation (Abbas *et al.* 1997). Secreted Ab circulate in the blood (also known as circulating antibody) to function as the effectors of humoral immunity. They bind to Ag and neutralize it or facilitate the elimination of Ag by complementing macrophage activity. Membrane-bound Ab subserves the recognition phase of humoral immunity and denotes the antigenic specificity of B cells (Kuby 1994).

Antibody have an immunoglobulin (Ig) structure. The basic functional unit consists of 2 heavy chains and 2 light chains linked by disulphide bonds. On the basis of enzyme digestion, this structure is further divided into Fab portions with two Ag binding sites and Fc portion. The Fab portion consists of both heavy and light chain components whereas the Fc portion consists of only heavy chain components (Winkelhake 1978). On the basis of individual differences in structure and function, five Ab isotypes are recognised: IgM, IgG, IgA, IgE and IgD. Among them, IgM, IgG, IgA are important in viral infections (Weiner & Fleming 1984).

IgM is produced during the "initial phase' Ab response, which appears in primary infection. It is expressed before isotype switching, *i.e.,* before the B cell undergoes somatic hypermutation, and is short-lived. The individual binding sites of IgM are generally of low affinity, it has high avidity due to its pentameric structure, which effectively gives it 10 Ag-binding sites. IgM plays a crucial role in controlling bloodstream infection via the efficient activation of the complement system (Janeway *et al.* 2001). IgG constitutes the major source of specific Ab both in the blood and extracellular fluid and persists for life. IgG neutralizes viral Ag, opsonizes Ag for phagocytosis, and activates complement. IgA represents secretory Ab and is involved in mucosal immunity (Ogra *et al.* 1975). IgE is

found in the blood and extracellular fluid at low levels. It is bound by receptors on mast cells and basophils (Winkelhake 1978). It is involved in immediate hypersensitivity reactions. IgD is involved in the activation of B cells by an Ag but its functions are incompletely understood (Janeway *et al.* 2001).

1.4.2.1.1. Role of antibody in viral encephalitis

Circulating Ab, acquired as a result of natural infection or passive transfer of specific Ab, plays an extremely important role in limiting viral infections by terminating the primary infection, limiting the spread of viraemia and preventing disease, as well as preventing reinfection. Several animal models of viral encephalitis have demonstrated the importance of Ab in viral infections although most of this research is based on passive transfer of either monoclonal or polyclonal Ab.

Levine *et al.* (1991) for the first time proposed that passive transfer of hyper immune serum (polyclonal Ab) can clear Sindbis virus (SBV) from neurones by non-cytolytic mechanisms. Such mechanisms precipitate prolonged presence of viral RNA in the neurones (Levine & Griffin 1992). Similarly, Wright and Buchmeier (1991) showed that pre-existing Ab, passively transferred, can prevent T-cell-mediated immunopathology in LCMV infection. Moreover, passive transfer of specific monoclonal Ab to SBV-infected IFN-deficient mice, which are extremely susceptible to SBV, resulted in complete clearance of virus and survival (Byrnes *et al.* 2000), suggesting that Ab can control viral infection even in the complete absence of IFN. Ab has been found to be involved in preventing the spread of virus in the CNS (McKendall *et al.* 1979; Levine *et al.* 1991) as well as in restricting viral gene expression in the CNS (Dietzschold *et al.* 1992). Studies on B-cell-deficient mice further provides evidence for the role of Ab in viral encephalitis. Liu & Chambers (2001) showed that B-cell-deficient mice have increased susceptibility to YF virus infection, compared to the wild type mice. This is supported by the findings of Beland *et al.* (1999) in HSV-1 infection. Similarly, mice with B cell suppression showed increased neuronal infection and increased incidence of latent infection with HSV compared to control mice (Simmons & Nash 1987; Kapoor *et al.* 1982).

1.4.2.2. Cell-mediated immunity: a major antiviral defence mechanism

The cellular branch of the immune system involves interaction of T lymphocyte (thymus-dependent) with Ag and their subsequent proliferation and differentiation into memory T cells and various effector T cells. T cells express a unique Ag-binding receptor on their membranes, known as the T cell receptor (TCR), that recognises Ag only in association with MHC molecules. Each T cell expresses about 10^5 receptors/cell, all of which have an identical Ag specificity (Kuby 1994). Unlike the humoral immunity, which can be transferred by serum Ab, cell-mediated immunity can only be transferred by immune T cells.

T helper (T_H) cells and T cytotoxic (T_C) cells are subsets of T cells, which can be distinguished on the basis of their cell surface glycoprotein expression. T cells displaying CD4 function as T_H cells, whereas T cells displaying CD8 function as T_C cells (Abbas *et al.* 1997). In response to the recognition of an Ag-MHC-II complex by the TCR, T_H cells are activated and become effector cells which secrete various cytokines. These play an important role in activating B cells, T_C cells, macrophages, and various other cells participating in the immune response, as well, they stimulate one another to proliferate and differentiate further (Kuby 1994). On the basis of secreted cytokines profile, T_H cells are classified principally into T_H1 and T_H2 cells (Mosmann *et al.* 1986). T_H1 cells produce proinflammatory cytokines, such as IL-2, IFN-γ and TNF, which activate macrophages and cytotoxic T lymphocytes. They are involved in cell-mediated immune responses that are particularly suitable for combating intracellular pathogens like viruses. In contrast, T_H2 cells secrete IL-4, IL-5 and IL-10 but not IFN- γ, and are more involved in humoral responses, contributing their help for strong Ab production, eosinophil activation, and inhibition of several macrophage functions, thus providing phagocyte-independent protective responses (Spellberg & Edward 2001; Zhao & Schwartz 1998). In addition T_H0 cells produce a mixture of both T_H1 and T_H2 cytokines. They are regarded as uncommitted cells, prior to the decision to respond as T_H1 or T_H2 cells.

Several factors influence the $T_H(CD4^+)$ cell differentiation. These include the cytokine profile of "natural immunity" secreted by different effector cells, the nature of the peptide

ligands derived from the microorganisms, as well as the activity of costimulatory molecules and microenvironmentally secreted hormones (Romagnani 1999). The balance between these two populations is critically important for the recovery or progression of many disease conditions (Young & Hardy 1995).

Under the influence of T_H-derived cytokines, T_c ($CD8^+$) cells recognise an array of Ag-MHC-I complexes (Lobigs *et al.* 1996) on infected cells and/or APC. $CD8^+$ T cells bearing cognate receptors for these complexes then proliferate and differentiate into cytotoxic T lymphocytes (CTL). This CTL play a key role in monitoring and eliminating cells infected with intracellular organisms. CTL kill their targets by programming them to undergo apoptosis. The cytoplasmic granules in CTL contain cytotoxic effector proteins such as perforin and granzymes that trigger apoptosis (Edwards *et al.* 1999). Moreover, these CTL also express Fas ligand which bind with Fas in the target cell membranes, which can also activate apoptosis by perforin-independent mechanisms (Razvi & Welsh 1995; Topham *et al.* 1997). Although, $CD8^+$ T cells exhibit mainly cytotoxic activity, they also can control viral infections by non-cytotoxic mechanisms (Kimura & Griffin 2000). This occurs via the secretion of antiviral cytokines, like IFN-γ and TNF (Ramshaw *et al.* 1997; Harty *et al.* 2000; Klavinskis *et al.* 1989), as well as via secretion of chemokines that contribute to the recruitment of inflammatory cells with microbiocidal activities, including macrophages and neutrophils (Harty *et al.* 2000).

- **Role of major histocompatibility complex**

The effector mechanisms of both $CD4^+$ and $CD8^+$ T cells depend absolutely upon recognition of MHC molecules. After infection, infected cells display peptide fragments derived from the proteins of the pathogen on the cell surface in conjunction with host-cell MHC molecules (Klein 1979). Although MHC molecules do not possess specific peptide Ag-binding receptors like B and T cells, MHC molecules bind a broad spectrum of individual peptide molecules, in a cleft in the distal region of the MHC molecules. With the Ag thus bound, MHC molecules can be recognised by T lymphocytes bearing a T cell receptor of the correct specificity (Kuby 1994; Abbas *et al.* 1997).

On the basis of function and structure, MHC molecules are classified as class I, II or III. Nearly all nucleated cells can express MHC-I molecules, always in association with a small stabilizing protein, β_2-microglobulin (Kuby 1994). MHC-I molecules present endogeneously synthesized peptide fragments, such as those derived from viruses in infected cells, which are recognised by specific killer cells (Springer 1990). $CD8^+$ T cells can recognise only MHC-I-associated Ag and thus, are known as class-I-restricted T cells (reviewed in Rothman *et al.* 1993). MHC-II molecules are constitutively expressed by APC. They present phagocytosed, processed peptide Ag to helper T cells (Springer 1990). $CD4^+$ T cells can recognise only MHC-II associated Ag, and thus are said to be MHC-II restricted (Glimcher & Kara 1992). A relatively restricted range of cells constitutively express MHC-II, but include macrophages/monocytes, B lymphocytes, dendritic cells, thymic dendritic cells, thymic epithelial cells, human vascular endothelial cells and Langerhans cells (Glimcher & Kara 1992). However, a wider range of cells can be induced to express MHC-II, including skin fibroblasts, neuroglial cells, pancreatic beta cells, thyroid epithelial cells and non human vascular endothelial cells (Kuby 1994; Mauerhoff *et al.* 1988). MHC-III is not a membrane protein. It plays no role in Ag presentation to T lymphocytes (Kuby 1994) and thus will not be reviewed here.

- **Role of T cells in viral encephalitis**

T cells are key players in antiviral immunity. They participate in the antiviral response both directly, by destroying viral infected cells (Edwards *et al.* 1999; Topham *et al.* 1997) and producing a range of antiviral cytokines (Ramshaw *et al.* 1997) that inhibit viral replication (Kundig *et al.* 1993; Schijns, 1991; Rossol-Voth *et al.* 1991), and indirectly, by providing help to B cells (Klein 1979). Several mouse models of viral encephalitis have shown the crucial role of T cells for the control of viral infection in the CNS (Flory *et al.* 1993; Binder & Kundig 1991; Domachowske *et al.* 2000).

Williamson & Stohlman (1990) showed that both $CD4^+$ and $CD8^+$ T cells are required for the effective clearance of mouse hepatitis virus (MHV) from the CNS. Although clearance of MHV from the CNS was mediated mainly by $CD8^+$ T cells (Williamson & Stohlman 1990), they required support from $CD4^+$ T cells. Without the help of $CD4^+$ cells, $CD8^+$ T

cells became apoptotic and were unable to clear the virus (Stohlman *et al.* 1998). Similarly in Borna disease, $CD8^+$ T cells can control Borna disease virus infection in the CNS only in cooperation with $CD4^+$ T cells (Noske *et al.* 1998). In contrast, in measles virus encephalitis, $CD4^+$ T cells alone are protective in resistant mice, however, in partially resistant mice, these cells need help from $CD8^+$ T cells to control infection (Weidinger *et al.* 2000). In flaviviral encephalitis, role of T cells has not been studied in detail in animal models. Jacoby *et al.* (1980) showed that adoptive transfer of immune spleen cells can protect naïve mice from lethal flaviviral encephalitis. In JE virus, the adoptive transfer of JE virus specific $CD8^+$ T cells via intracerebral (i.c.) route was found to be protective against lethal i.c. JE virus infection in adult mice only (Murali-Krishn & Manjunath 1996). Studies on T-cell-deficient as well as T-cell-suppressed mice further implicate the role of T cells in control of viral encephalitis. Liu & Chambers (2001) have demonstrated that $CD4^+$ T-cell-deficient mice are highly susceptible to YF viral encephalitis, compared to control mice.

Similarly, $CD8^+$ T cell-depleted mice are highly susceptible to coronavirus-induced encephalomyelitis (Flory *et al.* 1993) while $CD4^+$ T cell depletion with monoclonal Ab results in death from severe $CD8^+$ T cell-mediated immunopathology (Christensen *et al.* 2001). Taken together, the balance between resistance and susceptibility to disease depends on the functional composition of the respective T cell subsets (Weidinger *et al.* 2000). Both subsets of T cells are important in combating the viral infection. Defects in or deletion of one of the subsets precipitate severe disease or death either from overwhelming viral infection or immunopathology.

1.4.2.3. Cytokines: messengers of the immune system

Cytokines are a low molecular weight (approximately 8-80 kDa), soluble heterogeneous group of polypeptides that mediate intercellular communication. They are secreted by leukocytes, resident CNS cells and a wide variety of other cell types in the body in response to a number of stimuli. They act either in an autocrine or paracrine manner and thus contribute to a chemical signalling language in association with hormones and neurotransmitters to regulate development, tissue repair, haematopoiesis, inflammation and

immune responses (Balkwill 1997; Hopkins & Rothwell 1995). They have an extremely broad range of activities and may be synergistic or antagonistic, as well as having functional redundancy (Abbas *et al.* 1997). Cytokines exert their functions by binding to their specific receptors on the membrane of target cells. This sets off an intracellular signalling cascade leading to induction, enhancement or inhibition of a number of cytokine-regulated genes, with subsequent phenotypic changes in a variety of cells (Balkwill 1997; Miyajima *et al.* 1992).

Constitutive expression of most cytokines is low or undetectable. However, many increase massively in response to infection or injury, indicating a clear role in pathophysiological states (Hopkins & Rothwell 1995). The hallmark function of cytokines is the alteration of immune cells behaviour (Becher *et al.* 2000). They regulate the intensity and duration of the immune response, either by stimulating or inhibiting the activation, proliferation, and differentiation of various immune cells (Balkwill 1997). They also regulate secretion of Ab or cytokines from immune cells. In this manner they can activate the entire network of interacting cells of the immune system (Young & Hardy 1995; Balkwill 1997; Kuby 1994). Therefore, cytokines are also known as "messenger proteins" of the immune system (Kuby 1994). IL, IFN, TNF, colony stimulating factors (CSF), chemokines, growth factors, neurotrophins and neuropoietins are all cytokines (Hopkins & Rothwell 1995) and can influence CNS functions. The major members of each cytokine family and their functions are summarised in table 1.3. Most studies have been carried out on inflammatory cytokines, especially on IFN-γ and TNF. These contribute to CNS inflammation and antiviral responses, as well as to the generation of CNS pathology. Studies on cytokine/cytokine receptor-deficient mice, together with experiments blocking the functions of cytokine/cytokine receptor are allowing us to dissect out the role of these cytokines in inflammation and disease (Pasparakis *et al.* 1996; Huang *et al.* 1993 Dalton *et al.* 1993; Cantin *et al.* 1995).

1.4.2.3.1. IFN-γ: an immune interferon and antiviral cytokine

IFN-γ, or type II IFN, is a pleotropic, 17 kDa polypeptide cytokine. It plays a critical role in immune regulation. For this reason, it is also known as immune interferon (Popko *et al.* 1997). IFN-γ is produced by activated T lymphocytes (both $CD4^+$, T_H1 subset, and $CD8^+$ T

Table: 1.3 Summary of major activities and features of cytokine families

Family	Major members	Major activities and features
Chemokines	MIP-1α/β, RANTES, MCAF/MCP-1, IL-8 MGSA, NAP-1/2	Leukocyte chemotaxis and cellular activation
Colony stimulating factors (CSF)	G-CSF, M- CSF, IL-3, GM-CSF	Colony cell formation in the bone marrow and activation of mature leukocyte functions
Growth factors (GF)	EGF, FGF, PDGF, TGF- α/β and ECGF	Cell growth and differentiation
Interleukins (IL)	IL-1α, IL-1β, ILIra and IL-2 to IL-15	Multiple tissue and immunoregulatory activities
Interferons (IFN)	IFN - α/β and IFN-γ	Inhibition of intracellular viral replication and cell growth regulation, IFN-γ is primarily immu-noregulatory
Neurotropins	BDNF, NGF, NT-3 to NT-6 and GDNF	Growth and differentiation of neurons
Neuropoietins	CNTF, OM and IL-6	Cytokines acting on the nervous system, and acting via related receptor complexes
Tumor necrosis factors (TNF)	TNF and lymphotoxin α and β	Similar to IL-1, in addition to tumor cytotoxicity

Addapted from Hopkins & Rothwell 1995. Abbreviations: BDNF, brain-derived neurotrophic factor, CNTF, ciliary neurotrophic factor, E & FGF, epidermal & fibroblast GF, ECGF, endothelial cell GF, GDNF, glial-derived neurotrophic factor, G, M & GM-CSF, granulocyte, macrophage & granulocyte/macrophage-CSF, ILIra, IL-1 receptor antagonist, MCAF, monocyte chemotactic and activating factor, MCP-1, monocyte chemotactic protein, MGSA, melanoma growth stimulatory activity, MIP-1 α/β, macrophage inflammatory protein, NAP, neutrophil activating protein, NGF, nerve growth factor, NT, neurotrophin, OM, oncostatin M, PDGF, platelet-derived GF, RANTES, regulated upon activation normal T expressed and secreted, TGF- α/β, transforming GF-α/β.

cell), NK cells (Howard & Hardy *et al.* 1995) and macrophages (Gessani & Belardelli 1998). It acts on cells which posses the IFN-γ receptor (IFN-γR) and induce increased expression of several genes. Therefore, many organs and systems have been found to be affected by IFN-γ since IFN-γR are present on virtually all cells of the body (Billiau 1996).

IFN-γ facilitates the differentiation of $CD4^+$ T lymphocytes into the T_H1 subset involved in cell-mediated immunity. Cells from this subset in their turn also secrete IFN-γ. In contrast, IFN-γ inhibits the stimulation of T_H2 cells, which are involved in humoral immunity (Young & Hardy 1995). Several studies have demonstrated that endogenous production of IFN-γ is essential for host defence against virus infection (Huang *et al.* 1993; Bouley *et al.* 1995; Karupiah *et al.* 1990). IFN-γ is an antiviral cytokine that inhibits viral replication either directly (Ruby 1997), or indirectly by activating other effector cells of the immune system. Effector cells activated by this cytokine include CTL, NK cells and macrophages. These cells control viral replication by eliminating infected cells and themselves producing a variety of inflammatory cytokines, including IFN-γ (Utermohlen *et al.* 1996; Billiau 1996). IFN-γ produced by NK cells is transient compared to IFN-γ produced by T cells. Nevertheless, this brief response plays an important role in controlling pathogens during early stages of infection (Romani *et al.* 1997).

IFN-γ acts as a mediator of both innate and adaptive immunity. In innate immunity, it increases the antimicrobial capacity of macrophages by inducing increased production of reactive oxygen and nitrogen intermediates (H_2O_2, NO), increased expression of MHC molecules required to present Ag to lymphocyte, increased expression of FcR required for the opsonization of neutralized microbial pathogens (Loughlin *et al.* 1993; Kreil & Eibl 1995) and increased production of indoleamine-2-3-dioxygenase (IDO) enzyme, required for the metabolism of tryptophan (Thomas *et al.* 1994) (see below). In adaptive immunity, IFN-γ regulates Ab production via direct effects on B cells. IFN-γ thus promotes switching of Ig into IgG2a and IgG3 subclasses, but inhibits switching to IgG1 and IgE (Young & Hardy 1995). IFN-γ also induces increased expression MHC-I and MHC-II molecules on a wide variety of cell types (Grau *et al.* 1997; Huynh & Dorovini-Zis 1993; Momburg *et al.* 1986). It activates vascular endothelial cells to express high levels of cell surface CAM (Grau *et al.* 1997; Doukas & Pober 1990), which, with regulation of chemokine production

Table: 1.4 Summary of major activities and features of IFN-γ on CNS cells

Cell types	Effect	Functional response
Astrocytes	↑ ICAM-1, VCAM-1	Adhesion
	↑ NO	Astrogliosis
	↑ MHC-I	T cell cytotoxicity
	↑ MHC-II	Ag presentation
Microglia	↑ ICAM-1	Adhesion
	↑ Phagocytosis	Damage
	↑ NO, ROI	Cytotoxicity
	↑ MHC-I/MHC-II	T cell cytotoxicity /Ag presentation
Neurones	↑ ICAM-1/VCAM-1	Differentiation
	↑ ROI, NO	Damage
	↑ NO	Differentiation
	↑ MHC-I	Antigen presentation
Oligodendrocytes	↑ ICAM-1	Adhesion, death
	↑ NO	Damage

Derived from Munoz-Fernandez & Frenso 1998. Abbreviations: Ag: antigen, ICAM-1: intercellular adhesion molecule-1, MHC: major histocompatibility complex, NO: nitric oxide, NGF: neurotrophic growth factor, ROI: reactive oxygen intermediates, VCAM-1: vascular cell adhesion molecule-1, ↑: upregulation

by IFN-γ (Tran *et al.* 2000), facilitates the recruitment of different subpopulations of leukocytes to the sites of inflammation (Issekutz *et al.* 1988; Sethna & Lampson 1991).

IFN-γ has multiple effects on CNS cells. It is involved both in normal functioning of the brain as well as in the development and differentiation of neurones there (Munoz-Fernandez & Frenso 1998). IFN-γ may be either neuroprotective or neurotoxic depending upon the effects it may exert on different CNS resident cells. The major effects of IFN-γ on CNS resident cells are summarised in table 1.4.

- **Nitric oxide: an antiviral radical gas**

NO is a small membrane-permeable gas that serves as a mediator of many physiological functions. These include regulation of blood pressure, organ blood flow distribution, inhibition of the adhesion and activation of platelets and polymorphonuclear granulocytes, neurotransmission, insulin release and many others (Southan & Szabo 1996). It is water-and lipid-soluble and easily diffuses across the cell membrane. Thus, NO can exert its function not only in the cell where it is produced but can also interact with neighbouring cells and other molecules (Karupiah *et al.* 2000). It is produced by the oxidation of L-arginine by nitric oxide synthase (NOS) enzyme under both physiological and pathophysiological conditions, and converted into reactive nitrogen intermediates or other stable secondary products. Both forms are involved in normal tissue function and pathology (MacMicking *et al.* 1997). Many different cell types can be induced to produce NO (Boje & Arora 1992; MacMicking *et al.* 1997; Andrews *et al.* 1999; Komatsu *et al.* 1996), however, activated macrophages and neutrophils are the major source of NO (Karupiah *et al.* 2000).

NOS has 3 isoforms. NOS1 is expressed constitutively in neurones (Komatsu *et al.* 1999). NOS3 is expressed constitutively in endothelial cells (Karupiah *et al.* 2000). These isoforms are involved in the normal physiology and regulation in these cells. In contrast, NOS2 is readily inducible by IFN-γ, hence it is also known as inucible nitric oxide synthase (iNOS). It is typically associated with inflammatory and immune responses (Karupiah *et al.* 1998; Willenborg *et al.* 1999). The productions of NO is modalities used for controlling viral infections (Guidotti *et al.* 2000; Karupiah *et al.* 1993). Much evidence suggests that NO also

contributes to innate resistance against viral infections (Karupiah *et al.* 1998; Tucker *et al.* 1996) and that it can inhibit viral replication at an early stage. This prevents viral spread and promotes viral clearance and earlier recovery from infection (Reiss & Komatsu 1998). Growing evidence from experiments using NOS gene-deficient mice, or neutralizing NOS with aminoguanidine or treating mice with an analog of arginine, Nω-nitro-L-arginine methyl ester (L-NAME), have shown the crucial requirement of NO in antiviral defence (Saxena *et al.* 2000; Komatsu *et al.* 1999; Karupiah *et al.* 1998; Tucker *et al.* 1996).

The actual mechanism of antiviral action of NO is still not clear. They may be mediated by reaction with several possible cellular and viral targets. These include inhibition of ribonucleotide reductase, activation of cellular guanylate cyclase, modification of both cellular and viral transcription factors, inhibition of cellular metabolism (Mannick 1995; Komatsu *et al.* 1999) or inhibition of viral proteases (Saura *et al.* 1999). Although NO is important for early antiviral defence, its excessive production is harmful, leading to pathology in many neurotropic viral infections (Lane *et al.* 1999; Rose *et al.* 1998; Andrews *et al.* 1999; Fujii *et al.* 1999).

- **Indoleamine-2,3-dioxygenase: IFN-γ inducible enzyme**

IDO is a monomeric haemoprotein that catalyzes the oxidation of tryptophan into N-formylkynurenine, the first and rate limiting step in this metabolic pathway. Although IDO can be induced by several other cytokines, IFN-γ is the most potent inducer of IDO (Takikawa *et al.* 1990; Thomas *et al.* 1993). Yoshida *et al.* (1979) were the first to suggest the possible role of IDO in antiviral defence. Christen *et al.* (1990) have demonstrated the role of IDO as an antioxidant defence against viral pneumonia. Increased levels of IDO have been observed in viral encephalitides (Heyes 1992; Maloney 2000) and intracellular parasitic disease (Thomas *et al.* 1993). In addition to its antimicrobial properties, IDO also plays an important role in the development of fetus as demonstrated by Kamimura *et al.* (1991). Besides these functions, IDO may be involved in rejecting allografted tumors by damage to cells through tryptophan depletion (Takikawa *et al.* 1990).

Quinolinic acid (QA) is an end product of tryptophan metabolism. It is a neurotoxic agonist of the N-methyl-D-aspartate (NMDA) type excitatory amino acid receptor family. It's

neurotoxicity is mediated by overactivation of NMDA receptors, oxidative stress and reactive oxygen species production (Santamaria *et al.* 2001). On the other hand, kynurenic acid which is also produced during this metabolism protects neurones from the toxic effects of QA (reviewed in Sanni *et al.* 1998; Heyes *et al.* 1992). Therefore balanced production of QA and kynurenic acid is required for the proper function of CNS. Overproduction of QA causes neurodegeneration (Heyes *et al.* 1992).

1.4.2.3.2. TNF: a proinflammatory and antiviral cytokine

TNF is one of the many cytokines that make up the complex network of biological response modifiers active in the host response to infectious diseases (Czarniecki 1993). It is produced primarily by activated immune cells. Although TNF is produced by T and B lymphocytes, NK cells and mast cells, macrophages are the major source of TNF which is produced by these cells in response to various stimuli. Therefore, TNF is also seen as a mediator of both innate and adaptive immunity, and acts as an intermediate link between acute and adaptive inflammatory responses (Pasparakis *et al.* 1996, Abbas *et al.* 1997). In the CNS, it is produced by neurones, microglia and astrocytes upon stimulation (Acrain *et al.* 2000; Chen *et al.* 2000; Medana *et al.* 1997). TNF is produced predominantly as a secreted form, although it also exists as a transmembrane form on the surface of activated immune cells. Both forms are bioactive and bind to their receptors (Herbein & Brien 2000). This sets off an intracellular signaling cascade for the induction of many genes (Larrick & Wright 1990).

TNF plays an important role in inflammation by promoting the transmigration of inflammatory leukocytes to the sites of inflammation. This is mediated by inducing expression and upregulation of CAM in the vascular endothelium (de Jong *et al.* 1996; Dobbie *et al.* 1999) and increasing the permeability of endothelial cells (Medana *et al.* 2001). TNF also acts as an antiviral cytokine. It interferes with viral replication in several ways and thus plays an important role in many viral infections (Rossel-Voth et al 1991; Schijns *et al.* 1991). Some of its actions include directly inhibiting viral replication by preventing viral entry into the cell, inducing apoptosis in virus-infected cells and exerting antiviral effects in association with IFN (Czarniecki 1993; Herbein & Brien 2000). TNF further plays an important role in controlling T cell activation and proliferation by regulating IL-2 receptor expression (Pimentel-Muinos *et al.* 1994), required for T cell

Table: 1.5 Summary of major activities and features of TNF on CNS cells

Cell types	Effect	Functional response
Astrocytes	↑ ICAM-1, VCAM-1	Adhesion
	↑ NO	Astrogliosis
	↑ Proliferation	Astrogliosis
	↑ MHC-I/MHC-II	T cell cytotoxicity/Ag presentation
	↑ NGF	Nerve repair
Microglia	↑ ICAM-1	Adhesion, Ag presentation
	↑ Phagocytosis	Adhesion
	↑ NO, ROI	Cytotoxicity
	↑ MHC-IIII	Ag presentation
Neurones	↑ ICAM-1/VCAM-1	Adhesion/differentiation
	↑ ROI, NO	Damage
	↑ NO	Adhesion/differentiation
Oligodendrocytes	↑ Demyelination	Damage
	↑ ICAM-1	Adhesion, death
	↑ NO	Damage

Derived from Munoz-Fernandez & Frenso 1998. Abbreviations: Ag: antigen, ICAM-1: intercellular adhesion molecule-1, MHC: major histocompatibility complex, NO: nitric oxide, NGF: neurotrophic growth factor, ROI: reactive oxygen intermediates, VCAM-1: vascular cell adhesion molecule-1, ↑: upregulation

activation (reviewed in Pimentel-Muinos *et al.* 1994). Besides these functions, TNF acts as a regulator of the humoral immune response and is required in the formation of primary lymphoid follicles and germinal centers in the spleen (Pasparakis *et al.* 1996). Like IFN-γ, TNF exerts multiple effects in CNS cells. The summary of effects of TNF on CNS resident cells is presented in table 1.5. Although TNF is involved in antiviral defence, excessive production in the CNS is detrimental, and may exacerbate disease, resulting in death (Andrews *et al.* 1999; Choe *et al.* 1998).

1.4.2.3.3. IL-10 and TGF-β: anti-inflammatory cytokines

The anti-inflammatory cytokines are a series of immunoregulatory molecules which can modulate the proinflammatory cytokine response under pathophysiological conditions to limit the injurious effects of sustained or excess inflammatory reactions. Thus, a dynamic balance exists between proinflammatory and anti-inflammatory cytokines (Opal & Depalo 2000). IL-10 and tumor growth factor-β (TGF-β) are examples of anti-inflammatory cytokines that regulate the production of proinflammatory cytokines produced by activated T_H1 $CD4^+$ T cells and activated macrophages. Being anti-inflammatory in nature, these cytokines play a critical role in preventing uncontrolled T cell-mediated tissue destruction, and have thus become important therapeutic proteins for the treatment of organ-specific autoimmune diseases (Cua *et al.* 2001).

IL-10 is an 18 kDa molecule produced by a variety of cell types such as T_H2 T cells, B cells, macrophages, mast cells and glial cells (Chabot *et al.* 1999; Wagner *et al.* 1999) and is perhaps the most important anti-inflammatory cytokine found in the human immune response. It is a potent inhibitor of T_H1 cytokines, IL-2 and IFN-γ. Therefore IL-10 was previously known as cytokine synthesis inhibition factor (Opal & Depalo 2000). IL-10 regulate the activities of macrophages by inhibiting cytokine secretion, like TNF, IL-1, IL-12 and chemokines, and by reducing MHC-II and costimulators (eg., B7-1 and B7-2) to reduce T cell activation. In addition to this, IL-10 plays a crucial role in the proliferation of $CD4^+$ T cells into T_H0-T_H1-T_H2, as well as in the differentiation of B cell, thymocytes and mast cells (reviewed in Sawada *et al.* 1999). Moreover, IL-10 is a unique and potent modulator of the CNS cytokine network that regulates the expression of both cytokines and cytokine receptors by CNS resident cells (Sawada *et al.* 1999; Szczepanik *et al.* 2001). CNS

expression of IL-10 was found to abrogate EAE. The i.c. inoculation of replication-deficient adenovirus expressing human IL-10 into mice with active EAE blocked the progression of EAE (Cua *et al.* 2001) by reducing cell damage and enhancing lesion repair through the protection of oligodendrocytes and their progenitors (Molina-Holgado *et al.* 2001). However, intravenous (i.v.) inoculation of same vector was unable to protect the mice from EAE, despite high levels of circulating IL-10.

TGF-β is a group of cytokines (TGF-β1, TGF-β2 and TGF-β3) (Opal & Depalo 2000), produced by a variety of cells, including T cells, macrophages and glial cells (Abbas *et al.* 1997; Lehrmann *et al.* 1998). These cytokines play important regulatory roles in angiogenesis, osteogenesis, reproduction, development, cell growth and differentiation, wound healing and immune responses (Benveniste 1998). Like IL-10, the TGF-β cytokines are an important regulatory group that can shut off immune and proinflammatory responses. They can suppresses activation and proliferation of B and T cells and maturation of CTL. They inhibit production of proinflammatory cytokines (TNF, IL-1) from activated macrophages and can down-regulate MHC-II expression (Letterio 2000; Benveniste 1998). In the CNS, TGF-β reduces the incidence of neuronal death induced by trophic factor removal, excitotoxicity and oxidative injury (Prehn *et al.* 1994). Although IL-10 and TGF-β both are negative regulators of the immune response, their regulation of T_H1 activity is different. IL-10 blocks the activity of T_H1 T cell by suppressing macrophage activity, whereas TGF-β directly acts upon T_H1 T cells (Janeway *et al.* 2001).

1.4.2.3.4. Chemokines: chemoattractant cytokines

As previously mentioned (see the section on innate immunity, section 1.4.1.2.), neutrophils, macrophages, and NK cells, which are the effector cells of the innate immune response play important roles in neutralizing and clearing infectious pathogens before the development of adaptive immunity. Thus, migration of these cells into infectious sites and their subsequent activation is a critical step, enabling the host to achieve effective and efficient removal of pathogens. Among the cytokines released in the earliest phases of infection, are members of a family of chemoattractant cytokines known as chemokines. Chemokines are heparan-binding proteins that chemotactically guide the inflammatory cells in a unidirectional way through the microvascular cell wall (Ransohoff *et al.* 1996; De Groot &

Woodroofe 2000). They are secreted not only in response to infectious pathogens but also in response to a number of other different stimuli such as trauma, proinflammatory cytokines, and products of an activated immune response (McManus *et al.* 2000). On the basis of structural and genetic criteria, chemokines are generally classified into four subfamilies. This includes CC or β-chemokines, CXC or α-chemokines, CX_3C and C chemokines (De Groot & Woodroofe 2000). CXC chemokines are produced largely by activated macrophages as well as tissue cells such as endothelium and fibroblasts, and megakaryocytes. These chemokines are specific to neutroplils and act as a mediator of acute inflammation (Abbas *et al.* 1997). IL-8 was the first chemokine to be identified and belongs to the CXC family (Janeway *et al.* 2001). The CC chemokines are largely produced by activated T cells and act predominantly on T cells, monocytes, eosinophils and basophils, but not on neutrophils (Ransohoff *et al.* 1996). Macrophage inflammatory protein-1α (MIP-1α), regulated upon activation normal T expressed and secreted (RANTES), macrophage inflammatory protein-1β (MIP-1β), monocyte chemotactic protein-1 (MCP-1), etc., are the examples of CC group chemokines (Mahalingam & Karupiah 1999). Fractalkaline/neurotactin belongs to the CX_3C family and acts on T lymphocytes, NK cells and monocytes, whereas lymphotactin belongs to C chemokine and is chemotactic only for T lymphocytes (Mahalingam & Karupiah 1999; De Groot & Woodroofe 2000). Like cytokines, chemokines exert their functions through the specific receptors (Rollins 1997) present in wide variety of cells (Jiang *et al.* 1998; Meucci *et al.* 2000). They elicit a signalling cascade to attract inflammatory cells from the circulation to the sites of inflammation (Siebert *et al.* 2000). Chemokines play a critical role in the perivascular transmigration and accumulation of specific subsets of leukocytes to the sites of inflammation (Asensio *et al.* 1999).

Several studies on chemokine gene or chemokine receptor gene knock out mice in viral encephalitis have proven the importance of chemokine expression for the recruitment of inflammatory cells in the CNS (Liu *et al.* 2001; Salazar-Mather *et al.* 2000; Andrews *et al.* 1999). Moreover, recent studies have demonstrated antiviral properties of chemokines. Chemokine receptor, CC receptor-5, CCR-5, may function as a co-receptor for viruses like HIV-1 (Alkhatib *et al.* 1996; Deng *et al.* 1996) and natural mutation of such a specific co-receptor can confer resistance to the virus, and thus may have significant advantages in HIV-1 therapy (Yang *et al.* 1997). In addition to these, chemokines also have been found to

modulate different biological functions such as cell adhesion, phagocytosis, cytokine secretion, T cell activation, apoptosis, proliferation, angiogenesis, haematopoiesis and viral pathogenesis (Bacon & Harrison 2000; Rollins 1997).

1.5. The immune response within the central nervous system

As previously mentioned, the CNS has been considered to be an 'immune-privileged site" for many years due to the presence of the BBB which isolates the CNS from the peripheral immune system. This, coupled with lack of lymphatic drainage and low or absent expression of MHC molecules which effectively allow foreign Ag to hide from the immune system, helped to maintain this view. However, this has gradually changed due to recognition of the ability of activated T cells to pass across the BBB continuously to monitor the CNS (Hickey *et al.* 1991). More importantly, resident cells, such as microglia and astrocytes can themselves mount a potent response upon invasion by pathogens. Work from both animal models of virus-induced encephalitis, and *in vitro* culture systems have shown that both microglia and astrocytes can secrete numerous cytokines and chemokines, as well as express receptors that enable communication with the peripheral immune system (Chao *et al.* 1994; Merrill *et al.* 1996; Ransohoff *et al.* 1996; Dickson *et al.* 1993; Brodie *et al.* 1997; Schijns *et al.* 1991; Persidsky *et al.* 1999; Sauder *et al.* 2000; Asensio *et al.*1999). Moreover, when activated, microglia and astrocytes can function as APC. They express high levels of cell surface MHC molecules (Bo *et al.* 1994; Weissenbock *et al.* 2000). Therefore, it is presently widely accepted that these cells actively collaborate with peripheral immune cells to generate an effective inflammatory response within the CNS.

Interestingly, Neuman & Wekerle (1998) suggested that neurones, particularly physiologically active neurones, are the main player in regulating immune responses within the CNS by suppressing MHC-II inducibility and cytokine production in microglia and astrocytes through their electrical activity. This prevents unwanted immune-mediated damage of neurones. Under stress, however, neurones activate immunologically relevant molecules in these glial cells to enable them to become competent for interaction with infiltrating leukocytes (Neuman 2001).

1.5.1. CNS cells: factories for cytokines

Several studies, both *in vivo* and *in vitro*, have shown that CNS resident cells are the endogenous source of cytokines that act as the intercellular messengers in neurone-glia interactions, microglial-astroglial crosstalk, as well as in glial-T cell interactions during infection or injury (Acarin *et al.* 2000; Nohava *et al.* 1992; Streit *et al.* 1999).

From studies by Knoblach *et al.* (1999) and Acrain *et al.* (2000), it is likely that neurones are involved in initiation and propagation of inflammation through their production of TNF and IL-6 in response to injury. Moreover, neurones can regulate the activities of microglia/macrophages, leading to local expansion and enhanced function, in CNS inflammatory diseases. This occurs via production of macrophage-colony stimulating factor (M-CSF) (Nohava *et al.* 1992) (CSF-1 in mouse) (Kreutzberg 1996) which is mitogenic for microglia (Lodge & Sriram 1996). Lack of CSF-1 in mice results in an abnormal microglial response and increased neuronal vulnerability to injury (Berezovaskaya *et al.* 1995). Several *in vitro* studies have shown the ability of astrocytes to produce cytokines such as IL-6 and TNF upon stimulation (Chen *et al.* 2000; Schoneboom *et al.*1999). Acrain *et al.* (2000) have shown that astrocytes can also produce these cytokines within the CNS *in vivo* and actively pariticipate in the initiation of immune responses and inflammation within the CNS. Although, neurones and astrocytes can produce cytokines, activated microglia are the most abundant source. During neuronal stress these cells may become virtual factories for cytokines in the CNS (Graeber 1993).

In *in vitro* culture systems, microglia have been shown to express of IL-1 (Giulian *et al.* 1986; Giulian *et al.* 1994), TNF (Renno *et al.*, 1995; Medana *et al.* 1997), IL-12 (Lodge & Sriram 1996), IL-18 (Prinz & Hanisch 1999) and IL-1α and IL-6 (Mitrasinovic *et al.* 2001). Similarly, *in vivo* animal models have shown that upon stimulation, microglia can produce cytokines within the CNS, including IFN-1α (Yamada *et al.* 1994), IL-1α (Zhao *et al.* 2001), IL-1β and TNF (Acrain *et al.* 2000). These in turn induce upregulated CAM (Zielasek *et al.* 1993; Shen *et al.* 1997) and chemokine induction (McManus *et al.* 1998) which promotes recruitment of leukocytes across the BBB and may enhance inflammation in the CNS. Microglial production of IL-1β is also involved in remyelination via induction of growth-promoting factors, such as insulin-like growth factor-1, during pathological insult

within the CNS (Mason *et al.* 2001). Microglia have been found to express many cytokine receptors constitutively. These include receptors for IFN-1α (Yamada & Yamanaka 1995), M-CSF (Mitrasinovic *et al.* 2001), IL-12 (Taoufik *et al.* 2001), IL-1, TGF, GM-CSF and IFN-γ (Morris & Esiri 1998).

It is known that glial cells play a critical role in CNS inflammation, thus contributing to defence in the CNS against infection. However, several studies suggest that activated glial cells are involved in brain damage by secreting proinflammatory cytokines and neurotoxic metabolites (Choe *et al.* 1998; Gonzalez-Scarano & Baltuch 2000; Banati *et al.* 1993; Boje & Arora 1992). Therefore, perhaps not surprisingly, these glial cells can also release potent anti-inflammatory cytokines such as IL-10 and TGF-β (Wagner *et al.* 1999; Pratt & McPherson 1997) which inhibit the local production of inflammatory mediators as an emergency mechanism in circumstances of brain inflammation (Hu *et al.* 1999). These cytokines function as negative regulators in the CNS cytokine network, mainly by suppressing microglial function (Sawada *et al.* 1999; Lodge & Sriram 1996), including chemokine production (Hu *et al.* 1999), production of proinflammatory cytokines (Lodge & Sriram 1996) and neurotoxic metabolites, such as NO and reactive oxygen intermediates (Molina-Holgado *et al.* 2001; Chao *et al.* 1995; Ledeboer *et al.* 2000), and thus limit or prevent brain damage. IL-10 is not constitutively expressed in the CNS, whereas TGF-β is constitutively expressed in microglia at low levels contributing to CNS homeostasis (reviewed in Hu *et al.* 1999; Morris & Esiri 1998).

1.5.2. CNS cells: a source of chemokines

Experiments *in vivo* and *in vitro* have demonstrated that cells of the CNS can express chemokines and their receptors. This is likely to result in the chemoattraction of inflammatory cells to the sites of viral infections in the CNS. This notion is supported by Persidsky *et al.* (1999). His group has shown that both microglia and astrocytes can produce β-chemokines, including MIP-1α, MIP-1β, MCP-1 and RANTES, in HIV-1 infection in an *in vitro* culture system. Using SCID mice as an *in vivo* model, they found that β-chemokines secreted by glial cells play an important role in the transmigration of monocytes from circulation into the CNS. Similarly, Palm and Kim (2001) also observed secretion of β-chemokines such as RANTES, IP-10, MIP-1 α and MIP-1 β from glial cells, including

astrocytes, microglia and oligodendrocytes in Theiler's virus infection. Moreover, in a study carried out by Sauder et al (2000), glial cells, especially astrocytes, can express β-chemokines gene IP-10 and RANTES in the absence of inflammation in Borna disease.

Chemokines are not only chemotactic for inflammatory leukocytes, but also chemotactic for microglia (Peterson *et al.* 1997). Both human microglia (Peterson *et al.* 1997) and rodent microglia (Johnstone *et al.* 1999) have been demonstrated to migrate in response to β-chemokines, secreted by glial cells in a concentration-dependent manner. Besides chemokine synthesis, astrocytes and microglia can express several different types of chemokine receptors, including CX_3CR1, CCR1, CCR5, CCR2, etc., (Dorf *et al.* 2000; Gebicke-Haerter *et al.* 2001; Jiang *et al.* 1998). In addition to the traditional role of leukocyte attraction, several studies have shown a role for chemokines in normal CNS functions. For example, neurones can express chemokine receptor, CX_3CR1, the receptor for fractalkine, a chemokine that can directly modulate neuronal activities like synaptic transmission and neuronal survival (Meucci *et al.* 2000). This chemokine is produced by neurones themselves (Tong *et al.* 2000).

1.5.3. CNS cells: a source of nitric oxide

NO in the CNS has highly pleiotropic biological characteristics. It influences many aspects of CNS physiology, including synaptic plasticity, neuronal development and behavioural responses and reduces leukocyte extravasation (Munoz-Fernandez & Frenso 1998). The expression of NOS, which produces NO, has been characterized in numerous cell types of the CNS, either as a constitutive function or as a response to stimuli. NO can act as a physiological neurotransmitter in the CNS and has been found to inhibit viral replication in neurones. It is produced constitutively by neuronal constitutive NOS (NOS1) in neurones (Komatsu *et al.* 1999). Several *in vivo* and *in vitro* culture systems have shown that both microglia and astrocytes can be induced to express NOS2 for the production of NO upon immune stimulation (Grzybicki *et al.* 1997; Zhao *et al.* 1998; Hemmer *et al.* 2001; Banati *et al.* 1993; Boje & Arora 1992; Lane *et al.* 1999). Besides these cells, oligodendrocytes can also express NOS2 upon LPS and IFN-γ stimulation and thus can produce NO (Molina-Holgado *et al.* 2001).

According to Lane *et al.* (1999), generation of NO by NOS2 accelerates demyelination in MHV-infected animals by upregulating chemokines, such as MCP-1. In contrast, Okuda *et al.* (1997) have shown that excessive production of NO from NOS2 plays an important role in the control of demyelination in EAE through the elimination of inflammatory cells from the CNS, possibly via apoptosis. In conclusion, NO produced by CNS resident cells exerts variety of functions. These may be antiviral, anti-inflammatory, neuronal death-inducing or demyelinating, depending upon the nature of the stimulus.

1.5.4. CNS cells: an antigen presenting cells

It is now clear that glial cells, especially astrocytes and microglia, play a critical role in orchestrating the immune response in the CNS. Besides their physiological roles in CNS homeostasis, both can function as APC in association with MHC I and II on their surfaces. These molecules are inducible and regulated by cytokines, neurotransmitters and neuropeptides (Neumann & Wekerle 1998; Dong & Benveniste 2001). They enable the presentation of Ag to infiltrating lymphocytes (Raivich *et al.* 1999). Much evidence suggests that activated microglia and astrocytes can express increased levels of MHC-I and MHC-II molecules in viral encephalitis (Weissenbock *et al.* 2000; Bi *et al.* 1995), experimental allergic encephalomyelitis (EAE) (Gehrmann *et al.* 1993), Toxoplasma encephalitis (Deckert-Schluter *et al.* 1999), and ischaemia (Morioka *et al.* 1992). Similarly, several studies have shown the induction of MHC-I and MHC-II in astrocytes (Caplazi & Ehrensperge 1998; Liu *et al.* 1989; Mauerhoff *et al.* 1988). Although both microglia and astrocytes can present Ag and stimulate T cell proliferation in the CNS, recent evidence suggests that microglia are more efficient APC than astrocytes (Alsoi *et al.* 1998). In addition to this, Argall *et al.* (1991) have shown that Schwann cells of the PNS also can express MHC-I and MHC-II molecules upon viral infection.

In contrast to the glial cells, MHC-I inducibility is strictly regulated in the neurones (Neumann & Wekerle 1998) via their electrical activity (Neumann 2001), presumably because neurones are highly susceptible to the cytotoxic effect of $CD8^+$ T cells (Medana *et al.* 2000). Kimura & Griffin (2000) showed upregulation of MHC-I mRNA in the neurones in SBV infection, but they were unable to detect its surface expression. This may be due to a posttranscriptional block, mediated by neurones themselves. Recently, it has been found

that neurones are induced to express MHC-I molecules upon IFN-γ stimulation in *in vitro* culture systems (Neumann *et al.* 1997), however, this induction is limited only to those neurones which lack electric activity (Neumann & Wekerle 1998) or have been paralysed before stimulation by the neurotoxin, tetrodotoxin, which blocks sodium channels and neuronal electrical activity (Medana *et al.* 2000; Neumann *et al.* 1997). This has potentially important implications for the clearance of sick neurones in inflammatory responses in the CNS.

1.6. Immunopathology: the result of an uncontrolled immune response

The outcome of viral infection depends upon the balance between the ability of virus to replicate inside the host and the capability of host to generate and maintain an effective immune response. Although CNS resident cells can produce several different kinds of cytokines and chemokines (Benveniste 1992), the CNS requires help from the peripheral immune cells for the effective control of viral replication and clearance (Planz *et al.* 1997; Williamson & Stohlman 1990). During infection, the CNS microvascular endothelium is activated, with increased expression of CAM (Nansen *et al.* 1998). This facilitates the transmigration of inflammatory leukocytes through the BBB (Dopp *et al.* 1994) and thus creates a localized inflammatory reaction within the CNS parenchyma (Matyszak 1998). These inflammatory cells produce several different types of effectors, including proinflammatory cytokines, chemokines, neutralizing Ab and CTL which function to combat viral infection (Munoz-Fernandez & Frenso 1998; Hatalski *et al.* 1998; Noske *et al.* 1998) as well as enhance the activation of glial cells (Alsoi *et al.* 1998; Sedgwick *et al.* 1998). These glial cells then secrete more inflammatory cytokines as well as neurotrophic growth factors (Nakajima & Kohsaka. 1998; Benveniste 1992) and thus cooperate with the activities of infiltrating leukocytes (Alsoi *et al.* 1998).

Therefore, entry of inflammatory cells into the CNS and their retention and activation there, are crucial steps in the host immune response to neurotropic viral infection. However, occasionally, in the process of eliminating infected or dying cells, inflammatory reactions get out of hand, with the massive production of active mediators, including proinflammatory cytokines, which further increase the activation of inflammatory cells that can contribute to pathology in the CNS (Marten *et al.* 2001; Munoz-Fernandez & Fresno

1998) Moreover, activation of CNS resident cells, like microglia, is further enhanced and these cells then produce excessive amounts of many cytokines, as well as toxic metabolites such as reactive oxygen and nitrogen species, that can contribute to the lethal clinical manifestations of encephalitis and neurodegeneration (de Leo & Yezierski, 2001; Banati *et al.* 1993). For examples: several animal models of viral encephalitis have shown the importance of IFN and TNF in controlling the viral infections within the CNS (Brooks & Phillpotts 1999; Tishon *et al.* 1995; Rossel-Voth et al 1991), however, exaggerated production of these cytokines has been also implicated in the pathology of CNS viral infections, brain injury and neurodegenerative disorders (Munoz-Fernandez & Frenso 1998; Dickson *et al.* 1993; Ruddle *et al.* 1990).

Maloney *et al.* (2000) showed that excessive induction of IDO induced by IFN-γ is asoociated with immunopathology, by significantly decreasing the level of tryptophan within the CNS in human T cell lymphotropic virus type-1. Tryptophan is highly correlated with serotonin, which is an important neurotransmitter (reviewed in Kamimura *et al.* 1991). Decreased tryptophan reduces the level of serotonin, alters CNS function and causes neuronal death (Maloney *et al.* 2000). Similarly, NOS2 induced by IFN-γ (Karupiah *et al.* 1993) leads to excessive production of NO which precipitates pathology in viral encephalitis *eg.*, in HSV-1-induced encephalitis (Fujii *et al.* 1999). Andrews *et al.* (1999) have demonstrated the immunopathological role of TNF in MVE virus-induced encephalitis. In this model, increased production of TNF upregulates both microvascular CAM and neutrophil-specific chemokines N51/KC. This facilitates increased recruitment of neutrophils into the CNS parenchyma, which produces more inflammatory mediators, including NO, that disturb CNS homeostasis and neuronal function, leading to death. Initiation of EAE (Ruddle *et al.* 1990) and death from cerebral malaria (Medana *et al.* 1997) further illustrate the immunopathological role of TNF in the CNS. Akwa *et al.* (1998) have demonstrated that transgenic mice with CNS expression of IFN-α had significantly enhanced survival after i.c. inoculated LCMV infection. However, overproduction of IFN-α resulted in progressive inflammatory encephalopathy, with marked calcium mineralization, meningoencephalitis, gliosis and neurodegeneration (Campbell *et al.* 1999; Akwa *et al.* 1998).

Similarly, IL-1 has been found to produce immunopathology in the CNS. This cytokine is secreted by activated microglia (Giulian *et al.* 1994). It acts as a mitogen for astrocytes and these proliferate during embryonic development and injury in the brain (Giulian *et al.* 1986). Activated astrocytes enhance neuronal survival through the production of various neurotrophic growth factors and removal of neurotoxins (Mucke & Eddleston 1993). In a study of Giulian *et al.* (1994), increased production of IL-1 by microglia was observed in HIV-1 infection. This activated astrocytes produce excessive amounts of NOS2, leading to overproduction of NO and neuronal death (Zhao *et al.* 2001). Finally, in addition to the cytokines, B cells may also be associated with demyelination, resulting in immunopathology via the production of myelin-specific Ab (Cross *et al.* 2001).

1.7. Aims of this project

Most of the previous work on WNV encephalitis has been done in the young mouse model. We have therefore, developed an adult mouse model to understand better the mechanisms of pathogenesis and recovery from WNV encephalitis. Infection of IFN-γ-deficient mice with several different viruses has illustrated the importance of this cytokine for controlling virus infection. Therefore, IFN-γ-deficient mice were compared to wild types to evaluate the role of this cytokine in WNV encephalitis. The overall aim of this thesis is to evaluate the role of IFN-γ in WNV encephalitis in this model as well as the disease profiles of WNV encephalitis that result from different routes of virus inoculation. The following experimental approaches have been used:

1) To compare the susceptibility and disease profile of wild type and IFN-γ-deficient mice to WNV in the intraperitoneal (i.p.) route of WNV inoculation, specifically:

- To relate these to the development of CNS histopathology, kinetics of WNV replication and, clearance of WNV from the brain parenchyma.

- To compare the expression and upregulation of cell adhesion molecules in the CNS microvascular endothelium in the i.p. model and to relate these to the level of leukocyte infiltration in the brain parenchyma.

- To determine the activation of glial cells, especially microglia and astrocytes, and to relate these to the WNV clearance from the brain parenchyma in the i.p. model.

2) To compare the susceptibility and disease profile in the i.p. and intranasal route of WNV inoculation, specifically to relate these to the possible route of entry of WNV into the CNS and WNV replication in the brain parenchyma.

3) To evaluate the role of antibody in WNV encephalitis in both i.p. and i.n. models in wild type mice.

Chapter-2

General Materials and Methods

2.1. West Nile Virus: production and titre estimation

West Nile Virus (*Sarafend* strain) was passaged alternately in suckling mouse brain and cultured in vero cells. Working stocks consisted of culture supernatants from vero cells infected with brain-derived WNV.

2.1.1. Production of WNV

Frozen vero cells, derived from green monkey kidney, were thawed quickly in a 37°C water bath, washed in 10 ml complete medium (CM), *i.e.,* Dulbecco's modified eagles medium (DMEM) (JRH Biosciences, Lenexa, USA) supplemented with 10% fetal calf serum (FCS), by centrifuging at 450 xg at 20°C for 5 mins. The supernatant was discarded and the cell pellet was resuspended gently in 25 mls of CM, transferred into 175 cm^2 tissue culture flask and incubated at 37°C in a humidified atmosphere of 5% CO_2 in air for 24h. The vero cells were passaged and when they were confluent they were infected with mouse brain derived-WNV stock, provided by Dr. Nicholas J.C. King, University of Sydney.

The frozen brain virus (10^9 pfu/ml) was thawed at room temperature (RT°), mixed well in a vortex mixer and diluted 1:10 in CM. One ml of diluted brain (10^8 pfu/ml) virus was added into the vero cell culture flasks and incubated at 37°C in a humidified atmosphere of 5% CO_2 in air for 1h. The flasks were tilted every 10 mins for 1h to ensure even adsorption of virus. After 1h, the inoculum was removed by washing with DMEM and the cultures were incubated in 8 ml CM for 40h at 37°C. After 40h incubation, the culture medium was harvested and clarified by centrifugation at 480 xg for 20 mins at 4°C. The supernatants were pooled, aliquoted and stored at -70°C until required. This stock was titrated and used to infect mice and vero cells. The flasks with infected vero cells were then frozen at –70°C overnight and, thawed to release intracellular virus. One ml sterile PBS was added to the

flasks, contents were pooled and centrifuged as described before. The supernatant was aliquoted and stored at -70°C until required. This virus stock was used to coat ELISA plates.

2.1.2. Detection of virus titre: plaque assay

Virus concentration was determined by enumeration of antibody-labelled viral plaques in semiconfluent vero cell monolayers grown on glass coverslips. A sterile coverslip, 13 mm in diameter, was added in each well in a 24 well plate. One ml CM was added into each well, gently allowing the coverslips to settle to the bottom of the well. About 0.2 x 10^6 cells/ml was added in each well and incubated at 37°C for 24h. After 24h incubation, the vero cells were infected with 100μl of serially diluted vero grown WNV and incubated for 1h at 37°C, rocking the plate at 15 min intervals. After 1h adsorption of virus, the inoculum was removed by washing with DMEM and the culture was incubated in 2 ml CM for 24h at 37°C.

After 24h incubation, coverslips were washed 3 times in Tris-buffer (see appendix) and fixed in absolute ethanol at -20°C for 20 mins. Endogeneous peroxidase activity was then blocked with 0.3% H_2O_2 in methanol for 5 minutes. Coverslips were incubated with 10% normal goat serum (Gibco BRL, USA) at RT° for 30 mins followed by polyclonal rat anti-WNV antibody (Ab) (1:100 dilution). All subsequent incubations were done at RT°. Coverslips were then incubated with biotinylated anti-rat IgG, 1:200 dilution (BA-4000, Vector Laboratories, Burlingame, CA) for 30 minutes and then with horseradish peroxidase complex, 1:100 dilution (PK-4000, Vector Laboratories, Burlingame, CA) according to the manufacturer's instructions. The HRP was visualized using 3'3 diaminobenzidine tetrahydrochloride (DAB, 980681, ICN Biomedicals, Australia) and H_2O_2 for approximately 2 mins. Preparations were counter-stained with hematoxylin, mounted in DPX, and examined under transmitted light microscopy. Contiguous groups of labelled cells were counted as infected plaques and titres were calculated from the dilutions as pfu/ml. This technique is different from, and has considerable advantage over, previous techniques described by Taylor and Marshall (1975), for titrating WNV in that it takes only 24h, does not rely on plaques denoting cell death and uses single step kinetics.

2.1.3. Production of Rat anti-WNV antibody

Polyclonal anti-WNV Ab was made in a rat and was used for the detection of WNV Ag. Five rats were anesthesised with isoflorane (Lypards, Australia) in a rat chamber and were inoculated with 100μl of brain virus, containing $2x10^5$ pfu, via the intraperitoneal (i.p.) route. The rats were watched carefully for 14 days for any development of clinical symptoms and after 14 days post infection (p.i.), they were rechallenged again with a 10-fold higher dose of brain virus, $2x10^6$ pfu/rat. Seven days after rechallenge, blood was collected from cardiac puncture and pooled. The blood was kept at 4°C overnight to facilitate clot retraction and then centrifuged at 1851 xg for 20 mins at 4°C. Serum was collected, treated with 0.1% sodium azide (Ajax Chemicals, Sydney), aliquoted and kept frozen at -70°C until required.

2.1.4. Avertin anaesthetic

Avertin (Aldrich Chemical Co. Inc., Milwaukee, WI) was made by combining 2,2,2 tribromoethanol (1gm), 2- methyl-2 butanol (1ml) and dissolving in 50 mls boiled tap water. Avertin was aliquoted and kept at -20°C until required. The recommended dose for a mouse is 0.012 ml/gm/mouse, i.e. 250-300μl/mouse.

2.2. Experimental WNV-induced encephalitis models

In this thesis, pathogenesis of WNV encephalitis was studied in mice using the i.p. route of WNV inoculation (i.p. model) and intranasal (i.n.) route of WNV inoculation (i.n. model).

2.2.1. Mice

Eight-week-old Female C57BL/6 wild type (B6.WT), gamma interferon deficient (B6.IFN-γ-/-) mice backcrossed to C57BL/6 and 3-week-old female B6.WT were obtained from the Blackburn animal breeding establishment, The University of Sydney. Eight-week-old Female B cell-deficient mice backcrossed to C57BL/6 were obtained from John Curtin School, The Australian National University, Canberra, a kind gift from Dr. Gunasegaran Karupiah. During the experiments, all animals were housed under class II biohazard

conditions in hepa filter-top cages. The protocols for all animal experiments were approved by The Animal Care and Ethics Committee, The University of Sydney.

2.2.2. Virus infection of mice

2.2.2.1. Survival study and development of model

- **Titration of WNV in wild type mice**

After titration of vero-grown stock virus, groups of B6.WT mice were infected with serially diluted WNV to evaluate the development of disease and the survival rate in order to select an appropriate dose for the development of this model. Five different groups of mice (10 mice/group) were inoculated i.p. with 100μl of serially diluted WNV, from $3x10^6$ to $6x10^3$ pfu/mouse. The culture medium as well as diluent was CM. Therefore, supernatant from uninfected vero cells was used to mock-infect 10 mice for the control. Mice were monitored 3 times per day until day 30 p.i. Clinical symptoms and death were recorded in detail. Mice were sacrificed if they became moribund and were regarded as having succumbed to disease for statistical purposes.

- **B6.WT and B6. IFN-γ -/- mice: i.p. model**

After a series of titrations, $6x10^4$ pfu/mouse was chosen as the dose of WNV for the study of pathogenesis. Groups of 36 mice of B6.WT and B6.IFN-γ-/- strains were inoculated i.p. with $6x10^4$ pfu/mouse. Mice from each group were mock-infected as controls with the supernatant from uninfected vero cells. Mice were monitored 3 times per day until day 30 p.i. The clinical symptoms and death were recorded in detail. Mice were sacrificed if they became moribund and were regarded as having succumbed to disease for statistical purposes.

- **B6.WT and B6. IFN-γ -/- mice: i.n. model**

Groups of 20 mice of B6.WT and and B6.IFN-γ-/- strains were inoculated with 10μl via i.n. route of inoculation, containing $6x10^4$ pfu. Mice from each group were mock-infected as controls with supernatant from uninfected vero cells. Mice were monitored 3 times per day

until 7 days p.i. The clinical symptoms and death were recorded in detail. Mice were sacrificed if they became moribund and were regarded as having succumbed to disease for statistical purposes.

2.2.2.2. Time course experiment: Virus infection and tissue preparation

To determine the role of IFN-γ in the development of CNS histopathology and viral clearance, a time course experiment was performed. For the time course experiment described in the i.p. model, groups of 120 mice each of B6.IFN-γ-/- and B6.WT strains, respectively, were inoculated i.p., as described above and allocated randomly to groups representing timepoints. At least 7 mice were therefore in each group and were removed at the indicated timepoints from day 1 to 11 p.i. Groups of 3 mice were chosen for investigation on days 15 and 30 p.i. Mice were deeply anaesthesized i.p with avertin and perfused via the left ventricle with 10 ml PBS followed by 10 ml 2% paraformaldehyde in PBS, pH 7.5. In the i.n. model, groups of 21 mice, each of B6.IFN-γ-/- and B6.WT strains, respectively, were inoculated i.n., as described above. Groups of 3 mice were allocated to each timepoint from day 1 to 7 p.i.

Brains were removed with intact olfactory bulbs and post-fixed in 4% paraformaldehyde for 24h at 4°C. Cervical spinal cords were also collected from both groups at each timepoint in both i.p. and i.n. models and post-fixed with 4% paraformaldehyde. Brains were divided sagitally down the mid-line. Half of the brains were processed and embedded in paraffin. Spinal cords were cut into 3 pieces, processed and embedded in paraffin. Seven-micron sections of brains and spinal cords were cut, mounted onto slides precoated with 3-aminopropyltriethoxysilane (APTES, ICN Biomedicals, Australia) and used for histology and immunohistochemistry. The remaining halves of brains were washed twice in PBS and then cryopreserved in 30% sucrose (w/v) in PBS, pH 7.5 overnight at 4°C. Sucrose-infiltrated brains were then immersed in O.C.T medium (BDH Laboratories Supplies, England) and snap frozen using isopentane (BDH Laboratories Supplies, England), precooled in liquid nitrogen and then stored at -70°C until cryosectioning. Eight-micron sagital sections were cut, mounted onto slides precoated with APTES, air-dried overnight and stored at -70°C until they were used for immunohistochemistry. The flow chart of the time course experiment is presented in figure 2.1.

Methods: Time course experiment

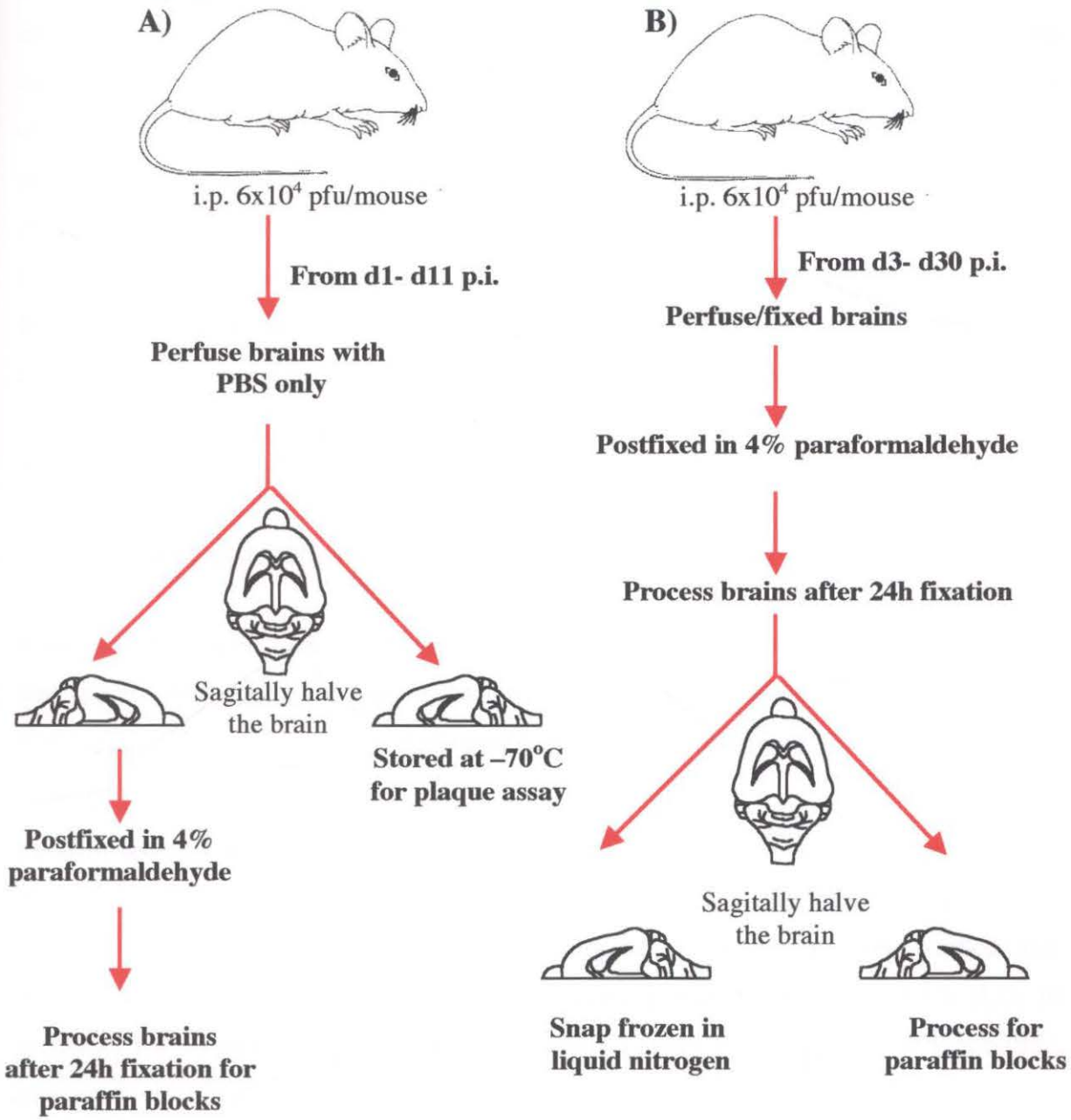

Figure: 2.1 Flow chart of steps used in time course experiment. Protocol in A was used to collect brain tissues for plaque assay and matched immunohistochemistry. Protocol in B was used to collect brain tissues for immunohistochemistry only.

A separate animal experiment was carried out to determine WNV brain titres. In the i.p. model, groups of 64 mice, each of B6.IFN-γ-/- and B6.WT strain, respectively, were inoculated i.p. as described above. At least 4 mice from each group were removed at the indicated timepoints from day 1 to 11 p.i. Mice were deeply anaesthesized i.p with avertin and perfused via the left ventricle with 20 ml PBS only. Brains were removed with intact olfactory bulbs and divided sagitally down the mid-line. Half of the brains were weighed and kept in eppendorf tubes with 50μl CM and stored at -70°C until they were used for plaque assays and the remaining halves of brains were processed and embedded in paraffin for matched immunohistochemistry. Similarly in the i.n. model, groups of 21 mice, each of B6.IFN-γ-/- and B6.WT strain, respectively, were inoculated i.n. as described above. Groups of 3 mice from each strain were removed at the indicated timepoints from day 1 to 7 p.i. Mice were perfused and brains were processed as described before in the i.p. model. The techniques used in this thesis are summarized in table 2.1.

2.2.3. Histology and immunohistochemistry

Paraffin sections were used for histology. Routine hematoxylin and eosin (H and E) staining was used to study histopathological changes occurring during encephalitis in both groups. Both paraffin and frozen sections were used for immunohistochemistry (IHC).

Paraffin sections were dewaxed in xylene, taken through graded (100-70%) ethanol and then fully rehydrated in water. Antigen was retrieved either by digestion of sections with enzymes or microwaved with citrate buffer (see appendix). The sections were washed once with Tris-buffer and endogeneous peroxidase activity was blocked with 0.3% H_2O_2 in methanol for 30 mins. The sections were washed 3 times for 10 mins with Tris-buffer, incubated with 100μl of 10% normal goat serum (Gibco BRL, USA) at RT° for 30 mins, for non-specific blocking, and incubated with 100μl of primary Ab. The incubation period for each Ag and isotype control used in this thesis are summarized in table 2.2. The sections were washed again with Tris-buffer 3 times for 10 mins and incubated with 1:200 dilution of 100μl secondary Ab for 30 mins at RT°. The sections were washed again with Tris-buffer 3 times for 10 mins and incubated with 100μl of horseradish peroxidase complex, 1:100 dilution (PK-4000, Vector Laboratories, Burlingame, CA) for 30 mins. The HRP was visualized using 3'3 diaminobenzidine tetrahydrochloride (DAB, 980681, ICN Biomedicals,

Australia) and H_2O_2 for approximately 5 mins. The sections were counter-stained with hematoxylin, mounted in DPX, and examined under transmitted light microscopy. Frozen sections were thawed out at RT°, air dried for 30 mins and rehydrated in Tris-buffer for 5 mins. After rehydration, all subsequent procedures were identical to those described for paraffin section.

2.2.4. TUNEL labelling

Paraffin brain sections were subjected to TUNEL staining to determine the incidence of neuronal death in the brain. This was achieved using the Apoptag® peroxidase *In situ* Apoptosis detection kit (Intergen Company). The labelling protocol followed was exactly according to the manufacturer's instructions.

2.3. Quantification of cell numbers in histological sections

Numbers of infected neurones were determined on anti-WNV-stained sections of brain parenchyma from both groups. To evaluate whether there were significant differences in WNV antigen-positive neurones between groups, the number of WNV-positive neurones were quantified as follows. The number of neurones positive for viral Ag was counted in 12 defined areas of brain as shown in figure 2.2. These areas included brain stem, cerebellum, superior colliculus, pyriform cortex (front cortex), cortex retrosplenalis (back cortex), hippocampus, thalamus, base of brain, olfactory bulb, base of olfactory bulb, corpus striatum and base of cerebellum. At least 5 high-power fields were counted in each area for each sample. Thus each mouse brain was evaluated on 60 high power fields. Numbers of infiltrating leukocytes, activated microglia, ICAM-1 and VCAM-1-expressing blood vessels were also quantified in this way.

2.4. Detection of hyper-immune serum efficiency and passive transfer

2.4.1. Production of hyper-immune serum and immune splenocytes

Hyper-immune (HI) serum was made in wild type mice and was used for passive serum transfer experiments. A group of 20 mice was infected i.p. with $6x10^4$ pfu/mouse and carefully watched for 14 days for any development of clinical symptoms or death. After 14

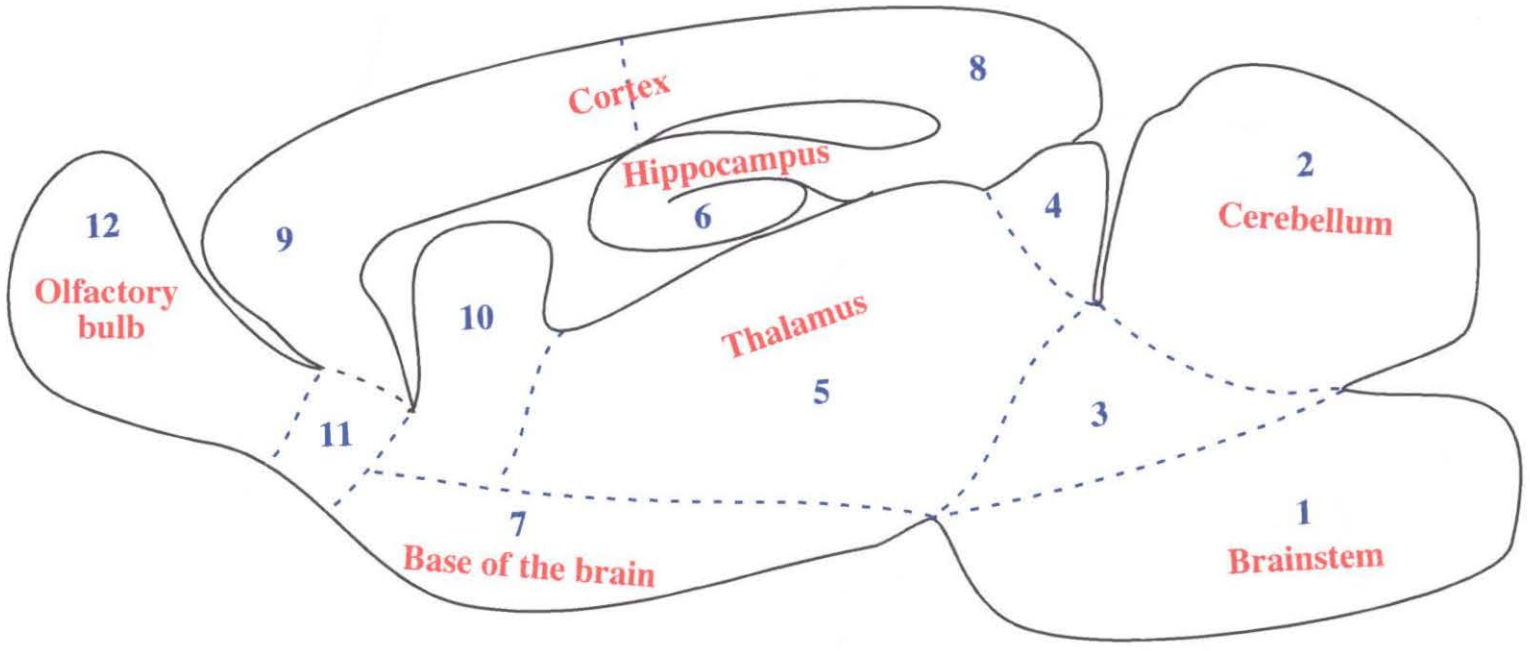

Figure: 2.2 Schematic diagram of sagittal brain section. Different numbers in the brain section show different areas of the brain used for counting as described above. 1, brainstem, 2, cerebellum, 3, base of cerebellum, 4, superior colliculus, 5, thalamus, 6, hippocampus, 7, base of the brain, 8, cortex retrosplenalis, 9, pyriform cortex, 10, corpus striatum, 11, base of olfactory bulb, 12, olfactory bulb

days, they were rechallenged with a 50-fold higher dose of virus, *i.e.*, $3x10^6$ pfu/mouse. Seven days after rechallenge, they were again rechallenged with $3x10^6$ pfu/mouse. Blood and spleens were collected after this 3rd challenge *i.e.*, 28 days after the first inoculation, by exsanquination under anaesthesia. The blood was kept at 4°C overnight to facilitate clot retraction and centrifuged at 1851 xg for 20 mins at 4°C. Serum was collected, aliquoted and stored at -70°C until required. The neutralizing capacity of hyper-immune serum was assessed before passive transfer into naïve mice. Spleens from hyper-immune mice were kept in a small petri dish containing CM and processed immediately for adoptive transfer of splenocytes into naïve mice (see below).

2.4.2. Direct ELISA

Direct, enzyme linked immunosorbent assay (direct ELISA) was performed to determine IgG titre in hyper-immune serum. Intracellular virus, as described in section 2.1.1, was used to coat the plate. It was diluted at a 1:5 dilution in a carbonate buffer (see appendix). Diluted WNV, 50μl, was added in each well of the ELISA plate using a multichannel pipette. Some wells were coated only with carbonate buffer as a negative control for WNV Ag. The plate was sealed with plastic film (glad wrap) and incubated overnight at 4°C, and then wells were washed 5 times with PBS/Tween-20 (PBS with 0.5% Tween-20) to remove unbound WNV Ag. Fifty microlitres of serially diluted immune and normal serum samples were added to the coated plate (serially diluted with PBS-T20 in a separate 96 well plate before adding to ELISA plate). Then the plate was incubated at RT° for 2h and rinsed 5 times with PBS/T20. Duplicate samples were used for each dilution. Fiffty microlitres of HRP-conjugated 1:3000 diluted secondary Ab, rabbit anti-IgG (P0406, DAKO) was added to each well and incubated at RT° for 1h. After rinsing the plate 5 times with PBS/T20, 50μl of TMB one step substrate (S1600, DAKO) was added to each well for visualization of the reaction product, and incubated at RT in the dark for 15 minutes. Blue to sky blue colour developed, depending upon the concentration of IgG. The colour intensity was measured using a 650 nm filter in the ELISA plate reader.

2.4.3 Plaque reduction neutralization test

A plaque reduction neutralization test (PRNT) was performed in a 6 well plate, containing vero cell monolayers on 22 mm diameter round coverslips. The vero cell monolayer was

grown in the sterile coverslips as described above, one day before PRNT. The number of vero cells required to give a semiconfluent growth was $0.3x10^6$ cells/ml. Stock WNV was diluted in CM to give 100 pfu in 100μl. Serum was serially diluted in CM and 100μl of diluted seum was incubated with 100μl of diluted virus containing 100 pfu in an eppendorf tube for 30 mins at 37°C. Vero cell monolayers were infected with WNV preincubated with the serially diluted immune sera and incubated for 1h at 37°C. After 1h adsorption, the mixed inoculum was removed, washed with CM and the cells incubated with 2 ml CM for 24h at 37°C. The following day WNV titres were determined using the Ab-labelling method as decribed above and the number of infected cells was counted on the whole coverslip. The dilution of serum required for 50% plaque reduction was determined as described previously by Reed and Muench (1938) and was defined as the 50% neutralization titre (NT_{50}). Undiluted normal serum was used as a negative control whereas undiluted immune serum was used as a positive control for the neutralization of WNV.

2.4.4. *In vitro* efficiency of neutralizing antibodies

To test whether neutralizing Ab could influence the release of virus *in vitro*, presence of WNV in the vero cell culture supernatant was assessed in 12 well plates. Vero cell monolayers were grown on coverslips as described above, infected with $6x10^4$ pfu/coverslip and incubated for 1h at 37°C. Both immune and normal serum was serially diluted in CM. Virus inoculum was removed after 1h adsorption and 2 ml CM and 300μl of serially diluted serum was added to each well. The plate was incubated at 37°C for 48h. After 48h of infection, culture supernatants of infected vero cells were harvested and diluted 1:10-1:50. Fresh vero cell monolayers were infected (200μl) with this diluted culture supernatant. The plate was incubated for 1h at 37°C, supernatant was removed and 2 ml fresh CM was added. The plate was incubated for 24h at 37°C. The following day WNV plaques were determined using the Ab-labelling method as decribed above and the number of plaques was counted as described above. The number of plaques were counted for each dilution and compared.

2.4.5. Passive transfer of hyper-immune serum

Passive transfer of HI serum was performed only in B6.WT mice. Hyper-immune or normal sera, 200μl of 1:3 diluted was transferred i.p. to 8-week-old B6.WT mice, 24h before

infection. In both i.p. and i.n. models, groups of 30 mice, 10 mice/subgroup were used, i.e. 3 groups of mice were used in each model. In both models, one group received 200μl HI serum/mouse, the second group received normal serum and third group was left untreated. After 24h, all groups of mice were inoculated with $6x10^4$ pfu/mouse, either i.p. or i.n. and were monitored 3 times per day until day 14 p.i. The clinical symptoms and death were recorded. Mice were sacrificed if they became moribund and were regarded as having succumbed to disease for statistical purposes.

2.5. Preparation of splenocytes and adoptive transfer

2.5.1. Preparation of splenocytes

As described earlier in section 2.4.1, spleens were collected from hyper-immune mice and immediately placed in a small petri dish containing 5 ml CM. Spleens were washed once with 70% ethanol and twice in PBS and were transferred into clean petri dish containing CM and a small piece of filter gauze. Spleens were placed on the top of filter gauze and very gently, using a syringe plunger, strained into the CM. The splenocytes were then transferred into a falcon tube using a pipette and centrifuged at 450 xg at RT° for 5 mins. Supernatant was discarded and the pellet was resuspended in 2 ml RBC lysis buffer (see appendix) for 1 min to allow lysis of RBC and then 2 ml CM was added to stop the process. The suspension was centrifuged at 450 xg at RT° for 5 mins. The supernatant was discarded, the pellet was resuspended in 10 ml PBS and splenocytes were counted using a haemocytometer and trypan blue. The number of splenocytes need to transferred was $5x10^7$ cells/mouse. The volume was adjusted to 200μl PBS and the cells injected i.p. Splenocytes from normal or pre-immune mice were processed similarly as the control.

2.5.2. Adoptive transfer of splenocytes

Adoptive transfer of splenocytes was performed only in B6.WT mice. Two hundred microlitres of cell suspension containing $5x10^7$ splenocytes were adoptively transferred i.p. to 8-week-old B6.WT mice using a 28 gauge needle, 24h before infection. In this experiment groups of 30 mice, 10 mice/subgroup were used, *i.e.*, 3 groups of mice were used. One group received $5x10^7$ immune splenocytes/mouse, the second group received $5x10^7$ normal splenocytes/mouse and third group was left untreated. After 24h, all groups of

mice were inoculated i.n. with $6x10^4$ pfu/mouse and were monitored 3 times per day until day 7 p.i. The clinical symptoms and death were recorded. Mice were sacrificed if they became moribund and were regarded as having succumbed to disease for statistical purposes.

2.6. Data analysis

All data derived from immunohistochemistry and lectin histochemistry shown in the figures are mean values ± SEM for the total number of fields examined from the indicated number of mice, n. Data were analysed using unpaired two-tailed Student's *t* test for single comparisons, or by ANOVA, where multiple comparisons were required. The Fisher exact probability test was used for survival analysis. Data were considered significant if $p = <0.05$.

Table 2.1 Summary of techniques described in this thesis.

Techniques	Parameters detected
Hematoxylin and eosin staining	Identification of histopathology and enumeration of leukocyte infiltration in the brain parenchyma and meninges
Anti-WNV immunohistochemistry	Cells infected with WNV and the areas of infection
Plaque assay	Virus titre in the brain
Griffonia simplicifolia isolectin B-4 (GS-lectin) histochemistry	Distribution and morphology of activated microglia, vascular endothelial cells and macrophages
Anti-ICAM-1 and VCAM-1 immunohistochemistry	Cells expressing ICAM-1 and VCAM-1
Anti-GFAP immunohistochemistry	Distribution and morphology of normal and activated astrocytes
Anti-MHC-II immunohistochemistry	Distribution and morphology of cells expressing MHC-II molecules
Anti-fibrinogen immunohistochemistry	Leakage of vessel, area and extent of leakage
Double labelling (labelling of 2 Ag) in the same brain section using immunohistochemistry	Confirmation of cells infected with WNV and glial cells expressing ICAM-1
Passive transfer of WNV-immune and normal sera	Role of Ab in the i.n. and i.p. model
Plaque reduction neutralization assay	Titre of neutralizing Ab
Adoptive transfer of WNV-immune and normal splenocytes	Role of immune cells in the i.n. model
Serum ELISA	Titre of WNV- immune serum IgG
TUNEL assay	Apoptosis

Table: 2.2 Summary of antibodies and lectin used for immunohistochemistry.

Primary antibody	**Dilution used**	**Isotype control**	**Incubation temperature for primary antibody**	**Types of section**	**Method of antigen retrieved**	**Company**
Rat anti-WNV Antibody	1:100	Normal rat serum	1h at RT°	Paraffin section	100µl protease enzyme for 4 mins at RT°	Prepared in our laboratory as described above.
Biotinylated Isolectin-B4	1:50	None	3h at 4°C	Paraffin section	Microwaved for 8 mins in 500 ml citric buffer	Sigma Chemical Company Cat # L-2140
Rat anti-mouse ICAM-1	1:10	Rat IgG_2a	1.5h at 4°C	Frozen section	Not used	Hybridoma supernatant ATCC, YN 1/1.7.4 CRL 1878
Rat anti-mouse VCAM-1	1:50	Rat IgG_2a	Overnight at 4°C	Frozen section	Not used	Pharmingen Cat # 01811D
Rabbit anti-human Fibrinogen	1:500	Polyclonal rabbit IgG	1h at RT°	Paraffin section	Microwaved for 29 mins in 500ml citric buffer	Dako Cat # A0080
Rabbit anti-cow GFAP	1:750	Polyclonal rabbit IgG	1h at RT°	Paraffin section	Not used	Dako Cat # Z0334
Rat anti-mouse MHC-II	undiluted	Monoclonal rat IgG_2b	overnight at 4°C	Paraffin section	100µl papain enzyme for 5 mins at RT°	Hybridoma supernatant (TIB 120 ATCC, M5/114.15.12)

Chapter-3

IFN-γ exacerbates disease in WNV encephalitis

3.1. Introduction

Virus infection presents a profound challenge to host survival. There are numerous antiviral defence mechanisms that include both innate and adaptive defences. Cytokines are among these several sophisticated defence mechanisms and are produced by a variety of cell types in response to viral infection (Ramshaw *et al.* 1997). Of these, IFN-γ, is one of the most important. A pleiotropic cytokine, it is produced by T_H1 cells, $CD8^+$ T cells, NK cells (Harty *et al.* 2000; Salazar-Mather *et al.* 2000; Christensen *et al.* 1999) and macrophages (Gessani & Belardelli 1998). IFN-γ regulates immune (Boehm *et al.* 1997) and inflammatory events (Benveniste 1998). Therefore, it is regarded as both immune (Young & Hardy 1995) and antiviral (Kohonen-Corish *et al.* 1990) in function.

Several experimental animal models of viral encephalitis demonstrated the importance of endogeneous production of IFN-γ for adequate host defence against virus infection (Nansen *et al.* 1998; Huang *et al.* 1993; Bouley *et al.* 1995; Karupiah *et al.* 1990). IFN-γ may either directly inhibit viral replication (Kohonen-Corish *et al.* 1990) or activate and orchestrate the collaboration of several other effector molecules as part of antiviral defence (Billiau 1996). Thus, IFN-γ activates CTL and NK cells (Utermohlen *et al.* 1996) which selectively eliminate virus-infected cells, as well as secreting IFN-γ themselves (Harty *et al.* 2000; Biron *et al.* 1999). IFN-γ activates macrophages to release several proinflammatory and antiviral cytokines, including TNF, IL-1, IL-6 (Janeway *et al.* 2001) and IFN-γ (Gessani & Belardelli 1998), as well as increasing their microbicidal activities (Munoz-Fernandez & Fresno 1998). It is also required for the maturation and effector function of $CD8^+$ T cells (Stohlman *et al.* 1998) and regulation of Ab production, especially in switching of Ig into IgG2a and IgG3 subclasses (Young & Hardy 1995). IFN-γ also induces MHC-I and MHC-II molecules on a wide variety of cell types (Grau *et al.* 1997; Huynh & Dorovini-Zis 1993;

Momburg *et al.* 1986). Moreover, IFN-γ induces increased production of NO and IDO enzymes (Guidotti *et al.* 2000; Karupiah *et al.* 1993; Takikawa *et al.* 1990), which are antiviral (Saxena *et al.* 2000; Yoshida *et al.* 1979). However, despite extensive studies, details of the mechanisms of the antiviral effects of IFN-γ are not fully understood.

Recruitment of inflammatory cells into the CNS is a critical step in antiviral host defence mechanisms. Until recently, the CNS has been seen characterized as an immune privileged site due to the presence of several unique features. First, the CNS parenchyma is separated from the blood circulation by the BBB. This prevents the entry of leukocytes, plasma proteins and cytokines. However, although access to the CNS is relatively restricted (Fontana 1987; Cserr *et al.* 1992), a small number of activated T lymphocytes, irrespective of their Ag receptor specificity, can pass through the BBB and subsequently migrate into the CNS (Hickey *et al.* 1991). Second, the normal CNS lacks professional APC such as B cells, dendritic cells and macrophages and this has been thought to prevent the initiation and propagation of Ag-specific immune responses (Becher *et al.* 2000). However, during CNS infection and inflammation microglia can act as APC (Bo *et al.* 1994; Weissenbock *et al.* 2000). Finally, in the normal CNS, the expression of MHC molecules are very low or undetectable (Benveniste 1992; Neumann 2001). Therefore, the CNS cells are not recognized by activated T lymphocytes under normal conditions, even though these cells can enter the CNS parenchyma. While this is true, it is clear that interaction with CNS cells does occur, probably due to upregulated immune recognition molecules during infection, damage and inflammation.

In viral encephalitis, massive amounts of inflammatory cells migrate into the CNS. When these cells find their respective target Ag in the CNS, an inflammatory reaction is started through the production of many proinflammatory cytokines, including IFN-γ (Liu & Chambers 2001; Christensen *et al.* 1999), leading to upregulation of CAM (Nansen *et al.* 1998; Irani & Griffin 1996) in the neurovascular endothelium (Fabry *et al.* 1992) and local production of chemokines (Asensio *et al.* 1999), which further help to recruit more inflammatory effector cells into the CNS. This initiates a cascade of inflammation in the CNS (Lassmann 1997). The mechanism of brain inflammation thus follows the same basic pattern that operates in inflammation at other sites of the body.

Although IFN-γ plays a critical role in viral infection, the role of IFN-γ has not been studied in WNV encephalitis to date. Moreover, due to the lack of defined *in vivo* animal models, understanding of the pathogenesis of WNV encephalitis is incomplete. Most previous studies on WNV encephalitis have been carried out in a neonatal or young (3-4 week-old) mice. These models do not reflect the disease profile of adult mice. Encephalitis develops more readily and severely in young mice, often with 100% mortality presumably due to the immature immune system. Therefore, an adult mouse model using 8-week-old, inbred C57BL/6 wild type (B6.WT) and gamma interferon deficient (B6.IFN-γ-/-) mice backcrossed to C57BL/6 was developed in this project to define the pathogenesis of WNV encephalitis and to determine the role of IFN-γ in this process.

3.2. Materials and Methods

3.2.1. Mice

Female, specific-pathogen free, 8-week-old B6.WT and B6.IFN-γ-/- mice, backcrossed to C57BL/6, and 3-week-old B6.WT were used.

3.2.2. Virus infection of mice and tissue preparation

To adopt an appropriate dose of WNV to develop this model, WNV was titrated in B6.WT mice as described in section 2.2.2.1. Five different doses were used: $3x10^6$ pfu/mouse, $3x10^5$ pfu/mouse, $1.2x10^5$pfu/mouse, $6x10^4$ pfu/mouse and $1.2x10^4$ pfu/mouse. From this titration series, a dose of $6x10^4$ pfu/mouse was chosen for the study of pathogenesis. Groups of 36 mice of B6.WT and B6.IFN-γ-/- strains were inoculated with $6x10^4$ pfu/mouse and their survival rate was evaluated as described in section 2.2.2.1. To determine the kinetics of viral infection and leukocyte infiltration in the CNS parenchyma, a time course experiment was carried out. Groups of 120 mice/strain were inoculated with $6x10^4$ pfu/mouse, tissues were collected and processed as described in section 2.2.2.2. To evaluate the route of access of WNV in a young mouse, 3-week-old B6.WT mice were used. Although these mice were not weighed, due to their smaller size compared to 8-week-old mice, 10 fold less virus *i.e.*, $6x10^3$ pfu/mouse, was inoculated i.p. using groups of 16 mice, as described before. Mice were sacrificed on days 2, 3, 4 and 5 p.i. Brains and cervical spinal cords were collected and processed as described before.

3.2.3. Histopathology and immunohistochemistry

Serial sections from paraffin-embedded tissues were stained with H and E, and were examined to evaluate the pathological changes occurring in the brain parenchyma of both groups of mice during encephalitis.

- **Detection of WNV antigen**

After dewaxing the paraffin sections, Ag was retrieved with digestion of sections in the protease enzyme derived from *Streptomyces griseus* (P-5005, Sigma Chemical Company), 0.05% w/v made in PBS, pH 7.5 for 4 mins at RT° and washed in Tris-buffer. After endogeneous peroxidase activity and non-specific blocking, sections were then incubated with 100μl of 1:100 diluted rat anti-WNV Ab for 1h at RT°. After this, the remaining procedures were identical to those described in section 2.2.3. Mock-infected brain sections were used as controls for rat anti-WNV serum labelling and normal *i.e.,* pre-immune rat serum was used as an isotype control for the primary Ab.

- **Detection of fibrinogen leakage**

Rabbit anti-human fibrinogen, 1:500 dilution (A0080, Dako, Denmark) was used to detect fibrinogen in the infected brain parenchyma, as a marker of blood-brain barrier damage in WNV encephalitis. After dewaxing and endogeneneous peroxidase blocking, sections were microwaved on high power in citrate buffer for 8 mins and boiled for 21 mins at medium high power. Sections were allowed to stand at RT° for 30 mins in citrate buffer, and then washed in Tris-buffer. After blocking endogeneous peroxidase activity and non-specific blocking, sections were then incubated with 100μl of primary antibody for 1h at RT°. After this, the remaining procedures were identical to those described in section 2.2.3. Mock-infected brain sections were used as control for rabbit anti-human fibrinogen labelling. Polyclonal rabbit IgG was used as an isotype control for the primary antibody.

3.2.4. Determination of brain titre

As described in section 2.1.2, virus titres in the brain were determined by plaque assay with slight modifications. The frozen brains collected from both groups of mice were thawed at RT°. The brains were homogenized and 950μl of CM was added to the tube. The brain homogenates were centrifuged at 2500 xg for 20 mins at 4°C. The supernatant was collected, serially diluted in CM and 100μl plated onto vero cell monolayers grown in coverslips in 24 well plates. The plate was incubated for 1h at 37°C, washed 2 times with CM and incubated for 24h at 37°C with 2 ml CM. After 24h incubation, the plaques were determined as described in section 2.1.2. Contiguous groups of labelled cells or individual labeled cell were counted over the whole cover slip as infected plaques and titres were calculated from the dilutions as pfu/gram.

3.2.6. Quantification of cells and data analysis

Quantification of cells and data were analysed as described in section 2.3 and 2.6 respectively. Figures are mean values ± SEM for the total number of fields examined from the indicated number of mice, n.

3.3. RESULTS

3.3.1. Survival in WNV encephalitis

3.3.1.1. Titration of WNV in B6.WT mice

Since one of the aims of this study was to establish and study a reliable adult model of WNV encephalitis, WNV was titrated in 8-week-old B6.WT mice. Five different doses were used. Mice were highly susceptible with 100% mortality to $3x10^6$, $3x10^5$ and $1.2x10^5$ pfu/mouse. Mortality was 60% using $6x10^4$ pfu/mouse, whereas it was only 40% using $1.2x10^4$ pfu/mouse. Clinical symptoms occurred from day 6 p.i. onwards, regardless of the dosage used. Mortality occurred between day 6-11 p.i. No further deaths occurred after day 11 p.i. and mice appeared healthy. The cumulative comparative survival after infection in all groups is presented in figure 3.1.

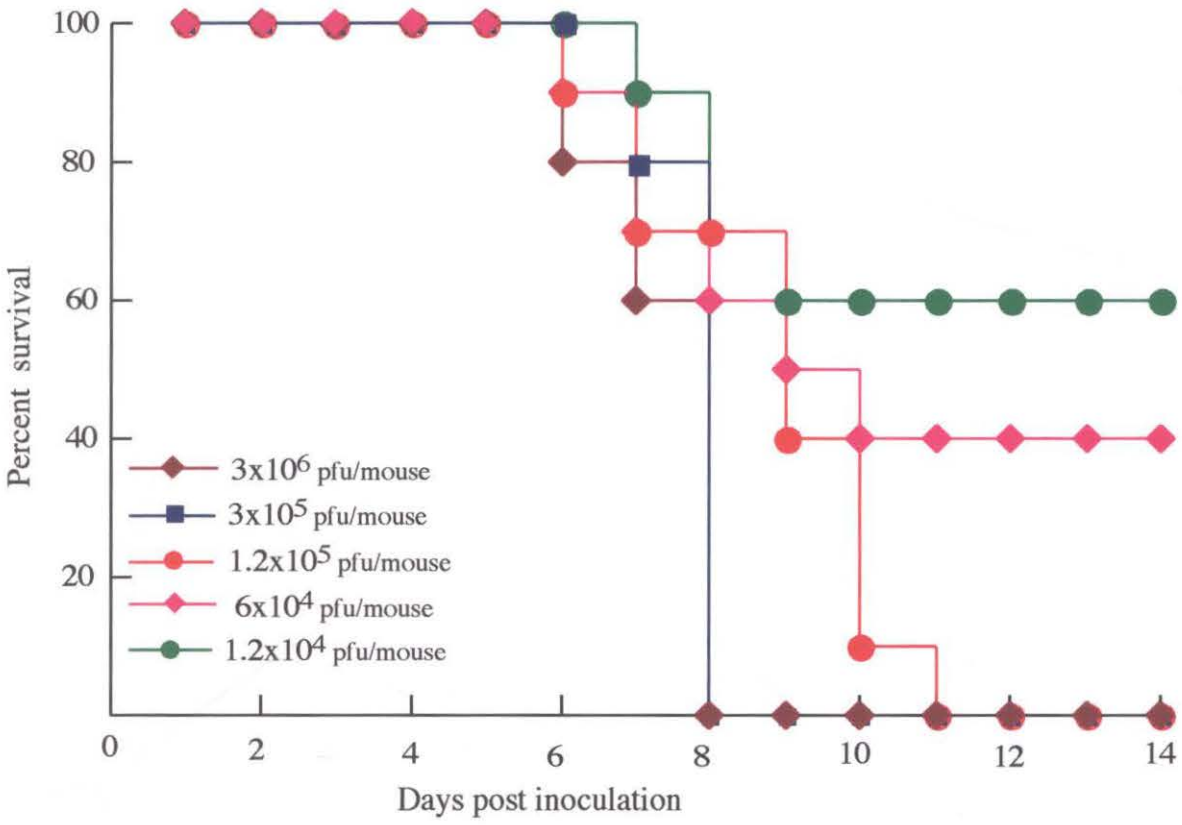

n = 10 mice/group

Figure: 3.1 Titration of stock vero-grown WNV in 8 week-old B6.WT mice. Groups of 10 female mice/dose were inoculated i.p. with different doses of WNV and monitored for signs of illness 3 times a day over 14 days. The percent survival at each time point is shown. Mock-infected mice did not develop signs of illness.

3.3.1.2. Role of IFN-γ in survival in WNV encephalitis

After a series of titrations, a dose of WNV was selected, which was normally lethal for 60% of B6.WT, so that a positive and negative role of IFN-γ could be evaluated in WNV encephalitis. In all groups, therefore, $6x10^4$ pfu/mouse was used. This dose resulted in the first clinical signs of infection by day 6 p.i. These included general signs such as ruffled hair, reduced activity and hunching, as well as exudative conjunctivitis, weight loss and/or weakness, with or without CNS symptoms. Such symptoms included hind limb paralysis, tremors and occasionally convulsions. Since IFN-γ is crucial to the effective immune response in many viral infections, the responses of B6.WT to WNV was compared with those of B6.IFN-γ-/- mice. The cumulative comparative survival after infection in both groups is presented in figure 3.2. In both groups mortality occurred between day 7 and 11 p.i. and once clinical signs were observed, death invariably followed within 12-48h. Occasionally, however, the onset of disease was sudden and mice died without observable illness. Survival from infection in B6.IFN-γ-/- was approximately 83%, significantly greater (p=0.002) than that of B6.WT, at approximately 40%. No further deaths occurred after day 11 p.i. and mice appeared healthy in both groups. Surviving mice from both groups were rechallenged i.p. with 50-fold the original dose of WNV ($3x10^6$pfu/mouse) and observed for 3 weeks for signs of illness. No signs of illness were observed at this time from either group (data not shown). This demonstrates that IFN-γ is not critical for survival either in primary or secondary WNV infection. Moreover, IFN-γ may contribute to clinical illness and death in primary WNV infection.

3.3.2. Histopathology

Routine H& E staining of sagittal brain sections from B6.WT and B6.IFN-γ-/- is shown in figure 3.3. Histopathological changes were clearly visible in the grey and white matter in both groups. These changes included diffuse infiltration of leukocytes consisting of both mononuclear and polymorphonuclear cells with occasional perivascular cuffing in both groups (Figure 3.3 c, d). Meningeal infiltration was also present at this time (Figure 3.3 e, f). Perineuronal microglial clusters and activated microglia were distributed throughout the brain in both symptomatic and asymptomatic mice from either group (Figure 3.3 c, f). Occasionally, at day 6 p.i., mice with high numbers of infected neurones throughout the

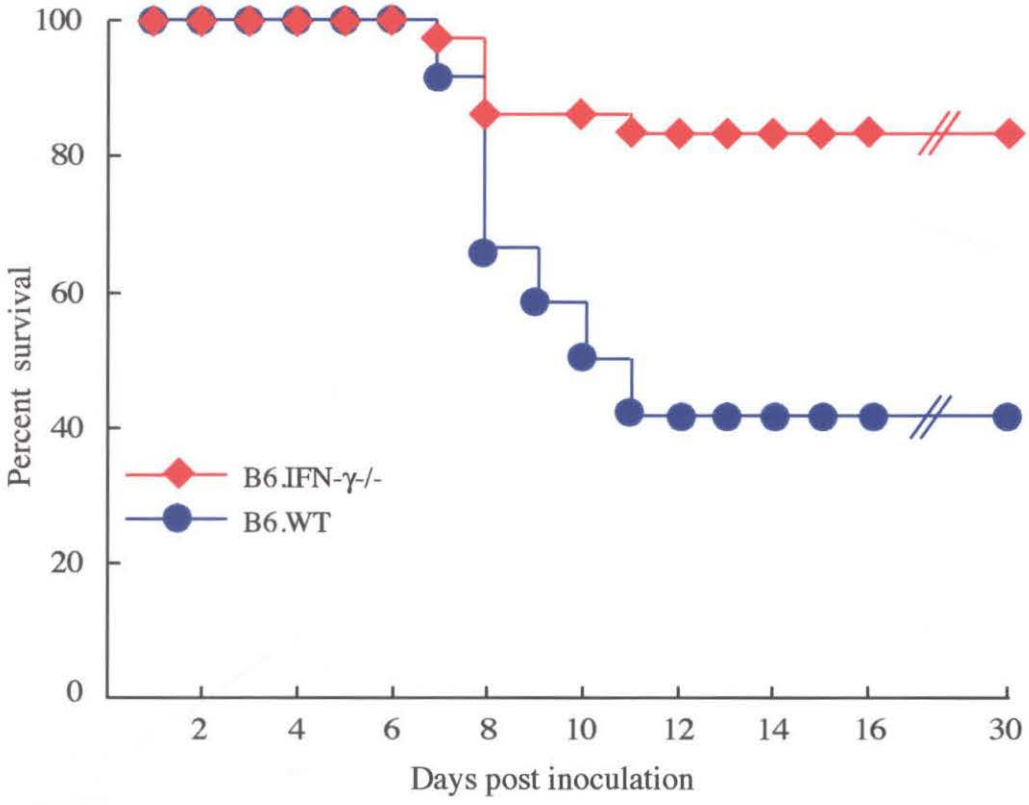

n = 36 mice/group

Figure: 3.2 Survival profiles of 8-week-old B6.WT and B6.IFN-γ-/- mice infected with WNV. Groups of 36 female mice/strain were inoculated i.p., $6x10^4$ pfu/mouse and monitored for signs of illness 3 times a day over 30 days. The percent survival at each time point is shown. There is a signifificant difference (P= 0.002 by Fisher Exact test) between survival data of B6.WT and B6.IFN-γ-/- mice. Mock-infected mice did not develop signs of illness.

Figure: 3.3 Brain sections stained with H and E from mock-infected and WNV-infected B6.WT and B6.IFN-γ-/- mice. Mock-infected brain parenchyma showing normal histology in B6.WT (a) and B6.IFN-γ-/- (b) mice. Infected brain parenchyma showing infiltration of leukocytes (solid arrows) and activated microglia with nodule (open arrow) in B6.WT (c) Infected brain parenchyma showing infiltration of leukocytes (solid arrows) in B6.IFN-γ-/- (d) mice. Marked meningitis was observed in both B6.WT (e) and B6.IFN-γ-/- (f) mice. Adherent inflammatory leukocytes (solid arrow) on cerebrovascular endothelium during infection in B6.WT (g). Occasional frank haemorrhage (solid arrow) was observed in the brain parenchyma of infected B6.WT, associated with agonal convulsions (h). Scale bar = 50μm. Abbreviation: BV- blood vessel.

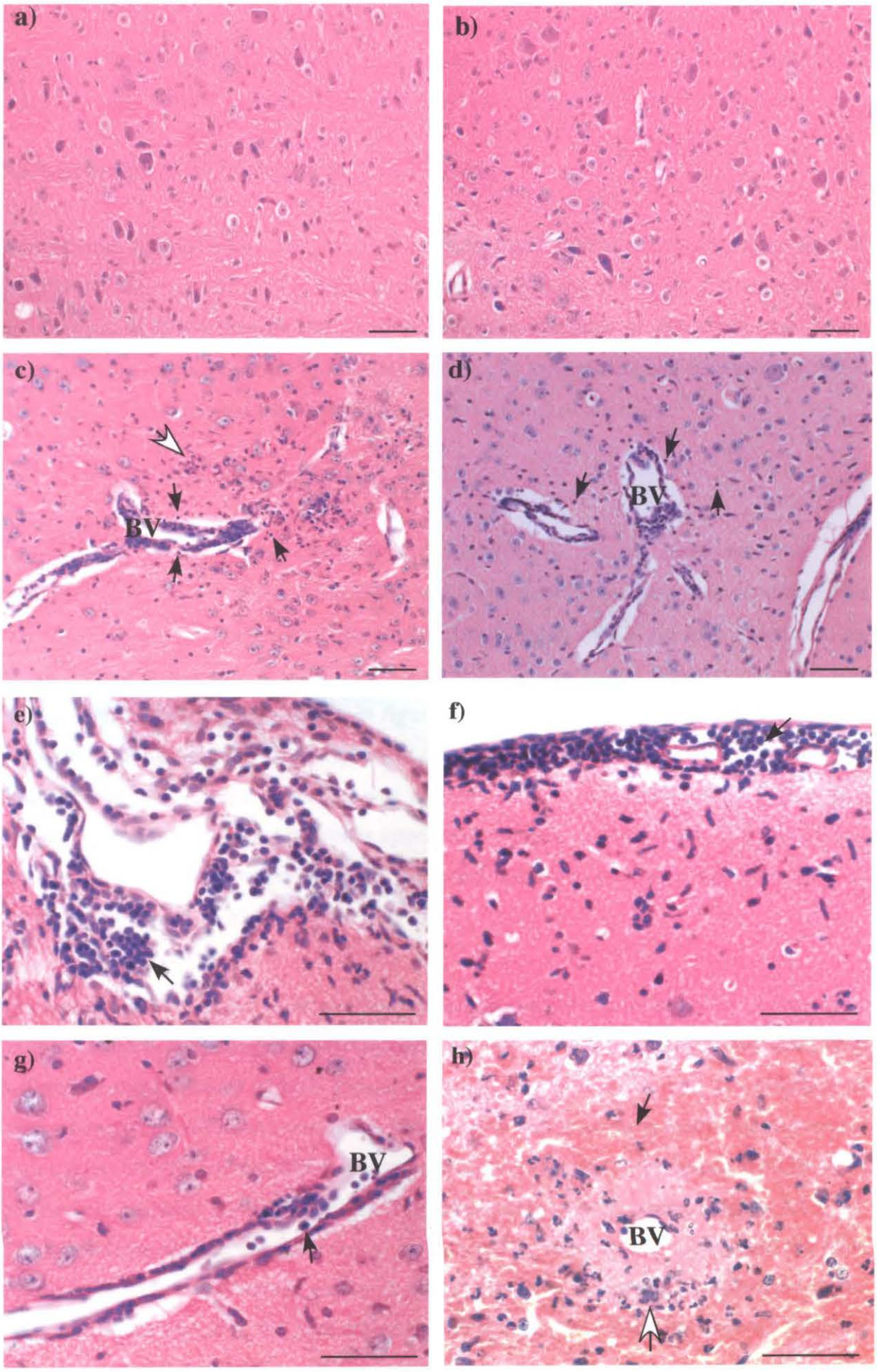
a)
b)
c)
BV
d)
BV
e)
f)
g)
BV
h)
BV

brain were observed to have frank haemorrhage into the brain parenchyma (Figure 3.3 h). In these mice, this finding was frequently associated clinically with agonal convulsions.

3.3.3. Detection of WNV antigen in the CNS tissue

Results from the preceding section clearly demonstrated that nearly twice the number of B6.IFN-γ-/- mice survived WNV infection compared to B6.WT mice. To elucidate the involvement of IFN-γ through the course of infection, the sites of WNV infection in the CNS, possible routes of access to the CNS, kinetics of progression and clearance of WNV from the CNS parenchyma was investigated in both groups of mice.

3.3.3.1. Sites of infection in the brain

Groups of 120 mice from B6.WT and B6.IFN-γ-/- strains were infected with $6x10^4$pfu/mouse, as described in Materials and Methods. Plaque assay was undertaken on brains from days 1-11 p.i. Immunoperoxidase labelling for WNV Ag was undertaken on brains from days 3, 5, 6, 7, 8, 9, 10, 11, 15 and 30 p.i. The pattern of infection observed was similar in both groups and is shown in figure 3.4. Positive staining was found only from day 6 p.i. in brain parenchyma, independent of clinical illness, and was first observed in the brainstem in both groups. Viral Ag was detected only in neurones and their processes (Figure 3.4 e, f) and infected neurones appeared morphologically normal. The number of infected neurones was increased after day 6 p.i. and was found predominantly in the base of the brain (Figure 3.4. g, h).

The brainstem, base of the brain and cerebral cortex were the principal sites of detectable virus infection in the brain. Occasional pyramidal cells of the hippocampus were detectably infected in some animals of both groups on day 9 p.i. (data not shown). No infection of other parenchymal cells was seen and no viral antigen was detected in mock-infected mouse brains from B6.WT and B6.IFN-γ-/- groups (Figure 3.4 a, b). Neurones in the OB were consistently negative for WNV antigen at all timepoints in both groups (Figure 3.4 c, d). The cerebellum was rarely observed to be infected in either group throughout the time course of infection. Extremely rarely (1 out of 194), microvascular endothelium in the brainstem stained positive for viral antigen in B6.WT on day 6 (data not shown). Infection of ependymal and choroid plexus cells and meninges was never observed.

Figure: 3.4 Brain sections from mock-infected and WNV-infected B6.WT and B6.IFN-γ-/- mice labeled for WNV antigen. Immunoperoxidase labelling with rat anti-WNV and DAB substrate was used for the detection of viral antigen. Sections were briefly stained with haematoxylin as a counterstain. Mock-infected brainstem showing negative labelling for WNV antigen in both B6.WT (a) and B6.IFN-γ-/- (b) mice. WNV antigen was first detected in the brainstem neurones in both B6.WT (e) and B6.IFN-γ-/- (f) mice on day 6 p.i. and was found only in the cytoplasm and processes of neurones (solid arrows). Olfactory bulbs of infected mice from both groups were negative on day 5 p.i. (c) and day 6 p.i (d) in both strains. The number of infected neurones was increased on day 8 p.i. in B6.WT (e) and B6.IFN-γ-/- (f), and was observed in the base of the brain at this timepoint. Scale bar = 50μm.

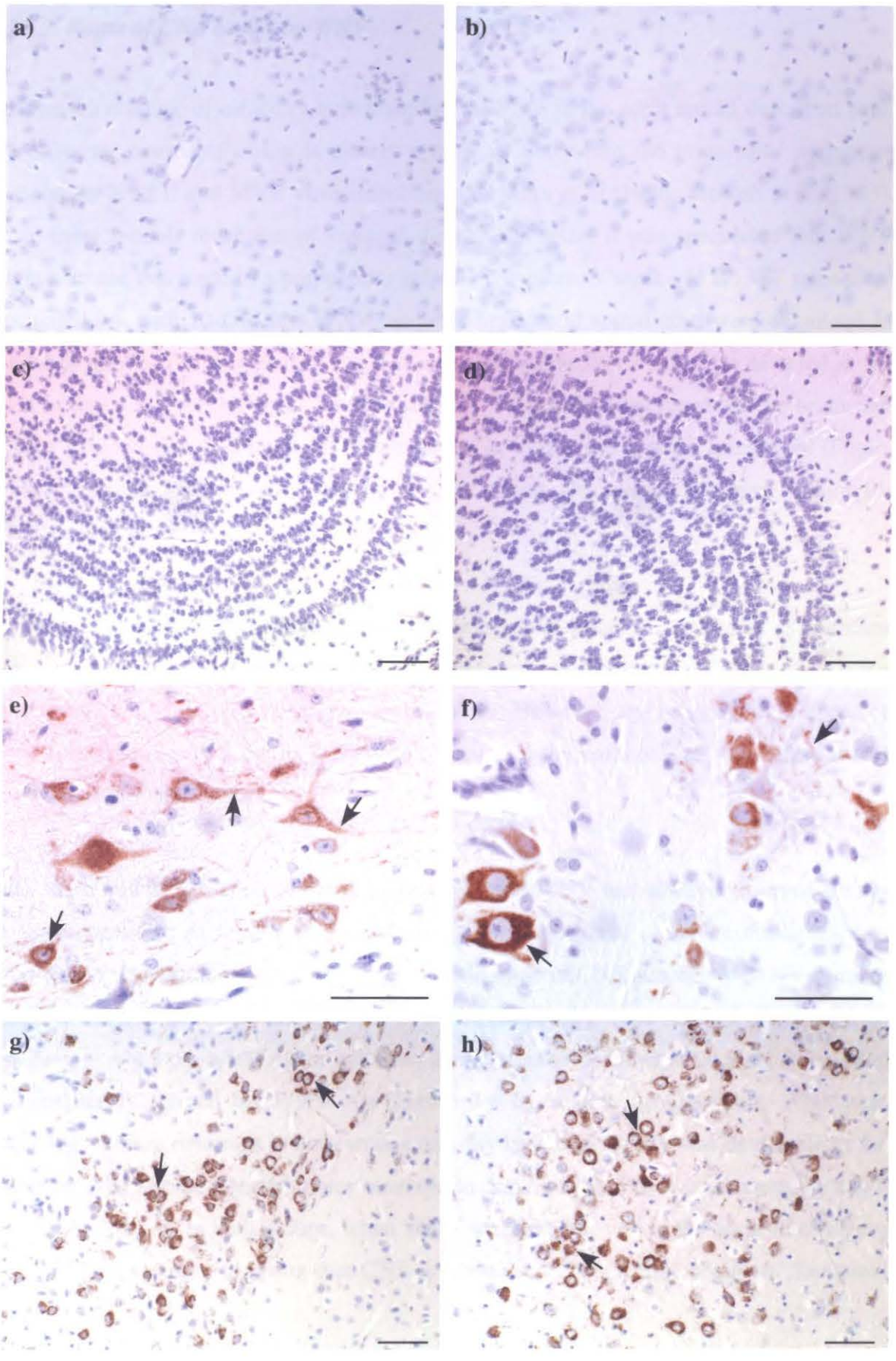
a)
b)
c)
d)
e)
f)
g)
h)

3.3.3.2. Route of CNS access by WNV

Despite the absence of olfactory bulb staining for WNV in the adult model described here, the olfactory neuroepithelium is clearly a route of entry into the brain after peripheral inoculation in SLE and MVE virus infections (McMinn *et al.* 1996; Monath *et al.* 1983). Since these models make use of young 3-4-week-old mice, it was speculated that WNV might also use this route in a prepubertal animal. Therefore, 3-week-old B6.WT mice were inoculated i.p. with 10-fold less WNV, and the brains and spinal cord were examined as described above. The time course experiment showed that WNV was first detected in the brain at day 4 p.i. At this time, positive staining was observed throughout the brainstem (Figure 3.5 a), thalamus (Figure 3.5 b) and cortex, as well as the cervical spinal cord (Figure 3.5 d), similar to the distribution seen in the adult mouse. However, no positive staining for WNV Ag was observed in the OB (Figure 3.5. b).

In young mice, viral Ag was detected only in the cytoplasm and the processes of neurones both in the spinal cords and the brain. These data indicate that age does not influence the route of infection and types of target cells for WNV. However, age influenced the speed of WNV spread to the CNS. Since WNV was observed in the brain at least 48h before it was detectable in the adult model.

Since there was no infection of the olfactory bulb and WNV was always observed first in the brainstem with extremely rare endothelial infection, spinal cords were examined to determine the infection of spinal cord and possible route of CNS access. No WNV staining at any level was observed in the spinal cord in both infected groups at day 4 (Figure 3.6 a). However, at day 5 p.i, a few motor neurones from the anterior horns of cervical spinal cord was postitively stained for WNV Ag (Figure 3.6 b) in both groups. Thus WNV was detectable in these neurones in both strains one day before WNV Ag was detectable in the brainstem. Numbers of infected motor neurones in the spinal cord further increased by day 6 p.i. (Figure 3.6 c, d) in both groups, when WNV was first detected in the brainstem (Figure 3.4 e, f). This strongly suggests that CNS infection with WNV first begins in the spinal cord.

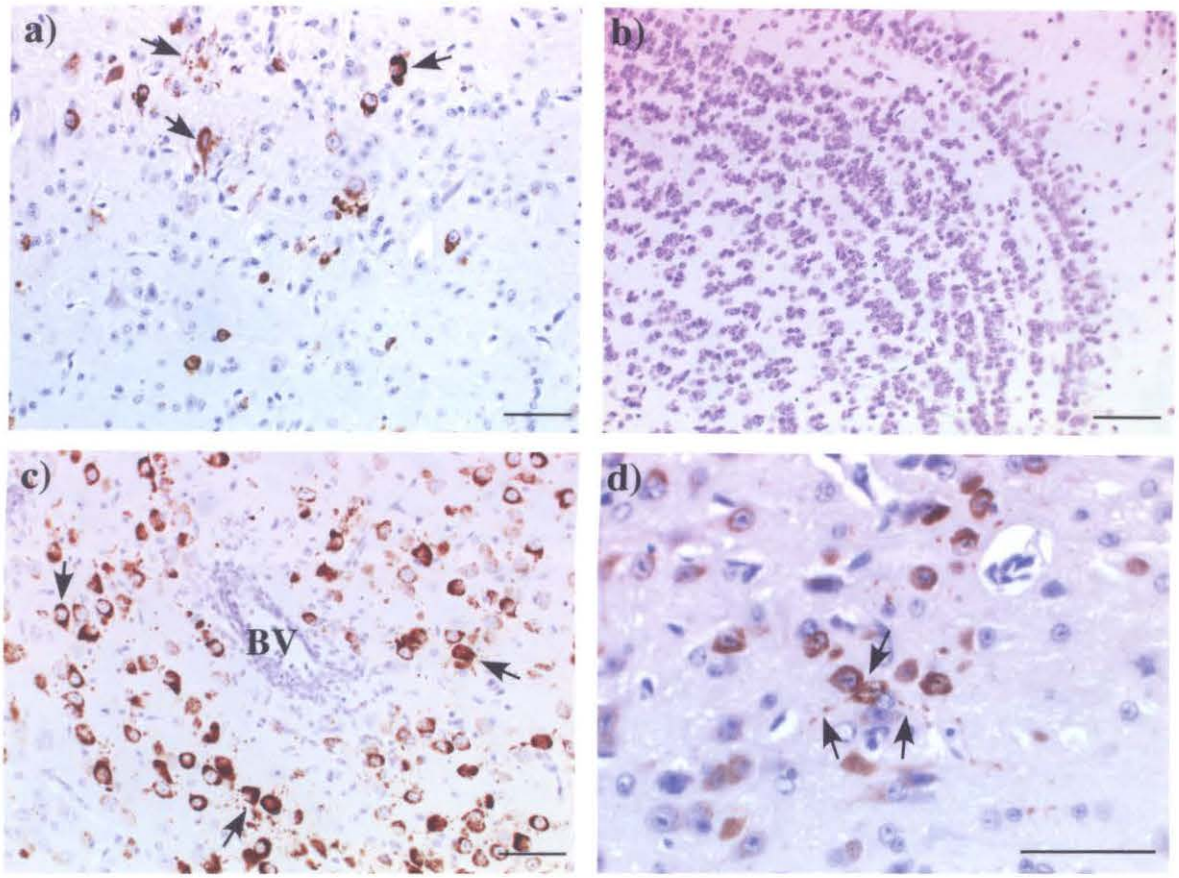

Figure: 3.5 Brain and cervical spinal cord sections from WNV-infected 3-week-old B6.WT mice labelled for WNV antigen. Immunoperoxidase labelling with rat anti-WNV and DAB substrate was used for the detection of viral antigen. Sections were briefly stained with haematoxylin as a counterstain. WNV antigen was detected in the brainstem (a) (solid arrows) and thalamus neurones on day 5 p.i. (c) (solid arrows). At the sametime, WNV antigen was also detected in the spinal cord neurones (d) (solid arrows). WNV antigen was found in the cytoplasm and processes of the neurones in both brain and spinal cord. However, olfactory bulbs of infected mice were consistently negative (b) on day 5 p.i. Scale bar = 50μm.
Abbreviation: BV- blood vessel.

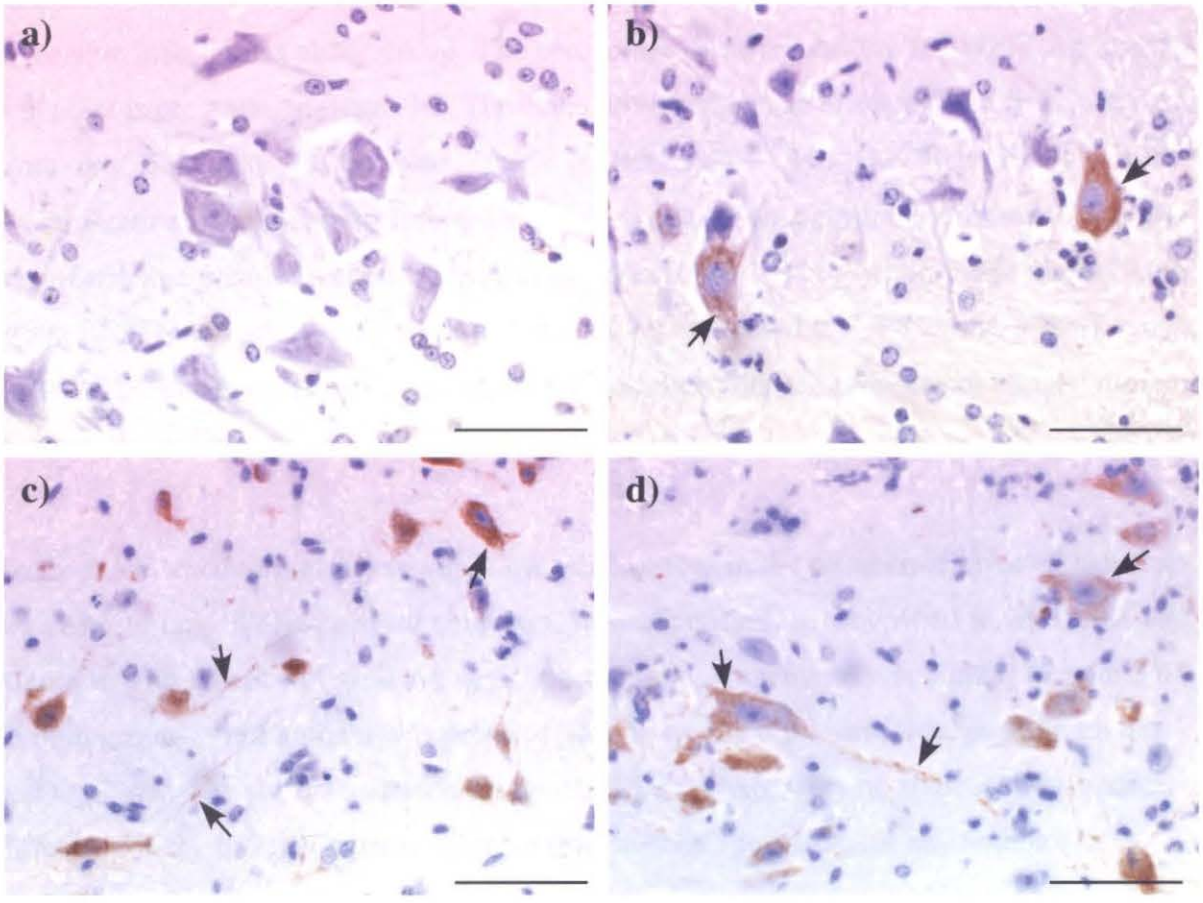

Figure: 3.6 Cervical spinal cord sections from WNV-infected B6.WT and B6.IFN-γ-/- mice labelled for WNV antigen. Immunoperoxidase labelling with rat anti-WNV and DAB substrate was used for the detection of viral antigen. Sections were briefly stained with haematoxylin as a counterstain. No WNV antigen was detected in the spinal cord on day 4 p.i. in either mouse strain (a). WNV antigen was detected in a few neurones of the spinal cord on day 5 p.i. (b) (solid arrows), 24h before it was detectable in the brainstem in both strains. The number of infected neurones was increased on day 6 p.i. in the spinal cords in both B6.WT (c) and B6.IFN-γ-/- (d) mice (solid arrows). Scale bar = 50μm.

3.3.3.3. Kinetics of progression and clearance of WNV

A greater proportion of B6.IFN-γ-/- than B6.WT mice had histologically detectable neuroneal infection between day 6 and 11 of infection. Outside of these days there was no detectable infection in either group. The percentage of mice positive for WNV Ag at each timepoint is presented in figure 3.7. The cumulative percentage of mice positive for viral Ag from day 6 to day 11 p.i. was 36.7% in B6.IFN-γ-/- and 14.9% in B6.WT mice. Quantification of numbers of infected neurones showed no significant difference between the groups that displayed signs of clinical disease. However, in asymptomatic mice, 29.6% of the B6.IFN-γ-/- group were positive for viral Ag compared to 7.4% of the B6.WT group (p=0.003). Thus the presence of virus did not correlate with the presence of clinical disease between the groups.

To evaluate whether there were significant differences in the number of infected neurones between groups, WNV-positive neurones were quantified, as described in Materials and Methods. The kinetics of viral Ag detection in brain parenchyma was similar (Figure 3.9). In both groups, viral antigen was detected only from day 6 p.i. onwards, peaking on day 7 and 8 p.i. and was always undetectable by day 15 p.i. There were no statistically significant difference in the mean number of infected cells between the groups at any timepoints.

Since there was no difference in the number of infected neurones between the groups, virus titres in the brain were determined by plaque assay to see whether there was a difference in virus load in the brain between the groups. These results can be seen in figure 3.8. In both groups of mice, replicating WNV was detected from day 6 p.i. This increased, peaking on day 8 p.i. and decreasing subsequently to be undetectable by day 10 p.i. in both groups of mice. The maximum virus titre was 2.22 $\log_{10}$ pfu/gram in B6.IFN-γ-/- and 2.23 $\log_{10}$ pfu/gram in B6.WT mice brain on day 8 p.i. Although there was a difference in the virus titres between the groups at earlier timepoints, there was no significant difference in the virus titres at any timepoints. This confirms the kinetics of WNV Ag detection in the brain parenchyma detected by IHC. Moreover, the virus titres suggest that WNV Ag detected by IHC on day 10 and 11 p.i. was from non-replicating WNV. These results indicate that IFN-γ does not play a critical role in the clearance of viral antigen from brain parenchyma.

Figure: 3.7 Percentage of mice positive for WNV-antigen: Groups, each of 120 mice, from B6.WT and B6.IFN-γ-/- strains were infected i.p. with $6x10^4$ pfu/mouse. Subgroups of mice in each strain were sacrificed from day 3 to 30 p.i. Immunoperoxidase labelling was used to detect viral antigen in the brain parenchyma of infected mice at each timepoint. Percentage of mice positive for WNV antigen throughout the time period is shown.

Figure: 3.8 Kinetics of WNV replication in the brain. Groups, each of 64 mice, from B6.WT and B6.IFN-γ-/- strains were infected i.p. with $6x10^4$ pfu/mouse. Subgroups of mice in each strain were sacrificed from day 1 to 11 p.i. Plaque assay was used to detect viral titre and replication in the brain of infected mice at each timepoint. Statistical analysis using ANOVA showed no significant difference in the titres between the groups. No viral antigen was detected in the brain of mock-infected mice from either group.

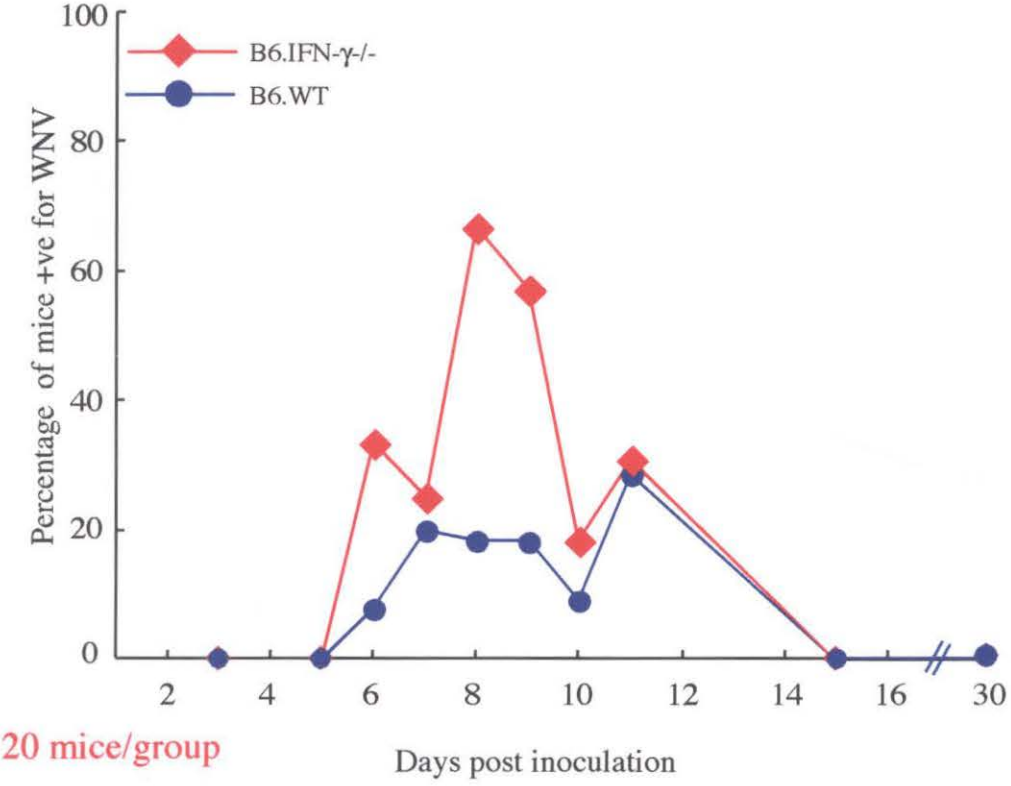

n = 120 mice/group

Figure: 3.7

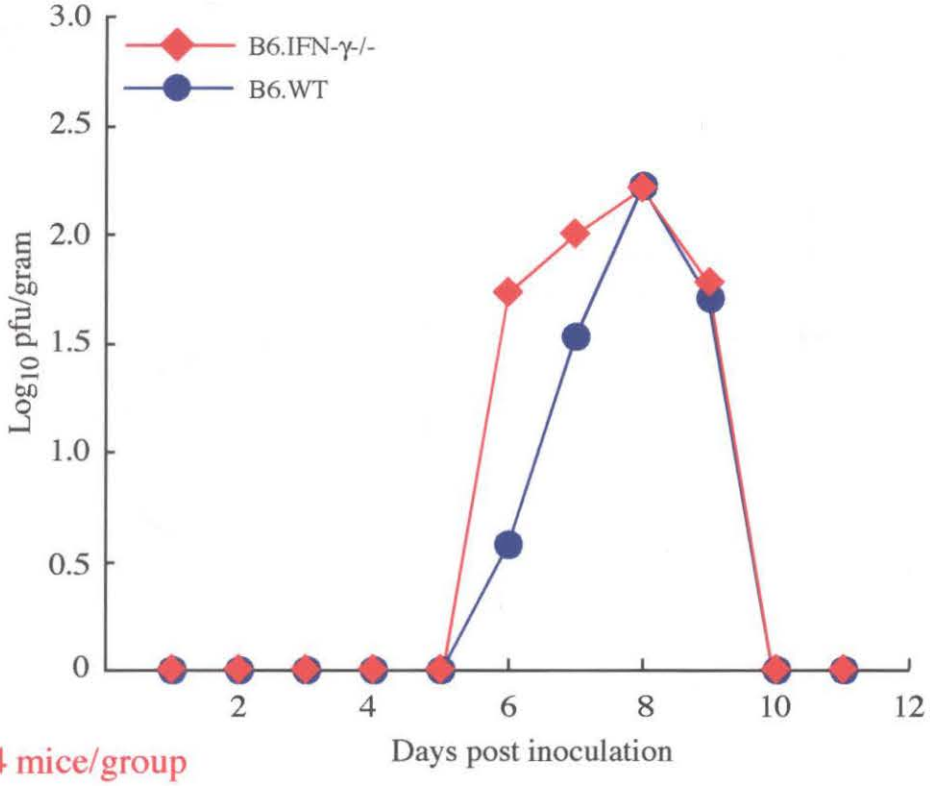

n = 64 mice/group

Figure: 3.8

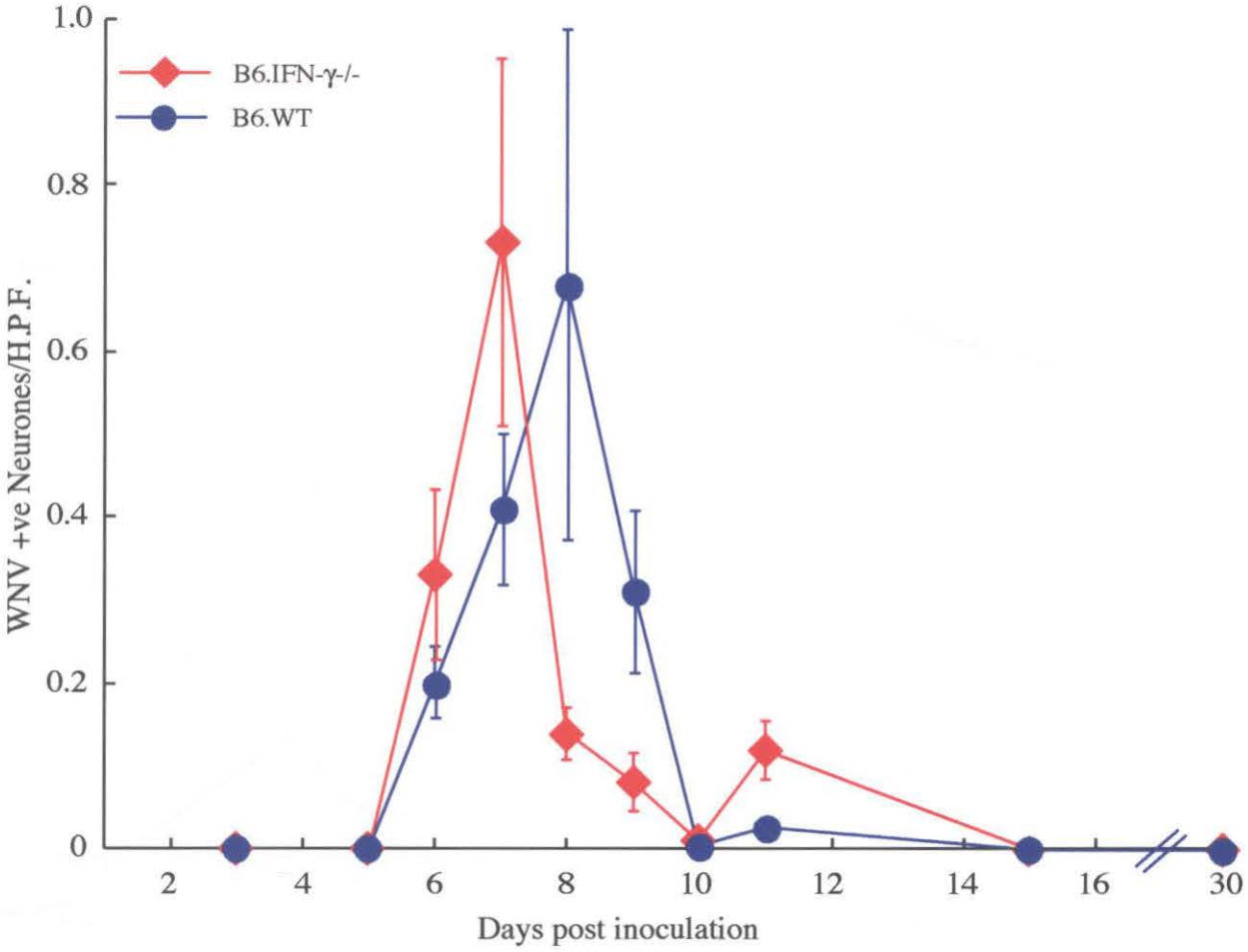

n = 120 mice/group

Figure: 3.9 Kinetics of WNV infection. Groups, each of 120 mice, from B6.IFN-γ-/- and B6.WT strains were infected i.p. with $6x10^4$ pfu/mouse. Subgroups of mice in each strain were sacrificed from day 3 to 30 p.i. Immunoperoxidase labelling was used to detect viral antigen in the brain parenchyma of infected mice at each timepoint. The number of neurones positive for viral antigen was counted, as described in materials and methods. Sixty H.P.F. were counted per mouse brain and values for each timepoint amalgamated and expressed as mean ± SEM. Statistical analysis using ANOVA showed no significant difference in the numbers of infected neurones between the groups. No viral antigen was detected in the brain parenchyma of mock-infected mice from either group.

However, absence of IFN-γ results in a greater number of mice acquiring detectable neuronal infection.

3.3.4. Kinetics of leukocyte infiltration

Since IFN-γ plays a role in the activation and recruitment of cells to inflammatory sites, the kinetics of appearance and disappearance of infiltrating leukocytes in brain parenchyma was assessed on H& E-stained brain sections from the same mice as used to determine the kinetics of viral Ag expression. In both groups, leukocytes initially appeared in the meninges and brain parenchyma from day 5 p.i. onwards. Numbers of leukocytes were counted in the defined areas of the brain parenchyma, as described in Materials and Methods, and are shown in figure 3.10.

In both strains, the kinetics of leukocyte infiltration was similar. However, the number of leukocytes infiltrating was significantly greater in the B6.WT than B6.IFN-γ-/- brains on day 7 (p=<0.001). In B6.WT, infiltration was clearly evident from day 6 p.i., although some leukocyte infiltration on day 5 was observed in a few mice. Infiltration was significantly higher on day 7 (p=<0.001), compared to day 6, significantly decreasing by day 9 p.i (p=<0.001), compared to day 7, and completely returning to baseline values in survivors by day 30 p.i. In B6.IFN-γ-/- mice, infiltration was observable from day 5, peaked on day 8, decreased by day 9 and returned to baseline values by day 30 p.i. However, there were no stastistically significant differences between the values obtained at any of these timepoints in this group. Despite the marked reduction of parenchymal leukocyte infiltration between days 11 and 15, conspicuous meningeal infiltration was still observed in both strains during this period, but this had returned to baseline levels by day 30 p.i. These data indicate that IFN-γ is important for the recruitment of the full complement of leukocytes to the brain.

3.3.5. Blood-brain barrier status

Fibrinogen is part of the blood clotting cascade as factor I and does not normally pass into the brain parenchyma in the presence of an intact blood brain barrier (BBB) (Reese *et al.* 1967). Thus extravascular detection in the brain parenchyma is considered a marker of increased BBB permeability. Fibrinogen lebelling has been used to demonstrate BBB breakdown in HIV encephalitis (Dallasta *et al.* 1999), Alzheimers disease (Mori *et al.*

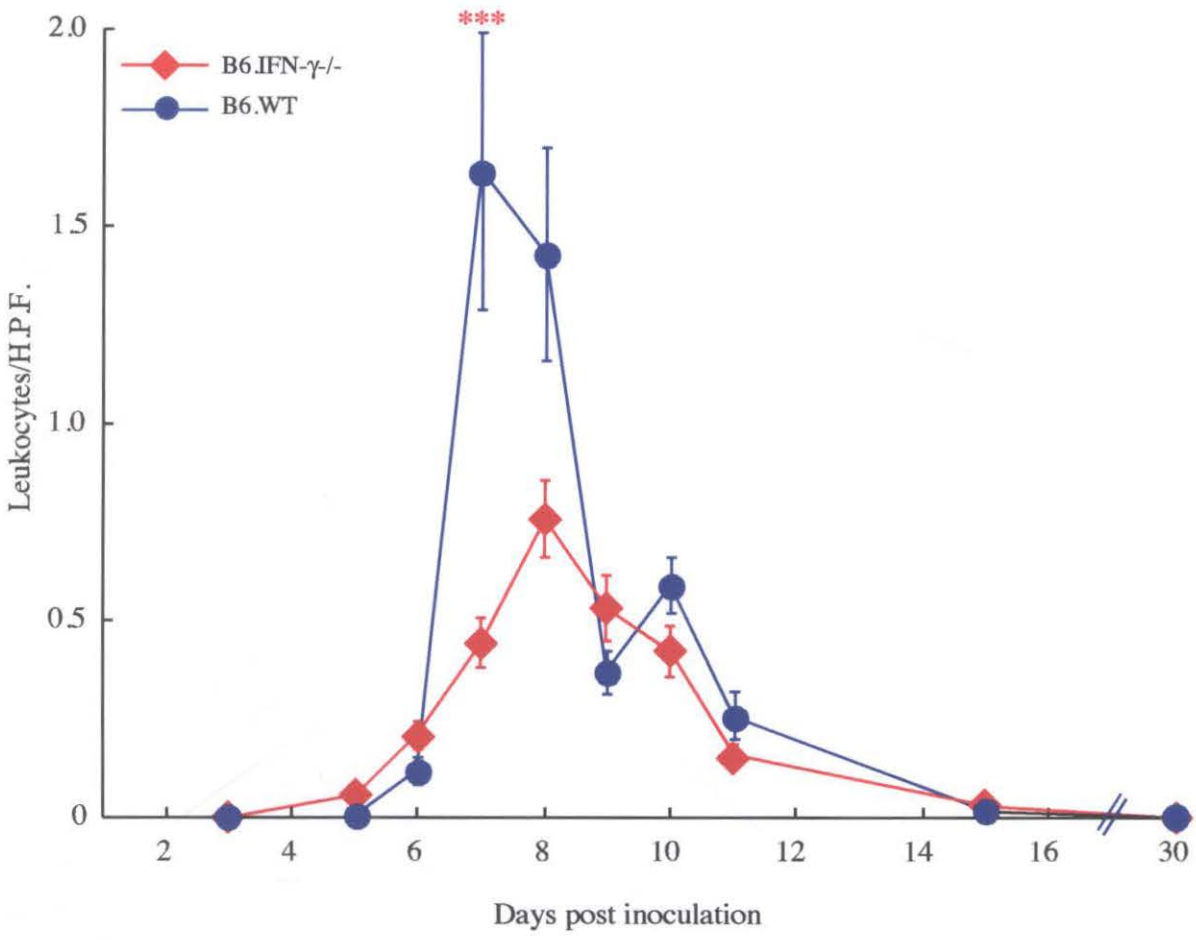

n = 120 mice/group

Figure: 3.10 Kinetics of leukocyte infiltration. Groups, each of 120 mice, from B6.WT and B6.IFN-γ-/- strains were infected i.p. with $6x10^4$ pfu/mouse. Subgroups of mice in each strain were sacrificed from day 3 to 30 p.i. H and E stained sections were used to quantify leukocyte infiltration in brain parenchyma. Sixty H.P.F. were counted per mouse brain, as described in materials and methods, and values for each timepoint amalgamated and expressed as mean ± SEM. There was a significant difference at day 7 p.i. between B6.WT and B6.IFN-γ-/- values (***p=<0.001 by ANOVA). No leukocyte infiltration was found in the brain parenchyma of mock-infected mice from either groups.

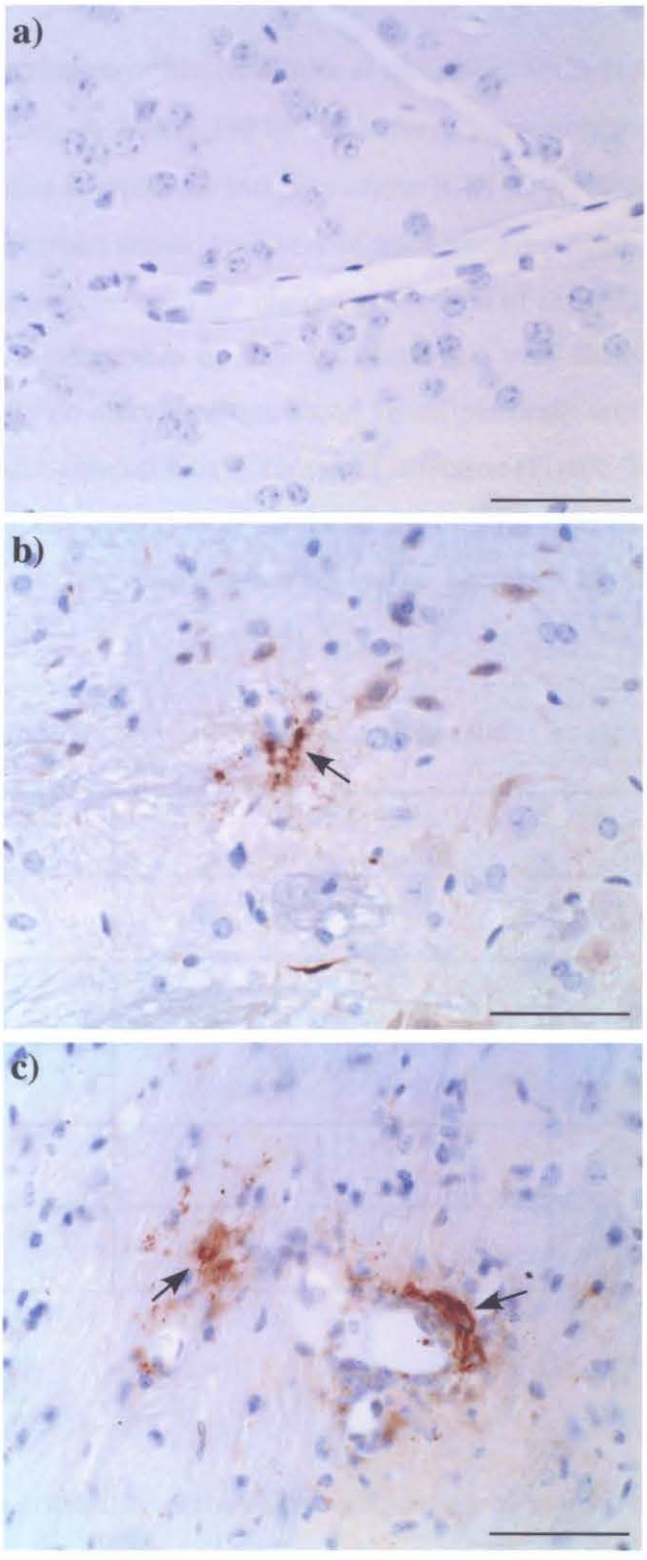

Figure: 3.11 Brain sections from mock-infected and WNV-infected B6.WT and B6.IFN-γ-/- mice labelled for extravascular fibrinogen. Immunoperoxidase labelling with rabbit anti-fibrinogen and DAB substrate was used for the detection of fibrinogen leaking blood vessels. Sections were briefly stained with haematoxylin as a counterstain. No extravascular fibrinogen was found in mock-infected brain parenchyma in both B6.WT and B6.IFN-γ-/- (a) mice. Extravascular fibrinogen was detected in very few mice in both B6.WT (b) (solid arrow) and B6.IFN-γ-/- (c) (solid arrows) mice. Scale bar = 50μm.

1991), SFV encephalomyelitis (Eralinna *et al.* 1996; Soilu-Hanninen *et al.* 1994) acute demyelination (Gay & Esiri, 1991). Therefore, immunohistochemical localization of fibrinogen was used to study the integrity of the BBB in WNV encephalitis using the same matched mice described above. Numbers of mice showing fibrinogen leakage are shown in Table 3.1. Leakage occurred in the highest proportion of animals between days 7 and 9 and was reduced or undetectable by day 10. However, very little perivascular staining for fibrinogen (usually no more than one blood vessel per brain section) was detected in either group of mice throughout the time course of infection (Figure 3.11 b, c). Moreover, it did not correlate with the detection of viral antigen or with sites of leukocyte infiltration and WNV antigen was frequently detected in the presence of an intact BBB during the observation period.

Table: 3.1 Proportion of mice showing fibrinogen staining at various timepoints p.i.

Days post infection	**B6.WT % (no. of mice/total)**	**B6.IFN-γ-/- % (no. of mice/total)**
6	0.0 (0/8)	14.2 (1/7)
7	12.5 (1/8)	28.5 (2/7)
8	0.0 (0/5)	0.0 (0/6)
9	33.3 (2/6)	25.0 (1/4)
10	16.6 (1/6)	0.0 (0/7)

3.4. Discussion

Since IFN-γ is a critical cytokine in the eradication of many viruses, the pathogenesis of WNV encephalitis in normal and IFN-γ-deficient mice was evaluated, using an adult model of WNV encephalitis developed in this project. Several studies on IFN-γ and IFN-γR gene knockout mice have shown that IFN-γ confers resistance to several microbial infections, including viruses (Nansen *et al.* 1998; Yu *et al.* 1996; Rodriguez *et al.* 1995; Utermohlen *et al.* 1996; Huang *et al.* 1993; Bouley *et al.* 1995; Karupiah *et al.* 1990), bacteria (Barbic *et al.* 1997; Rubbins *et al.* 1997), rickettsia (Li *et al.* 1987), fungi (Balish *et al.* 1998) and

parasites (Wang *et al.* 1994; Suzuki *et al.* 2000), although the response to influenza A (Graham *et al.* 1993), murine gammaherpesvirus 68 (Sarawar *et al.* 1997) and SFV, VSV (Muller *et al.* 1994) appears unchanged in the genetic absence of IFN-γ or IFN-γ receptor. In contrast, my study shows that absence of IFN-γ is associated with a marked reduction in mortality from approximately 60% in B6.WT to some 17% in B6.IFN-γ-/- mice (Figure 3.2) in WNV infection. IFN-γ gene knockout mice were more resistant to fatal disease compared to wild type and were completely resistant to secondary challenge WNV at a 50-fold higher dose than the first. Thus IFN-γ is not critical for survival in either primary or secondary WNV infection. Moreover, it may exacerbate disease.

Detection of WNV in the CNS was restricted to the cytoplasm and major dendrites of neurones in both groups of mice. There was no evidence of infection in glial cells, ependyma, choroid plexus or meninges. Thus absence of IFN-γ does not alter the susceptibility to infection of different types of resident brain cells. Due to the lack of MHC-I on neurones in response to cytokine stimulation (Neumann 2001; Neumann & Wekerle 1998) and viral infection *in vivo* (Kimura & Griffin 2000), neurones are more vulnerable to infection compared to other CNS resident cells and enable certain viruses to escape immune regulation by virus-specific $CD8^+$ T cells. Thus, neurones are a favoured site for the persistence of both productive and latent viral infection (Levine & Griffin 1992). Previous studies on neurotropic flaviviruses have also shown infection of neurones only, and not glia or endothelial cells (Shieh *et al.* 2000; McMinn *et al.* 1996; Iwasaki *et al.* 1986; Monath *et al.* 1983; Pogodina *et al.* 1983; Eldadah & Nathanson 1967). Since *in vitro* astrocytes and microglia readily become infected (Liu *et al.* 1989, Dr. Nicholas JC. King, USYD, personal communication), this apparent cellular specificity within the CNS seems unlikely to indicate the exclusive expression of specific receptors for WNV at the neuronal surface and seems more in keeping with a possible mode of neurone-to-neurone spread.

Neurotropic viruses can invade the CNS across the BBB via infected endothelial cells (Wisniewski *et al.* 1983), access presumably being further facilitated by destruction of the BBB (Soilu-Hanninen *et al.* 1994; Johnson 1964) or may be transported through the endothelial cells without replication (Coffin & Lu 1957; Liou & Hsu 1998) or via diapedesis of infected leukocytes (Dallasta *et al.* 1999). Despite their *in vitro* susceptibility

to infection (Shen *et al.* 1997), endothelial infection was rarely observed in the brain in my model. Moreover, while destruction of BBB in WNV encephalitis occurred in a few mice in both groups (Table 3.1 and Figure 3.11), WNV was usually detectable in neurones without evidence of BBB disruption. *Vice versa,* evidence of BBB destruction was not necessarily accompanied by detectable WNV in neurones. A similar result was found in Borna disease, in which viral Ag was detected in the brain parenchyma in the presence of intact BBB (Hatalski *et al.* 1998). Since no infection of infiltrating leukocytes in the brain parenchyma was observed at any timepoints in my study, this route of infection also seems unlikely. Thus in the absence of a meticulous transmission electron microscopic study to exclude it, a cerebrovascular transendothelial transport route of WNV entry into the brain remains a possibility in this model.

The olfactory neuroepithelium is thought to be a portal of entry into the CNS from the circulation after peripheral inoculation for several neurotropic viruses. For example, SLE (Monath *et al.* 1983), TBE (Albrecht 1962), MVE (McMinn *et al.* 1996), Venezuelan equine encephalitis (VEE) (Vogel *et al.* 1996; Charles *et al.* 1995) and neurovirulent influenza virus A (Reinacher *et al.* 1983). In my model there was no detectable WNV Ag in the OB at any point during the period of infection. In both groups, viral Ag was first detectable in the spinal cord at day 5 p.i., in the brainstem on day 6 and in other adjacent areas after this in a similar pattern in both groups (Figure 3.4 and 3.6). Since this WNV model is in adult mice, young 3-week-old mice were infected with WNV i.p. to evaluate whether age influences the route of access of WNV to the brain. Interestingly, patterns of WNV Ag detection in the young mouse model (Figure 3.5) were also similar to the adult model. It seems unlikely, therefore, that CNS invasion occurred via the OB in this model, or that the absence of IFN-γ influences this route of infection. This leaves open the possibility that peripheral nerves may be the route of CNS invasion in WNV in this model. Kundin *et al.* (1962) demonstrated that WNV can infect peripheral nerves and Shieh *et al.* (2000) have shown that WNV Ag was detectable in the neurones of brainstem and spinal cords of fatally infected human cases. The time course experiment in our model showed the infection of motor neurones in the cervical spinal cord one day before WNV Ag was detected in the brainstem. This suggests that infection of the spinal cord may occur via retrograde axonal transport in motor nerves supplying infected striated muscle. Several animal models of viral encephalitis have demonstrated that neurotropic viruses can use pheripheral nerves as a

route of CNS invasion from the periphery, such as rabies (Tang *et al.* 1999; Murphy *et al.* 1973), human poliovirus (Nathanson & Bodian 1961), Borna disease virus (Carbone *et al.* 1987) models, for example. These viruses replicate within nerves and are moved through the host by the axonal transport system of neurones.

Several studies in animal models of viral encephalitis have demonstrated the requirement of IFN-γ for the control of viral infection in the CNS (Bartholdy *et al.* 2000; Geiger *et al.* 1997; Parra *et al.* 1999; Christensen *et al.* 1999; Nansen *et al.* 1999; Rodriguez *et al.* 1995; Finke *et al.* 1995) Lewandowski *et al.* (1998) demonstrated that mice deficient in IFN-γ production in the CNS had increased neuronal infection and death from HSV infection. Tishon *et al.* (1995) showed that IFN-γ is required for the termination of persistent viral infection. Moreover, the athymic nude mouse model (immunodeficient mice) illustrate the role of IFN-γ in viral infection (Kohonen-Corish *et al.* 1990). In contrast, in the WNV model, both the kinetics of infection, virus titres and the numbers of neurones infected were similar in B6.WT and B6.IFN-γ -/- mice (Figure 3.8 and 3.9), although significantly greater numbers of B6.IFN-γ-/- mice manifested detectable neuronal infection, compared to B6.WT (Figure 3.7). However, virus was still cleared from the CNS in the absence of IFN-γ. This indicates that IFN-γ is not required for the clearance of WNV.

Inflammation is typical of a variety of CNS diseases and leukocyte recruitment to the CNS is a hallmark feature of viral encephalitis (Lassmann 1997). It is an important component of host defence and is often required for elimination of virus from the CNS. IFN-γ is thought to play a role in the recruitment of inflammatory leukocytes in numbers of viral infections (Liu & Chambers 2001; Baumgarth & Kelso 1996). Consistent with this, the numbers of infiltrating leukocytes in the CNS parenchyma were significantly reduced in the absence of IFN-γ in my model. In the B6.WT brain, maximal infiltration on day 7 p.i. was approximately 4-fold that in the B6.IFN-γ-/- (Figure 3.10), suggesting that IFN-γ plays an important role in the cerebral recruitment and extravasation of leukocytes in WNV encephalitis. There was no observable difference in morphology between the infiltrating cell populations seen in brains from either group. Whether there are functional differences in various leukocyte subsets infiltrating into the brain or whether the pathogenesis of

encephalitis is linked merely to quantitative differences in leukocyte infiltration is not clear yet.

In the CNS parenchyma, IFN-γ like immunoreactivity has been observed in the neurones previously (Kiefer & Kreutzberg 1990) and recently, it has been confirmed that neurones can produce IFN-γ (Mori *et al.* 2001). IFN-γ mRNA, although not IFN-γ protein, has been detected in purified cultures of astrocytes and microglia (Benveniste 1998). Recently, Morris & Esiri (1998) observed the constitutive expression of IFN-γ at low levels in scattered microglia and some microvascular endothelium both in the normal and inflamed brain. However, although CNS resident cells are capable of producing IFN-γ, the major source of IFN-γ in the CNS in many viral encephalitides and CNS disorders has been ascribed to infiltrating T cells (Binder & Griffin 2001; Hammarberg *et al.* 2000; Finke *et al.* 1995; Cantin *et al.* 1995; Krakowski & Owens 1996). Therefore, T cells play a decisive role in the course and clinical outcome of viral CNS infection via secretion of IFN-γ. The T cells that infiltrate into the CNS in viral encephalitis are activated and produce numbers of proinflammatory cytokines, including IFN-γ, which is essential for the elimination of virus from the CNS in numbers of viral infections as discussed before, however, my study suggests a role for IFN-γ in exacerbating disease in WNV encephalitis.

There is strong evidence that IFN-γ is a major disease-promoting cytokine. A small clinical trial during early 1980s using systemic administration of IFN-γ was found to exacerbate disease in MS patients (Popko *et al.* 1997). Detection of IFN-γ in *post mortem* samples of MS patients as well as detection of increased numbers of IFN-γ-secreting T cells in the CSF of patients further support a role for IFN-γ in disease exacerbation (Billiau 1996). MS is a chronic inflammatory neurological disease characterized by infiltration of leukocytes into the CNS, localized myelin destruction, and loss of oligodendrocytes and axons (Al-Omaishi *et al.* 1999). The role of IFN-γ in disease exacerbation has been studied well in EAE, an animal model for MS. In this model, IFN-γ produced by infiltrating activated T cells in the CNS is thought to be a key mediator of inflammation that induces pathogenesis of immune-mediated demyelinating disorders since these processes can be inhibited by anti-IFN-γ Abs (Olsson 1995). Moreover, adoptive transfer of IFN-γ-secreting T cells isolated

from animals affected by EAE can cause EAE themselves in naïve animals (Popko *et al.* 1997).

The immunopathological role of IFN-γ in viral infections is poorly understood. LCMV has been extensively studied as a model of viral induced immunopathology, mediated by $CD8^+$ T cells (Doherty & Zinkernagel 1974; Zinkernagel 1992). However, how T cells mediate immunopathology in LCMV infection is still unknown. Although, Leist *et al.* (1989) demonstrated that treatment of mice with sheep anti-IFN-γ Ab protect them from lethal LCMV infection despite enhanced LCMV replication in the CNS compared to control mice, it was not well clear that IFN-γ was the cause of immunopathology in this model.

In conclusion my model of WNV encephalitis clinically and histopathologically very similar to that seen in humans. This makes it relevant to the study of human disease. IFN-γ is not important for survival in WNV encephalitis or generation of secondary anti-WNV immunity and clearance of WNV from the CNS, but is on the contrary critically involved in exacerbating disease. Only neurones are infected in WNV encephalitis and lack of IFN-γ did not alter the susceptibility of CNS resident cells. WNV may enter into the brain via axonal pathways through the spinal cord both in the presence and absence of IFN-γ. Leukocyte recruitment is significantly reduced in the absence of IFN-γ and may be the major source of IFN-γ in wild type mice. IFN-γ on its own or in combination with other proinflammatory cytokines, could influence the CNS immune response as well as CNS functions via inducing to release several other cytokines, reactive oxygen species, NO and IDO. The precise mechanisms by which IFN-γ exerts its function in exacerbating disease in WNV encephalitis are unknown. Taken together, these results suggest that WNV encephalitis is an immunopathological disease.

Chapter-4

Microglia, not astrocytes are activated in WNV encephalitis

4.1. Introduction

Glial cells are supporting cells of the nervous system that help to maintain neuronal function and viability by providing both mechanical and metabolic support for neurones. Glial cells include microglia, astrocytes, oligodendrocytes and ependymal cells (Afifi & Bergman 1998). Oligodendrocytes provide support for neurones by producing the myelin sheath that insulates axons. Ependymal cells are modified to produce CSF by transport and secretion of materials derived from adjacent capillary vessels in the CNS and this provides a hydrostatic buffer in which CNS is suspended (Burkitt 1993; Afifi & Bergman 1998). Astrocytes provide trophic support for neurones, maintain the BBB, regulate extracellular pH and potassium ion levels, guide neuronal development, remove spent neurotransmitters and synthesize essential neurotrophic factors (reviewed in Schoneboom *et al.* 1999; Dong & Benveniste 2001; Patel *et al.* 1996). Microglia represent the defence cells of the CNS (Chao *et al.* 1994; Matyszak 1998; Kreutzberg 1996). Among glial cells, microglia and astrocytes represent two highly reactive glial cells which respond to infectious and inflammatory stimuli (Aloisi *et al.* 2000) by producing various kinds of cytokines, chemokines, cytotoxic metabolites and growth factors, as well as upregulating or inducing *de novo* expression of various receptor molecules that are implicated in immune reactivity in conjunction with the peripheral immune system (Chao *et al.* 1994; Merrill & Benveniste 1996; Brodie *et al.* 1997; Dallasta *et al.* 2000; Glabinski *et al.* 1999; Grzybicki *et al.* 1997; Benveniste 1992; Schijns *et al.* 1991; Persidsky *et al.* 1999; Sauder *et al.* 2000; Asensio *et al.* 1999)

Astrocytes are the largest of the glial cells and outnumber neurones 10-1 in the mammalian brain (Benveniste 1992). They are distributed throughout the CNS in close association with neurones and blood vessels. They can be distinguished by their large stellate shape comprising cell bodies with many radiating processes. Some of these processes form terminal expansions that are applied to the terminal blood vessels (Figure 4.2 a) (Carpenter

1991). Astrocytes contain bundles of intermediate filament of cytoskeletal protein, known as GFAP (Eddleston & Mucke 1993), having a molecular weight of 41-51 kDa depending upon the species (reviewed in Martin & O'Callaghan 1995). Several markers have been used for the identification of astrocytes, including S100β, GFAP and glutamate synthetase (reviewed in Mucke & Eddleston 1993). Morphological changes in astrocytes visualized with any of these markers are considered an indicator of a change in the function of these cells. Astrocytes are immunocompetent cells of the CNS. They can divide and multiply, and respond to various CNS infections and demyelinating diseases (Dong & Benveniste 2001; Benveniste 1992). This response is known as astrogliosis or reactive astrocytosis, characterized by an increase in the numbers and size of cells with enhanced expression of GFAP (Mucke & Eddleston 1993). Astrogliosis may also result from interference with blood supply (Buchanan 1951), since astrocytes extend their processes to the blood vessels for the exchange of metabolites and wastes to and from neurones (Dong & Benveniste 2001; Burkitt 1993). It has been observed that lack of astrogliosis in response to neuronal injury increases disease. Such dysfunction can lead to reduce neurotrophic support and increased neurotoxin levels with resultant neurological disease (Benveniste 1992).

In contrast to astrocytes, microglia are the smallest glial cells. They are ubiquitously distributed in the CNS, comprising up to 20% of the total glial cell population in the rodent brain and are located in close proximity to neurones in the grey matter and between fibre tracts in the white matter (Lawson 1990). It used to be thought that the CNS was an immune-privileged site due to the presence of the BBB, which isolates the CNS from peripheral immune system, lack of lymphatic drainage and low or absent expression of MHC molecules. But from several studies it is clear that microglia are part of a substantial immune response capability within the CNS (Cross & Woodroofe 2001; Mori *et al.* 2001; Chao *et al.* 1994) and are seen as the first line of defence in the CNS against infectious diseases, inflammation, brain tumors, neurodegeneration, etc., (Kreutzberg 1996). Microglia are considered to arise from the monocyte lineage that enter the brain during embryonic development in response to naturally occurring cell death (Moore & Thanos 1996) prior to the formation of the BBB (Davis *et al.* 1994). Within the developing CNS, monocytes transform into ramified cells through the intermediate form known as amoeboid microglia (Perry & Gordon 1988). Therefore, microglia are functionally related to peripheral tissue macrophages (Ling & Wong 1993). Like tissue macrophages, microglia are involved in the

local CNS immune responses. Once activated, they can destroy invading microorganisms (Kreutzberg 1996), remove cell debris and enhance neuronal survival by secreting many different neurotrophic factors, thus facilitating a return to normal tissue homeostasis (Nakajima & Kohsaka 1998).

In the normal adult brain, microglia display a ramified morphology with small somata and numerous processes radiating therefrom (Ling & Wong 1993). They exhibit a downregulated immunophenotype (Streit *et al.* 1999; Banati *et al.* 1993). These ramified microglia are thus known as resting microglia (Dickson *et al.* 1993) and are generally considered as inactive macrophages, capable of converting rapidly into the active phenotypes (Davis *et al.* 1994). These cells can divide and multiply during activation (Dickson *et al.* 1991) but do not divide while resting (Ling & Wong 1993). The function of resting microglia in the CNS is poorly understood, however, it has been suggested that they may contribute to the normal function of brain tissue by inactivating neurotransmitters, cleansing extracellular fluid and otherwise providing neurotrophic support (Davis *et al.* 1994). Unlike astrocytes, microglia and their processes are not specifically associated with blood vessels (Dickson *et al.* 1991).

Microglia function as intrinsic sensors to threats to the CNS, as indicated by rapid changes in their morphology (Greenfield 1997). The degree of activation or alteration in morphology reflects the severity of the injury (Streit *et al.* 1999). Activated microglia are characterized by larger cell bodies with shorter, stouter processes. This is the first stage of activation and these cells are still non-phagocytic in nature (Kreutzberg 1996). In the second stage of activation, microglia withdraw all processes and transform into phagocytic cells, and are termed microglia-derived brain macrophages (Streit *et al.* 1999). Phagocytic microglia are typically small and spherical, but also exhibit rod-shaped and other morphologies. These microglia are known as amoeboid or reactive microglia (Davis *et al.* 1994) and are a prominent feature of inflammatory conditions (Dickson *et al.* 1991). Thus, activation of microglia occurs in a graded fashion, however, this graded response can not be differentiated from the influx of monocytes with full macrophage capabilities, as can occur with destruction of the BBB from the circulation (Kato & Walz 2000). Both activated and phagocytic forms of microglia can return to the resting, ramified state (reviewed in Stence *et al.* 2001). Besides changes in morphology, activated microglia can also proliferate, migrate

to the site of injury (Cuadros & Navascues 1998), increase their synthesis of secretory products, as well as present Ag to infiltrating T cells by expressing MHC molecules (Moore & Thanos 1996; Stoll & Jander 1999; Havenith *et al.* 1998). Moreover, depending upon neuronal stress, microglia may displace synapses, known as synaptic stripping, to deafferentiate and isolate stressed neurones (Banati 1993). It has been suggested that microglial activation is induced by neurones (Sudo *et al.* 1998; Kreutzberg 1996). Moreover, increasing evidence suggests that glial cell activation is mediated by IFN-γ both *in vivo* and *in vitro* (Meda *et al.* 1995; Sethna *et al.* 1991; Yong *et al.* 1991). However, the actual mechanism by which microglia are activated and how this corresponds to the severity of neuronal injury is not fully understood.

Although astrocytes and microglia are activated in many viral infections of the CNS (Kure *et al.* 1990; Christian *et al.* 1996; Iwasaki *et al.* 1986; Sauder *et al.* 1999; Brodie *et al.* 1997) this process has not been studied in detail in any viral encephalitis model, including WNV encephalitis. For these reasons, the types of glial cells, the kinetics of their activation and the role of IFN-γ in this activation were investigated in WNV encephalitis by comparing CNS responses of IFN-γ-deficient mice with that of the congenic B6.WT mice.

4.2. Materials and Methods

4.2.1. Mice

Female, specific-pathogen free, 8-week-old B6.WT and B6.IFN-γ-/- mice, backcrossed to C57BL/6, were used.

4.2.2. Virus infection of mice and tissue preparation

A time course experiment was performed to determine the types of glial cell activated and the kinetics of activation, as well as their normalization in the CNS. Groups of 120 mice, each of B6.WT and B6.IFN-γ-/-, were inoculated with WNV i.p. at $6x10^4$ pfu/mouse. Tissues were collected and processed as described in section 2.2.2.2. Groups of 21 B6.WT mice were inoculated i.n. with $6x10^4$ pfu/mouse and tissues were collected and processed as described in section 2.2.2.2. Mice were mock-infected with DMEM as controls.

4.2.3. Histopathology

Serial sections from paraffin-embedded tissues used for immunohistochemistry and lectin histochemistry were routinely stained with H and E, and examined to evaluate the pathological changes, including glial cell activation, in both groups of mice.

4.2.4. Lectin histochemistry and Immunohistochemistry

Paraffin-embedded sections were used for both immunohistochemistry and lectin histochemistry.

- **Detection of activated microglia by lectin histochemistry**

Isolectin-B4 derived from *Griffonia simplifolia* (L-2140, Sigma Chemical Company) (GS-lectin) was used as a marker for the visualization of activated microglia in the brain. GS-lectin binds to glycoprotein α-D-galactose, which is important for cell recognition and adherence (Dickson *et al.* 1991). Cells of the monocyte/macrophage lineage, vascular precursor cells and vascular endothelium can be labelled with GS-lectin (Streit *et al.* 1987; Medana *et al.* 1997). Several reports suggest that increased staining intensity with GS-lectin correlate with activation of macrophages/microglia (Maddox *et al.* 1982; Streit *et al.* 1987; Medana *et al.* 1997).

After dewaxing, the sections were microwaved on high power in citrate buffer for 8 mins. After this treatment, sections were allowed to stand at RT° for 30 mins in citrate buffer, washed in Tris-buffer for 5 mins and endogeneous peroxidase activity was blocked, as described in section 2.2.3. Sections were washed 3 times with Tris-buffer for 10 mins and then incubated with 100μl of 1:50 diluted biotinylated GS-lectin for 3h at 4°C. After rinsing in Tris-buffer for 10 mins, sections were incubated with 100 μl of horseradish peroxidase complex, 1:100 dilution, according to the manufacturer's instructions. After this step, the rest of the procedure was identical to that described in section 2.2.3. Mock-infected brain sections were used as controls for GS-lectin labelling.

- **Detection of MHC-II expression**

After dewaxing the sections, Ag was retrieved with digestion of sections in papain (02310807, CSL, Australia) for 5 mins at RT°, according to the manufactures's instructions and washed in Tris-buffer. After blocking the endogeneous peroxidase activity and non-specific staining as described before, sections were then incubated with undiluted rat anti-mouse MHC-II Ab, a hybridoma (TIB 120: ATCC, M5/114.15.12) supernatant, overnight at 4°C. The rest of the staining procedure was identical to that described in section 2.2.3. Mock-infected brain sections from both groups of mice were used as controls for MHC-II expression and monoclonal rat IgG_2b was used as an isotype control for the primary antibody.

- **Detection of astrocyte activation by GFAP immunohistochemistry**

After dewaxing the sections, endogeneous peroxidase activity and non specific staining were blocked, as described in section 2.2.3. Sections were then incubated with 100μl of 1:750 diluted polyclonal rabbit anti-cow GFAP Ab (Z0334, Dako) for 1h at RT°. The rest of the staining procedure was as described in section 2.2.3. Mock-infected brain sections from both groups of mice were used as controls for GFAP upregulation and polyclonal rabbit IgG was used as an isotype control for the primary Ab.

- **Double labelling for WNV antigen and activated microglia**

Alkaline phosphatase substrate, 5-Bromo-4-Chloro-3-Indolyl Phosphate/Nitroblue Tetrazolium (BCIP/NBT, Vector Laboratories, Burlingame, CA), was used to give a blue cytoplasmic signal for WNV Ag whereas horseradish peroxidase substrate, DAB, was used to detect activated microglia. Activated microglia were detected as described above and WNV Ag was detected as described in section 3.2.3.

4.2.5. TUNEL labelling

After dewaxing, sections were stained for apoptosis using *In situ* Apoptosis detection kit, Apoptag® peroxidase (Intergen Company) according to the manufacturer's instructions.

4.2.6. Quantification of cells and data analysis

Quantification of cells and data were analysed as described in section 2.3 and 2.6 respectively. Figures are mean values ± SEM for the total number of fields examined from the indicated number of mice, n.

4.3. Results

4.3.1. Histopathological changes in the brain parenchyma during infection

The main aims of this study were to determine the extent and distribution of activated glial cells within the CNS in response to WNV infection and to characterize the types of activated glial cells. Brain sections from both groups of mice were stained routinely with H and E. Histology of mock-infected mouse brain was normal (Figure 4.1 a). Histopathological lesions were observed after infection in both groups. H and E stain showed activation of glial cells, including rod shaped morphology (Figure 4.1 b) with the formation of nodules (Figure 4.1 c) throughout the brain in B6.WT and B6.IFN-γ-/- mice as well as the presence of inflammatory cells. These were obsereved from day 7-11 p.i. in both groups of mice (Figure 4.1 b).

4.3.2. No Astrocytes activation in WNV encephalitis

Upregulation of GFAP was used as a marker for the activation of astrocytes in WNV encephalitis. Interestingly, no activation of astrocytes was observed at any of the timepoints in B6.WT and B6.IFN-γ-/- mice. Mock-infected brain parenchyma from both groups of mice showed low intensity GFAP staining of astrocytes (Figure 4.2 a). However, on day 10 p.i., in one B6.WT mouse a few astrocytes were activated in the brainstem, as demonstrated by increased GFAP staining (Figure 4.2 b), compared to astrocytes from mock-infected mice (Figure 4.2 a). This result suggests that astrocytes do not generally play a significant role in WNV encephalitis.

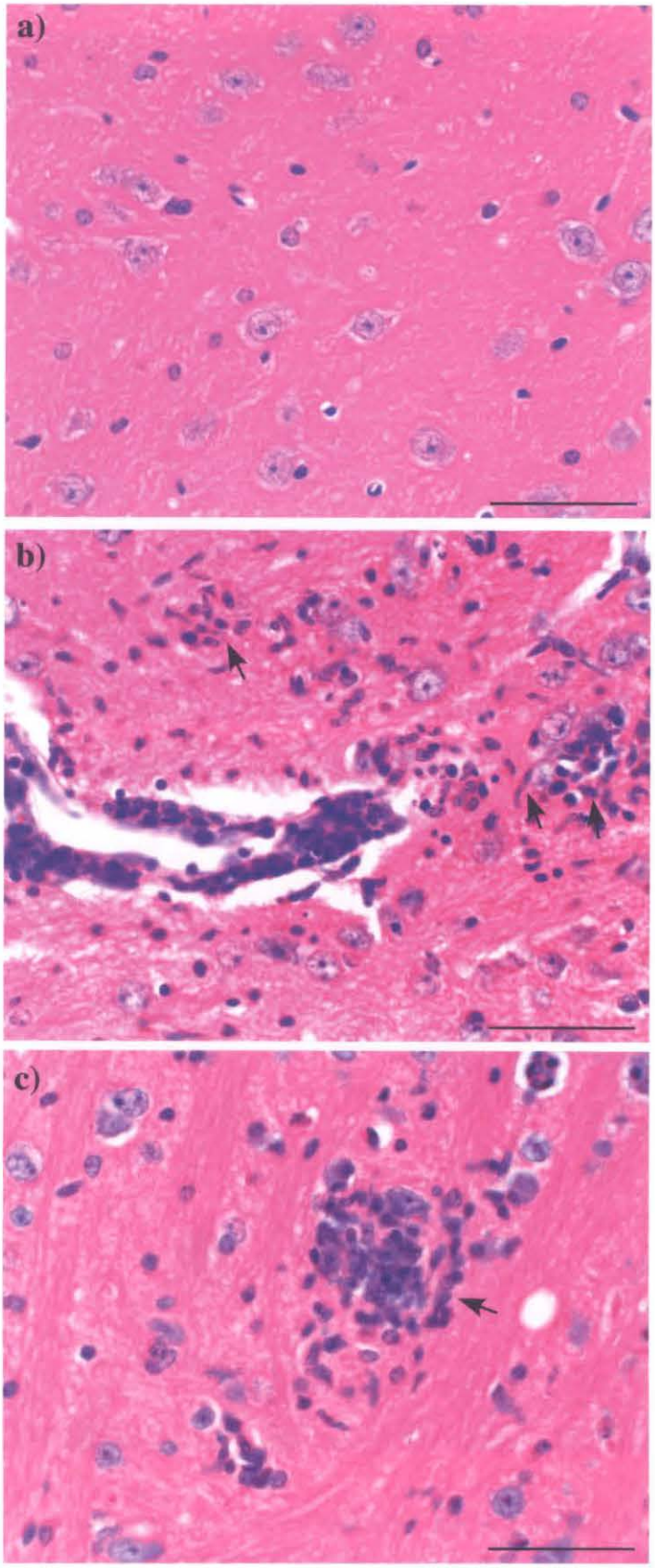

Figure: 4.1 H and E stained brain sections of mock-infected and WNV-infected mouse brain. Mock-infected brain parenchyma showing normal histology (a). Infected brain parenchyma showing microglial activation (solid arrows) on day 8 p.i. (b) and nodules (solid arrow) (c) on day 10 p.i. These micrographs are representative of histopathology observed in both B6.WT and B6.IFN-γ-/- mice. Scale bar = 50μm.

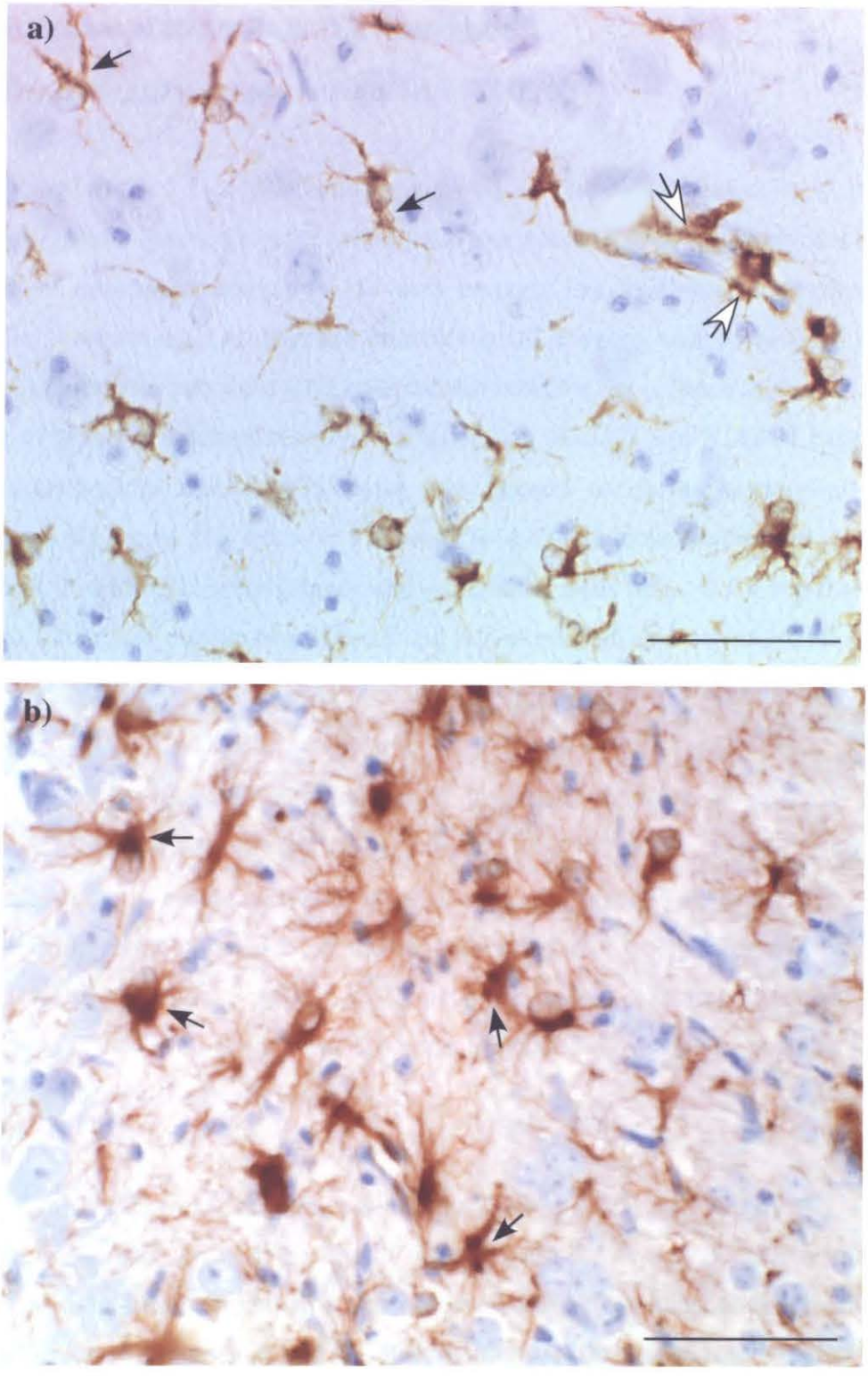

Figure: 4.2 Mock-infected and WNV-infected B6.WT mouse brain sections labelled for GFAP. Astrocytes were less intensely stained with anti-GFAP antibody in mock-infected brain (a) (solid arrows). Some of the *end feet* of astrocytes cover a blood vessel (a) (open arrows). Activated astrocytes showed intense staining with increased production of GFAP in the brainstem of only one WNV-infected B6.WT mouse brain on day 10 p.i. (b) (solid arrows). Scale bar = 50μm.

4.3.3. Activation of microglia in WNV encephalitis

4.3.3.1. Activation of microglia in the absence of IFN-γ

As described earlier, H and E staining showed activation of glial cells in B6.WT and B6.IFN-γ-/- mice. Since, astrocytes were poorly or not activated, this study was completely focused on microglial activation. Several markers are available to dectect activated microglia, however most of them are immunological markers, such as MHC-II expression, ICAM-1 expression, increased CR3 complement receptor, etc.,. Since this study focused on the role of IFN-γ in microglial activation, including MHC-II and ICAM-1 expression, the non-immunological marker, GS-lectin was chosed to define microglial activation throughout the study. GS-lectin is a ligand for α-D-galactose, embedded in the plasma membrane of microglia/macrophages and endothelial cells only. GS-lectin does not stain neurones, astrocytes or oligodendrocytes and this combined with cell morphology makes it a selective marker for activated microglia in the CNS (Cross & Woodroofe 2001).

Resting microglia under normal condition do not posses enough α-D-galactose residues to be prominently labelled with GS-lectin (Medana *et al.* 1996), however during activation they increase sugar residues, which labelled strongly with GS-lectin. Therefore, resting microglia from mock-infected brain showed either negative labelling or very faint labelling with GS-lectin throughout the brain (Figure 4.3 a, c and e). After infection, microglial activation was observed throughout the brain, indicated by intensely positive labelling in both groups of mice (Figure 4.3 b, d and f).

Activated microglia were first detectable in the brain at day 7 p.i., within 24h of WNV Ag detection in the brain in both groups of mice (Figure 4.4 A and B). Since infiltration of leukocytes in the brain parenchyma was observed 48h before microglial activation in both groups of mice (Figure 4.5 A and B), it was important to investigate whether microglial activation was mediated by infiltrating leukocytes or in response to the neuronal infection in the i.p. model. To confirm this, groups of mice were infected i.n. and, brain sections were stained with GS-lectin and anti-WNV Ab. The kinetics of WNV Ag detection and microglial activation in the i.n. model is presented in figure 4.4 C. The kinetics of leukocyte infiltration and microglial activation in the i.n. model is presented in figure 4.4 C. In the i.n.

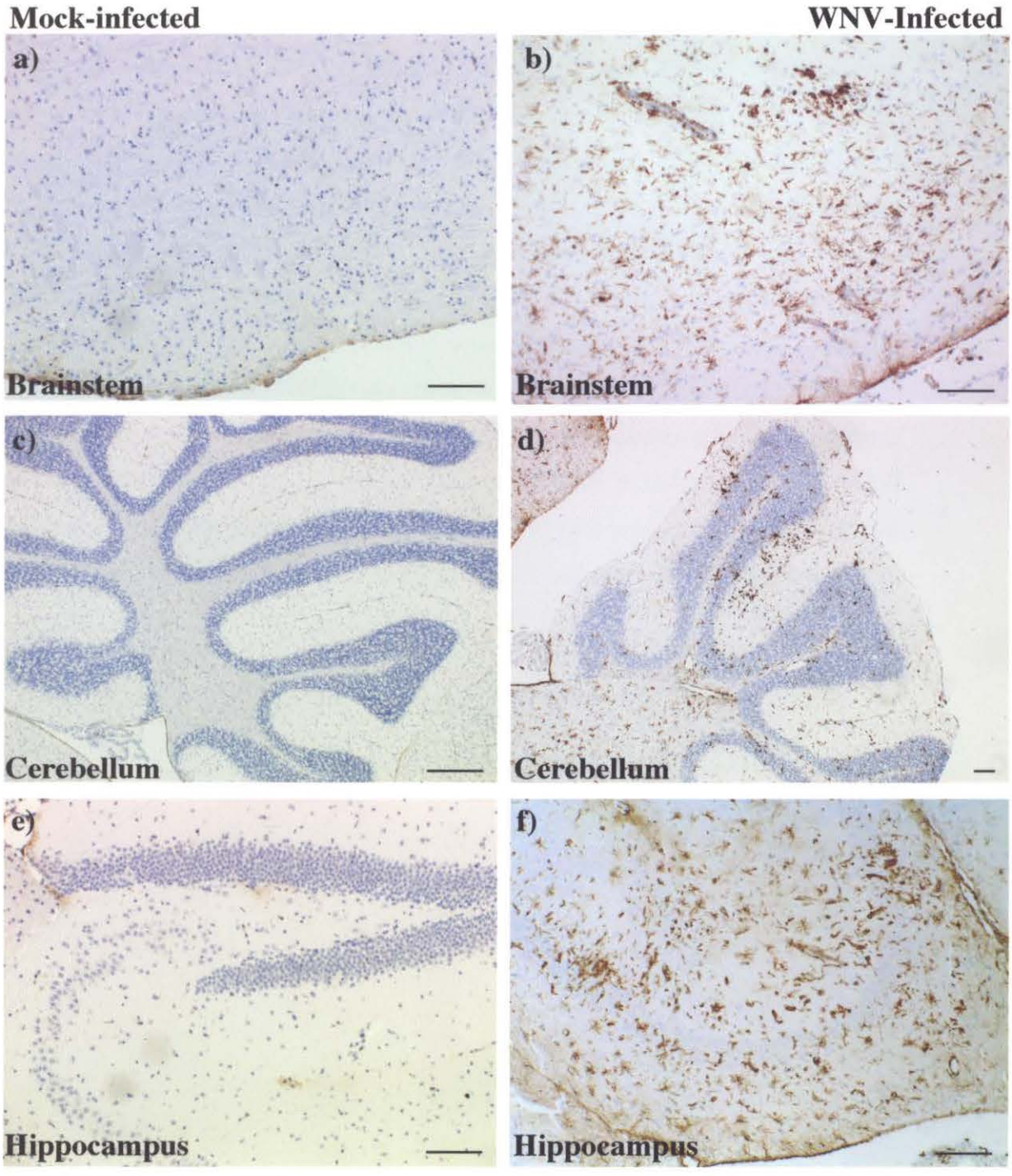

Figure: 4.3 Microglial activation in different parts of the brain section stained with GS-lectin. No microglial activation was observed anywhere in the brain parenchyma of mock-infected brain (a, c and e). Microglia were highly activated throughout the brain in infected mice (b, d and f). These micrographs are representative of both B6.IFN-γ-/- and B6.WT mice.
Scale bar = 100μm.

Figure: 4.4 Kinetics of microglial activation and WNV antigen detection in the i.p. and i.n. model. Groups, each of 64 mice, from B6.WT and B6.IFN-γ-/- strains were infected i.p. with $6x10^4$ pfu/mouse and groups of 15 mice from B6.WT were infected i.n. with $6x10^4$ pfu/mouse. Subgroups of mice in each strain in each model were sacrificed from day 3 to 7 p.i. in both models. Lectin histochemistry was used to detect activated microglia and immunoperoxidase labeling was used to detect WNV antigen in the brain of infected mice. The number of +ve cells labelled with GS-lectin and anti-WNV antibody were counted, as described in Materials and Methods. Sixty H.P.F. were counted per mouse brain and values for each timepoint amalgamated and expressed as mean ± SEM. Kinetics of microglial activation and WNV antigen detection in B6.WT (A) and B6.IFN-γ-/- mice in the i.p. model (B) and B6.WT in the i.n. model (C) are shown. Arrows indicate first appearance of infiltrating leukocytes. Note the change of scale at 4 positive cells/H.P.F. (broken line) in figure C.

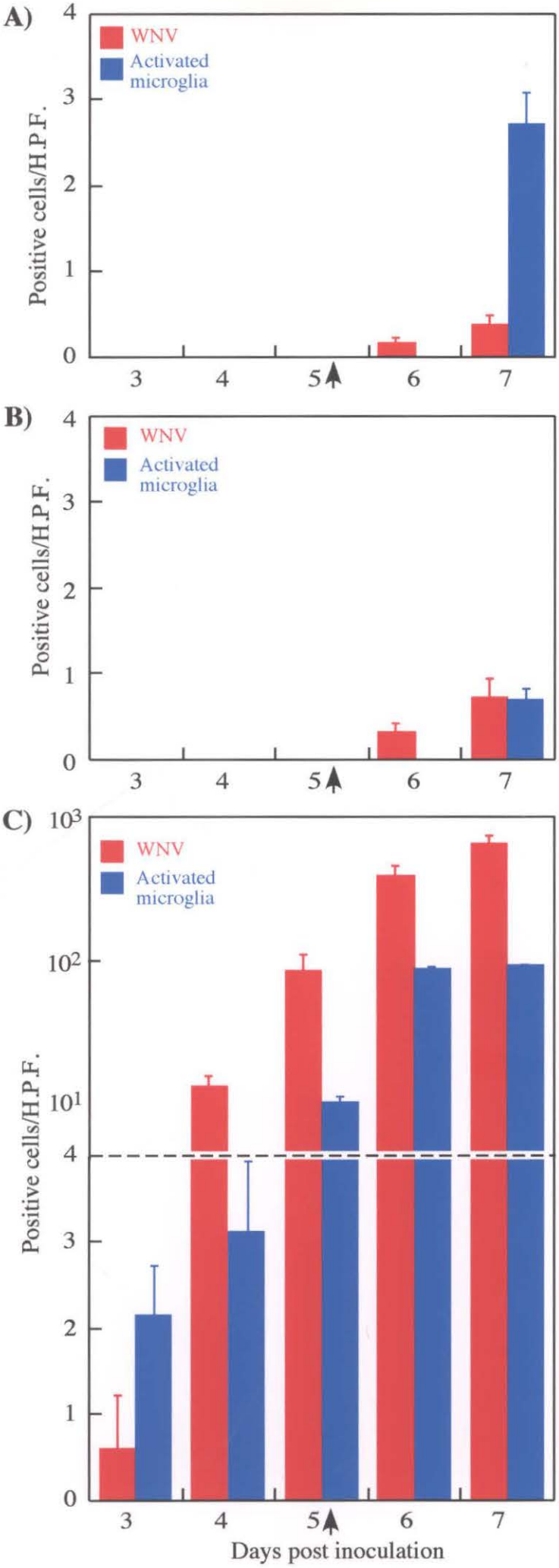
A)
WNV
Activated microglia
Positive cells/H.P.F.
0
1
2
3
4
3
4
5
6
7
B)
WNV
Activated microglia
Positive cells/H.P.F.
0
1
2
3
4
3
4
5
6
7
C)
WNV
Activated microglia
Positive cells/H.P.F.
10^3
10^2
10^1
4
3
2
1
0
3
4
5
6
7
Days post inoculation

Figure: 4.5 Kinetics of microglial activation and detection of leukocytes in the brain parenchyma in the i.p. and i.n. model. Groups, each of 64 mice, from B6.WT and B6.IFN-γ-/- strains were infected i.p. with $6x10^4$ pfu/mouse and groups of 15 mice from B6.WT were infected i.n. with $6x10^4$ pfu/mouse. Subgroups of mice in each strain in each model were sacrificed from day 3 to 7 p.i. in both models. Lectin histochemistry was used to detect activated microglia and, H and E stain was used to detect leukocyte infiltration in the brain parenchyma of infected mice. The number of +ve cells labelled with GS-lectin and leukocytes were counted, as described in Materials and Methods. Sixty H.P.F. were counted per mouse brain and values for each timepoint amalgamated and expressed as mean ± SEM. Kinetics of microglial activation and leukocytes detection in B6.WT (A) and B6.IFN-γ-/- in the i.p. model (B) and B6.WT in the i.n. model (C) are shown. Arrows indicate first detection of WNV antigen in the brain. Note the change of scale at 4 positive cells/H.P.F. (broken line) in figure C.

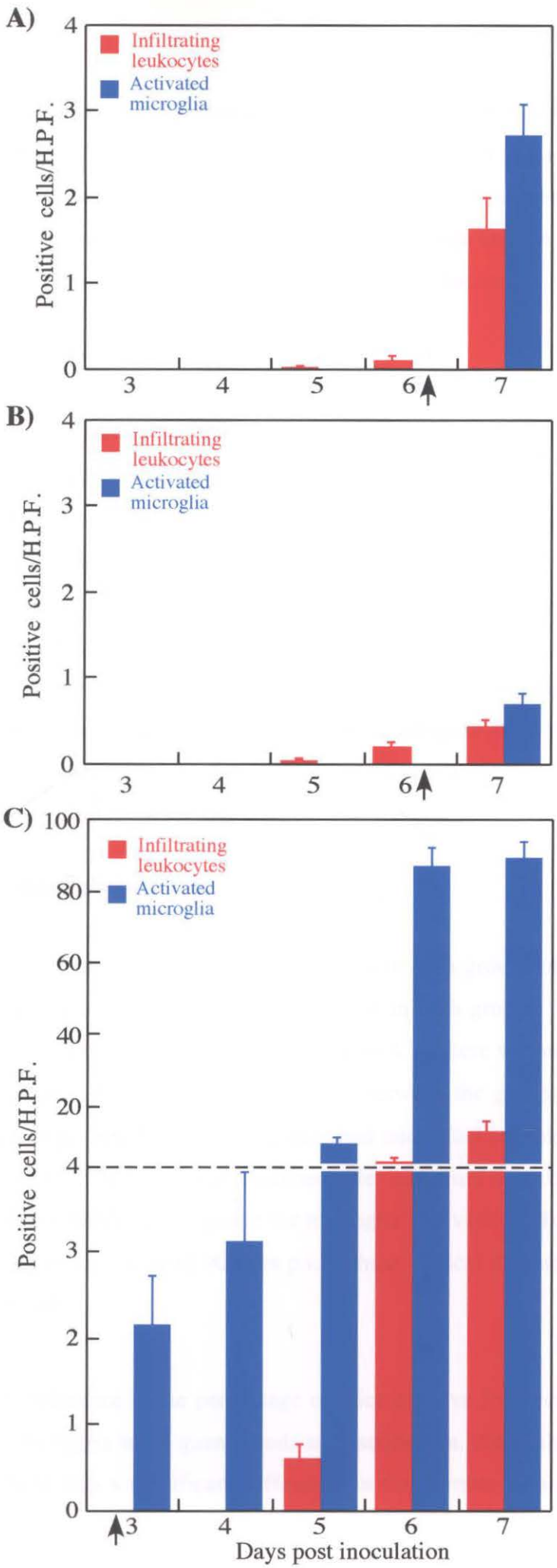
A)
Infiltrating leukocytes
Activated microglia
Positive cells/H.P.F.
0
1
2
3
4
3
4
5
6
7
B)
Infiltrating leukocytes
Activated microglia
Positive cells/H.P.F.
0
1
2
3
4
3
4
5
6
7
C)
Infiltrating leukocytes
Activated microglia
Positive cells/H.P.F.
0
1
2
3
4
20
40
60
80
100
3
4
5
6
7
Days post inoculation

model, activated microglia were detected at the same time as WNV Ag was detected in the OB, co-localising with WNV-positive neurones in the OB at day 3 p.i., while leukocyte infiltration was observed 48h after microglial activation. These results indicate that microglial activation is independent of both leukocyte infiltration and the presence of IFN-γ and suggest that they were activated in response to neuronal infection.

4.3.3.2. Morphology of microglial changes during activation

Microglia were activated throughout the brain with markedly altered morphology between day 7-11 p.i. in B6.WT and B6.IFN-γ-/- mice. The progression of activation can be seen in figure 4.6. During early activation, microglia showed highly branched processes, exhibiting ramified morphology, with little GS-lectin labelling (Figure 4.6 a). During activation, the processes became thicker with increased staining intensity (Figure 4.6 b), ultimately withdrawing (Figure 4.6 c, d and e). In the last step of activation, microglia became round or elongated (rod shaped). These are known as amoeboid or reactive microglia (figure 4.6 f). Amoeboid microglia were clustered around neurones (Figure 4.6 h). The morphology and staining characteristics of microglial cells returned to normal by day 30 p.i. in both groups of mice. These results indicate that microglial activation is independent of IFN-γ.

4.3.3.3. Kinetics of microglial activation

As discussed earlier, although microglia were activated in both groups of mice from day 7 p.i., not all mice were positive for microglial activation in both groups. The percentage of mice positive for microglial activation is shown in figure 4.7. There was no difference in the percentage of mice positive for microglial activation between the groups. Interestingly, in both groups of mice more than 85% surviving mice had microglial activation on day 11 p.i., and at this timepoint WNV Ag was nearly undetectable (discussed in section 3.3.3.3). None of the mice positive for WNV was negative for microglial activation. Mice surviving after day 11 p.i. continued to survive until 90 days p.i. without clinical symptoms. After day 90 p.i., mice were sacrified.

Since there was no difference in the percentage of mice positive for microglial activation, GS-lectin-positive microglia were quantitated, as described in Materials and Methods to evaluate whether there was a significant difference in the number of activated microglia

Figure: 4.6 WNV-infected B6.WT mouse brain sections stained with GS-lectin showing different morphologies of activated microglia. Microglia during early activation showed highly branched processes exhibiting a ramified morphology, lightly stained with GS-lectin (a) (solid arrows). During activation, the processes became more thicker with increased staining intensity (b, c and d) (solid arrows), and begin to withdraw (d and e) (solid arrows). They finally achieve an amoeboid morphology, including rod (f) (solid arrows) or spherical forms (g) (solid arrows). These amoeboid microglia were the predominant type clustered around neurones (h) (solid arrow). These micrographs are representative of both B6.WT and B6.IFN-γ-/- mice. Scale bar = 50μm.

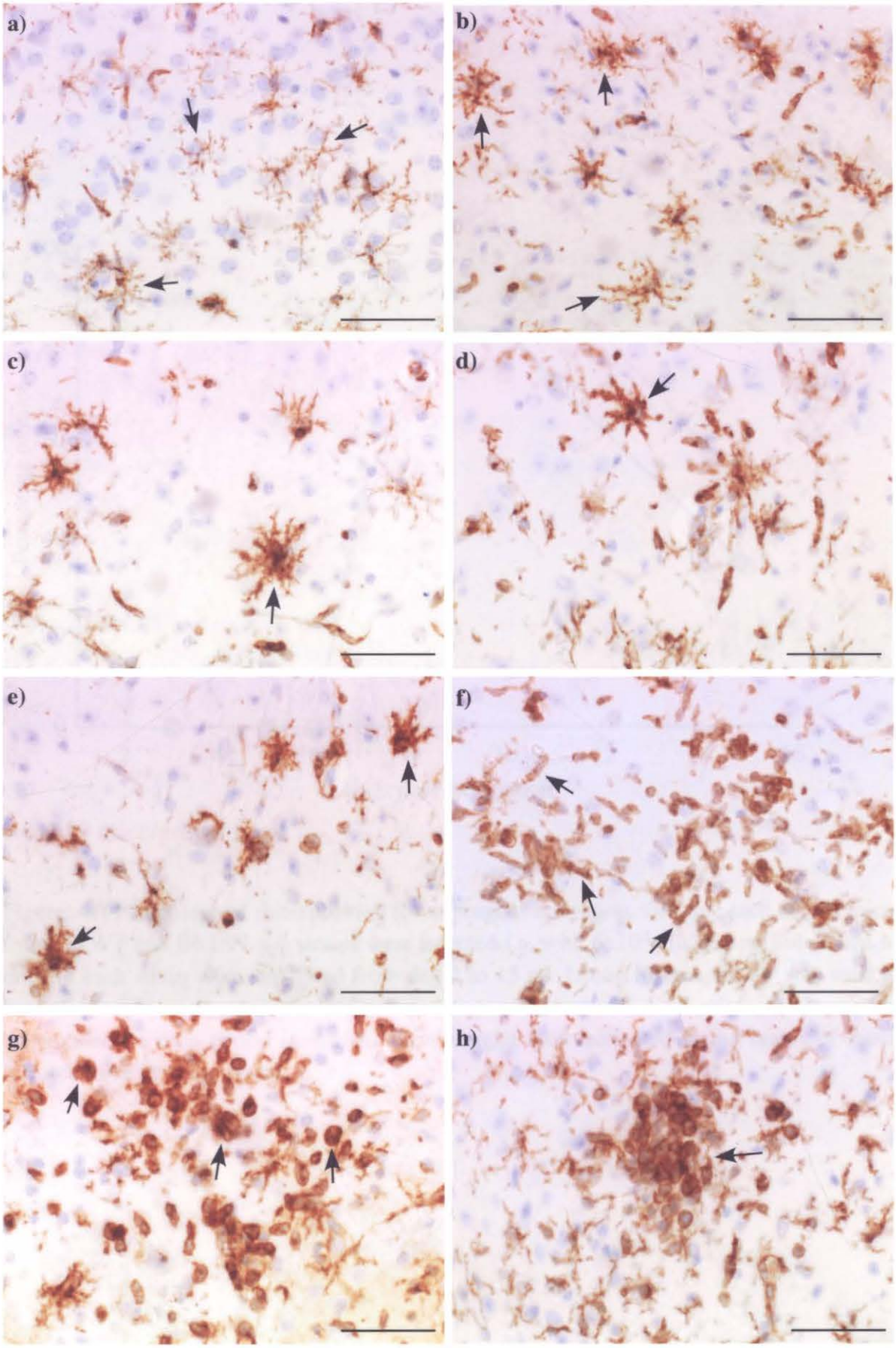
a)
b)
c)
d)
e)
f)
g)
h)

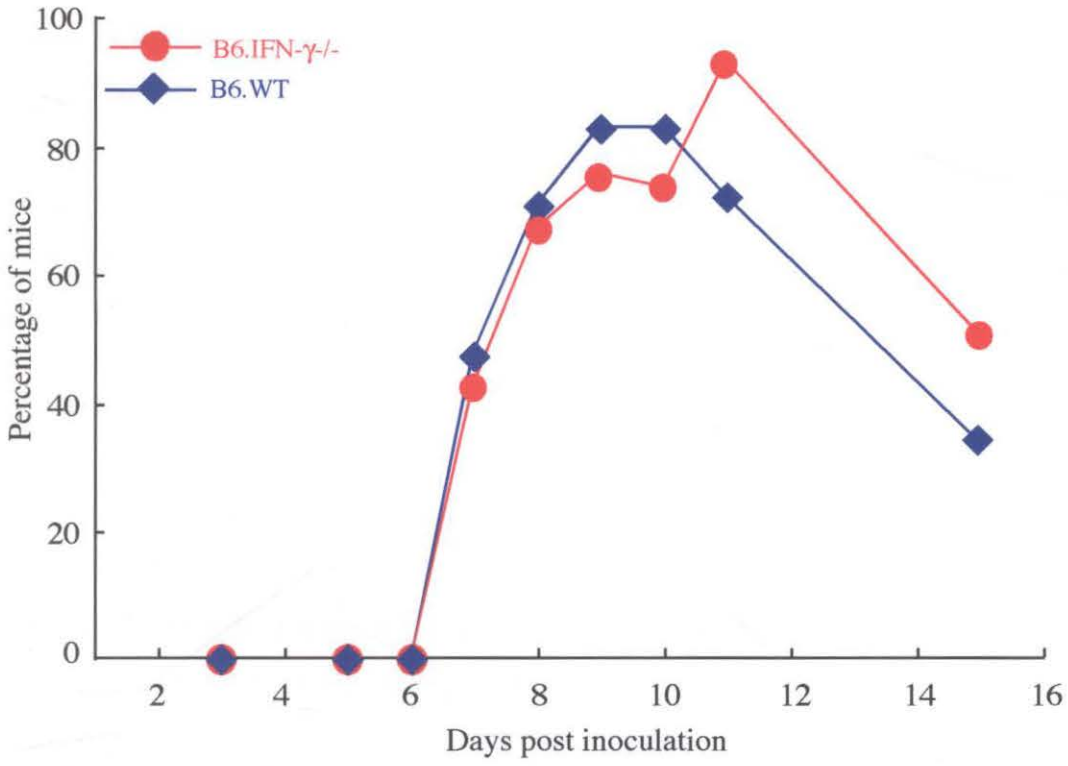

Figure: 4.7 Percentage of mice positive for microglial activation. Groups, each of 110 mice, from B6.WT and B6.IFN-γ-/- strains were infected i.p. with $6x10^4$ pfu/mouse. Subgroups of mice in each strain were sacrificed from day 3 to 15 p.i. Lectin histochemistry was used to detect activated microglia in the brain. Percentage of mice positive for microglial activation throughout the time period is shown. No microglia were activated in the brains of mock-infected mice in either group.

between the groups. The kinetics of microglial activation were similar and are shown in figure 4.8. In B6.WT mice, microglial activation was significantly increased on days 7-11 (p=<0.001), peaking on day 10 p.i. and reduced nearly to baseline values in survivors by day 15 p.i. In B6.IFN-γ-/- mice, microglial activation was significantly increased on days 8-11 (p=<0.001), peaking on day 9 p.i. and reduced nearly to baseline values in survivors by day 15 p.i. These numbers returned completely to baseline values in survivors by day 30 p.i. in both groups of mice (Figure 4.8) after WNV Ag was completely undetectable from day 15 p.i. These results provide further support for the hypothesis that microglial activation was in response to neuronal infection. Although the kinetics of microglial activation was similar between the groups, the number of activated microglia was significantly higher (p=<0.001) in B6.IFN-γ-/- mice compared to B6.WT on day 9 p.i. This result suggests that lack of IFN-γ enhanced microglial activation in WNV encephalitis.

4.3.3.4. Kinetics of microglial nodules formation

Microglial nodules are a hallmark of viral encephalitis (Dickson *et al.* 1991; Dickson *et al.* 1993). In aggrement with this, microglial nodules were also observed in WNV encephalitis from day 7 onwards (Figure 4.1 c and Figure 4.6 h) in both groups of mice. The size and number of nodules were also increased between days 7-11, consisting of approximately 3-30 microglia displaying amoeboid morphology/nodule. In the beginning, at day 7-8 p.i., the nodules were small and consisted of loose aggregates of activated microglia in both groups of mice. After day 8 p.i. in B6.IFN-γ-/- and after day 9 p.i in B6.WT mice, the nodules were larger with densely aggregated activated microglia. To evaluate whether there was a significant difference in the numbers of nodules formed between the groups, they were counted in whole brain sections stained with GS-lectin. The number of nodules peaked on day 10 and 11 p.i. in B6.WT, whereas in B6.IFN-γ-/- mice, nodules were maximal on day 9 p.i. (Figure 4.9). The number and size of nodules were decreased from day 15 p.i. in both groups of mice. The kinetics of nodule formation was similar and there were no statistically significant differences in the total numbers of nodules formed between the groups at any timepoints.

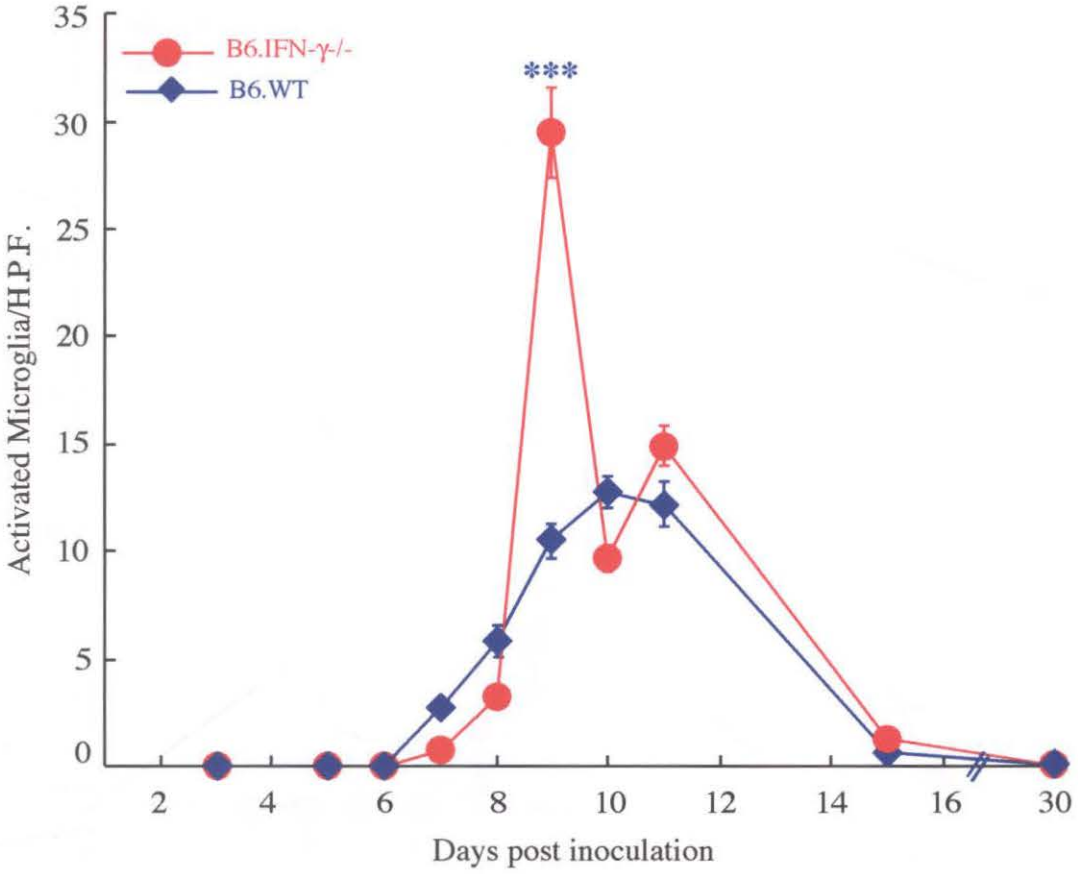

n = 120 mice/group

Figure: 4.8 Kinetics of microglial activation. Groups, each of 120 mice, from B6.WT and B6.IFN-γ-/- strains were infected i.p. with $6x10^4$ pfu/mouse. Subgroups of mice in each strain were sacrificed from day 3 to 30 p.i. Lectin histochemistry was used to detect activated microglia in the brain parenchyma of infected mice. The number of activated microglia was counted, as described in materials and methods. Sixty H.P.F. were counted per mouse brain and values for each timepoint amalgamated and expressed as mean ± SEM. No microglia were activated in the brains of mock-infected mice in either group. (***p = <0.001 by ANOVA).

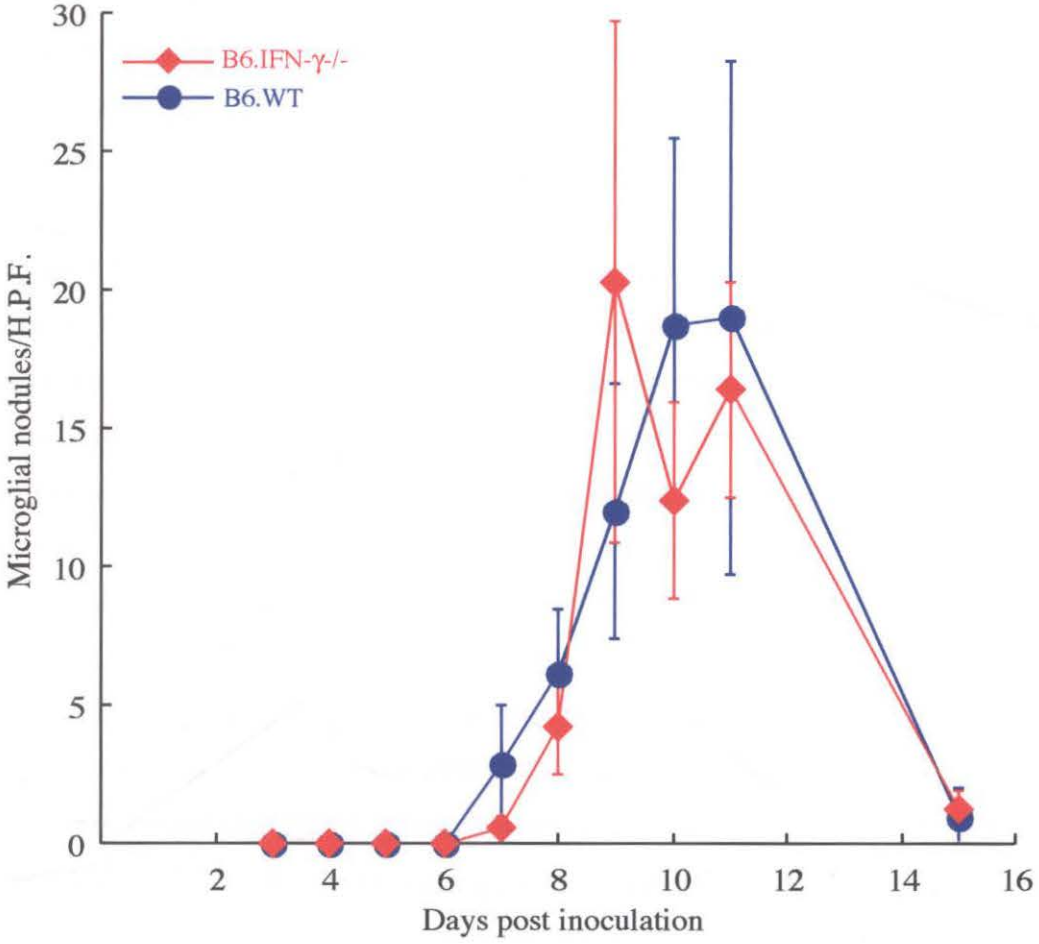

n = 110 mice/group

Figure: 4.9 Kinetics of microglial nodule formation. Groups, each of 110 mice, from B6.WT and B6.IFN-γ-/- strains were infected i.p. with $6x10^4$ pfu/mouse. Subgroups of mice in each strain were sacrificed from day 3 to 15 p.i. Lectin histochemistry was used to detect activated microglia in the brain parenchyma of infected mice. The number of nodules was counted in a whole brain section, values for each timepoint amalgamated and expressed as mean ± SEM. Statistical analysis using ANOVA showed no significant difference in the numbers of nodules formed between the groups.

4.3.3.5. Formation of microglial nodules did not correlate with neuronal death

It has been suggested that clustering of amoeboid microglia around the neurones reflect neuronal cell death (Adams *et al.* 1994; Raivich *et al.* 1999). Therefore, in order to determine whether neurones at the centre of these clusters were dead or dying, we used a TUNEL assay on these brain sections. Mock-infected brain from both groups showed no cell death (Figure 4.10 a). Brain sections showing maximum neuronal infection were chosen for TUNEL assay. Very few cells were labelled with TUNEL in both groups of mice (Figure 4.10 b and c). All TUNEL-positive cells were counted in whole brain sections and compared with the total number of infected neurones. Interestingly, it was found that less than 0.1% of neurones were apoptotic, compared to the total number of neurones infected while only 1% of neurones at the centre of a nodule were apoptotic compared to the total number of nodules from either group. Moreover, the number and sites of TUNEL-positive neurones did not correlate with the number and sites of microglial clustering in the brain parenchyma (data not shown). It follows that most neurones surrounded by activated microglia had not undergone cell death. Since microglia were highly activated in both groups of mice, a double-labelling for viral Ag and activated microglia was carried out to confirm that only neurones were infected and also to determine the numbers of microglia clustering around detectably infected neurones. In no case were microglia found to be infected with WNV. However, microglia surrounded infected neurones, showing typical phagocytic morphology in both groups (Figure 4.11). Indeed, many apparently uninfected neurones detected by immunoperoxidase were also associated with microglial nodules from day 7 onwards of the time course.

4.3.3.6. Unimpared MHC-II expression in microglia in the absence of IFN-γ

Microglia act as an APC in the CNS. Expression of MHC-II in microglia is inducible and IFN-γ is a potent inducer of microglial MHC-II expression both *in vivo* and *in vitro* (Raivich *et al.* 1999; Deckert-Schluter *et al.* 1999). Therefore, the status and role of IFN-γ in MHC-II upregulation in microglia was determined. Mock-infected mice from either group were negative for MHC-II expression (Figure 4.12 a). After infection, MHC-II expression was observed in both groups of mice (Figure 4.12 b and c). In B6.IFN-γ-/- mice MHC-II expression was observed only on a very few neurovascular endothelial cells on day 6 p.i. From day 7 p.i., a few infiltrating leukocytes, the neurovascular endothelial cells,

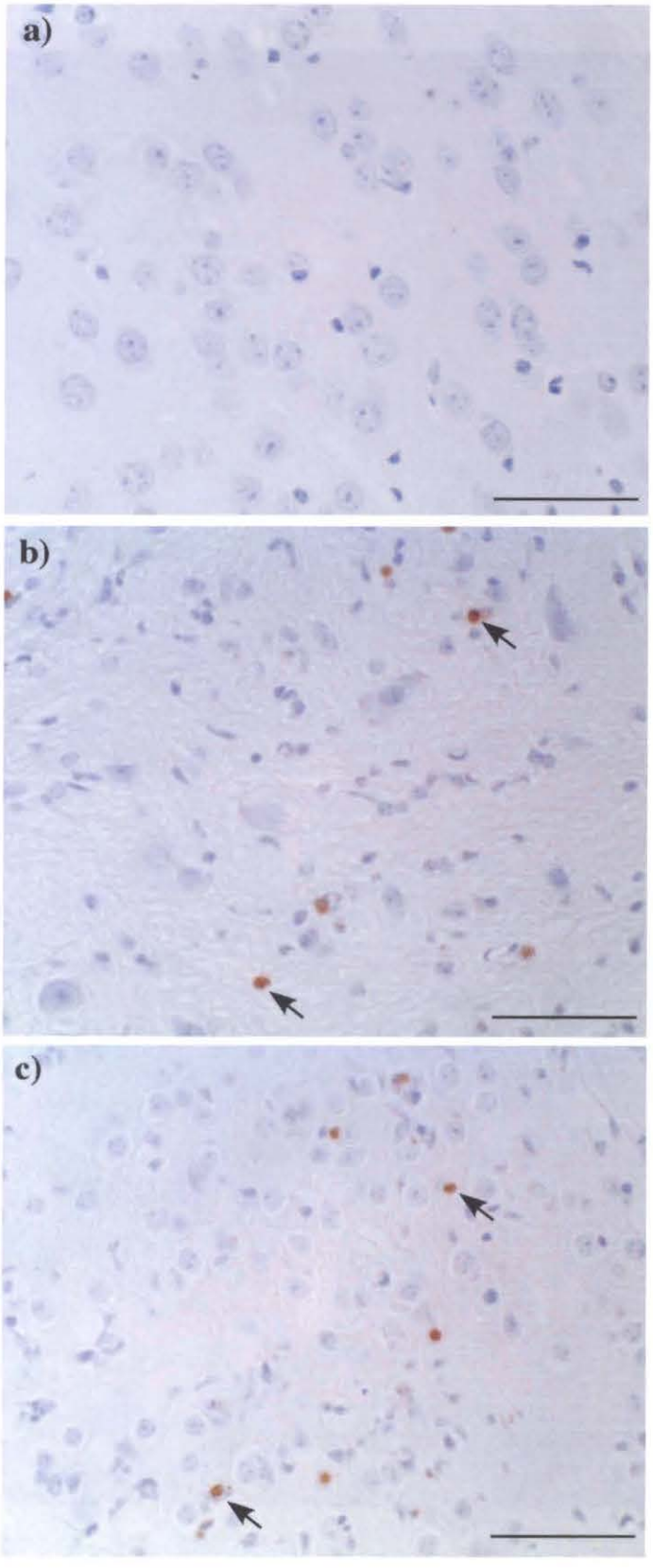

Figure: 4.10 Brain sections from mock-infected and WNV-infected B6.WT and B6.IFN-γ-/- mice on day 9 p.i. labelled for apoptosis by TUNEL assay. No cell death was found in the mock-infected brain parenchyma in both B6.WT and B6.IFN-γ-/- mice (a). Brain sections showing maximum WNV antigen were selected for TUNEL assay. Few cells were labelled with TUNEL (solid arrows) in both B6.WT (b) and B6.IFN-γ-/- (c) mice. Scale bar = 50μm.

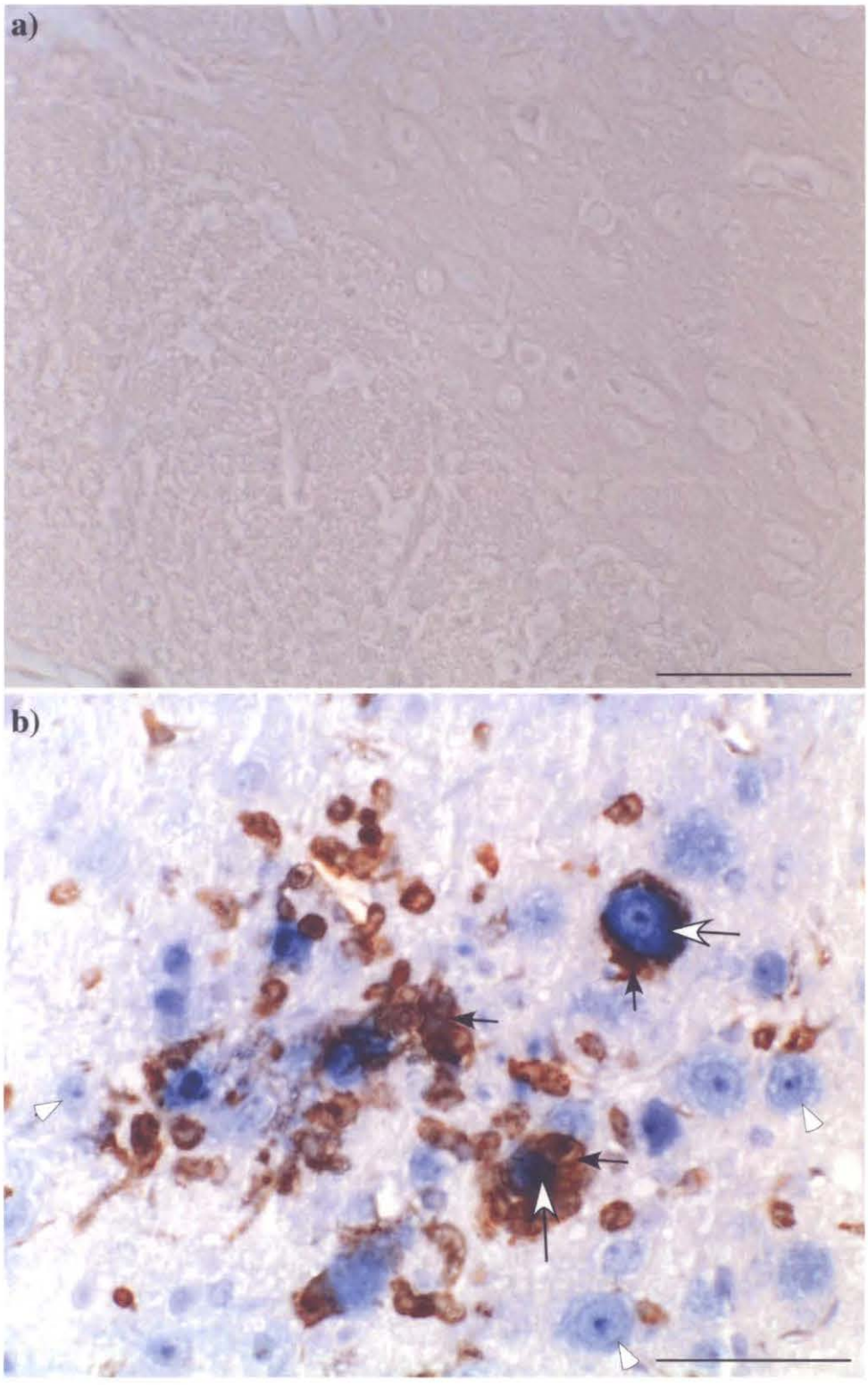

Figure: 4.11 Mock-infected (a) and WNV-infected B6.IFN-γ-/- (b) mouse brain parenchyma double-labelled for WNV antigen and activated microglia on day 9 p.i. Alkaline phosphatase labelling using rat anti-WNV and BCIP/NBT substrate for WNV antigen detection is shown in blue. GS-lectin and DAB substrate were used for the detection of activated microglia and these displayed a phagocytic morphology (brown). Infected neurones (open arrows) were surrounded by clusters (nodules) of activated microglia (solid arrows). Uninfected neurones are indicated by arrow heads. These micrographs are representative of histopathology observed in both B6.WT and B6.IFN-γ-/- mice. Scale bar = 50μm.

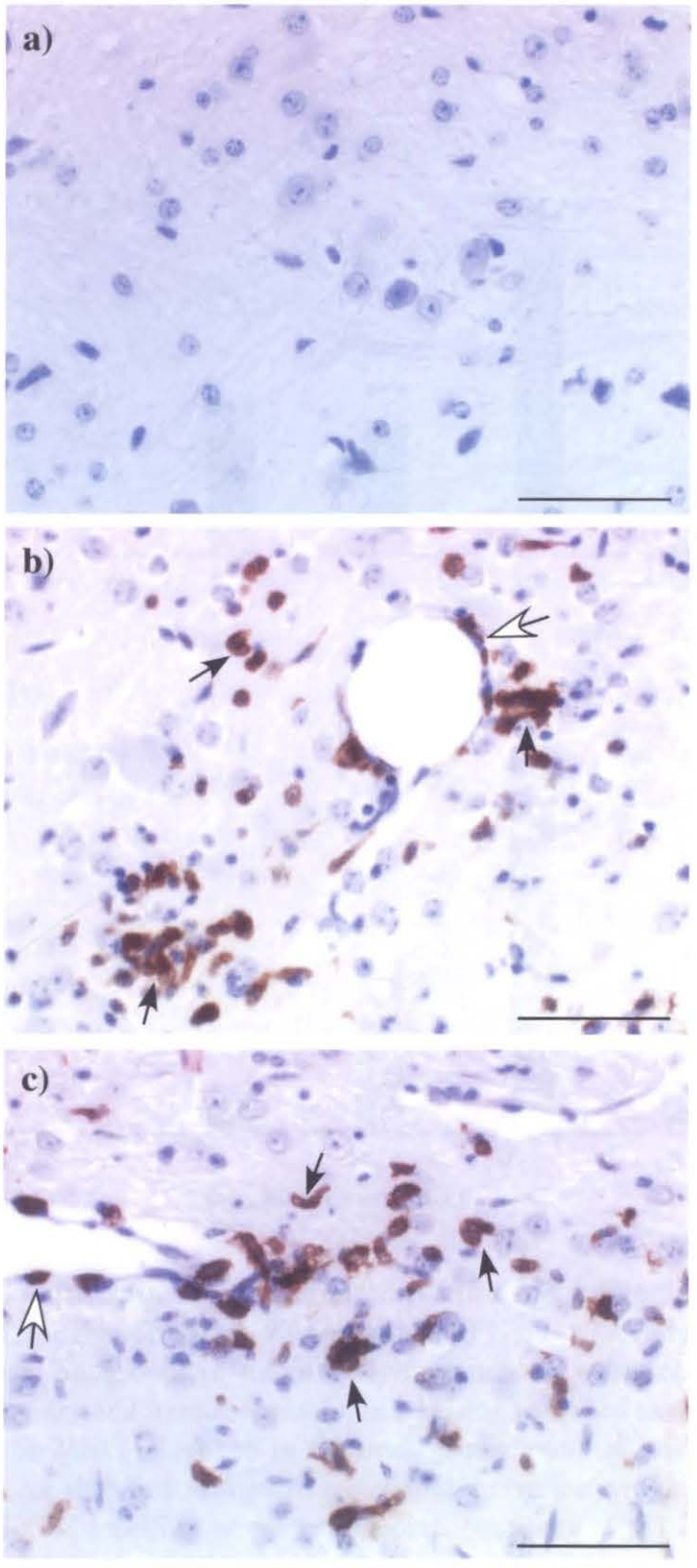

Figure: 4.12 MHC-II expression in the brain parenchyma. Immunoperoxidase labelling was used to detect MHC-II in mock-infected and WNV-infected mouse brains on day 11 p.i. from B6.WT and B6.IFN-γ-/- mice. There was no constitutive expression of MHC-II in the brain parenchyma in either group (a). After WNV infection, MHC-II was expressed in microglia (solid arrows) and perivascular cells (open arrows) in both B6.WT (b) and B6.IFN-γ-/- mice (c). Only activated microglia displaying ameboid morphology were labelled with anti-MHC-II antibody in both groups of mice (solid arrows).
Scale bar=50μm.

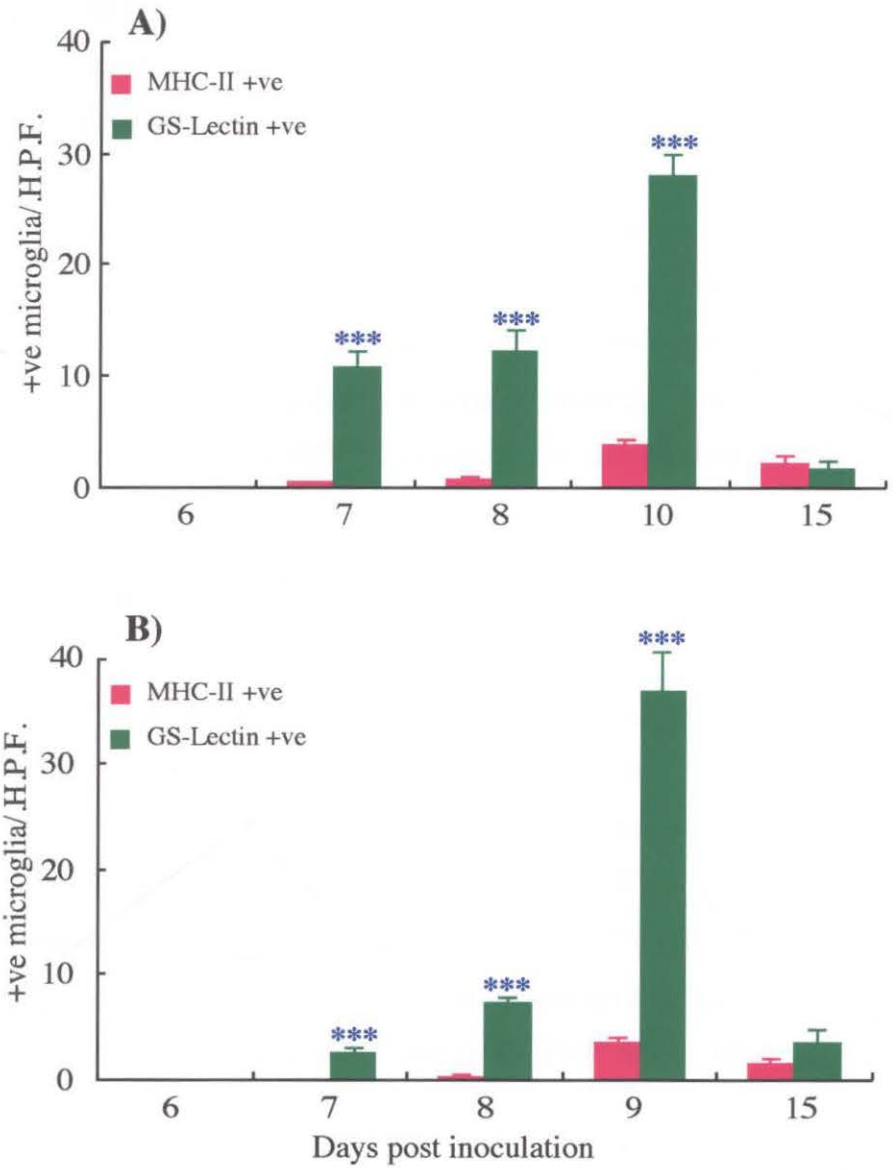

Figure: 4.13 Comparision of microglial activation and microglial MHC-II expression. Groups, each of 70 mice, from B6.WT (A) and B6.IFN-γ-/- (B) strains were infected i.p. with $6x10^4$ pfu/mouse. Subgroups of mice in each strain were sacrificed from day 3 to 15 p.i. Lectin histochemistry and immunoperoxidase labelling was used to detect activated microglia and expression of MHC-II antigen in the brain parenchyma of infected mice, respectively. The brain sections showing maximum microglial activation as detected by GS-lectin, was selected for MHC-II labelling at each timepoint. Numbers of GS-lectin-positive microglia and MHC-II-positive microglia were counted, as described in materials and methods. Sixty H.P.F. were counted per mouse brain and values for each timepoint amalgamated and expressed as mean ± SEM. No microglia were activated or expressed MHC-II antigen in the brains of either strain of mock-infected mice. (***p = <0.001 by ANOVA). n=3 from d6-d10 p.i. and n=1 on day 15 p.i. in both groups.

perivascular macrophages and microglia only those displaying amoeboid morphology expressed MHC-II in both strains of mice. These MHC-II-positive cells were scattered throughout the brain. The brain sections showing high microglial activation were chosen for the study of MHC-II expression to determine the relationship between microglial activation detected by GS-lectin and MHC-II expression on microglia. The number of MHC-II-positive microglia were counted, as described in Materials and Methods and compared with GS-lectin-positive microglia. It was found that the number of MHC-II expressing microglia was significantly less (p=<0.001) compared to the GS-lectin positive microglia from either group at any timepoints from day 7-10 p.i. (Figure 4.13). These data indicate that induction of MHC-II expression is independent of IFN-γ and relatively few activated microglia are induced to express MHC-II in WNV encephalitis.

4.4. Discussion

The glial cells, predominantly microglia and astrocytes, represent highly reactive CNS cells that respond to infectious and inflammatory stimuli by upregulation or *de novo* expression of various cell surface molecules, which are implicated in the control of CNS infections. Several experiments have shown the importance of IFN-γ in glial cell activation. Therefore, to investigate types and kinetics of glial cell activation, and the role of IFN-γ in glial cell activation in WNV encephalitis, the brain parenchyma of infected B6.WT and B6.IFN-γ-/- mice was stained with GS-lectin and anti-GFAP Ab to label microglia and astrocytes, respectively.

Astrocytes play a key role in the normal CNS and have a number of important physiological properties related to the CNS homeostasis (Benveniste 1998). They can be identified by *de novo* expression of GFAP (Martin and O'Callaghan 1995), which is enhanced during activation (Eddleston & Mucke 1993). Therefore, upregulation of GFAP was used in this study as a marker of astrocyte activation. Astrocytes can respond during infection of the CNS as well as in inflammatory demyelinating disease (Mucke & Eddleston 1993; Brodie *et al.* 1997; Schonrock *et al.* 1998) with an increase in number and size of enhanced GFAP-expressing cells, *i.e.*, astrogliosis (Eddleston & Mucke 1993). Several experiments have demonstrated the activation of astrocytes in CNS infections both *in vivo* and *in vitro* (Weissenbock *et al.* 2000; Schoneboom *et al.* 1999; Bi *et al.* 1995; Chen *et al.* 2000; Liu *et*

al. 1989; Medana *et al.* 1996). *In vitro* experiments suggest that astrogliosis is mediated by IFN-γ (Balasingam *et al.* 1994; Yong *et al.* 1991). However, in WNV encephalitis, only extremely rarely were astrocytes activated in both B6.WT and B6.IFN-γ-/- mice, suggesting that astrocytes do not play a significant role in WNV encephalitis. Moreover, the presence of IFN-γ neither induced astroglial activation nor reduced its activation, suggesting that activation of astrocytes is not mediated by IFN-γ.

Since, astrocytes were not activated in WNV encephalitis, this study thus mainly focused on microglial activation. Microglia are found to be activated in several CNS diseases. These include human neurological disorders (Banati *et al.* 1993; Paresce *et al.* 1996; Schluesener *et al.* 1996), EAE (Bauer *et al.* 1995), ischemia (Morioka *et al.* 1992), viral encephalitis (Sampson *et al.* 2000; Shieh *et al.* 2000, Kure *et al.* 1990; Christian *et al.* 1996; Iwasaki *et al.* 1986; Sauder *et al.* 1999; Mokhtarian *et al.* 1996; Bi *et al.* 1995), parasite infection (Deckert-Schluter *et al.* 1999; Medana *et al.* 1997) and radiation injury of the CNS (Kyrkanides *et al.* 1999). Being extremely sensitive in nature, hardly any disease of the nervous system occurs without microglial activation. Microglial activation in all CNS diseases is characterized by proliferation, increased or *de novo* expression of marker molecules, such as MHC Ag, and migration, with the eventual change into a macrophage-like phenotype and the production of a variety of secretory molecules, including cytokines, chemokines, reactive oxygen and nitrogen species (Banati *et al.* 1993; Benveniste 1992). In WNV encephalitis, microglia were highly activated throughout the brain (Figure 4.3), as identified by their enlarged size and dramatic alteration in their morphology with intense GS-lectin staining. Resting microglia labelled very weakly or not at all with GS-lectin.

Meddana *et al.* (1997) showed that breakdown of BBB would facilitate microglial activation. However, in WNV encephalitis microglia were activated in the presence of an intact BBB (see section 3.3.5), suggesting that microglial activation is independent of BBB permeability. In this model, microglial activation was observed within 24h of WNV Ag detection in the the brain at or near the sites of neuronal infection in both groups of mice (Figure 4.4). Sudo *et al.* (1998) suggested that microglial activation is induced by stressed neurones. Therefore, I speculate that microglia in this study may be activated in response to the infected neurones. However, it has been also suggested that activated T cells and

monocytes/macrophages induce microglial activation (Langford & Masiah 2001; Gehrmann *et al.* 1993, Aloisi *et al.* 2000; Sedgwick *et al.* 1998; Bauer *et al.* 1995). Since, infiltration of leukocytes were observed 48h before microglia were activated in my model (Figure 4.4), it was hypothesized that microglial activation may be mediated by these infiltrating leukocytes. To confirm this hypothesis, groups of mice were infected i.n. with the same dose of WNV and brain parenchyma were examined for microglial activation, leukocyte infiltration and WNV Ag. Interestingly, it was found that microglia were activated near the sites of neuronal infection at the same time, day 3 p.i. in the OB, in the absence of any infiltrating leukocytes (Figure 4.5). Moreover, the progress of microglial activation through the brain closely matched that of the advancement of WNV infection of neurones from rostral to caudal in the i.n. model. Leukocyte infiltration was observed only after 48h of microglial activation, suggesting that microglial activation was independent of leukocyte infiltration and was mediated by infected neurones. This finding is supported by facial-nerve transection model. In this model, after facial nerve axotomy microglia were activated in the absence of any infiltrating haematogenous cells (Kreutzberg 1996).

Upon induced, stressed neurones rapidly change their gene expression to stimulate nearby microglia via neurotransmitters or neuropeptides. Microglia respond immediately (Banati *et al.* 1993) and undergo graded changes in their morphology (Raivich *et al.* 1999, Davis *et al.* 1994). In WNV encephalitis, activated microglia displayed all the different stages of activation (Figure 4.6) between day 7-11 p.i. These different stages of activated microglia may have different roles in WNV encephalitis. Double-labelling experiments confirmed that microglia were not infected with WNV (Figure 4.11). Mori *et al.* (2001) suggested that the transformation of resting microglia into amoeboid form is dependent on IFN-γ. However, in WNV encephalitis the amoeboid form of microglia occurred in the complete absence of IFN-γ.

Increasing evidence from both *in vivo* and *in vitro* studies suggests that IFN-γ plays an important role in microglial activation (Grau *et al.* 1997; Meda *et al.* 1995; Sethna *et al.* 1991). In contrast, in WNV encephalitis lack of IFN-γ did not reduce microglial activation. The kinetics of activation and the percentage of mice showing microglial activation in B6.WT and B6.IFN-γ-/- (Figure 4.7) was similar between the groups. Furthermore,

significantly higher microglial activation occurred in the absence of IFN-γ on day 9 p.i in B6.IFN-γ-/- mice (Figure 4.8), indicating that microglial activation is independent to IFN-γ; moreover, its absence enhanced microglial activation in WNV encephalitis.

Formation of microglial nodules, consisting of amoeboid microglia are the prominent features of viral encephalitis (Dickson *et al.* 1991). In the WNV model, microglial activation was associated with significant numbers of microglial nodules (Figure 4.9). These were observed from day 7 p.i. in both groups of mice. The number of nodules increased subsequently and peaked on day 11 p.i. At this timepoint WNV was nearly undetectable. The formation of microglial nodules is thought to indicate neuronal death (Neumann 2001; Adam 1994). However, the incidence of neuronal death in WNV encephalitis, compared to the numbers of microglial nodules is not consistent with the current notion that nodules are indicative of neuronophagia. Thus, the presence of microglial nodules does not equate with neuronal death in WNV encephalitis.

As discussed earlier, microglial activation was observed within 24h of WNV Ag detection at or near the sites of neuronal infection and was maximal between day 9-11 p.i. in both groups of mice. The number and morphology of activated microglia, as well as the number of nodules, had reduced to nearly baseline levels only when WNV Ag was undetectable, at day 15 p.i. These results suggest that these activated microglia may play a role in the control of WNV in the neurones. Recently, Cheeran *et al.* (2001) demonstrated the antiviral role of microglia *in vitro*. He infected the coculture of astrocytes and microglia with cytomegalovirus (CMV) and found 60% reduction in viral gene expression compared to the CMV infected purified astrocytes culture lacking microglia. These microglia were found to produce antiviral cytokines, like TNF, soon after CMV infection and this may have helped control infection of astrocytes. It has been also shown that microglia can produce potent antiviral cytokines like IFN-α and their receptors (Yamada *et al.* 1994; Akiyama *et al.* 1994; Yamada & Yamanaka 1995). Several experiments on animal models of neurotropic viral infections showed that these antiviral cytokines dramatically reduce the viral gene expression in the CNS (Akwa et al 1998; Carr *et al.* 1998; Schijns *et al.* 1991). Moreover, microglia express FcR and CR3 receptors on their surface (Dickson *et al.* 1991), which increase during activation (Nakajima & Kohsaka 1998). Thus, in my model, activated

microglia may be involved in the control of WNV in conjunction with Ab produced locally by infiltrating leukocytes in the brain via non-cytotoxic mechanisms.

Work on neurological disorders and viral encephalitis suggest that activated microglia may play a cytotoxic role through the production of various cytotoxic metabolites, as well having phagocytic properties (Banati *et al.* 1993; Bauer *et al.* 1994; Benveniste *et al.* 2001; Gonzalez-Scarano & Baltuch 1999; McGeer *et al.* 1993). As discussed earlier, in WNV encephalitis presence of nodules did not correlate with neuronal death in either B6.WT or B6.IFN-γ-/- mice. Moreover, more than 85% of surviving mice showed high microglial activation with only rare neurone degeneration. Despite extensive microglial activation, surviving mice after day 11 p.i. did not show any signs of clinical illness for 90 days p.i. These data, therefore, suggest that activated microglia in this model may play a protective role rather than a cytotoxic role. Increasing evidence supports the potential role of activated microglia in neuronal survival (Nakajima & Kohsaka 1998). For example, production of neurotrophic factors such as nerve growth factor (NGF) and brain derived neurotrophic factor (BDNF) promote the development and normal function of neurones and glia (Elkabes *et al.* 1996; Mallat *et al.* 1989). Basic fibroblast growth factor regulates the development and regeneration of neurones (Shimojo *et al.* 1991). Plasminogen enhances neuronal outgrowth (Nakajima *et al.* 1992) and similarly, thrombospondin, secreted by amoeboid microglia, stimulate neurite growth and regeneration (Chamak *et al.* 1994).

In addition, different cytokines produced by activated microglia *eg.*, IL-6, IL-1, IL-1β, TGF-β and IL-3 support neuronal survival and remyelination (Mason *et al.* 2001; Hama *et al.* 1989; Kamegai *et al.* 1990; Frei *et al.* 1989; Giulian *et al.* 1994; Pratt & McPherson 1997). Soontornniyomkikj *et al.* (1998) demonstrated that in HIV-1 encephalitis, BDNF protein is produced only by activated microglia and suggest that these cells may therefore provide a local supplementary source of BDNF to the neurones to survive. The production of these neurotropic factors from activated microglia may therefore, play a role in trophic support for injured neurones. Importance of microglial activation in neuronal survival has been investigated by Berezovskaya *et al.* (1995) in the ischemic lesion model in CSF-1-deficient mice. Since, CSF-1 acts as a potent mitogen for microglia (Giulian & Ingeman 1988), lack of CSF-1 resulted abnormal microglial activation, which increased neuronal vulnerability to ischemia, compared to control mice.

Microglia are major APC within the CNS (Shrikant 1996). MHC-II can be expressed constitutively in the human microglia (Gehrmann *et al.* 1993) and rat microglia (Sedgwick *et al.* 1993), although it was once thought not to be (Griffin *et al.* 1992). In contrast, in the WNV encephalitis model, microglia from mock-infected mice were consistently negative for MHC-II (Figure 4.12 a) significant expression was induced after infection. The induction of MHC-II is required to present Ag to $CD4^+$ T cells. Induction of MHC-II in microglia has been shown in many human neurological disorders and encephalitic models (Deckert-Schluter *et al.* 1999; Bo *et al.* 1994; Song & Jia 1999; Schmitt *et al.* 1998; Morioka *et al.* 1992; Caplazi & Ehrensperger 1998; Gehrmann *et al.* 1993). Increasing evidence suggests that similar to the MHC-II induction in peripheral cells, IFN-γ is a potent inducer of MHC-II in microglia (Deckert-Schluter *et al.* 1999; Pazmany *et al.* 2000; Aloisi *et al.* 1998). In contrast, in WNV encephalitis, MHC-II was induced in microglia in both infected B6.WT and B6.IFN-γ-/- mice. Thus, the presence of IFN-γ did not massively upregulate MHC-II in B6.WT; nor did the absence of IFN-γ reduce the expression of MHC-II in microglia in the B6.IFN-γ-/- mouse (Figure 4.12 a, b and 4.13). Moreover, the kinetics of MHC-II expression was similar between the groups. These results suggest that MHC-II induction in microglia is independent of IFN-γ.

Since the numbers of activated microglia detected by GS-lectin were significant in both groups of mice, numbers of GS-lectin positive microglia and MHC-II-expressing microglia were compared. Interestingly, it was found that the MHC-II-expressing microglia were significantly less (p=<0.001) compared to the number of GS-lectin-positive microglia except on day 15 p.i.(Figure 4.13). Moreover, almost all MHC-II-expressing microglia displayed amoeboid morphology in both groups of mice (Figure 4.13 and b). These results suggest that microglia are relatively resistant to MHC-II induction during WNV encephalitis and may perhaps not actively participate in Ag presentation to T cells. It has been suggested that MHC-II expression is regulated by neurones and blockade of neuronal activity significantly increased microglial MHC-II expression (Neumann & Wekerle 1998). The low levels of MHC-II induction, despite high activation of microglia coupled with the observation that only amoeboid microglia expressed MHC-II, therefore may mean that neurones induce MHC-II expression on microglia as a last resort in WNV encephalitis.

In conclusion, only microglia, not astrocytes are activated in WNV encephalitis. Microglial activation is independent of IFN-γ. In both groups of mice, microglia were activated within 24h of WNV Ag detection in neurones and returned to normal only after WNV Ag was undetectable, suggesting that microglial activation are induced by infected neurones. Moreover, the low incidence of neuronal death, despite formation of large numbers of microglial nodules with highly activated microglia, further suggest that microglia may play an active role in controlling and/or eradicating WNV directly or indirectly in the neurones via non-cytotoxic mechanisms and may furthermore provide trophic support to these neurones. MHC-II expression on microglia is independent of IFN-γ, but relatively little MHC-II expression was induced, compared to levels of activation detected by GS-lectin. The functional significance of activated microglia seen in areas/nodules surrounding WNV-infected neurones need to be further investigated.

Chapter-5

Enhanced expression of cell adhesion molecules in the CNS in the absence of IFN-γ in WNV encephalitis

5.1. Introduction

Leukocyte recruitment to the CNS parenchyma is a feature of viral encephalitis. Under normal conditions, the CNS parenchyma is separated from the peripheral immune system through the BBB formed by interendothelial tight junctions, which form an impermeable seal between the cells. Thus, the BBB plays a critical role in regulating cell trafficking through the CNS (Andjelkovic & Pachter 1998) (See section 1.2.3.). A number of studies have explored inflammatory responses in the CNS in infectious, inflammatory and autoimmune demyelinating diseases. All are characterized by the migration of acute and chronic inflammatory cells from blood into the CNS across the extravascular tissue (Caplazi & Ehrensperger 1998; Eralinna *et al.* 1996; Krakowski & Owens 1996; Johnson *et al.* 1985). Similar to peripheral inflammation, the upregulation of CAM on the surface of neurovascular endothelial cells and the production of cytokines and chemokines at the site of the BBB play an important role in mobilizing peripheral inflammatory cells into the CNS (Clark *et al.* 1995; Sobel *et al.* 1990; Matyszak 1998; Stanimirovic & Satoh 2000).

The process of leukocyte migration to sites of inflammation is believed to begin with the activation of endothelial cells by inflammatory mediators, leading to increased expression of CAM, including selectins and the immunoglobulin superfamily of CAM (Meager 1999; Imhof & Dunon 1995). During extravasation, leukocytes make initial transient contact with neurovascular endothelial cells lining the vessel wall, roll along the endothelial cells, firmly adhere and extravasate out of the vasculature. As described earlier in section 1.4.1.4., selectins play an important role in initial attachment and rolling of leukocytes along the vessel wall, where firm adhesion is produced by the interaction of leukocyte integrins with immunoglobulin superfamily of CAM, including ICAM-1 and VCAM-1, expressed on

endothelial cells during inflammation. Therefore, the expression of ICAM-1 and VCAM-1 on the cerebral endothelium, which do not express these molecules under normal condition (Matyszak 1998), is critical for transmigration of leukocytes into the CNS parenchyma. ICAM-1 is a ligand for LFA-1 and VCAM-1 is a ligand for VLA-4. Both of these integrins are constitutively expressed on the surface of leukocytes. ICAM-1 and VCAM-1 have been extensively studied in *in vitro* culture systems (Linke *et al.* 2000; Shen *et al.* 1997; Wong & Dorovini-Zis 1995; Brankin *et al.* 1995; Wong & Dorovini-Zis 1992) and have been found to be induced by proinflammatory cytokines such as IFN-γ, TNF and IL-1 (Barten & Ruddle 1994; Dobbie *et al.* 1999; Lee *et al.* 1999; de Jong *et al.* 1996). These cytokines not only induce the cerebral endothelium to express ICAM-1 and VCAM-1, but also induce expression of these molecules in astrocytes and microglia (Kyrkanides *et al.* 1999; Shrikant *et al.* 1994; Zielasek *et al.* 1993).

The expression and upregulation of ICAM-1 and VCAM-1 in the cerebral endothelium allows recruitment of cells from blood to the CNS parenchyma and thus, initiates inflammation within the CNS. This process is the first step in the immune response and is required for host defence, as well as tissue repair. Infiltrating NK and T lymphocytes help to eliminate virus-infected cells from the CNS, plasma cells produce neutralizing Ab, which inactivates extracellular virus and hence, prevents virus spread in the CNS, and infiltrating macrophages help to clear cellular debris (Hatalski *et al.* 1998; Williamson & Stohlman 1990; Fehniger *et al.* 1998; Chan *et al.* 1989). Moreover, these infiltrating cells produce different kinds of cytokines that enhance the activation of resident CNS cells and induce them to produce many different kinds of cytokines and neurotrophic growth factors which help to return the CNS to normal homeostasis (Aloisi *et al.* 2000). Therefore, ICAM-1 and VCAM-1 play a crucial role in neuroinflammation during viral encephalitis.

The physiological role of adhesion molecule expression on glial cells has not been characterized. However, from the general role of CAM in other cell types, it is inferred that expression of CAM in glial cells may guide infiltrating leukocytes into and through the CNS parenchyma (Merrill & Benveniste 1996). A diagrammatic representation of interactions among inflammatory leukocytes, endothelial cells and glial cells expressing ICAM-1 is presented in figure 5.1. It has also been reported that neurones can express both

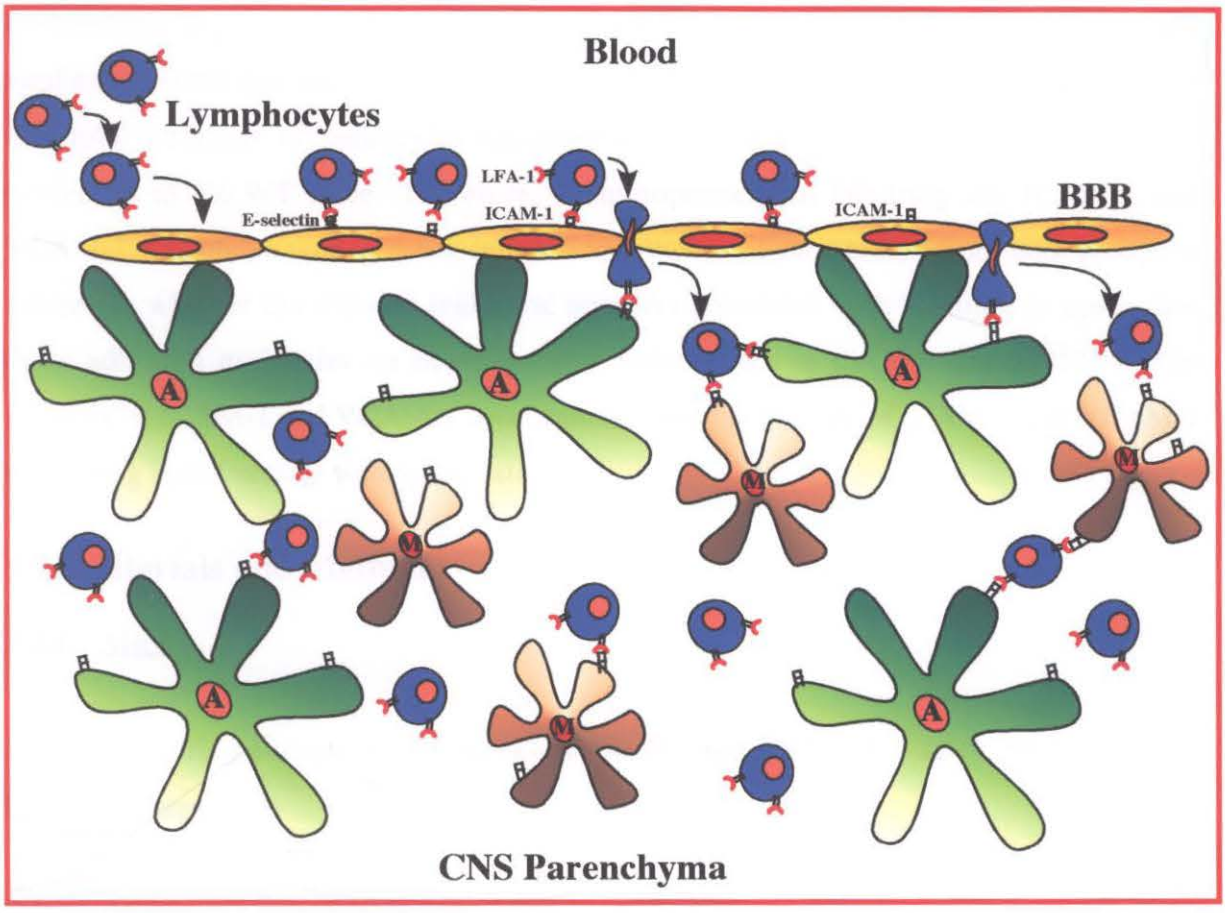

Figure: 5.1 Interactions among lymphocytes, endothelial cells, astrocytes and microglia. T lymphocytes interacting with E-selectin and ICAM-1$^+$ endothelial cells and astrocytes of the BBB, followed by extravasation through the BBB, and then migration through brain parenchyma via further interactions with ICAM-1$^+$ astrocytes and microglia. In addition VLA-4 expression by T cells and VCAM-1 expression by endothelial cells and glial cells leads to the same interactions as dipicted for ICAM-1 and LFA-1. Abbreviations: BBB, blood-brain barrier, ICAM-1, intercellular adhesion molecule-1, LFA-1, lymphocyte function-associated antigen, VLA-4, very late antigen-4, VCAM-1, vascular cell adhesion molecule-1, A, astrocyte, M, microglia. Symbols: lymphocyte , endothelial cell , astrocyte , microglia . Modified from Merrill & Benveniste 1996.

ICAM-1 and VCAM-1 in *in vitro* culture upon stimulation with cytokines (Hery *et al.* 1995), however, this has not been reported *in vivo*.

Despite their importance in inflammation, the upregulation of ICAM-1 and VCAM-1 in any viral encephalitis has not been studied in detail. Results in chapter 3 clearly demonstrated that total numbers of leukocytes recruited to the brain were reduced in B6.IFN-γ-/- compared to B6.WT mice. Therefore, immunoperoxidase labelling for ICAM-1 and VCAM-1 was undertaken in mock-infected and WNV-infected brains from both groups to determine whether the reduced leukocyte numbers correlated with a failure to upregulate these adhesion molecules on neurovascular endothelium in the absence of IFN-γ. The intensity of ICAM-1 and VCAM-1 was evaluated and the number of ICAM-1 and VCAM-1 expressing blood vessels were quantitated.

5.2. Materials and Methods

5.2.1. Mice

Female, specific-pathogen free, 8-week-old B6.WT and B6.IFN-γ-/- mice, backcrossed to C57BL/6, were used.

5.2.2. Virus infection of mice and tissue preparation

To determine the kinetics of ICAM-1 and VCAM-1 expression in the CNS, a time course experiment was carried out. Groups of 120 mice/strain were inoculated with $6x10^4$ pfu/mouse. Tissues were collected and processed as described in section 2.2.2.2.

5.2.3. Immunohistochemistry

Serial sections from paraformaldehyde-fixed, frozen tissues were stained with anti-ICAM-1 and anti-VCAM-1 antibodies, and examined to determine the kinetics of expression and upregulation of these CAM during encephalitis in both groups.

- **Detection of ICAM-1 expression**

Hybridoma supernatant from rat anti-mouse ICAM-1 (CD54) at 1:10 dilution (YN1/1.7.4; ATCC CRL 1878) was used as the primary antibody for labelling ICAM-1 expression. Frozen sections were rehydrated with Tris-buffer for 5 mins. After endogeneous peroxidase and non-specific blocking procedures, as described before in section 2.2.3, sections were incubated with primary Ab at 4°C for 1.5h. The rest of the staining procedure was identical to that described in section 2.2.3. Mock-infected brain sections from both groups were used as controls for ICAM-1 labelling. Monoclonal rat IgG2a was used as an isotype control for the primary antibody.

- **Detection of VCAM-1 expression**

Rat anti-mouse VCAM-1 (CD106) Ab at 1:50 dilution (01811D, Pharmingen, San Diego, CA) was used as the primary antibody for labelling VCAM-1 expression. Frozen sections were rehydrated with Tris-buffer for 5 mins and endogeneous peroxidase activity was blocked with 2.0% H_2O_2 in Tris-buffer for 30 mins. After endogeneous peroxidase and non-specific blocking procedures, sections were incubated with primary Ab for overnight at 4°C. The rest of the staining procedure was identical to that described in section 2.2.3. Mock-infected brain sections from both groups were used as controls for VCAM-1 labelling. Monoclonal rat IgG2a was used as an isotype control for the primary Ab.

- **Double labelling for ICAM-1 expression and activated microglia**

Alkaline phosphatase substrate, 5-Bromo-4-Chloro-3-Indolyl Phosphate/Nitroblue Tetrazolium (BCIP/NBT, Vector Laboratories, Burlingame, CA), was used to give a blue signal for activated microglia, whereas horseradish peroxidase substrate, DAB, was used to detect ICAM-1 expression in microglia. ICAM-1 expression was detected by the procedure described above and activated microglia was detected by the procedure described in section 4.2.4.

5.2.4. Quantification of cells and data analysis

Quantification of cells and analysis of data was carried out as described in section 2.3 and 2.6, respectively. Figures are mean values ± SEM for the total number of fields examined from the indicated number of mice, n.

5.3. Results

5.3.1. Expression of ICAM-1 on neurovascular endothelium

Since IFN-γ plays an important role in the activation of neurovascular endothelium and the induced expression of immunoglobulin superfamily of CAM, the kinetics of ICAM-1 expression in the brain parenchyma was assessed using anti-ICAM-1 immunohistochemistry. Brains of mock-infected B6.WT mice showed no labelling for ICAM-1 on neurovascular endothelium (Figure 5.2 a), indicating that ICAM-1 is not constitutively expressed in wild type mice. In contrast, ICAM-1 was constitutively expressed at low levels in mock-infected B6.IFN-γ-/- mice (Figure 5.2 b). During infection, activated leukocytes migrate into the brain. They bind to cell surface molecules such as ICAM-1, expressed on endothelium (Figure 5.2 c, open arrow) and transmigrate into the brain parenchyma (Figure 5.2 d, open arrows). After infection, much greater expression of ICAM-1 was observed in the blood vessels of B6.IFN-γ-/- mice (Figure 5.2 f) compared to B6.WT (Figure 5.2 e).

To evaluate whether there was a significant difference in the number of blood vessels expressing ICAM-1 between the groups, ICAM-1-positive blood vessels were quantitated as described in Materials and Methods. The kinetics, intensity of staining and number of blood vessels expressing ICAM-1 in B6.IFN-γ-/- mice were very different from that of B6.WT (Figure 5.3). In B6.WT mice, vessels expressing ICAM-1 at low levels were initially observed at day 3 p.i. The number of ICAM-1-expressing vessels increased at day 6 p.i., and was maximal on day 9 p.i. In B6.IFN-γ-/- mice, vessels expressing ICAM-1 were upregulated from day 3 p.i., numbers peaking on days 8 and 10 p.i. The number of ICAM-1-positive vessels was significantly higher (p=<0.001 on each day) in B6.IFN-γ-/- mice from day 6 onwards compared to B6.WT. However, in both groups expression of ICAM-1 and number of vessels expressing increased levels returned to the nearly baseline values of the

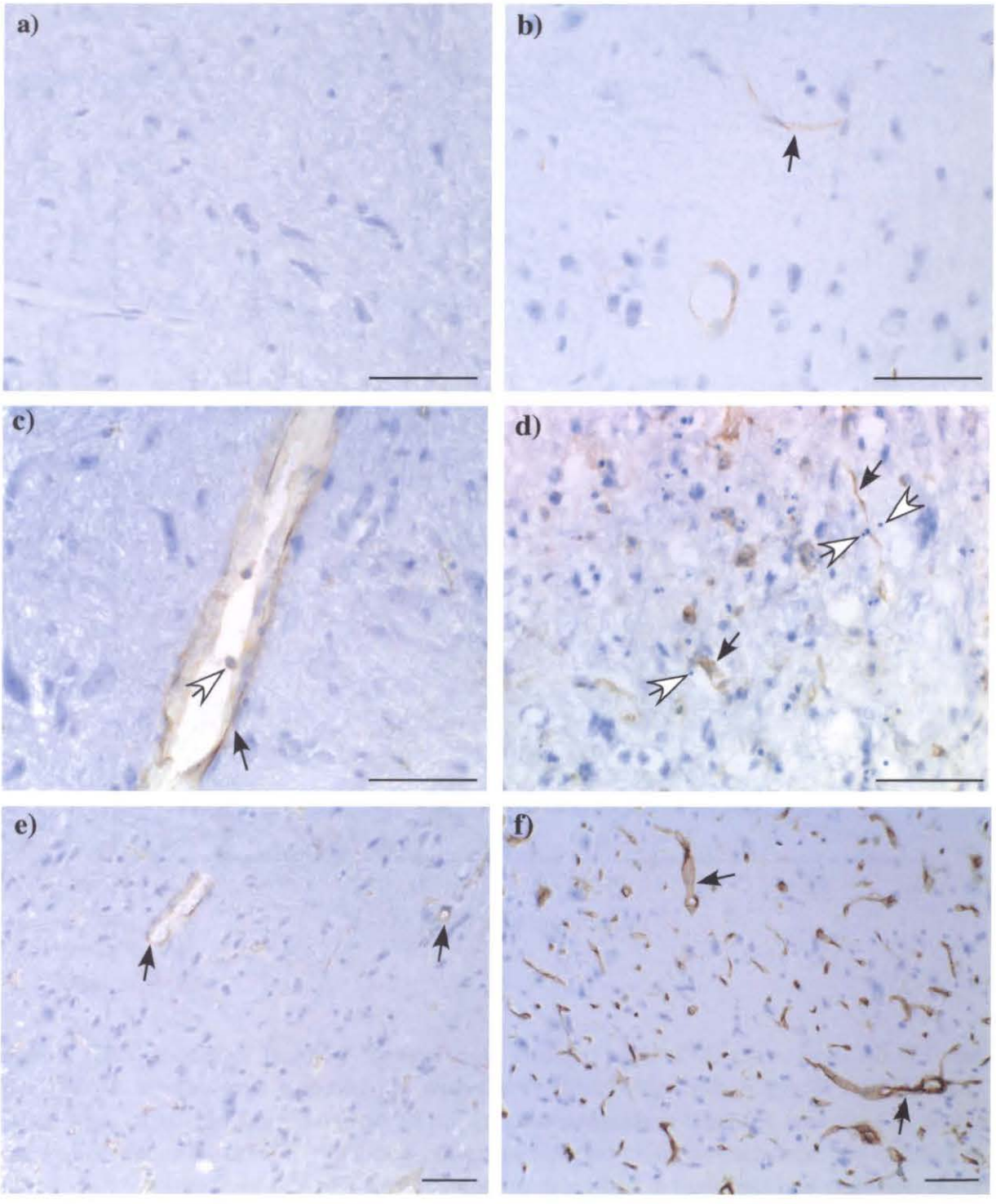

Figure: 5.2 ICAM-1 expression in WNV encephalitis. Immunoperoxidase labelling was used for the detection of ICAM-1 in mock-infected and WNV-infected mouse brains from both groups There was no constitutive expression of ICAM-1 in the mock-infected brain of B6.WT mice (a). In contrast, ICAM-1 was constitutively expressed in the mock-infected brain of B6.IFN-γ-/- mice (b). During leukocyte migration to the brain parenchyma, leukocytes bind to ICAM-1 (c) (open arrow), expressed on endothelium of infected B6.WT mouse brain (c) (solid arrow) and transmigrate to the parenchyma (d) (open arrows). ICAM-1 expressed in the blood vessels (d) (solid arrows) facilitates the entry of leukocytes to the brain parenchyma. Both the number of ICAM-1$^+$ blood vessels and their staining intensity was higher in the infected brain parenchyma from B6.IFN-γ-/- (f) compared to B6.WT mice. Scale bar-50μm.

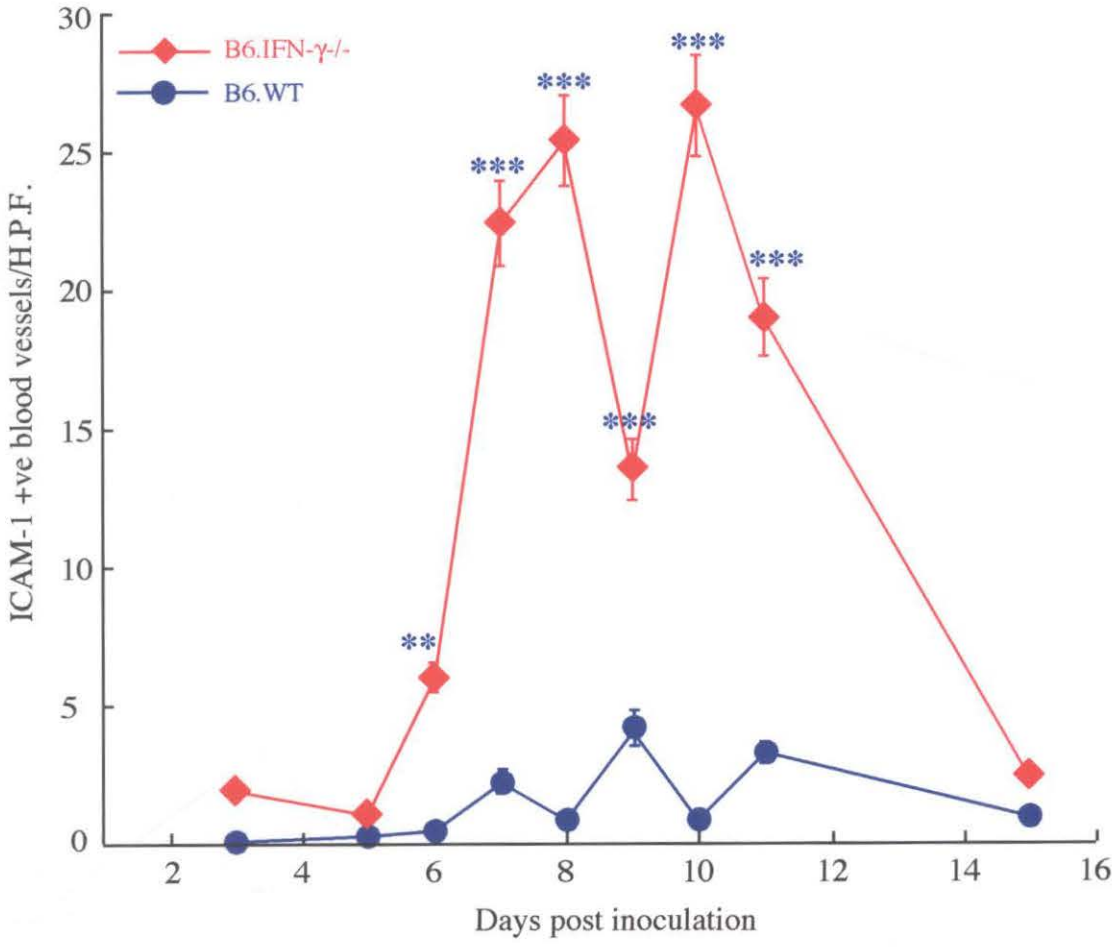

n = 70 mice/group

Figure: 5.3. Kinetics of ICAM-1 upregulation. Groups, each of 70 mice, from B6.WT and B6.IFN-γ-/- strains were infected i.p. with $6x10^4$ pfu/mouse. Subgroups of mice in each strain were sacrificed from day 3 to 15 p.i. Immunoperoxidase labelling was used to detect the expression of ICAM-1 in the blood vessels of infected brain parenchyma. The number of blood vessels expressing ICAM-I was counted, as described in materials and methods. Sixty H.P.F. were counted, per mouse brain and values for each timepoint amalgamated and expressed as mean ± SEM. There were significant differences at days 6-11 p.i. between B6.WT and B6.IFN-γ-/- values (**p=<0.01 and ***p=<0.001 by ANOVA). Brains from mock-infected B6.WT mice were negative for ICAM-1 whereas B6.IFN-γ-/- mice showed constitutive expression of ICAM-1.

respective groups by day 15 p.i (Figure 5.3). These data show that IFN-γ does not play a critical role in ICAM-1 upregulation in the neurovascular endothelium. Moreover, its absence is associated with a massive upregulation of ICAM-1 in WNV encephalitis.

5.3.2. Expression of ICAM-1 in microglia

5.3.2.1. Microglia express ICAM-1 in the absence of IFN-γ

As described earlier in section 5.3.1, lack of IFN-γ resulted in massive ICAM-1 upregulation in blood vessels in B6.IFN-γ-/- mice compared to B6.WT. In addition to the blood vessels, glial cells were also expressing ICAM-1 in B6.IFN–γ-/- mice (Figure 5.4). Unlike blood vessels, microglia did not constitutively express ICAM-1 in mock-infected brain parenchyma (Figure 5.4 a). After infection, glial cells were positive for ICAM-1 expression only from day 6 p.i. (Figure 5.4. b) and were observed only in the brainstem at this timepoint. On day 11 p.i., an increased number of glial cells were positive for ICAM-1 as well as showing significantly increased staining intensity (Figure 5.4.c). Nodules were also positive for ICAM-1 (Figure 5.4 d).

It has been reported that both astrocytes and microglia can express ICAM-1 (Lee & Benveniste 1999; Zielasek *et al.* 1993). However, in my model, astrocytes were seldom activated, while microglia were highly activated (chapter 4). I speculated that ICAM-1-expressing glial cells could be microglia, since the morphology of glial cells expressing ICAM-1 was similar to that of microglia. Therefore, double labelling of histological sections for both ICAM-1 and GS-lectin were performed to confirm the identity of these ICAM-1-expressing glial cells. Almost all ICAM-1-expressing glial cells, as well as nodules, co-labelled with GS-lectin, a marker for activated microglia (Figure 5.5 a, b). This result confirms that these ICAM-1 expressing cells were activated microglia.

Although ICAM-1 was expressed in the blood vessels from day 3 p.i. in B6.WT mice (section 5.3.1), not all mice expressed ICAM-1 in the blood vessels, initially. However, after day 3 p.i. this increased to 100% ICAM-1 expression at day 11 p.i. (Figure 5.6 A). Interestingly, no microglia were observed to express ICAM-1 at any timepoint in B6.WT (Figure 5.6 B). These results further confirm that lack of IFN-γ not only enhanced the

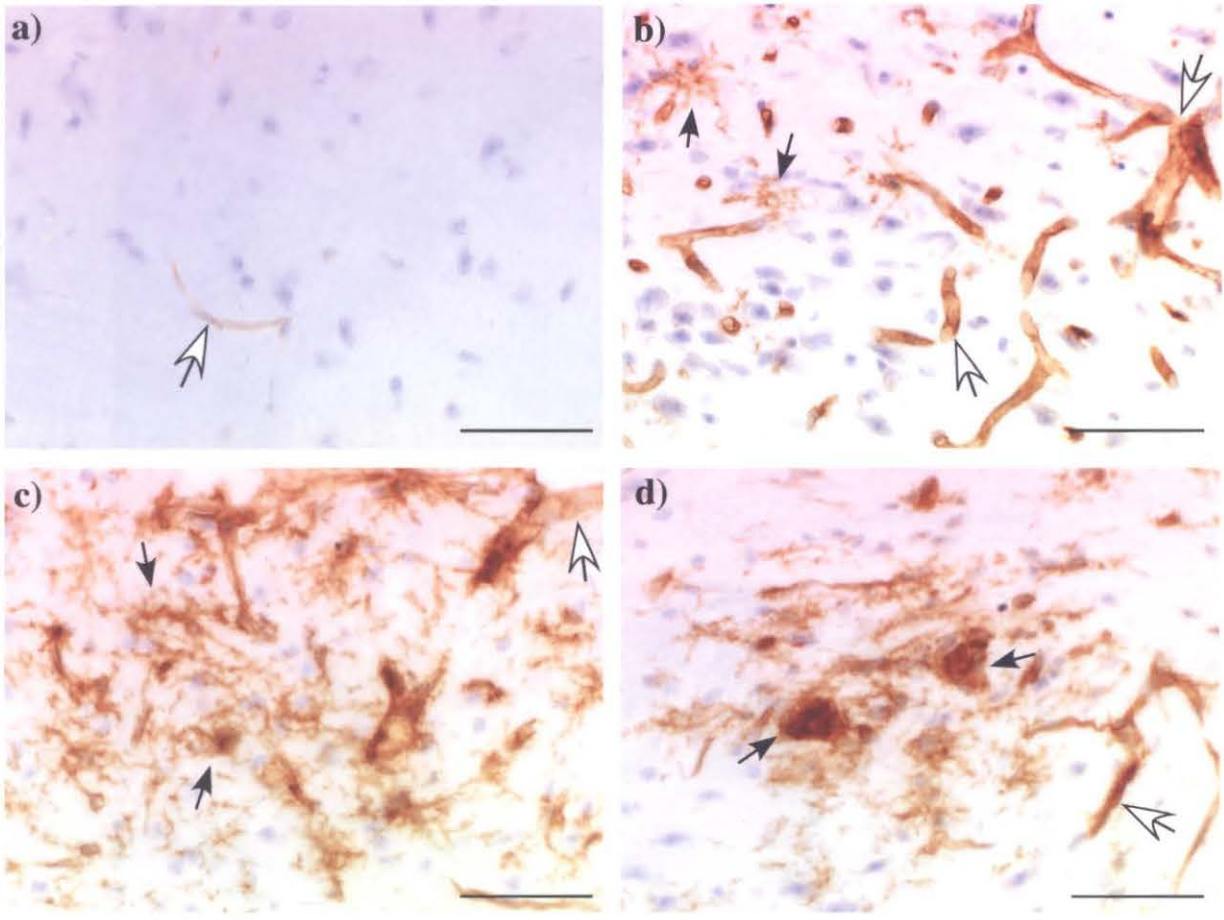

Figure: 5.4 Microglia express ICAM-1 only in the absence of IFN-γ in WNV encephalitis. Immunoperoxidase labelling was used for the detection of ICAM-1 in mock-infected and WNV-infected B6.IFN-γ-/- mouse brain. ICAM-1 is constitutively expressed only in the blood vessels (open arrow) but not in glial cells (a). On day 6 p.i., ICAM-1 was strongly expressed both in the blood vessels (open arrows) and glial cells (closed arrows) (b). The expression of ICAM-1 was massively increased on day 11 p.i.(c). At this time, nodules (closed arrows) were also postive for ICAM-1 labelling (d). Open arrows in all figures show ICAM-1 expression in the blood vessels and closed arrows show ICAM-1 expression in the glial cells. Scale bar = 50μm.

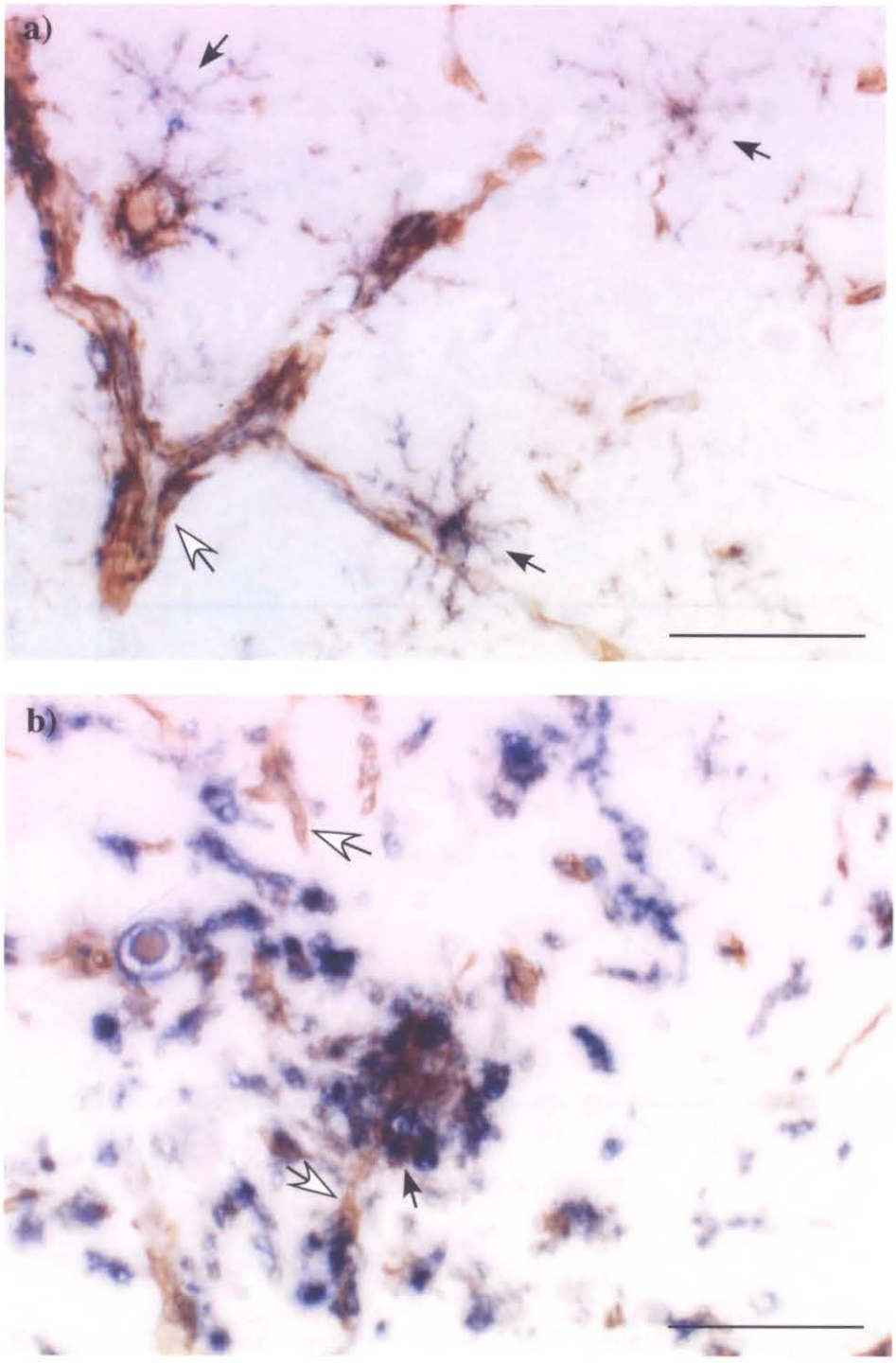

Figure: 5.5 Double labelling of WNV-infected B6.IFN-γ-/- mouse brain for ICAM-1 (brown) and activated microglia (blue) on day 10 p.i. ICAM-1 was expressed in both microglia and blood vessels in B6.IFN-γ-/- mice. Astrocytes and microglia both can express ICAM-1. Double labelling was performed to confirm the identity of ICAM-1$^+$ glial cells. Nearly all of ICAM-1$^+$ microglia were labelled with GS-lectin (a) (solid arrows) confirming that ICAM-1 positive glial cells were microglia. Microglial nodules also expressing ICAM-1 (b). Solid arrows in a) and b) show double labelled microglia and nodules with GS-lectin and ICAM-1, whereas open arrows show blood vessels expressing ICAM-1. Scale bar- 50μm.

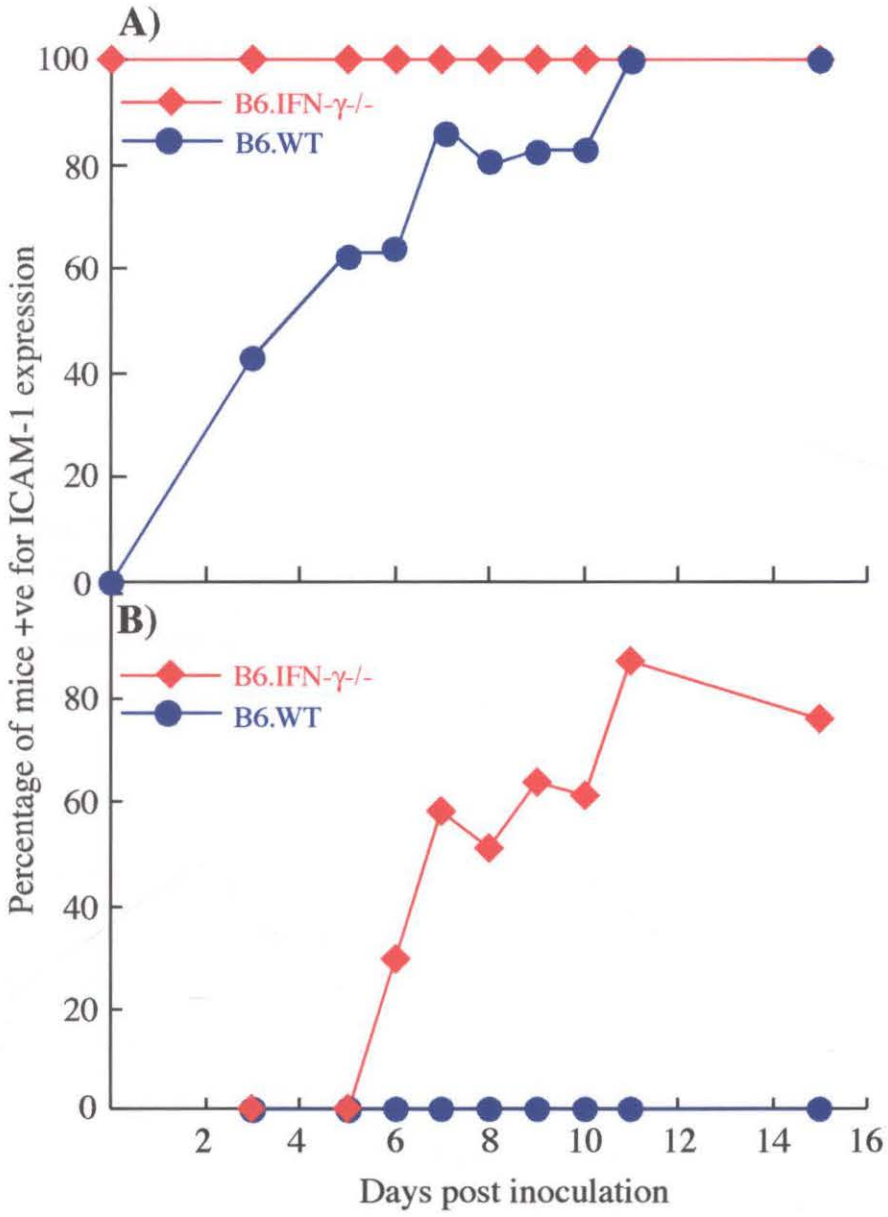

n = 70 mice/group

Figure: 5.6 Percentage of mice positive for ICAM-1 expression. Groups, each of 70 mice, from B6.WT and B6.IFN-γ-/- strains were infected i.p. with $6x10^4$ pfu/mouse. Subgroups of mice in each strain were sacrificed from day 3 to 15 p.i. Immunoperoxidase labelling was used to detect the expression of ICAM-1 in the brain parenchyma. A) In B6.WT, there was no constitutive expression of ICAM-1, but it was expressed on blood vessel endothelium from day 3 p.i. in few mice and increased subsequently at later timepoints. In contrast, in B6.IFN-γ, ICAM-1 was expressed constitutively on endothelium. B) Interestingly, ICAM-1 was also expressed in microglia in B6.IFN-γ-/- from day 6 p.i., the number of mice positive for microglial ICAM-1 increasing further in later timepoints. In contrast, no microglia of B6.WT were positive for ICAM-1 at any timepoints.

upregulation of ICAM-1 in the blood vessels in B6.IFN–γ-/-, but also that not withstanding microglia were induced to express ICAM-1 in the absence of IFN-γ.

5.3.2.2. Kinetics of microglial and endothelial ICAM-1 expression in B6.IFN-γ-/- mice

In B6.IFN-γ-/- mice, unlike the constitutive expression of ICAM-1 in blood vessels, not all mice were positive for microglial ICAM-1. A very small percentage of mice was positive for microglial ICAM-1 on day 6 p.i. By day 11 p.i., however, more than 85% mice expressed ICAM-1 on the microglia (Figure 5.6 B). The number of ICAM-1-positive microglia and blood vessels were counted, as described in Materials and Methods. The kinetics of ICAM-1-positive blood vessels and ICAM-1-positive microglia are presented in figure 5.7. Blood vessels expressing ICAM-1 increased at least 24h before microglia, and with much steeper kinetics. The increase in microglial ICAM-1 was slower. Thus, microglia and blood vesels express ICAM-1 with different kinetics.

Although microglial activation was detectable from d7 p.i. by GS-lectin, microglia expressed ICAM-1 from day 6 p.i in B6.IFN–γ-/- mice. However, the percentage of mice expressing microglial ICAM-1 and activation detected by GS-lectin was similar after day 6 p.i. To evaluate whether there was a significant difference between these cells, the number of GS-lectin-positive microglia and ICAM-1-positive microglia were compared. The kinetics of microglial ICAM-1 expression and GS-lectin positive microglia can be seen in figure 5.8. At the earlier timepoints from day 6-8, a significantly higher number of microglia were expressing ICAM-1 (p=<0.05), compared to lectin-positive microglia, however, on day 9 and 10 p.i., the numbers of cells expressing both were nearly equal. Interestingly, on day 11 p.i., significantly higher numbers of microglia were expressing ICAM-1 (p=<0.001), compared to lectin-positive microglia. However, the number of both ICAM-1-positive and lectin-positive microglia returned to nearly baseline levels on day 15 p.i.

5.3.3. Expression of VCAM-1 on neurovascular endothelium

Since there was an enhanced ICAM-1 expression in the absence of IFN-γ in B6.IFN-γ-/- mice, the status of VCAM-1 expression in the brain parenchyma was assessed, as with ICAM-1 expression, in both groups of mice. Unlike ICAM-1 expression, VCAM-1 was not

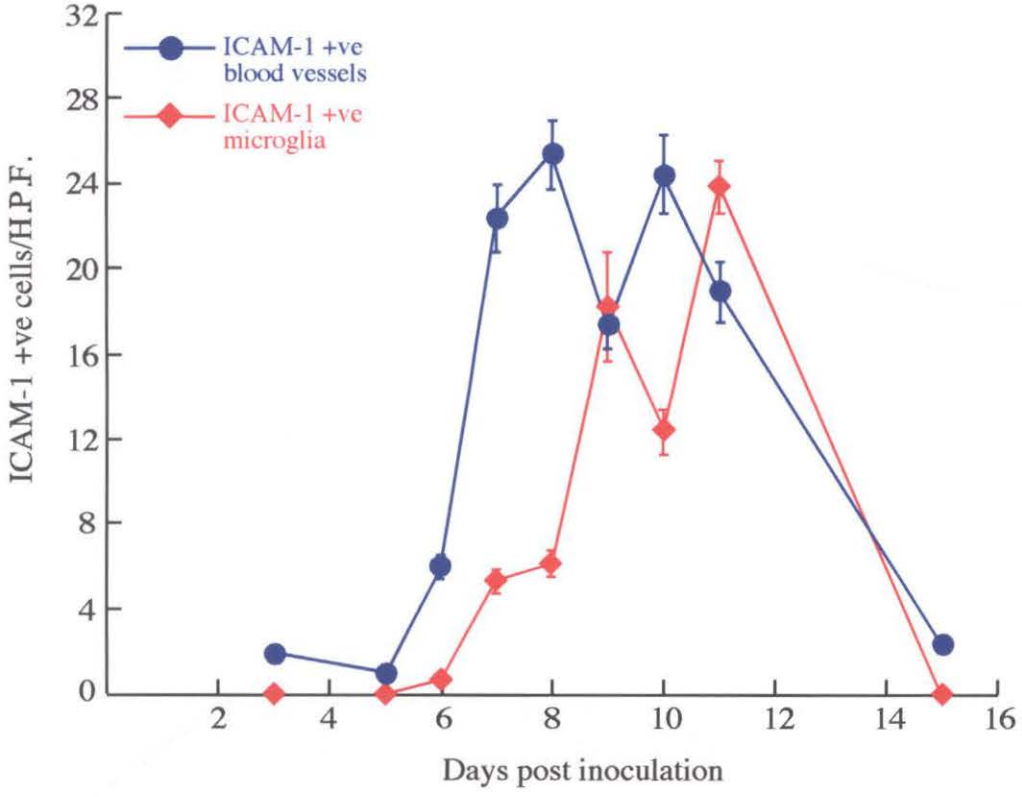

n = 70 mice/group

Figure: 5.7 ICAM-1 expression in blood vessels and microglia in B6.IFN-γ-/- mouse brain. Groups, each of 70 mice, from B6.WT and B6.IFN-γ-/- strains were infected i.p. with $6x10^4$ pfu/mouse. Subgroups of mice in each strain were sacrificed from day 3 to 15 p.i. Immunoperoxidase labelling was used to detect the expression of ICAM-1 in the brain parenchyma. The number of blood vessels and microglia expressing ICAM-I was counted, as described in materials and methods. Expression of ICAM-1 in the blood vessels increased earlier than that in the microglia.

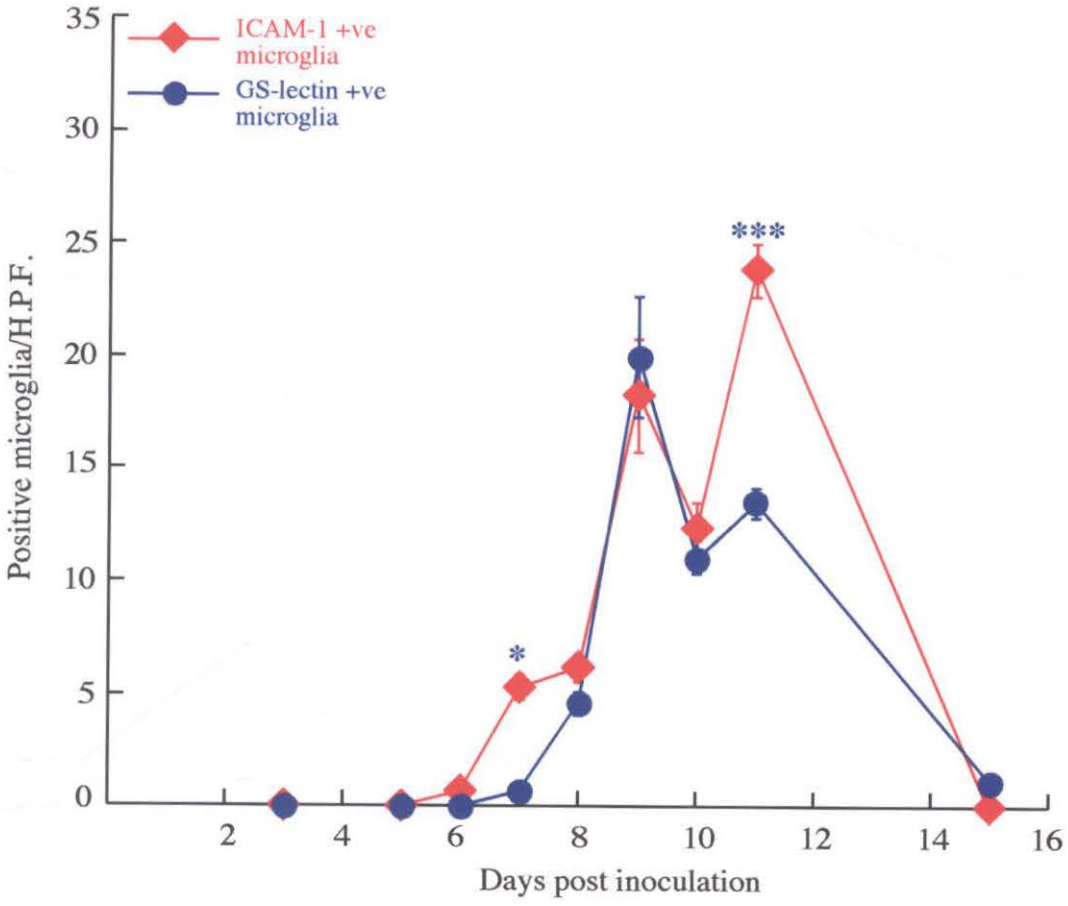

n = 70 mice

Figure: 5.8 Comparison between kinetics of ICAM-1 expression in microglia and microglial activation in B6.IFN-γ-/- mouse brain. Groups, each of 70 B6.IFN-γ-/- mice were infected i.p. with $6x10^4$ pfu/mouse. Subgroups of mice in each strain were sacrificed from day 3 to 15 p.i. Immunoperoxidase labelling was used to detect the expression of ICAM-1 and GS-lectin was used as a marker to detect the activation of microglia of infected brain parenchyma. The numbers of ICAM-1 expressing microglia and GS-lectin$^+$ microglia were counted, as described in materials and methods. Sixty H.P.F. were counted per mouse brain and values for each timepoint amalgamated and expressed as mean ± SEM. (*p=<0.05, and ***p=<0.001 by ANOVA).

expressed constitutively in either group (Figure 5.9 a, b). Furthermore, after infection, VCAM-1 expression was observed only in the blood vessels in both groups (Figure 5.9 c,d). The number of blood vessels expressing VCAM-1 was quantitated in both groups, as described in Materials and Methods to evaluate whether there was a significant difference between the groups. The kinetics of VCAM-1 expression in both groups is presented in figure 5.10. In B6.WT mice, VCAM-1 was expressed only from day 5 p.i. It was maximal on day 9 and returned to almost baseline levels by day 15 p.i. On the other hand, in B6.IFN-γ-/- mice, expression of VCAM-1 was detectable from day 3 p.i. Similar to the B6.WT, the increasing number of vessels expressing VCAM-1 also peaked on day 9 p.i., at approximately 3-fold higher than the B6.WT (p=<0.001) and returned to almost baseline levels by day 15 p.i. The kinetics of VCAM-1 expression was very similar between the groups, although it was expressed 24h earlier than B6.WT mice. These data indicate that IFN-γ is not required for upregulation of VCAM-1 in the CNS blood vessels during WNV infection. Moreover, lack of IFN-γ is associated with upregulation of VCAM-1 in WNV encephalitis.

5.3.4. Comparison between ICAM-1 and VCAM-1 expression in blood vessels

Results from preceeding sections show that both ICAM-1 and VCAM-1 were expressed and upregulated in WNV encephalitis. Moreover, in both cases it shows that lack of IFN-γ was associated with enhanced their expression, compared to wild type mice. Comparison between the kinetics of ICAM-1 and VCAM-1 expression in the blood vessels of each strain were also evaluated. In B6.WT the number of blood vessels expressing ICAM-1 was significantly higher (p=<0.001) on day 7, 9 and 11 p.i. than the VCAM-1-expressing blood vessels (Figure 5.11 A). Similarly, in B6.IFN-γ-/- mice, the number of blood vessels expressing ICAM-1 was very much higher from day 6-11 p.i. (p=<0.001) than the VCAM-1 expressing blood vessels. Thus, greater numbers of blood vessels express ICAM-1 compared to VCAM-1 in both groups of mice in WNV encephalitis.

5.4. Discussion

CNS infection with viruses can result in vigorous inflammatory responses with large numbers of leukocytes recruited into the CNS. These are required for the evolution of pathological and host-defence processes (Christensen *et al.* 2001; Weidinger *et al.* 2000;

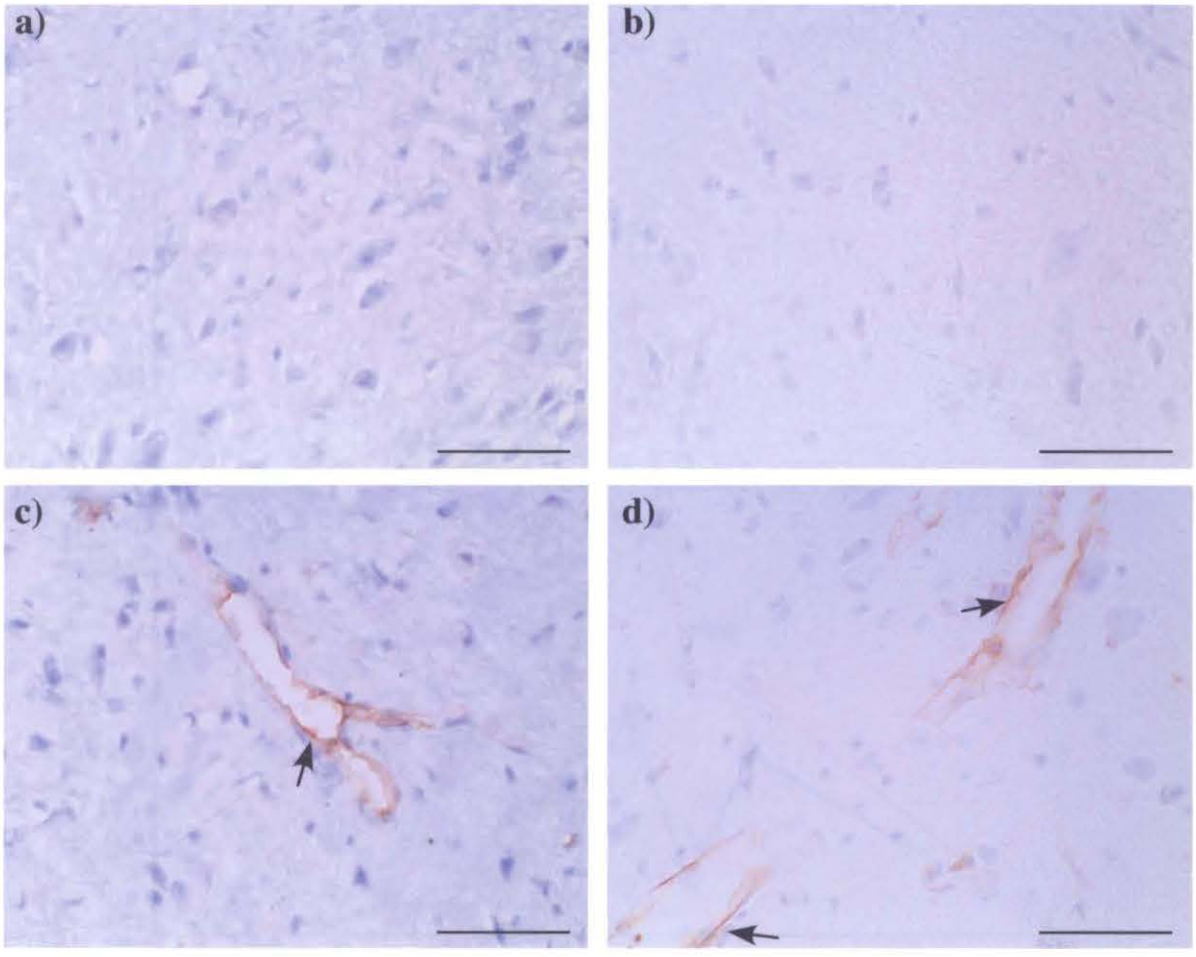

Figure: 5.9 Immunoperoxidase labelling of VCAM-1 in the blood vessels of mock-infected and WNV-infected mouse brains on day 9 p.i. from both groups. VCAM-1 expression was constitutively negative in the mock-infected brain parenchyma from both B6.WT (a) and B6.IFN-γ-/- (b). Infected brain parenchyma from B6.WT (c) and B6.IFN-γ-/- (d) showing VCAM-1 expression. Scale bar=50μm.

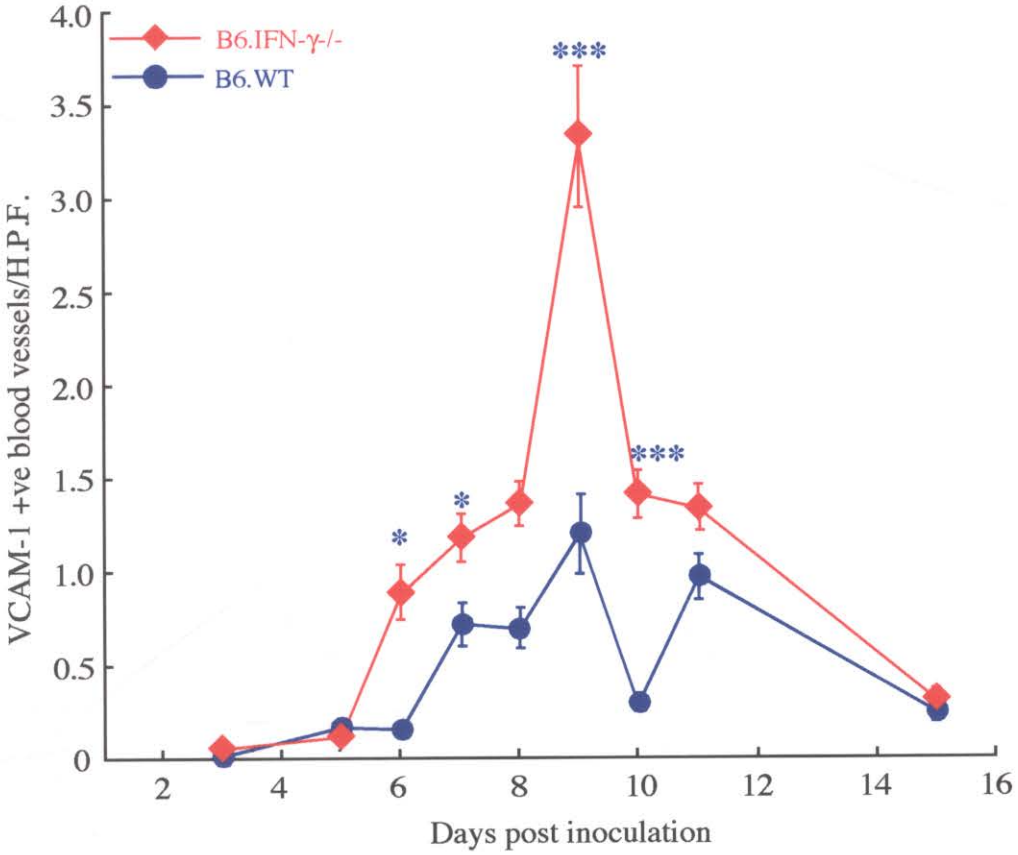

n = 70 mice/group

Figure: 5.10 Kinetics of VCAM-1 upregulation. Groups, each of 70 mice, from B6.WT and B6.IFN-γ-/- strains were infected i.p. with $6x10^4$ pfu/mouse. Subgroups of mice in each strain were sacrificed from day 3 to 15 p.i. Immunoperoxidase labelling was used to detect the expression of VCAM-1 in the blood vessels of infected brain parenchyma. The number of blood vessels expressing VCAM-I was counted, as described in materials and methods. Sixty H.P.F. were counted per mouse brain and values for each timepoint amalgamated and expressed as mean ± SEM. There were significant differences at days 6, 8, 9 and 10 p.i. between B6.WT and B6.IFN-γ-/- values (*p=<0.05, and ***p=<0.001 by ANOVA). Brains from both mock-infected B6.WT and B6.IFN-γ-/- mice were negative for VCAM-1.

Figure: 5.11 Kinetics of ICAM-1 and VCAM-1 upregulation. Groups, each of 70 mice, from B6.WT and B6.IFN-γ-/- strains were infected i.p. with $6x10^4$ pfu/mouse. Subgroups of mice in each strain were sacrificed from day 3 to 15 p.i. Immunoperoxidase labelling was used to detect the expression of ICAM-1 and VCAM-1 in the blood vessels of infected brain parenchyma. The number of blood vessels expressing ICAM-I and VCAM-1 was counted, as described in Materials and Methods. Sixty H.P.F. were counted per mouse brain and values for each timepoint amalgamated and expressed as mean ± SEM. The number of ICAM-1 expressing blood vessels was significantly higher than those expressing VCAM-1 in both B6.WT (A) and B6.IFN-γ-/- (B) mouse brains. (**p=<0.01, ***p=<0.001 by ANOVA. Note the change of scale at 5 positive blood vessels/H.P.F. (broken line).

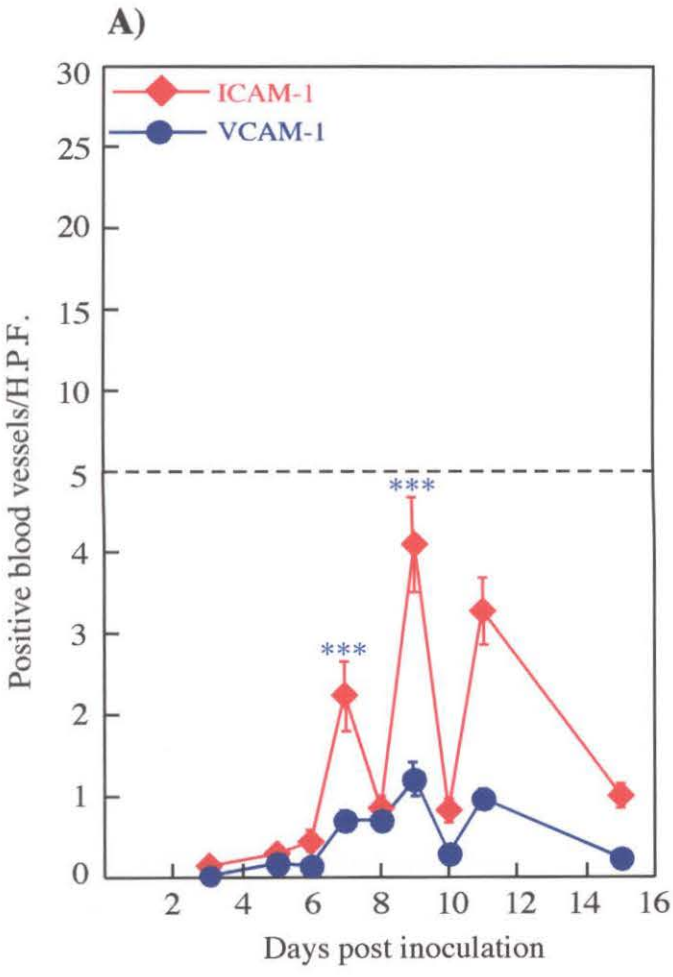

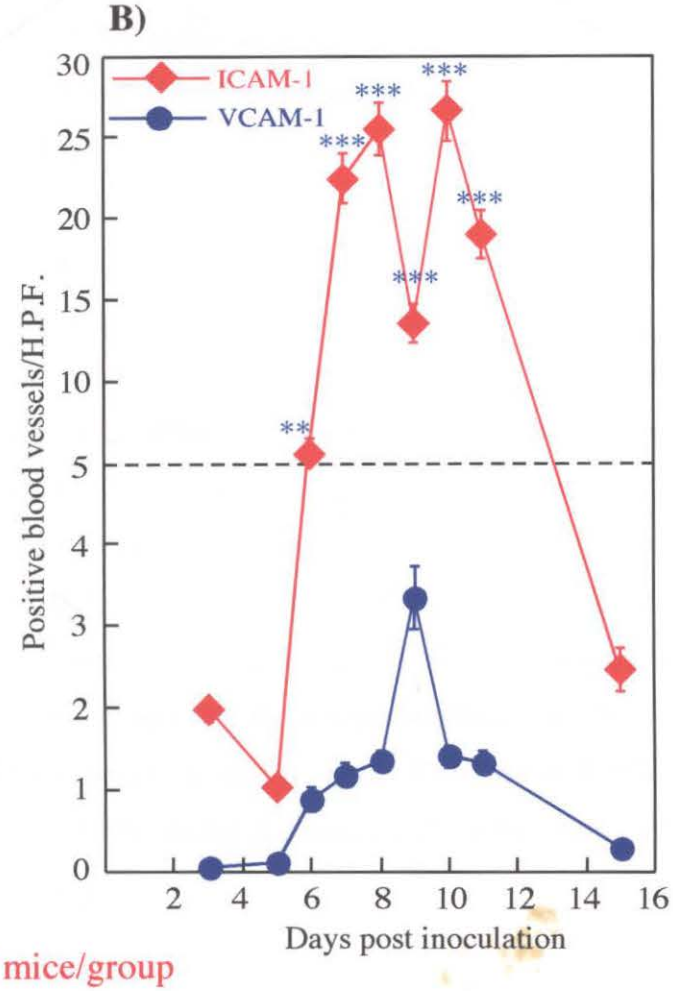

n = 70 mice/group

Lane *et al.* 2000; Adler *et al.* 1999; Noske *et al.* 1998; Zinkernagel 1992). The unique position of the neurovascular endothelial cells at the interface between the blood and the brain makes them a principal regulator of peripheral inflammatory cell recruitment into the CNS (Rubin 1999). Circulating leukocytes are non-adherent, whereas extravasation requires strong adhesion to the endothelial cells. Thus, phenotypic alterations in the neurovascular endothelial cells, including expression of CAM are required for extravasation, which is induced during inflammation (Irani & Griffin 1996; Engelhardt *et al.* 1994). ICAM-1 and VCAM-1 have emerged as a key players in leukocyte-endothelial cell interactions, since they provide firm adhesion via interaction with leukocyte integrins (Carlos & Harlan 1994). It was shown in chapter 3 that lack of IFN-γ significantly reduced leukocyte recruitment into the brain parenchyma in B6.IFN-γ-/- mice. Therefore the status of ICAM-1 and VCAM-1 expression in the neurovascular endothelial cells was evaluated in this model.

Animal models of viral encephalitis (Eralinna *et al.* 1996; Irani & Griffin 1996; Finke *et al.* 1995; Sasseville *et al.* 1992; Soilu-Hanninen *et al.* 1994) as well as several neurological disorders (Dopp *et al.* 1994; Barten *et al.* 1994; Brosnan *et al.* 1995) have shown increased expression of both ICAM-1 and VCAM-1 in the neurovascular endothelium, as part of the development of CNS inflammation (Raine *et al.* 1990; Hartung *et al.* 1993). Deckert-Schluter *et al.* (1999) demonstrated that up-regulation of ICAM-1 and VCAM-1 is totally dependent on IFN-γ in Toxoplasma encephalitis. In contrast, Nansen *et al.* (1998) showed normal induction of ICAM-1 and VCAM-1 in IFN-γ deficient mice in LCMV infection. In aggrement with the latter, expression and upregulation of ICAM-1 and VCAM-1 in WNV encephalitis has also been shown to be independent of IFN-γ in this work (Figure 5.2 and 5.9). However, unlike the LCMV model, both ICAM-1 and VCAM-1 upregulation, as measured both by the number of positive vessels and the intensity of endothelial staining, was significantly increased in the absence of IFN-γ compared to B6.WT mice. These results clearly indicate that upregulation of these adhesion molecules in WNV encephalitis is not dependent on IFN-γ and indicate that different signaling pathways upregulate these molecules in response to particular pathogenetic mechanisms. It has been demonstrated that in addition to being inducible by IFN-γ, endothelial ICAM-1 and VCAM-1 expression are upregulated by other cytokines, IL-1α/β, TNF and IL-4 (Meager 1999; Shen *et al.* 1997; Mickelson *et al.* 1995; Wong & Dorovini-Zis 1992; Fabry *et al.* 1992; Masinovsky *et al.* 1990).

In both groups, the first detectable increases in VCAM-1 expression occurred later than that of ICAM-1, although the kinetics of VCAM-1 expression between the groups remained similar. The number of vessels showing upregulated VCAM-1 expression in B6.IFN-γ-/- mice was significantly different (p=<0.001) from B6.WT at day 9 p.i. At this timepoint, it was approximately 3-fold higher than that of the WT mice. On the other hand, the upregulation of ICAM-1 expression in B6.IFN-γ-/- mice had different kinetics compared to the B6.WT. The increase in number of ICAM-1-positive vessels was significantly different (p=<0.001) on days 6-11, at times being >10-fold higher than the corresponding infected B6.WT mice. The different kinetics of VCAM-1 expression is presumably due to regulation by different cytokines from those inducing ICAM-1.

Experiments both *in vivo* and *in vitro* have demonstrated that glial cells, including both astrocytes and microglia are capable of expressing ICAM-1 and VCAM-1 (Weener *et al.* 2001; Dallasta *et al.* 2000; Shrikant *et al.* 1994; Lee *et al.* 1999; Lee & Benveniste 1999; Zielasek *et al.* 1993). However in WNV encephalaitis, glial cells expressed only ICAM-1, and moreover, only in the absence of IFN-γ (Figure 5.4, 5.6 B and 5.9). As mentioned in chapter 4, there was little or no activation of astrocytes in B6.IFN-γ-/- mice and the morphology of ICAM-1-expressing glial cells was similar to the morphology of microglia, which suggested that these ICAM-1-expressing glial cells could be microglia. This was confirmed by double labelling for ICAM-1 and GS-lectin (Figure 5.5). Nearly almost all GS-lectin positive microglia expressed ICAM-1 (Figure 5.5 a), except on day 11 p.i (Figure 5.8).

At day 11 p.i., significantly higher numbers (p=<0.001) of microglia were ICAM-1-positive, compared to GS-lectin-positive microglia (Figure 5.8), however, both parameters decreased to nearly baseline levels on day 15 p.i. Expression of ICAM-1 in microglia has been reported in many encephalitis models (Deckert-Schluter *et al.* 1999; Dallasta *et al.* 2000; Weissenbock *et al.* 2000). It has been reported that IFN-γ is responsible for the induction of ICAM-1 expression in microglia (Zielasek *et al.* 1993; Deckert-Schluter *et al.* 1999). In contrast, my work shows ICAM-1 was expressed in microglia only in the absence of IFN-γ in WNV encephalitis. Moreover, unlike blood vessels, microglial ICAM-1 was not constitutively expressed in B6.IFN-γ mice (Figure 5.4 a) and after infection not all mice

showed microglial ICAM-1 expression (Figure 5.7 A). Dallasta *et al.* (2000) suggest that microglia expressing ICAM-1 may be involved in the development of neurodegeneration in murine retroviral infection. However, neurodegeneration rarely occurred in B6.IFN-γ mice. Thus these ICAM-1-expressing microglia are unlikely to play a role in neurodegeneration in WNV encephalitis. Why there was the discrepancy between the B6.IFN-γ mice in terms of microglial ICAM-1 expression, and what the functional significance of these ICAM-1 positive microglia may be, especially since leukocyte recruitment into the brain parenchyma is so low, warrant further investigation.

Endothelial ICAM-1 and VCAM-1 expression are important for the adhesion and migration of all leukocyte subsets *in vivo* and *in vitro*. Increased expression increases the avidity of cell-cell interactions and subsequent transendothelial migration (Bochner *et al.* 1991; Shimizu *et al.* 1991). Deckert-Schluter *et al.* (1999) suggested that low levels of CAM induction is sufficient to recruit leukocytes into the CNS of IFN-γ-deficient mice. However, despite markedly higher adhesion molecule expression, significantly lower numbers of infiltrating leukocytes were observed in the brain parenchyma of infected B6.IFN-γ-/- mice compared to B6.WT in WNV encephalitis. Coupled with this, few ICAM-1 and VCAM-1-positive parenchymal vessels were associated with adjacent inflammatory cell infiltrates (Figure 5.2 d). Thus increased expression of endothelial ICAM-1 and VCAM-1 was not sufficient to mediate the migration of compensatory numbers of inflammatory leukocytes into the brain in WNV encephalitis in the absence of IFN-γ. This is similar to the findings of other investigators in other model systems (Willenborg *et al.* 1993; Engelhardt *et al.* 1994). These observations suggest that IFN-γ-mediated chemokines may play a role in guiding the movement of leukocytes into the brain parenchyma (Lane *et al.* 2000; Liu *et al.* 2001).

It is hypothesized that chemokines, along with CAM play a major role in leukocyte reorientation and migration in response to stimuli (Asensio *et al.* 1999; Lane *et al.* 2000; Ransohoff *et al.* 1996; Liu *et al.* 2001; Liu *et al.* 2000; Godiska *et al.* 1995). Chemokines are synthesized locally at sites of inflammation variously, by leukocytes, endothelial cells and CNS resident cells that may localized at or near the endothelial surface. These are secreted in association with other molecules, and establish a concentration gradient down which target cell populations migrate (Boehm *et al.* 1997). Recent studies in chemokines

have shown that many chemokines that are important for the recruitment of inflammatory cells to the CNS are strongly and consistently induced by IFN-γ, such as IP-10 (Simpson *et al.* 2000), MCP-1 (McManus *et al.* 2000), Mig (Liu *et al.* 2001), RANTES and MIP-1α/β (Boehm *et al.* 1997). The expression of chemokines in the brain is not the focus of this study; however, it can be speculated that these IFN-γ inducible chemokines would be poorly induced in IFN-γ-deficient mice.

In conclusion, IFN-γ is not critical for the induction of ICAM-1 and VCAM-1 in WNV encephalitis. In contrast, these molecules were strongly upregulated in the absence of IFN-γ in WNV encephalitis. Moreover, the greater upregulation of these adhesion molecules was not in itself sufficient to facilitate the endothelial transmigration of the high numbers of leukocytes into the brain seen in the WNV-infected B6.WT mice. It follows that IFN-γ-mediated chemotactic signals are likely to be required for successful recruitment of inflammatory cells before increased ICAM-1 and VCAM-1 expression fulfil their roles in leukocyte migration to the sites of WNV infection in the CNS. What the functional significance is and which candidate(s) is/are responsible for such massive upregulation of ICAM-1 and VCAM-1 in IFN-γ-deficient mice in WNV encephalitis is unknown.

Chapter-6

Route of infection determines disease profile in WNV encephalitis

6.1. Introduction

Several neurotropic viruses regularly produce lethal infections when inoculated into the experimental animals via the i.c. route, while peripheral inoculation produces only sub lethal infection (Hase *et al.* 1990; Richards *et al.* 1981; Nathanson & Cole 1970). Neurotropic viruses need to replicate in the peripheral organs before invasion of the CNS, when introduced peripherally (Carbone *et al.* 1987; Monath *et al.* 1983). Peripheral inoculation reflects the usual route of inoculation into the host. It induces host defences several days prior to the CNS invasion, leading to the generation of defence mechanisms that anticipate and can control the infectious process in the CNS. With the i.c. route of inoculation, virus is directly introduced into the brain tissue. Being neurotropic, it quickly replicates in neural tissue, often before development of a peripheral immune response. This results in fatal encephalitis with 100% mortality. For WNV, the i.c. route of inoculation does not reflect natural infection at all; normally the virus enters the body through the bite of an insect vector.

Similar to i.c. inoculation, the i.n. route may also result in lethal infection in many animal models of viral encephalitis (Thach *et al.* 2000; Carbone *et al.* 1987). In i.n. inoculation, neurotropic viruses are introduced into the nasal cavity, innervated by both olfactory and trigeminal nerves (reviewed in Barnett & Perlman 1993). After i.n. inoculation, virus can easily be transported to the CNS via these nerves. Some viruses use the olfactory nerve, strictly as a portal of entry into the brain, while some use only the trigeminal nerves. Some use both routes (Barnett & Perlman 1993; Plakhov *et al.* 1995; Babic *et al.* 1994; Perlman *et al.* 1990). Via peripheral inoculation, neurotropic viruses can get access to the CNS via many different pathways. These include the haematogenous route, transmigration of

infected immune cells into the brain, endocytosis, axonal migration via spinal cord, etc., (see chapter 3).

Little literature exists about i.n. inoculation of neurotropic viruses in experimental animal models, much less about comparative studies between i.p. and i.n. models. To date no one has studied the pathogenesis of WNV encephalitis after i.n. inoculation. Nir *et al.* in 1965 studied WNV infection in mice with WNV aerosol exposure. However, he used 3-week-old mice and did not compare the disease profile with that induced by i.p exposure. Therefore, this study was undertaken to understand better the mechanisms involved in the pathogenesis of WNV encephalitis comparing these 2 routes of inoculation in the adult mouse as a model. The preceding chapters have clearly demonstrated that WNV encephalitis is an immunopathological disease, mediated at least in part by IFN-γ. To further explore the role of IFN-γ in survival and its influence in the pathogenesis of disease after i.n. inoculation, B6.WT mice and B6.IFN-γ-/- mice were infected via both i.p. and i.n. route.

6.2. Materials and Methods

6.2.1. Mice

Female, specific-pathogen free, 8-week-old B6.WT and B6.IFN-γ-/- mice, backcrossed to C57BL/6, were used.

6.2.2. Virus infection of mice and tissue preparation

For the survival study, groups of 36 mice of B6.WT and B6.IFN-γ-/- strains were inoculated i.p. with $6x10^4$ pfu/mouse and groups of 20 mice of B6.WT and B6.IFN-γ-/- strains were inoculated i.n. with $6x10^4$ pfu/mouse, as described in section 2.2.2.1. The survival rates were evaluated, as described in section 2.2.2.1. To determine the kinetics of viral infection, leukocyte infiltration and microglial activation in the CNS parenchyma, a time course experiment was carried out. Groups of 120 mice/strain were used in the i.p. model and 21 mice/strain were used in the i.n. model. Tissues, including brains and cervical spinal cords were collected and processed as described in section 2.2.2.2. Mice were mock-infected with DMEM as controls.

6.2.3. Histopathology

Serial sections from paraffin-embedded tissues were routinely stained with H and E, and examined to evaluate the pathological changes occurring in the brain parenchyma in the i.p. and i.n. models.

6.2.4. Determination of brain titre

This was done as described in section 3.2.4.

6.2.5. Lectin histochemistry and immunohistochemistry

Paraffin-embedded sections were used for both immunohistochemistry and lectin histochemistry.

- **Detection of activated microglia by lectin histochemistry**

This was done as described in section 4.2.4. Mock-infected brain sections were used as controls for GS-lectin labelling.

- **Detection of WNV antigen**

This was done as described in section 3.2.3. Mock-infected brain sections were used as controls for WNV Ag labelling.

6.2.6. Quantification of cells

Cells were quantified as described in section 2.3 and figures are mean values ± SEM for the total number of fields examined from the indicated number of mice, n.

6.3. Results

6.3.1. Survival after i.p. and i.n. route of WNV inoculation

Since 40% B6.WT mice survived after i.p. inoculation (section 3.3.1.2.), mice were infected i.n. with the same dose of WNV to evaluate the disease profile in WNV encephalitis induced via a different route of infection. Therefore, a survival study was undertaken in B6.WT mice infected both i.n. and i.p. with $6x10^4$ pfu/mouse. First signs of clinical illness were observed from day 6 p.i. in both models. However, there was a difference in the signs of clinical illness. In the i.p. model, the clinical signs included ruffled hair, reduced activity, hunching, weight loss and/or weakness. Occasionally, CNS symptoms were observed such as hindlimb paralysis (0-3%), tremors and occasionally convulsions (chapter 3). Mortality occurred between day 6-11 p.i. In contrast, in the i.n. model, mice were suddenly sick on day 6 p.i. They often exihibited a swollen head, hyperactivity and aggressive behaviour. This occurred without weight loss or hunching posture, as signs of clinical illness. Mice were frequently observed standing on their hind limbs, rocking back and forth. All mice were moribund on day 7 p.i. However, none of the mice was paralysed in this model. Mortality occurred in 100% of mice between day 6-7 p.i. after i.n. inoculation. The cumulative comparative survival after infection in both models is presented in figure 6.1 A.

Mortality of B6.IFN-γ-/- mice was also compared after i.p. and i.n. inoculation. Similar to B6.WT, in B6.IFN-γ-/- mice, the clinical signs were observed from day 6 p.i. in both i.p. and i.n. models and mice exihibited clinical signs in both models similar to those described in B6.WT mice. In the i.p. model, mortality occurred in approximately 17% of mice bewteen day 6-11 p.i. whereas in the i.n. model, mortality occurred in 100% of mice between day 6-7 p.i. The cumulative comparative survival after infection in both models is presented in figure 6.1 B.

Unlike the i.p. model, there was no difference in survival between the groups in the i.n. model, which showed 100% mortality in both groups of mice. These data suggest that mice are highly susceptible to the i.n. route of infection compared to the i.p. route. Unlike in the i.p. model, IFN-γ does not play a role in exacerbating disease in the i.n. model.

Figure: 6.1 Survival after i.p. and i.n. inoculation of WNV in B6.WT and B6.IFN-γ-/- mice. Groups of 36 mice/strain were inoculated i.p., $6x10^4$ pfu/mouse, and groups of 20 female mice/strain were inoculated i.n., $6x10^4$ pfu/mouse. They were monitored for signs of illness 3 times per day over 21 days. The percent survival at each time point is shown. A) Survival profiles of B6.WT after i.p. and i.n. inoculation. B) Survival profiles of B6.IFN-γ-/- mice after i.p. and i.n. inoculation. Mock-infected mice did not develop signs of illness in either model.

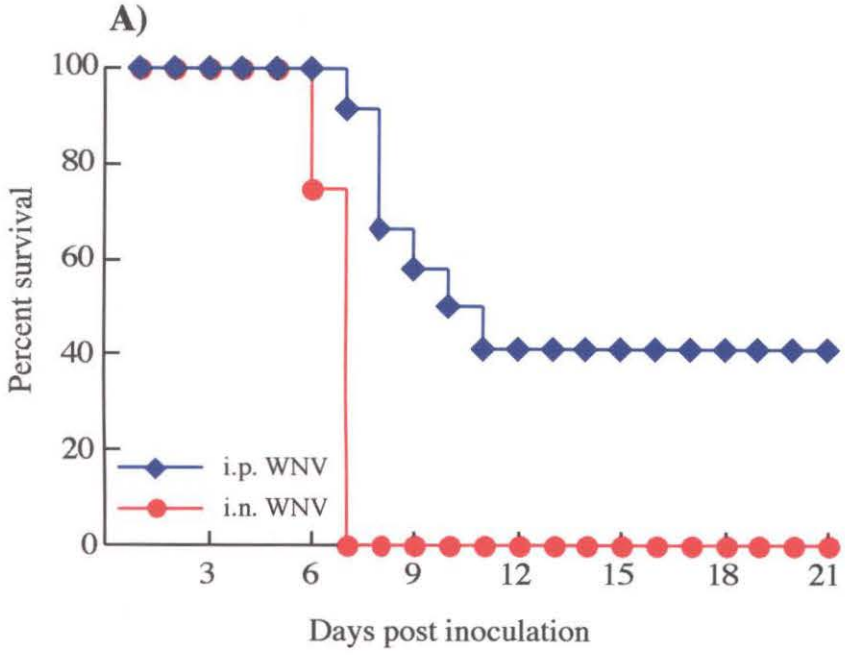
A)
100
80
60
40
20
0
Percent survival
i.p. WNV
i.n. WNV
3
6
9
12
15
18
21
Days post inoculation

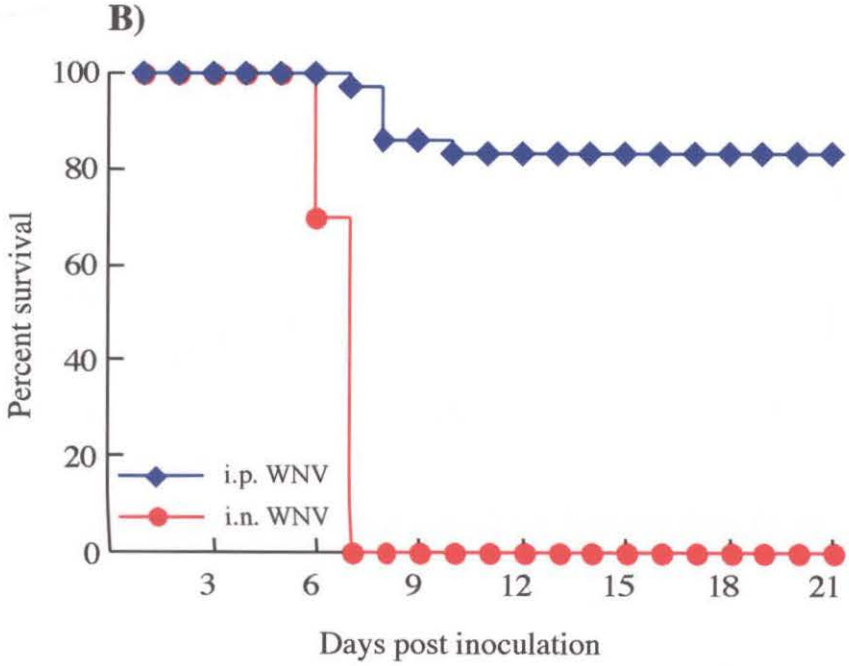
B)
100
80
60
40
20
0
Percent survival
i.p. WNV
i.n. WNV
3
6
9
12
15
18
21
Days post inoculation

6.2.3. Detection of WNV antigen in the brain

6.3.2.1. Detection of WNV titre in the brain

Results from the preceding section clearly demonstrated that mice from both strains were highly susceptible to infection via the i.n. route of WNV inoculation. Mortality occurred in 100% of mice within 24h of clinical symptoms appearing, unlike the i.p. model. Therefore, the virus load in the brains of these mice was determined as a first approach, using a plaque assay. In the i.p. model, groups of 64 mice from B6.WT and B6.IFN-γ-/- strains were infected i.p. with $6x10^4$ pfu/mouse. In the i.n. model, groups of 21 mice from B6.WT and B6.IFN-γ-/- strains were infected i.n. with $6x10^4$ pfu/mouse. Plaque assay was performed from day 1-7 p.i. in the i.n. model and from day 1-11 p.i. in the i.p. model.

As described in section 3.3.3.3., in B6.WT mice, replicating WNV was detected only from day 6 p.i. It increased, peaking on day 8 p.i. and decreased thereafter to become undetectable by day 10 p.i. in the i.p. model. The maximum virus titre was 2.23 $\log_{10}$ pfu/gram on day 8 p.i. in this model. In contrast, replicating virus was detected from day 3 p.i. (Figure 6.2 A) in the i.n. model in B6.WT. At this timepoint, virus titre was 4.85 $\log_{10}$ pfu/gram, *i.e.,* 2 log-fold higher than the peak virus titre detected in the i.p. model. Within 48h of detection, virus titre was increased by a further 2 log-fold in the i.n. model. At the time of death, on day 7 p.i., the WNV titre was 9.72 $\log_{10}$ pfu/gram.

Similar to the B6.WT, replicating WNV was detected from day 3 p.i. in B6.IFN-γ-/- mice after i.n. inoculation of WNV (Figure 6.2 B). Like B6.WT, the virus titre on day 3 p.i. was 4.98 $\log_{10}$ pfu/mouse and within 48h of detection, the titre was increased almost a further by 2 log-fold. At the time of death, the virus titre was 9.72 $\log_{10}$ pfu/mouse. In contrast, in the i.p. model (section 3.3.3.3). WNV was detected only from day 6 p.i., increased and peaked on day 8 p.i. Replicating WNV was undetectable from day 10 p.i. The titre of WNV at the peak was 2.22 $\log_{10}$ pfu/gram, which was <2 log-fold less than the titre detected on day 3 p.i. in the i.n. model.

Like the i.p. model, the kinetics of WNVgrowth in the brain parenchyma was similar between B6.WT and B6.IFN-γ-/- mice in the i.n. model (Figure 2 C). Titres of WNV on day

Figure: 6.2 Virus titres in the brain after i.p. and i.n. inoculation of WNV in B6.WT and B6.IFN-γ-/- mice. Groups of 64 mice/strain were inoculated i.p., $6x10^4$ pfu/mouse and groups of 21 female mice/strain were inoculated i.n., $6x10^4$ pfu/mouse. Brains were collected from day 1-11 p.i. in the i.p. model and from day 1-7 p.i. in the i.n. model. Virus titres were detected by plaque assay. A) Virus titres of B6.WT after i.p. and i.n. WNV inoculation. B) Virus titres of B6.IFN-γ-/- mice after i.p. and i.n. WNV inoculation. C) Virus titres of B6.WT mice and B6.IFN-γ-/- after i.n. WNV inoculation. No WNV was detected in the mock-infected mice from either group in either model.

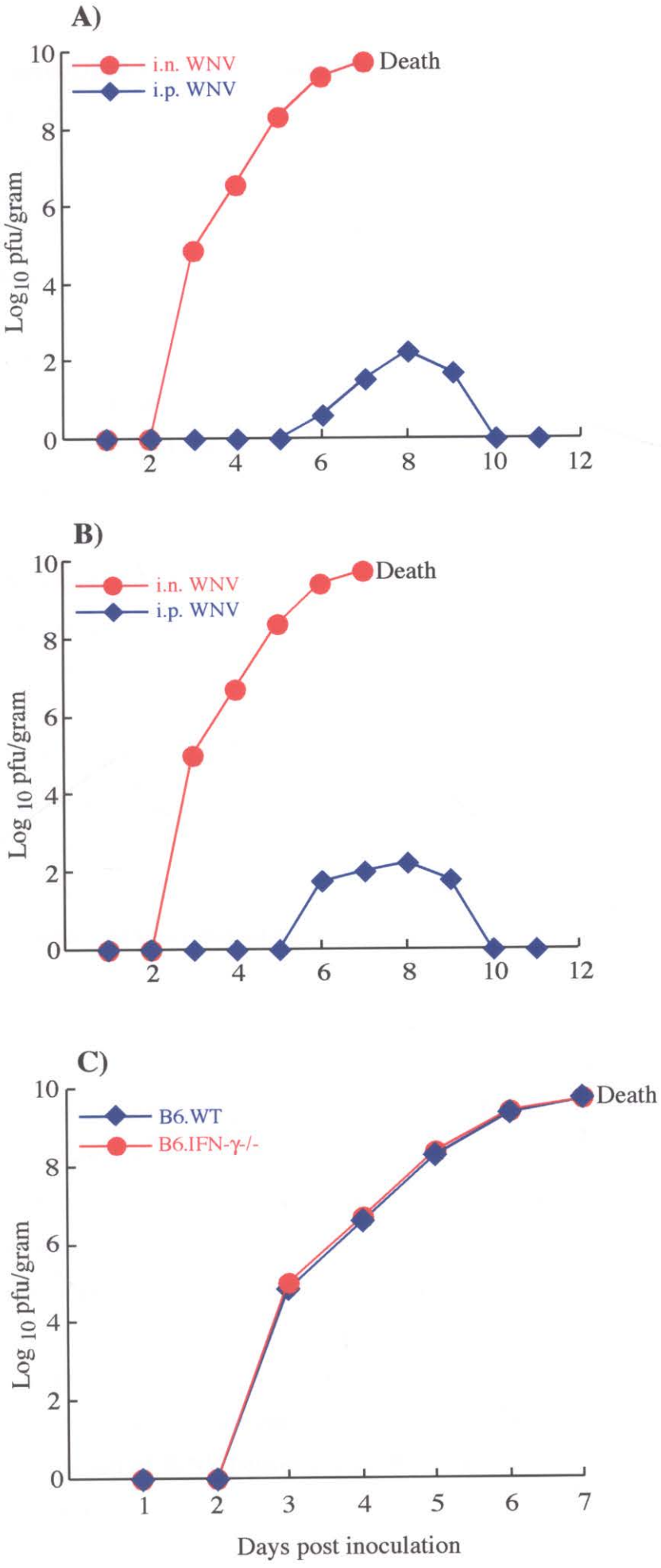
A)
i.n. WNV
i.p. WNV
Death
Log10 pfu/gram
B)
i.n. WNV
i.p. WNV
Death
Log 10 pfu/gram
C)
B6.WT
B6.IFN-γ-/-
Death
Log 10 pfu/gram
Days post inoculation

3 p.i. were approximately similar between the groups. The titres were also similar at the time of death between the groups. These data suggest that death of mice was due to overwhelming WNV infection, regardless of the strain of mice in the i.n. model, whereas in the i.p. model, death of mice was due to the activity of IFN-γ.

6.3.2.2. Kinetics of WNV progression in the i.n. model

Since, extremely high virus titres were detected in the i.n. model, brain sections from both strains, B6.WT and B6.IFN-γ-/- mice, were labelled with anti-WNV Ab and examined for progression of infection. In both groups of mice, a few neurones were infected in the outermost layer of the OB on day 3 p.i. (Figure 6.3 a). On day 5 p.i., the number of infected neurones had markedly increased and WNV Ag was observed in other areas of the OB. Many neurones were infected in the base of the OB, front cortex (Figure 6.3 b) and a few infected neurones were seen in the base of the brain. At this timepoint few neurones were infected in the hippocampus. On day 6 p.i., most of the neurones in the OB and cortex were infected (Figure 6.3 C). Most of the neurones in the hippocampus were also infected. Similarly, high neuronal infection was observed in the base of the brain, striatum and thalamus. Compared to the cortex, fewer neurones were infected in the brainstem but no detectable cerebellar infection was observed. On day 7 p.i., nearly all neurones of the OB (Figure 6.3 d), cortex, striatum (Figure 6.3 e), hippocampus (Figure 6.3 e and 6.4 c) were detectably infected. At this timepoint, many brainstem neurones were also infected (Figure 6.3 f). In the hippocampus, both pyramidal cells (Figure 6.4 c and d) and granular cells of the dentate gyrus (Figure 6.4 c) were highly infected. At the time of death all areas of the brain, except cerebellum were heavily infected. Interestingly, only occasional cerebellar neurones were infected in both groups of mice (Figure 6.3 g). There was no difference in the pattern and kinetics of infection between the groups. These data confirm that WNV is highly neurotropic and replicates quickly in neurones if inoculated i.n. These data further suggest that death of mice was due to the overwhelming brain infection. Despite such extensive and marked brain infection, no infection of glial cells, ependymal cells or meninges was observed in either group of mice. Like the i.p. model, WNV was confined to the neurones (Figure 6.3 h) and their processes (Figure 6.4 b and d) in the i.n. model, possibly suggesting that only neurones have a specific receptors for WNV or reflecting the mode of transmission of WNV between cells. However, on day 7 p.i., 1 blood vessel in 1

Figure: 6.3 WNV-infected B6.WT mouse brain sections labelled with anti-WNV antibody showing progression of infection in the i.n. model. WNV antigen first appeared in the outermost layer of the olfactory bulb (OB) at day 3 p.i. (a) (solid arrows). On day 5 p.i. WNV antigen was observed in other parts of the OB with increased numbers of infected neurones (b) (solid arrows). At this timepoint, WNV antigen was also found in the OB base (OBB) (Solid arrows) and front cortex (FCO) (solid arrow). On day 6 p.i. the number of infected neurones increased in the OB, OBB, FCO, striatum (ST) (c) (solid arrows). At the time of death, on day 7 p.i, large numbers of neurones were infected in the OB (d) (solid arrows), FCO, ST, hippocampus (HIP) (e) (solid arrows). At this timepoint many neurones in the thalamus (TH) (e) (solid arrows) and brainstem (f) (solid arrows) were also infected. Only occasional neurones were infected in the cerebellum (CB) at the time of death (g) (solid arrows). Despite extensive infection, WNV antigen was confined only to the neurones (h) (solid arrows). These micrographs are representative of both B6.WT and B6.IFN-γ-/- mice. Scale bar = 400μm from a-f, 100μm from g-h. Anatomic orientation of the brain sections: Right, anterior brain (fore brain), left, posterior brain (hind brain).

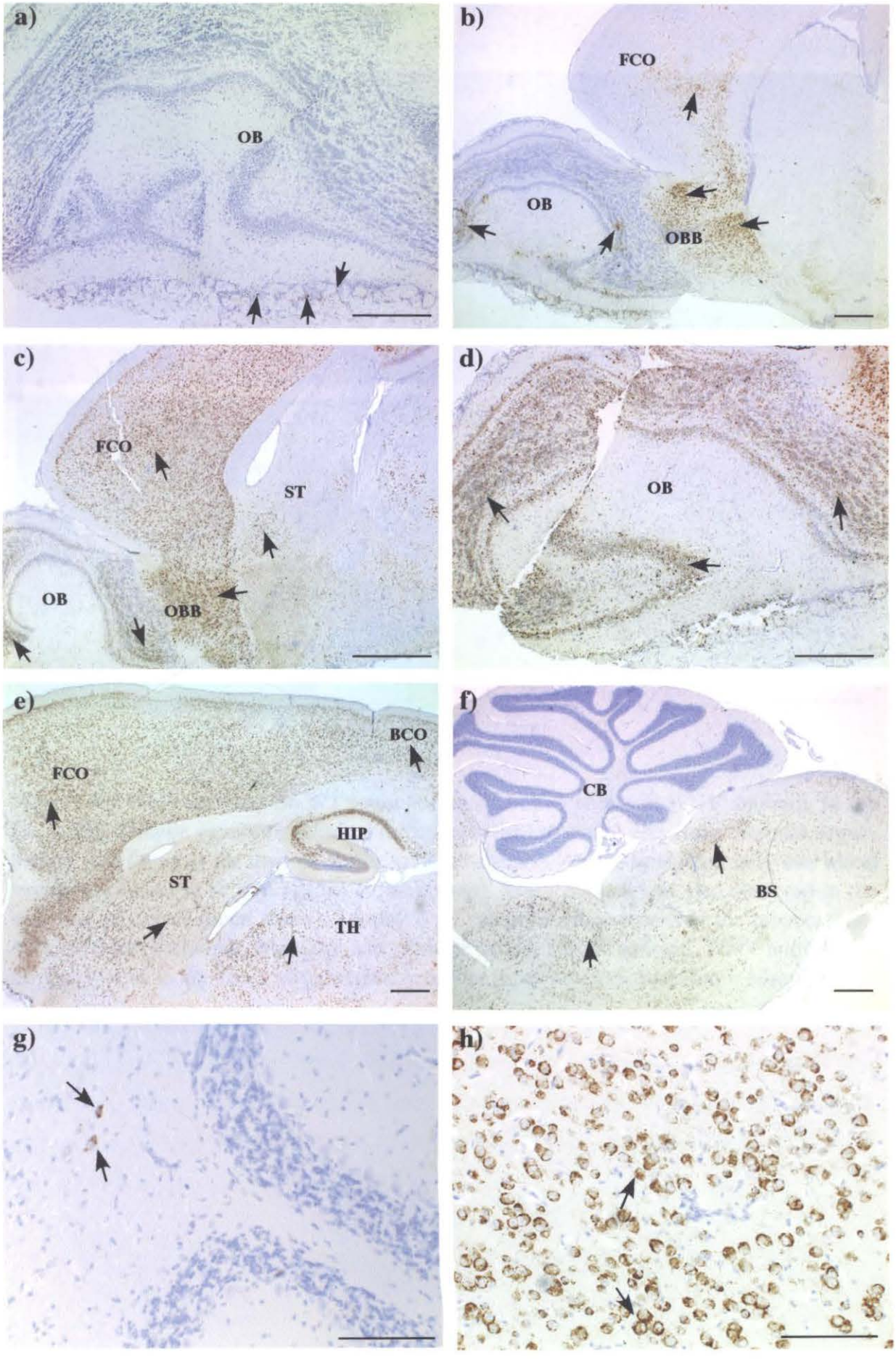
a)
OB
b)
FCO
OB
OBB
c)
FCO
ST
OB
OBB
d)
OB
e)
BCO
FCO
HIP
ST
TH
f)
CB
BS
g)
h)

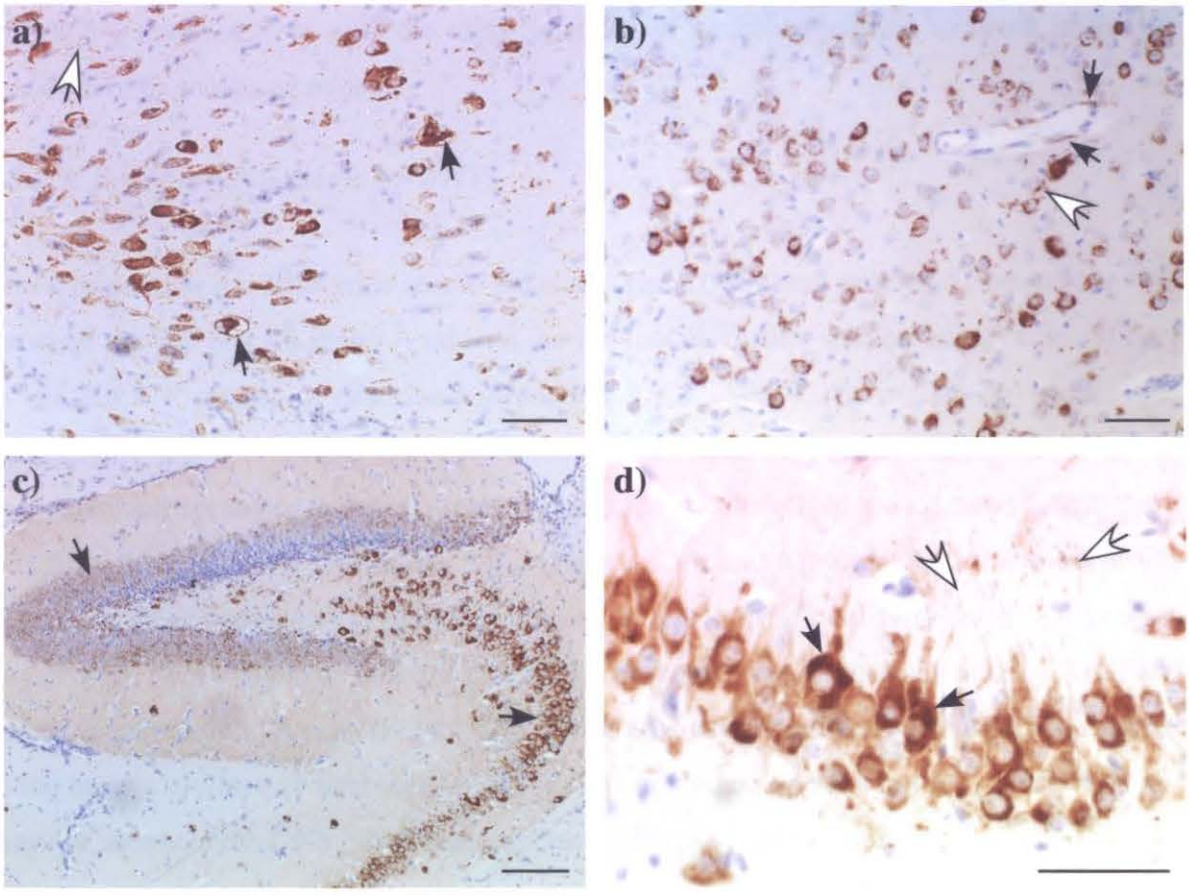

Figure: 6.4 WNV-infected B6.WT brain sections labelled with anti-WNV antibody in the i.n. model. Despite extensive neuronal infection in the i.n. model very little neuronal degeneration was found at the time of death (a) (solid arrows). At this timepoint, only one blood vessel was found to be infected (b) (solid arrows). WNV antigen was also observed in the neuronal processes (open arrow). On day 7 p.i., most of the neurones of the hippocampus were infected, including pyramidal and granular cells (c) (solid arrows). WNV antigen can be clearly seen in the axons of pyramidal neurones (open arrows). Scale bar = 50μm.

out of 42 mice, was found to be infected (Figure 6.4 b). Very few neurones showed abnormal morphology or evidence of degeneration, on day 7 p.i. (Figure 6.4 a), suggesting that WNV may interfere with the vital functions of neurones leading to death in the i.n. model in both groups of mice.

6.3.2.3. Route of CNS access by WNV

Since there was no difference in the survival, virus titres and pattern of brain infection between B6.WT and B6.IFN-γ-/- mice in the i.n. model, further studies were continued only in the B6.WT mice. As described in section 3.3.3., WNV Ag in the i.p. model was consistently negative in the OB throughout the timeperiod. It was first detected in the brainstem and spread in the caudo-rostral direction. In contrast, in the i.n. model, WNV Ag was first detected in the OB on day 3 p.i. (Figure 6.5 b and 6.3 a). In the i.n. model, at this timepoint, both brainstem (Figure 6.5 c) and cervical spinal cords (Figure 6.5 d) were negative for WNV Ag. The number of infected neurones was increased from day 3 p.i. and spread from rostral to caudal (Figure 6.3). These data strongly suggest that WNV get access to the brain via olfactory neuroepithelium in the i.n. model, whereas in the i.p. model, WNV may get access to the CNS via axonal migration along the spinal cord.

6.3.3. Histopathology

The histopathology in the i.n. model was very similar to the i.p. model. Histopathological changes in the i.p. model were described in section 3.3.2. Routine H and E staining of brain sections from the i.n. model are shown in figure 6.6. Histopathological changes in the i.n. model included infiltration of leukocytes consisting of both mononuclear and polymorphonuclear cells. Interestingly, infiltrating leukocytes accumulated predominantly in the OB (Figure 6.6 b). Very little perivascular cuffing was observed in the brain parenchyma at the time of death, despite extremely high neuronal infection in the parenchyma. Meningeal infiltration was also observed at this timepoint. Activated microglia with rod morphology were observed around the blood vessels. The OB from mock-infected mice showed normal histology (Figure 6.6 a).

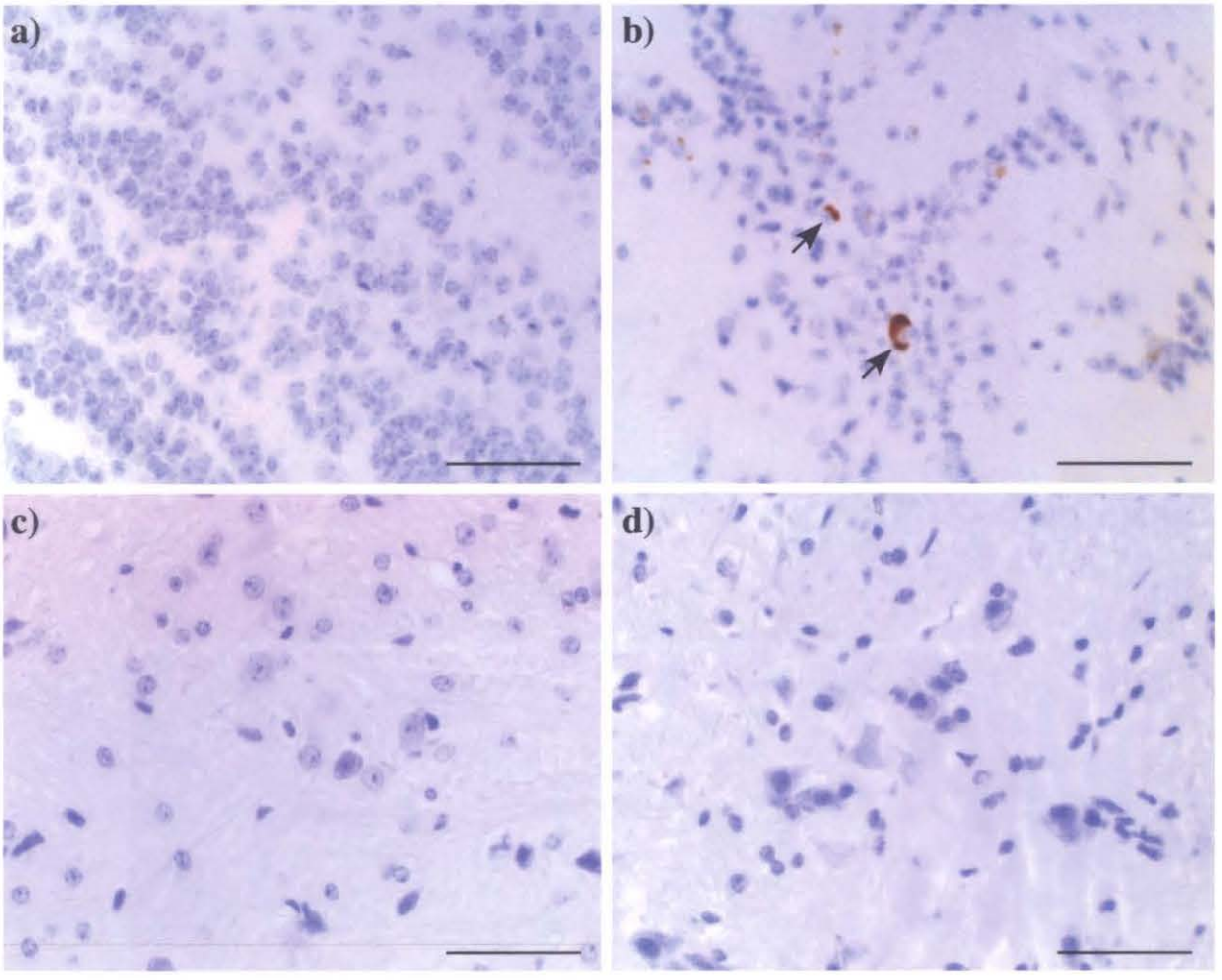

Figure: 6.5 WNV-infected B6.WT brain and cervical spinal cord sections labelled with anti-WNV antibody in the i.n. model. WNV antigen was first detected in the outermost layer of the olfactory bulb on day 3 p.i. (b) (solid arrows). At this timepoint, no WNV antigen was detected in the brainstem (c). Similarly, WNV antigen was also undetectable in the cervical spinal cord at this timepoint (d). No WNV antigen was detected in the olfactory bulb from mock-infected mouse brain (a). Scale bar = 50μm.

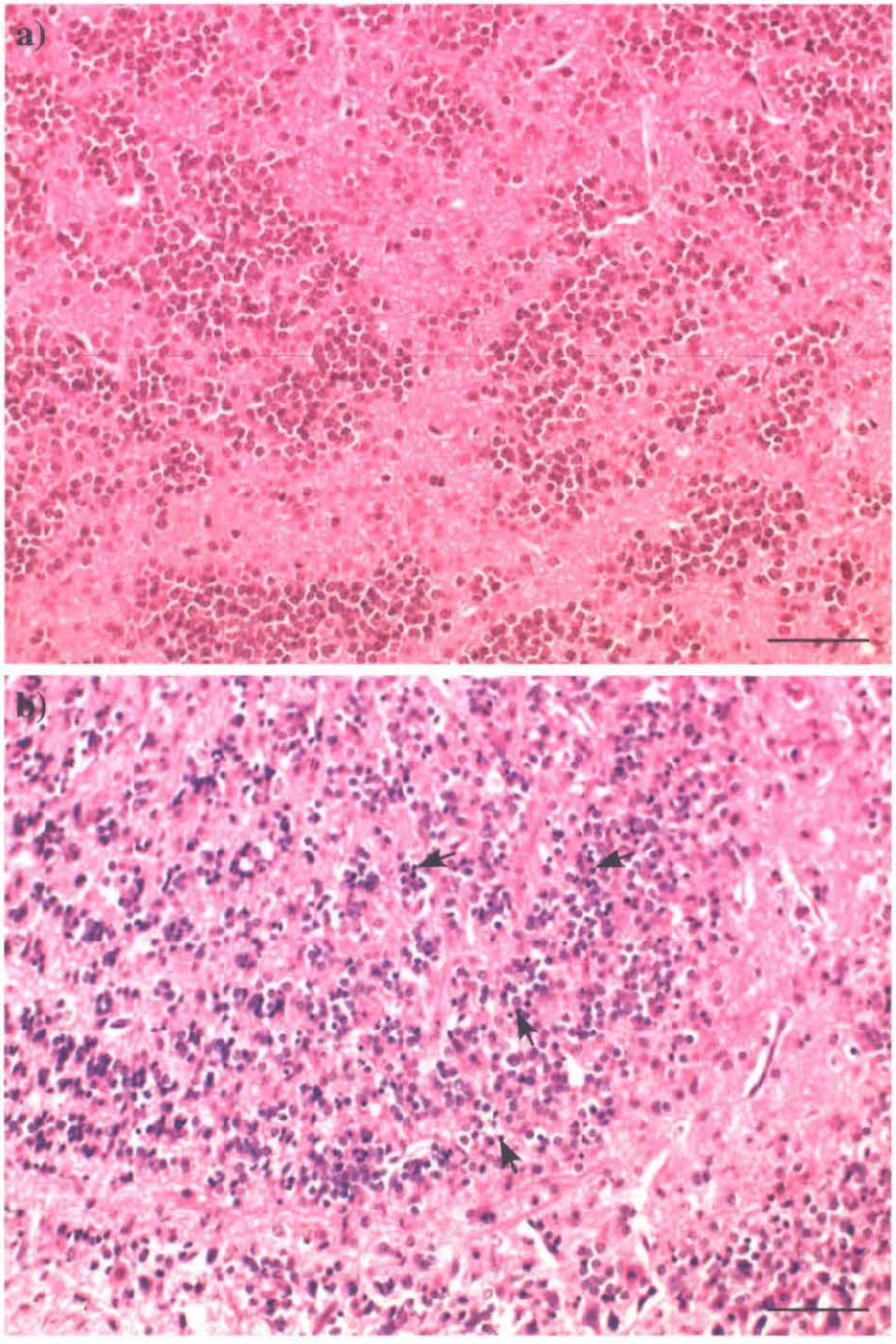

Figure: 6.6 H and E stained brain sections of B6.WT mice in the i.n. model. Olfactory bulb from mock-infected mouse brain showing normal histology (a). Olfactory bulb from infected mouse showing high infiltration of leukocytes on day 7 p.i. (b) (solid arrows).
Scale bar = 50μm.

6.3.4. Kinetics of microglial activation in relation to WNV infection and infiltration

GS-lectin was used to detect activated microglia in this study. Microglia were activated from day 3 p.i., concurrently with the detection of WNV Ag (Figure 6.7 a). At this timepoint activated microglia were detected only in the outermost layer of the OB (Figure 6.7 b). The number of activated microglia had increased by day 6 (Figure 6.8 c) and was highest at the time of death on day 7 p.i. (Figure 6.8 d). The detection of activated microglia was co-incident with the detection of WNV Ag, occurring in a wave, just ahead of the advancing front of WNV-infected neurones. Interestingly, unlike in the OB, relatively few microglia were activated in the brain parenchyma and most were found around blood vessels, exhibiting amoeboid morphology (Figure 6.8 a and b). Moreover, unlike the i.p. model, very few microglial nodules were observed at the time of death. In the i.p. model, microglia were highly activated throughout the brain parenchyma with the formation of large numbers of nodules. Activated microglia were first observed in the i.p. model within 24h of WNV Ag detection at or near the sites of neuronal infection (section 4.3.3).

The number of activated microglia, leukocytes and infected neurones were counted as described in Materials and Methods to compare the kinetics. In the i.n. model, the number of infected neurones was extremely high, compared to the number of activated microglia. The number of leukocytes was near to base line value compared to the number of infected neurones (Figure 6.9 A). In contrast, in the i.p. model, the reverse was the case. The number of activated microglia was extremely high, compared to the number of infected neurones, and the number of inflammatory leukocytes was also higher than the number of infected neurones in the i.p. model. The number of inflammatory leukocytes and activated microglia returned nearly to baseline values once WNV Ag was undetectable (Figure 6.9 B). These data suggest that in the i.n. model, the uncontrolled growth of WNV in the brain may be due to the low numbers of activated microglia, compared to the number of infected neurones.

6.4. Discussion

The i.n. route of WNV inoculation was used to characterize the i.n.-induced disease profile and compare it with the i.p. route of WNV inoculation. In the i.p. model, WNV seems to get access to the brain via ascending axonal migration along the spinal cord. Therefore, the

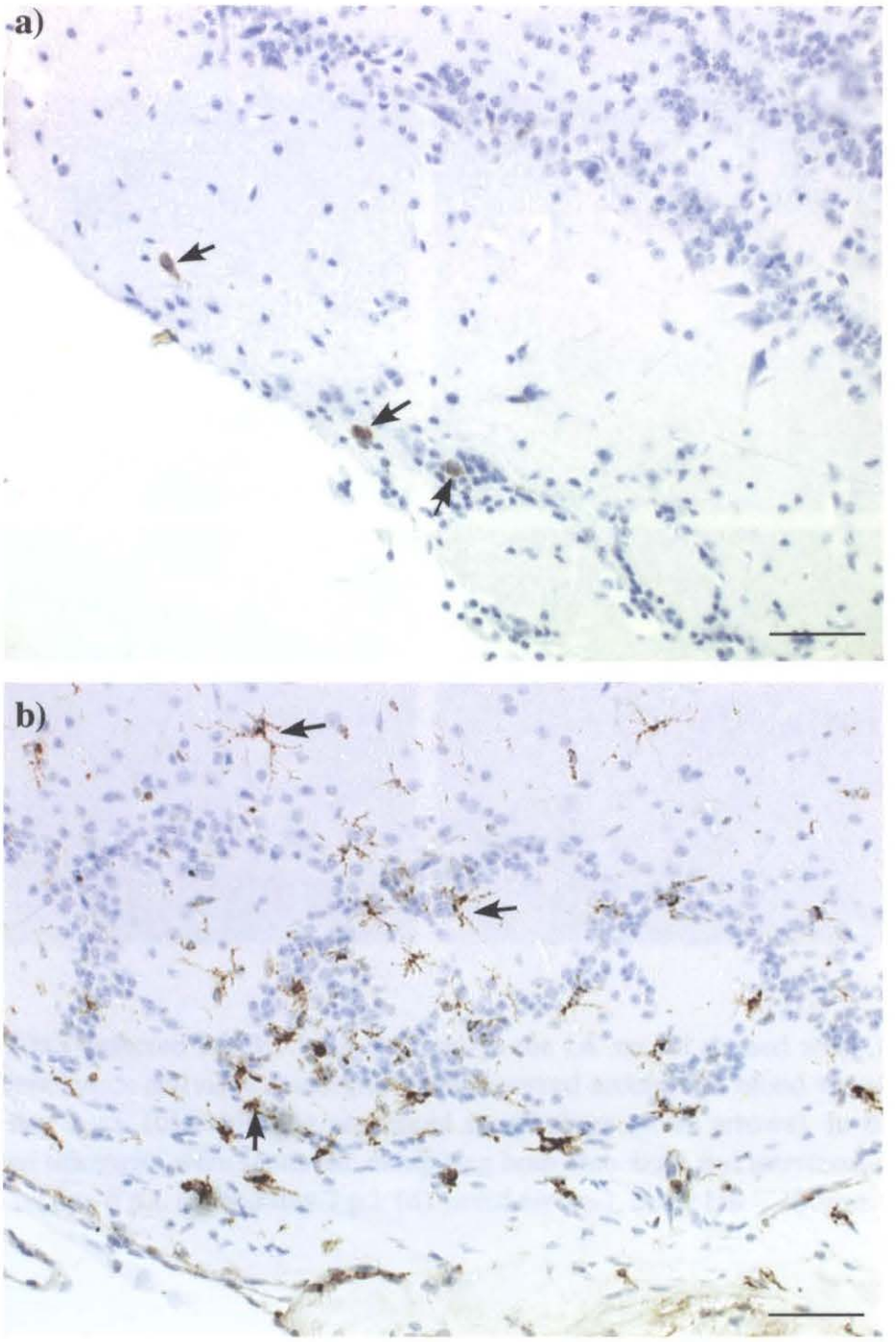

Figure: 6.7 WNV immunohistochemistry and lectin histochemistry of brain sections of B6.WT mice in the i.n. model. WNV antigen first appeared in the outermost layer of olfactory bulb on day 3 p.i. (a) (solid arrows). Activated microglia were also detected coincidently with the detection of WNV antigen in the outermost layer on day 3 p.i. (b) (solid arrows), but no where else in the brain. Scale bar = 50μm.

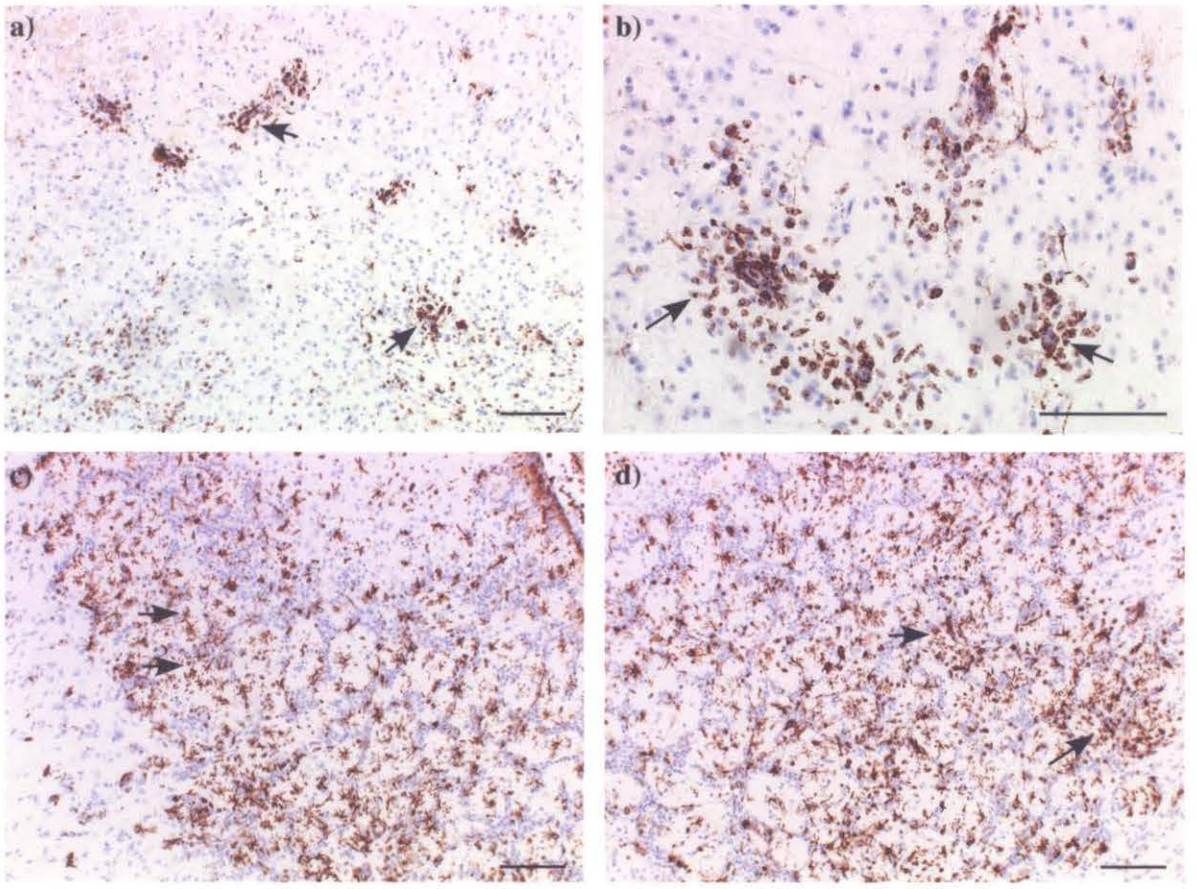

Figure: 6.8 WNV-infected B6.WT brain sections in the i.n. model stained with GS-lectin. In the brain parenchyma, activated microglia were observed around the blood vessels on day 6 p.i. (a) and day 7 p.i. (b) exhibiting amoeboid morphology (solid arrows). In the olfactory bulb, activated microglia were scattered, exhibiting both amoeboid and intermediate activated morphology on day 6 p.i. (c) and day 7 p.i. (d) (solid arrows). Scale bar = 100μm.

Figure: 6.9 Kinetics of WNV infection, microglial activation and leukocyte infiltration in B6.WT mice in the i.n. model (A) and i.p. model (B). In the i.n. model, extensive neuronal infection was observed in 100% of mice with similar pattern throughout and with 100% mortality by day 7 p.i. Therefore, relatively fewer numbers of mice were needed in the i.n. model, compared to the i.p. model. Groups of 110 mice in the i.p. model and groups of 21 mice in the i.n. model were infected with $6x10^4$ pfu/mouse. Subgroups of mice in each strain were sacrificed from day 3 to 15 p.i. in the i.p. model and from day 1-7 p.i. in the i.n. model. Immunoperoxidase labelling was used to detect viral antigen in the brain parenchyma of infected mice. H and E stain was used to detect leukocyte infiltration in the parenchyma. Lectin-histochemistry was used to detect activated microglia in the brain parenchyma. The number of neurones positive for viral antigen, leukocytes and activated microglia were counted, as described in Materials and Methods. Sixty H.P.F. were counted per mouse brain and values for each timepoint amalgamated and expressed as mean ± SEM.

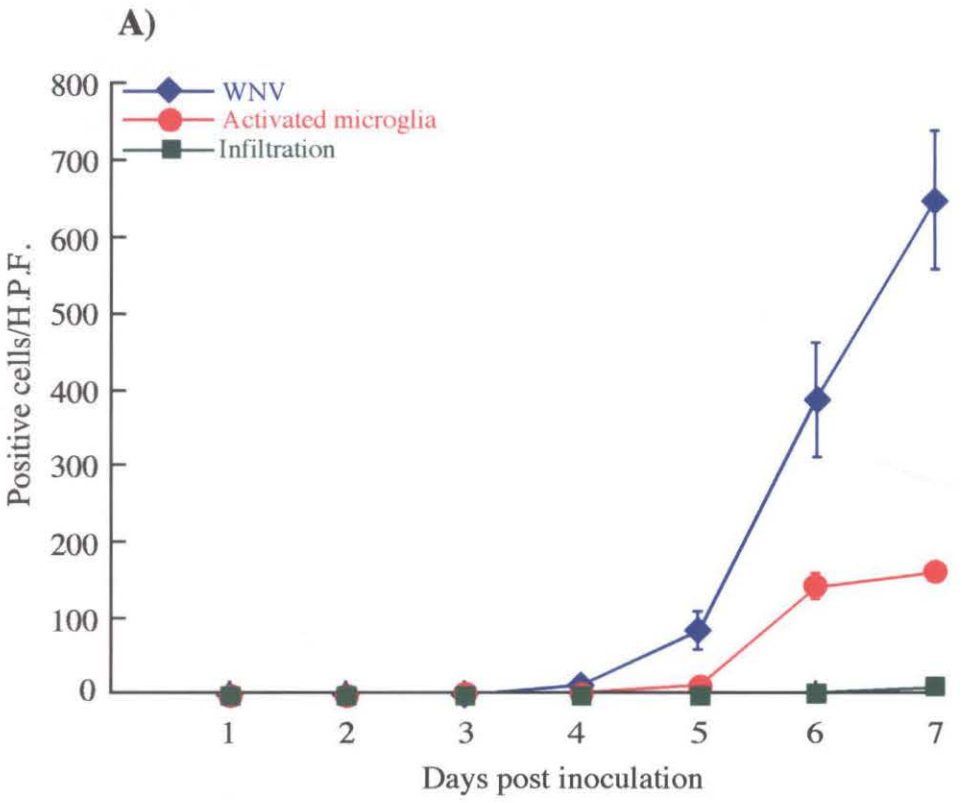
A)
WNV
Activated microglia
Infiltration
Positive cells/H.P.F.
800
700
600
500
400
300
200
100
0
1
2
3
4
5
6
7
Days post inoculation

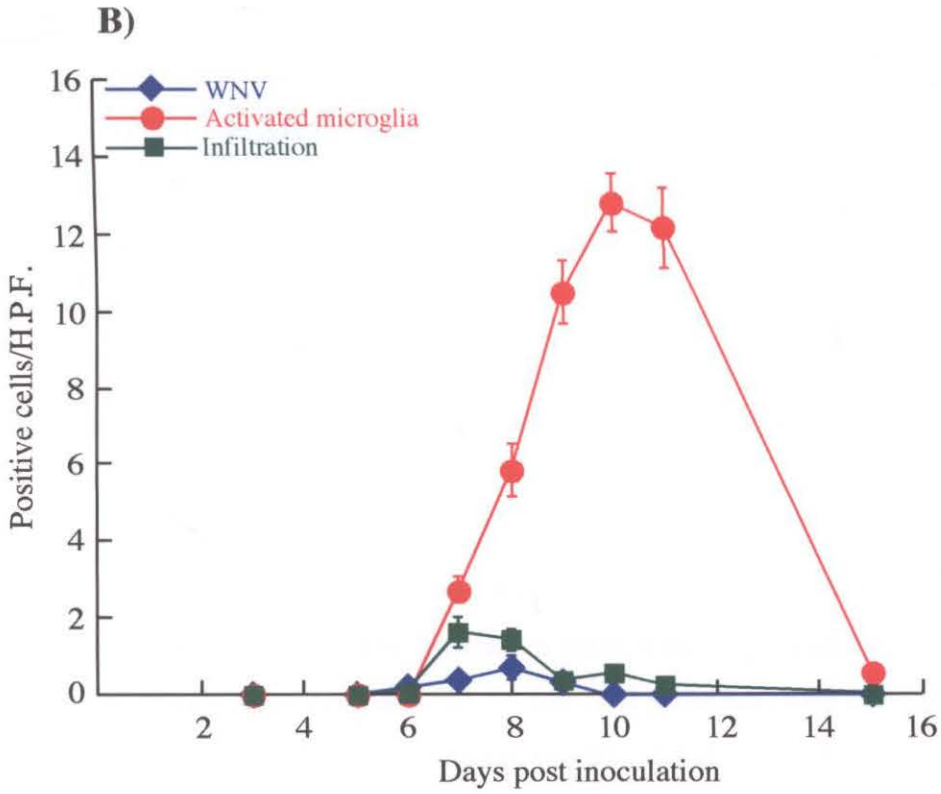
B)
WNV
Activated microglia
Infiltration
Positive cells/H.P.F.
16
14
12
10
8
6
4
2
0
2
4
6
8
10
12
14
16
Days post inoculation

route of access to the CNS in the i.n. model was also evaluated in this study. More importantly, in the i.p. model, IFN-γ clearly exacerbates disease. Therefore, it was important to determine in the i.n. model whether IFN-γ exerted a similar action to the i.p. model. To address these questions, mice were inoculated i.n. and i.p. in both strains of mice with the same dose of WNV, $6x10^4$ pfu/mouse. Their survival rates, clinical symptoms, virus burden in the brain, pattern of brain infection, as well as activation of microglia and kinetics of leukocyte infiltration were studied.

As described earlier in section 3.3.1.2., in the i.p. model, there was >2 fold better survival in B6.IFN-γ mice compared to B6.WT. In contrast, mice inoculated i.n. with WNV became sick suddenly and moribund the following day, with mortality rates of 100% in both strains. In both strains, mortality occurred between day 6-7 p.i. with identical kinetics (Figure 6.1 A and B), indicating that IFN-γ does not influence the outcome of disease in this model at this dose of virus. Although signs of clinical illness were observed from day 6 p.i. in both models in both strains of mice, the clinical signs exhibited by these mice were different between the models. In the i.p. model, some of the mice showed hindlimb paralysis whereas in the i.n. model, none of the mice from either strain was paralysed. This is supported by the early involvement of the spinal cord prior to brain involvement in the i.p. model, while in the i.n. model the brain was always involved before the spinal cord. These data suggest that paralysis is a result of spinal cord involvement, not pathology in the brain. In a study by Thach *et al.* (2000) mice lost up to 30% of their original body weight after i.n. inoculation of SBV. In this study, although the infected mice were not weighed during the experiment in either model, there was no visually obvious weight loss in the i.n. model, whereas inanition was clearly obvious in the i.p. model.

Since 100% mortality occurred with acute illness in the i.n. model in both strains of mice, the replicating virus load was determined by plaque assay. There was a massive difference in the titres between the models (Figure 6.2). In the i.p. model in both groups of mice, replicating WNV was detected from day 6 p.i. whereas in the i.n. model, replicating WNV was observed from day 3 p.i. The maximum titres were approximately 10 $\log_{10}$ pfu/gram brain in both groups of mice. This was >4 log-fold different from the i.p. model and was accompanied by 100% mortality. In the i.p. model, detection of WNV in the brain did not invariably reflect clinical illness or mortality. In contrast, the extensive growth of WNV in

the i.n. model was most likely be the cause of death in both B6.WT and B6.IFN-γ-/- mice, unlike the i.p. model, where mortality is clearly independent of WNV.

Immunoperoxidase labelling was used to determine the types of cells infected, the kinetics of disease progression as well as the possible route of WNV entry into the CNS in the i.n. and i.p. models. WNV first appeared in the cervical spinal cord 24h before it was detectable in the brainstem in the i.p. model. Consistently negative OB neurones and extremely rare infection of neurovascular endothelium as well as associated clinical features of hindlimb paralysis strongly suggests that WNV enters the brain via ascending axonal migration along the spinal cord in this model (section 3.3.3). In contrast, in the i.n. model, WNV first appeared in the outermost layer of the OB (Figure 6.3 a and 6.7 a) when both cervical spinal cord and brainstem were negative for WNV Ag. WNV spread to other parts of the OB and brain in a caudal-to-rostral direction, indicating that in the i.n. model, WNV uses the OB to enter the brain. The involvement of the outermost layer of the OB is consistent with the fact that this layer contains the incoming axons from the receptor neurones of the neuroepithelium. Similar results were also found in other viral encephalitis models using the i.n. route of infection, including SBV, VSV, HSV, MHV (Thach *et al.* 2000; Huneycutt *et al.* 1994; Barnett & Perlman 1993; Barnett *et al.* 1993; Anderson *et al.* 1983). These viruses use the olfactory nerve to enter the brain from the nasal cavity. However, several experiments show that after i.n. inoculation, it is not necessarily the olfactory pathway that is used to enter the brain. Shinya *et al.* (2000) demonstrated that in avian influenza virus encephalitis, virus was first detected in the brainstem, not in the OB after i.n. inoculation. Similarly, Babic *et al.* (1994) have shown that pseudorabies virus used 3 different routes, including the trigeminal, sympathetic and parasympathetic routes to enter into the CNS after i.n. inoculation. These data show that the manner of CNS involvement is clearly dependent on the route of inoculation. This in turn influences host survival in viral encephalitis.

As in the i.p. model, WNV Ag was observed only in the neurones and their processes in the i.n. model. However, extremely rarely, blood vessels may be infected (Figure 6.4 b). In the i.p. model, relatively localized and restricted infection of neurones were observed throughout all timepoints. In contrast, in the i.n. model, WNV spreads very rapidly (Figure 6.3), infecting almost all neurones of all brain except the cerebellum, demonstrating that WNV is highly neurotropic. This suggests either that only neurones have receptors for

WNV *in vivo* (this is clearly not true *in vitro*) or that WNV spreads from neurone to neurone via the axons and dendrites across the synaptic junctions. Very few necrotic neurones were observed, despite extensive neuronal infection at the time of death (Figure 6.4 a). WNV in the i.n. model regularly infected all the parts of hippocampus (Figure 6.3 e and 6.4 c), whereas in the i.p. model, these areas were only rarely infected. This may be due to the direct connections between the OB and hippocampus (Barr & Kiernan 1983). Like the i.p. model, detectable WNV Ag was rarely observed in the cerebellum, despite extensive neuronal infection in the rest of the brain in the i.n. model. This suggests that cerebellar neurones are perhaps not as accessible anatomically or are resistant to WNV infection.

It is clear that viral encephalitis is accompanied by infiltration of leukocytes into the brain parenchyma (Liu & Chambers 2001; Christensen *et al.* 1999; Kimura & Griffin 2000; Liu *et al.* 2001; Lane *et al.* 2000). In the i.n. model, infiltration of leukocytes was first observed in the OB, and increased to a maximum by the time of death. These inflammatory cells include both mononuclear and polymorphonuclear leukocytes, although the predominant cell type was mononuclear. Despite extensive infection throughout the brain, comparatively few leukocytes were observed in the brain parenchyma and very little perivascular cuffing was seen. Leukocytes were seen predominantly in the OB (Figure 6.6 b). In the i.p. model, infiltrating leukocytes were seen predominantly in the parenchyma, not the OB. Infiltration of leukocytes was observed 24h before WNV Ag detection in the brain parenchyma. In contrast, in the i.n. model, infiltration of leukocytes was observed 48h after WNV Ag detection in the OB. However, WNV spread rapidly throughout the brain before infiltration of leukocytes increased further (Figure 6.9 A). Interestingly, similar to the i.p. model, infiltration of leukocytes was observed from day 5 p.i., suggesting that the time required for activation of immune system with migration of leukocytes to the brain required at least 4-5 days in both models and suggests that leukocyte infiltration is part of the adaptive immune response, rather than the innate response.

Since neuronal infection was extensive in the i.n. model, the status of microglial activation was also evaluated. Activated microglia first appeared, co-incident with the detection of WNV Ag from day 3 p.i. in the OB (Figure 6.7). The number of activated microglia increased subsequently and was maximal at the time of death (Figure 6.9 A). As in the i.p. model, activated microglia showed different activated morphologies, including intermediate

and amoeboid forms and were scattered throughout the brain parenchyma and OB (see chapter 4). However, in the i.n. model, microglial activation was confined either to the OB (Figure 6.8) or found around the blood vessels in the i.n. model with very little nodule formation. Microglial activation was much higher in the OB, compared to the rest of the brain. Activated microglia are highly motile and mitotic in nature (Dickson *et al.* 1991). They can migrate to the sites of injury (Kreutzberg 1996) in response to chemokines (Johnstone *et al.* 1999; Peterson *et al.* 1997) they themselves can produce (Persidsky *et al.* 1999). The accumulation of activated microglia in the OB begs the question as to why they are not migrating to other parts of the brain or being activated in other areas when there is such extensive infection in these areas. Evidently high numbers of activated microglia migrate towards the early sites of infection in the OB. However, in the i.p. model, activated microglia were not concentrated only in the brainstem, but were scattered throughout the brain parenchyma, including the brainstem.

In the i.p. model, extremely high microglial activation was observed after 3-4 days of WNV detection in the brain parenchyma (Figure 6.9). This was normalized only after WNV antigen was undetectable (See chapter 4 for detail). In contrast, in the i.n. model, despite extremely high neuronal infection, significantly fewer microglia were activated after 3-5 days of WNV detection (Figure 6.9 A). It is known that microglial activation is under the strict control of neurones (Neumann 2001). Also, neurones are potential sources of M-CSF (Nohava *et al.* 1992), a potent mitogen for microglial proliferation (Lodge & Sriram 1996). Since WNV replicated and spread so quickly through the brain neurones, it is possible that these cells were not able to generate the mitogenic and chemoattractant gradient required to enable activation and migration of microglia. Further studies of soluble factors production by neurones in the i.p. and i.n. models may help to answer this question.

The responses of microglia in the i.p. model suggests that the control of WNV in the neurones may be mediated by activated microglia, since the number of activated microglia were extremely high, compared to the number of infected neurones. It is possible that the fewer numbers of activated microglia allowed the uncontrolled WNV growth in the brain in the i.n. model.

In conclusion, the disease profile was completely different, depending on the route of WNV inoculation. Mice in the i.n. model were highly susceptible to WNV infection with 100% mortality within 7 days p.i. due to acute encephalitis, compared to the mice in the i.p. model. In the i.n. model, WNV replicated very quickly and infected almost all neurones in most areas of the brain. The virus titres were approximately 10 $\log_{10}$ pfu/gram at the time of death, which is >4 log-fold higher than the peak titres observed in the i.p. model in both groups of mice. Unlike in the i.p. model, IFN-γ did not influence disease progression in the i.n. model. The small amount of neuronal degeneration, despite extensive infection suggests that the fatal outcome from i.n. inoculation may be associated with the functional insufficiency of the large numbers of WNV-infected neurones in the brain.

In the i.n. model, WNV used the olfactory pathway to gain access into the brain, whereas in the i.p. model WNV probably used the neural pathways through the spinal cord to gain entry into the brain. Infiltration of leukocytes occurred 48h after WNV Ag was detected in the brain parenchyma, but infiltrating cell numbers were significantly lower than the number of neurones infected. In the i.p. model, infiltration of leukocytes occurred 24h before WNV Ag was detected and leukocyte numbers were higher than infected neurones. Microglia were activated in response to neuronal infection in the i.n. model. However, significantly lower numbers of microglia were activated, compared to the number of neurones infected. In the i.p. model, extremely high numbers of microglia were activated compared to the number of neurones infected. This may contribute to controlling WNV in the neurones in the i.p. model. The, i.p., not the i.n. model, exhibits the pathology seen in human WNV encephalitis. The i.n. model represents direct neuronal infection whereas the i.p. model delays the access of WNV to the CNS, allowing the host to mount an effective adaptive immune response. Ironically, this may lead to death from immunopathology in this model.

Chapter-7

Role of antibody depends on the route of infection in WNV encephalitis

7.1. Introduction

The antiviral host defence mechanism is orchestrated by both natural and adaptive immune components. The immune mechanisms which mediate natural antiviral defence include macrophage activity, IFN-α/β, complement and natural Ab. Those that mediate adaptive antiviral defence include cell-mediated and humoral immune responses. Several animal models of neurotropic viral infection have shown that cell-mediated immune mechanisms play a major role in controlling viral infections in the CNS. This is mediated by T cells, either via CTL or by producing antiviral cytokines such as IFN-γ or TNF (Binder & Kundig 1991; Binder & Griffin 2001; Christensen *et al.* 1999; Harty *et al.* 2000; Kundig *et al.* 1993; Noske *et al.* 1998; Stohlman *et al.* 1998; Weidinger *et al.* 2000; Geiger *et al.* 1997; Rossol-Voth *et al.* 1991). However, in addition to cell-mediated immunity, humoral immune mechanisms also play an important role in controlling viral infection in the CNS and hence in disease outcome (Matthews *et al.* 2001; Wright & Buchmeier 1991; Griffin *et al.* 1997; Levine *et al.* 1991; Dietzschold *et al.* 1992; Kapoor *et al.* 1982).

Humoral immunity is mediated by Ab which is produced by B cells in both membrane bound and secreted forms. Since secreted Ab circulates in the blood, it functions as an effector molecule of humoral immunity for terminating primary infection, reducing the level of viraemia and may thus prevent disease. Although natural Ab has been shown to play a role in controlling viral infections (Ochsenbein *et al.* 1999; Ochsenbein & Zinkernagel 2000), most Ab-mediated protection is attributable to specific antiviral Ab (Thach *et al.* 2000; Kapoor *et al.* 1982; Kimura-Kuroda & Yasui 1988; Levine *et al.* 1991). Antiviral Ab can directly bind and neutralize virus particles and this opsonizes them to facilitate phagocytosis. Ab can also stimulate Ab-dependent cell cytotoxicity or activate the complement cascade (Kuby 1994). Antiviral Ab is generated after primary infection, or

after viral vaccination, but may also be effective after passive administration of HI or specific monoclonal Ab. Antiviral Ab which can neutralize virus infectivity is known as neutralizing Ab. Although viruses induce the host to produce both neutralizing and non-neutralizing Ab, neutralizing Ab plays a vital role in limiting virus spread and preventing disease. Circulating neutralizing Ab is the basis of protection against viral reinfection. Increasing evidence shows the importance of Ab in neurotropic viral infection, where it is thought to clear infectious virus and viral RNA from neurones (Levine *et al.* 1991; Dietzschold *et al.* 1992; Byrnes *et al.* 2000). This work is based predominantly on passive transfer of HI serum or monoclonal Ab. In the absence of effective antiviral therapy for neurotropic virus infection, passive protection with Ab can thus play an important role in prophylactic prevention or amelioration of viral infections. However, although Ab is important in antiviral defence mechanisms, it has been also postulated that Ab may be involved in enhancing disease in viral infections (Gould *et al.* 1987; Barrett & Gould 1986).

In WNV encephalitis, in the i.p. model, surviving mice from either strain (B6.WT and B6.IFN-γ-/-) rechallenged with a 50-fold higher dose of WNV than the original dose showed no clinical or histopathological features of encephalitis and 100% of mice survived. However, in the i.n. model, fatality was 100% during the primary infection in both groups of mice. Although Camenga *et al.* (1974) have studied the role of Ab in WNV encephalitis by passive transfer of HI serum using the i.p. route of WNV inoculation, the role of Ab in the i.n. model has not been studied. Therefore, a preliminary investigation was undertaken in B6.WT mice to determine the role of Ab in increasing survival and limiting the extent of CNS infection in the both i.p. and i.n. model, using passive transfer of HI serum. A preliminary study was also carried out in B cell-deficient mice (B6.μMT-/-) compared to control (B6.WT) mice to further explore the role of Ab in the immune response to WNV.

7.2. Materials and Methods

7.2.1. Mice

Female, specific-pathogen free, 8-week-old B6.WT and B6.μMT-/- mice (deleted μ chain of Ab), backcrossed to C57BL/6 were used.

7.2.2. Titration of WNV in the i.n. model

To determine the sublethal dose of WNV in the i.n. model, WNV was titrated in both B6.WT and B6.IFN-γ-/-mice. Three different doses were used: $6x10^4$ pfu/mouse, $6x10^3$ pfu/mouse and $1x10^2$ pfu/mouse. Groups of 24 mice, each of 8 mice/group/strain were inoculated i.n. with different doses of WNV. Their survival rate was evaluated as described in section 2.2.2.1. Surviving mice from this titration series were rechallenged i.n. with $6x10^4$ pfu/mouse. Their survival rate was evaluated as described in section 2.2.2.1.

7.2.3. Generation of hyper-immune serum and measurement of efficacy

HI serum was produced in B6.WT mice and its efficacy, including IgG titre, plaque reduction neutralization titre (PRNT) and *in vitro* efficacy as a neutralizing antibody was determined as described in section 2.4.

7.2.4. Passive transfer of hyper-immune serum and virus infection of mice

Only B6.WT mice were used for passive transfer experiments in i.n. and i.p. models. Groups of 30 mice in each model were treated with 200μl of 1:3 diluted serum (HI and normal serum) and WNV and their survival rates were evaluated as described in section 2.4.5. Another group of 10 mice was also treated with 200μl of 1:3 diluted HI serum i.p. at 48h p.i. in the i.p. model. A group of 35 mice was treated with 500μl of undiluted serum (HI and normal serum) and WNV only in the i.n. model. Infected mice in this group showing signs of hindlimb paralysis on day 11 and 13 p.i. were sacrificed for detection of WNV in the brain and spinal cord. The survival rate was evaluated as described. Brains and whole spinal cords were collected and processed as described in section 2.2.2.2.

Groups of 20 B6.WT mice and 15 B6.μMT-/- mice were inoculated i.p. with $6x10^4$ pfu/mouse and their survival rates were evaluated as described in section 2.2.2.1. Brains and cervical spinal cords were collected and processed as described in section 2.2.2.2.

7.2.5. Generation of hyper-immune splenocytes

Hyper-immune splenocytes were obtained from the same HI mice whose sera was used for passive transfer experiments, and cells were processed as described in section 2.5.1.

7.2.6. Adoptive transfer of hyper-immune splenocytes and virus infection of mice

B6.WT mice were used for adoptive splenocyte transfer experiments only in the i.n. model. Groups of 30 mice were treated with 200μl containing $5x10^7$ splenocytes/mouse (HI or normal splenocytes) and WNV. Their survival rates were evaluated as described in section 2.5.2.

7.4.7. Histopathology

Serial sections from paraffin-embedded tissues were stained with H and E stain, and were examined for histopathology.

7.2.8. WNV immunohistochemistry

This was done as described in section 3.2.3. Mock-infected brain sections were used as controls for WNV Ag labelling.

7.3. Results

7.3.1. Titration of WNV in the i.n. model

In the preceeding chapter it was shown that WNV was lethal in B6.WT and B6.IFN-γ-/-, with 100% mortality in both strains of mice when inoculated i.n. at $6x10^4$ pfu/mouse. Mice from both groups succumbed to extensive neuronal infection. Therefore, WNV was titrated in this model to determine the sublethal i.n. dose of WNV. The cumulative comparative survival after infection in all groups is presented in figure 7.1. In both strains of mice, 100% mortality occurred by day 7 p.i. after inoculation of $6x10^4$ and $6x10^3$ pfu/mouse, whereas $1x10^2$ pfu/mouse resulted in extended survival in both strains. In mice given $1x10^2$ pfu i.n., mortality occurred from day 7 p.i. in both groups and by day 9 p.i. mortality was 85% in B6.WT mice and 65% in B6.IFN-γ-/-. No further deaths occurred after day 9 p.i. and mice

Figure: 7.1 Titration of stock vero-grown WNV in 8-week-old B6.WT (A) and B6.IFN-γ-/- (B) mice in the i.n. model. Groups of 8 mice/strain/dose were inoculated i.n. with different doses of WNV and monitored for signs of illness 3 times a day over 21 days. The percent suvival at each timepoint is shown. Mock-infected mice did not develop signs of illness.

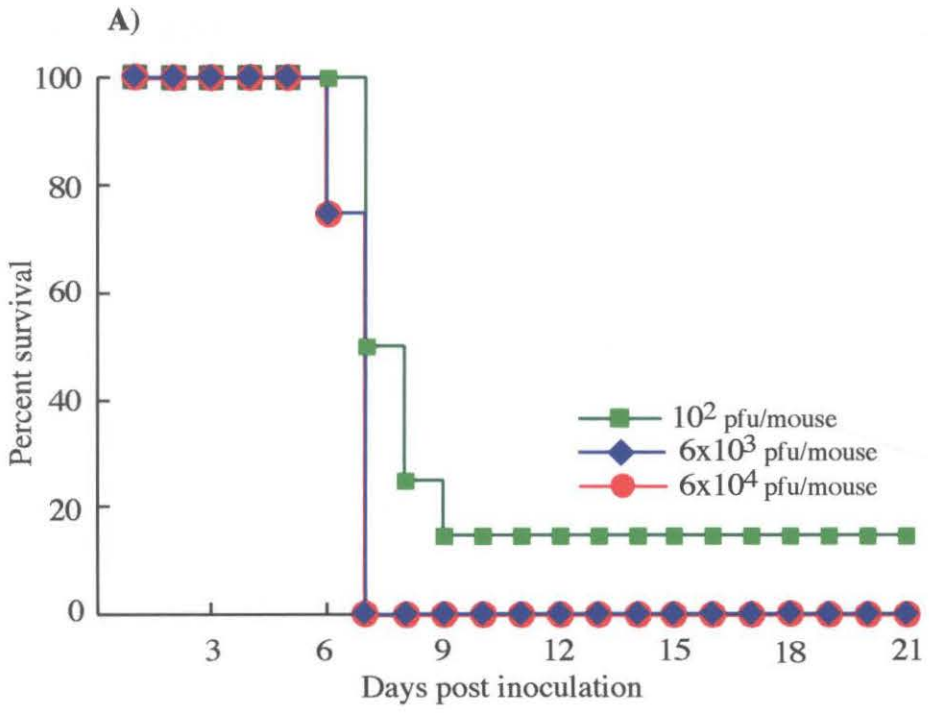

n = 8 mice/group

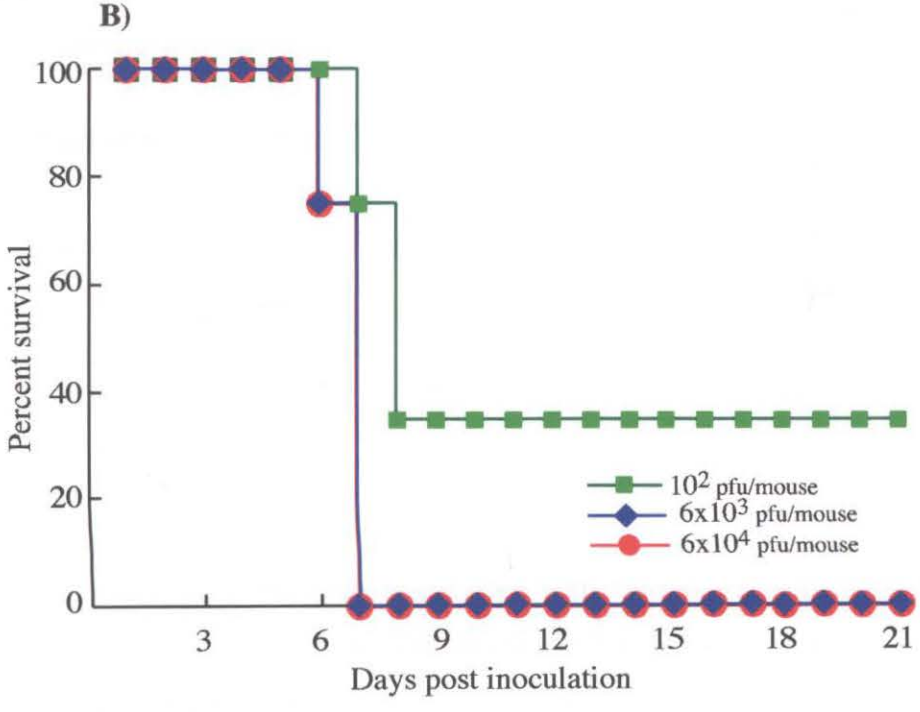

n = 8 mice/group

appeared healthy. Surviving mice from both strains were rechallenged with a 600-fold higher dose of WNV than the original dose, *i.e.*, $6x10^4$ pfu/mouse. This showed 100% protection from disease. These data suggest that the lethality of WNV is dose-dependent in the i.n. model and similar to the i.p. model, secondary immunity can be generated in the i.n. model.

7.3.2. Measurement of Hyper-immune serum efficiency *in vitro*

Before passive transfer of HI or normal sera into naïve mice, their antiviral activity was measured by 2 different methods. The IgG titre was determined by direct ELISA. The titre was determined as the dilution of serum where the optical density of HI and normal sera were equal. HI serum had an IgG titre of log 4.8 (Figure 7.2). The log of the highest dilution reducing 100 WNV plaques on vero cells by 50% was considered to be the PRNT or neutralizing $titre_{50}$ (NT_{50}). HI serum had a NT_{50} of log 5.4 (Figure 7.3). The efficacy of HI serum was further confirmed by its ability to neutralize WNV released from vero cell monolayers into the supernatant. In this assay, the presence of replicative WNV in the culture supernatant was determined after 48h infection in the presence of undiluted HI serum. It was found that undiluted HI serum could completely neutralize all supernatant WNV released from vero cells by 48h and this was dose-dependent, whereas undiluted normal sera had no effect on WNV released from infected vero cells (Figure 7.4). These data indicate that mice develop high levels of neutralizing Ab upon exposure to WNV.

7.3.3. Effect of passively transferred hyper-immune serum on survival

After analyzing the efficiency of HI serum *in vitro*, 200μl of 1:3 diluted HI and normal sera were passively transferred i.p., as described in Materials and Methods. This dose of HI serum could completely neutralize $6x10^4$ pfu *in vitro*. Another group of mice was treated with the same dose of HI serum at 48h p.i. in the i.p. model. Mice were observed for 2 weeks for clinical signs of illness.

In the i.p. model, mice passively transferred with normal serum or untreated and infected with WNV showed signs of clinical illness by day 6-10 p.i. with 60-70% mortality. In contrast, mice passively transferred with HI serum on p.i. day-1 or p.i. day+2 did not show any signs of clinical illness for 14 days p.i and appeared completely healthy (Figure 7.5 A).

Figure: 7.2 Detection of IgG titre in hyper-immune serum: IgG titre in the hyper-immune serum was determined by ELISA as described in Materials and Methods. IgG titre was defined as the log dilution of the serum where the optical density of hyper-immune and normal serum were equal.

Figure: 7.3 Kinetics of WNV neutralization by hyper-immune serum. Plaque reduction neutralization titre or neutralizing $titre_{50}$ was determined as described in Materials and Methods. The highest dilution of the hyper-immune serum that reduced plaques by 50% was regarded as the plaque reduction neutralizing titre.

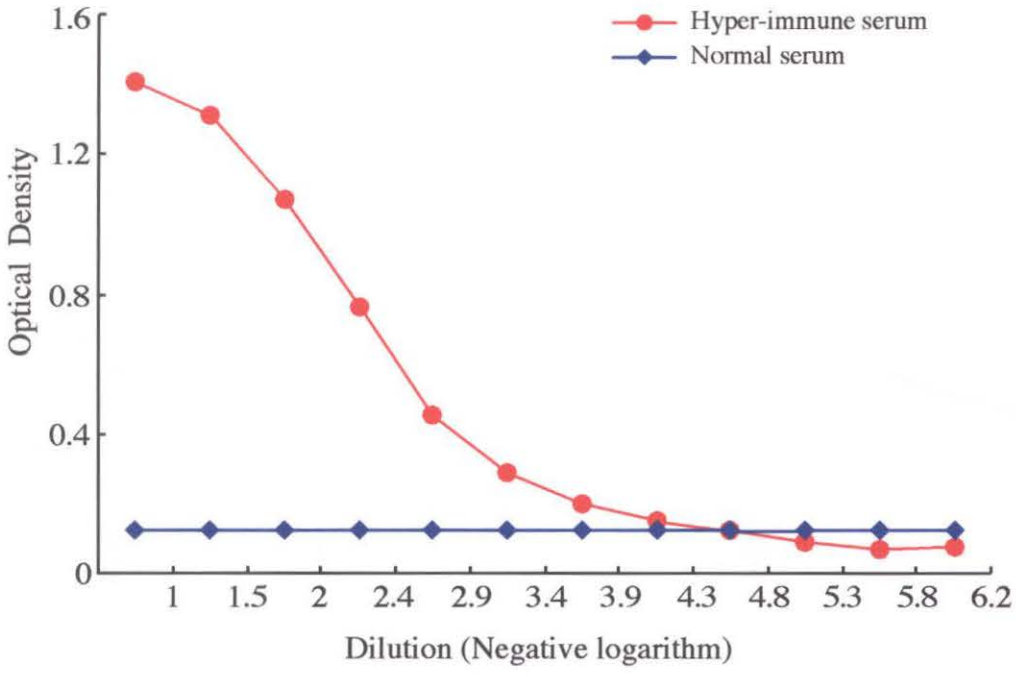

Figure: 7.2

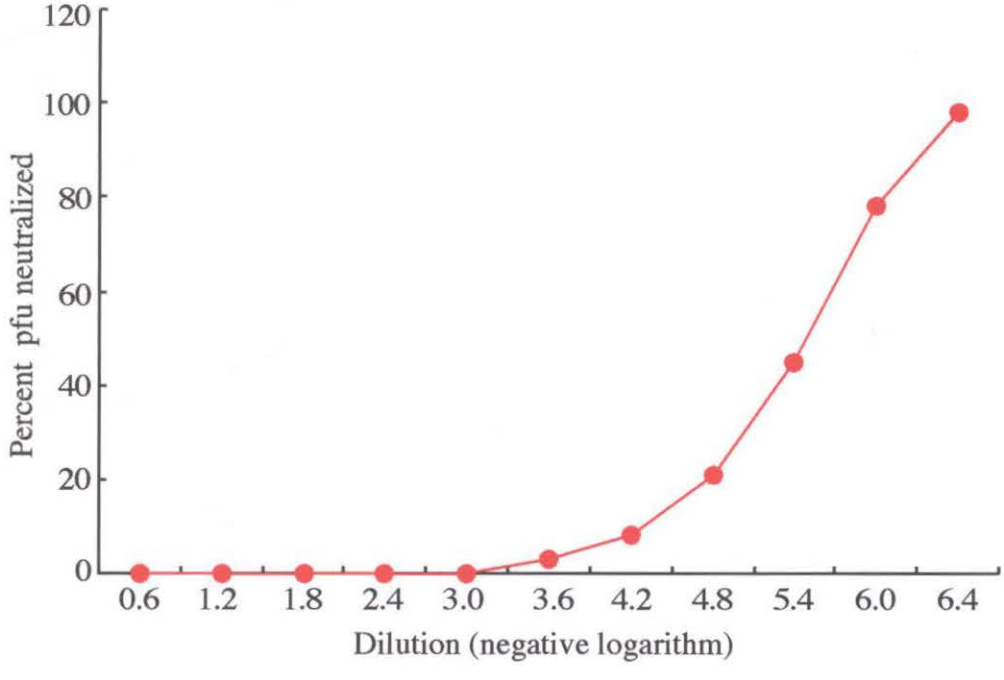

Figure: 7.3

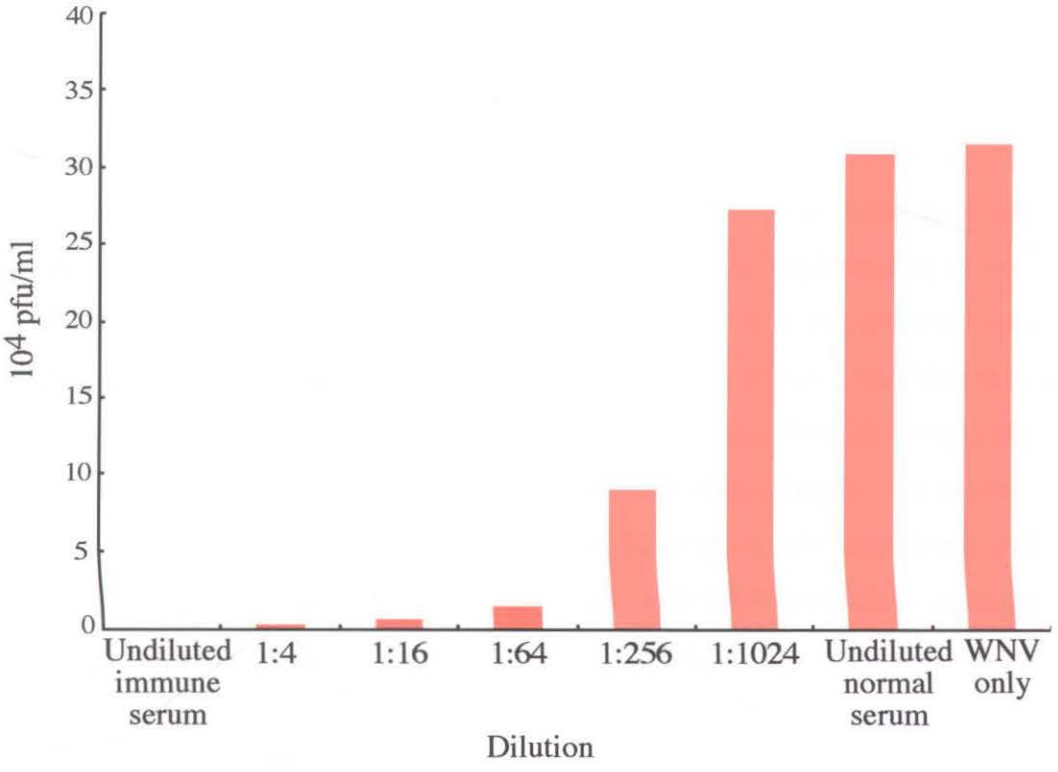

Figure: 7.4 *In vitro* efficacy of neutralizing antibody: The efficacy of neutralizing antibody was performed in an *in vitro* culture system, as described in materials and methods. In this assay, the effect of neutralizing antibody on WNV released from infected vero cells into the supernatant was measured. Normal serum was used as a control for hyper-immune serum and untreated infected vero cells were used as a control for both immune and normal sera. Undiluted normal serum could not inhibit WNV released from infected vero cells. Undiluted hyper-immune serum completely inhibited WNV released from infected vero cells into supernatant and no WNV plaques were detected by plaque assay of the supernatant. This effect was dose-dependent.

After 14 days p.i., 50% of mice were sacrificed, sera were pooled and assessed. Interestingly, 100 μl of this serum could still neutralize $6x10^4$ pfu, the dose originally given to infect these mice. The remaining 50% mice were rechallenged with a 50-fold higher dose of WNV than the original dose and observed for 14 days. No signs of clinical illness was observed in this time period (data not shown).

In contrast, in the i.n. model, mice passively transferred with HI or normal sera or left untreated, showed signs of clinical illness by day 6 p.i. and had all died by day 7 p.i. (Figure 7.5 B). It was speculated that the amount of serum given to the naïve mice may not have been enough to protect mice in this model. Therefore, 500μl undiluted HI or normal serum, *i.e.,* 750-fold higher than the neutralizing dose in the first experiment, was passively transferred, as described, one day prior to WNV infection. It was found that this dose of HI serum could extend the survival of mice in this model (Figure 7.6). However only 13% mice survived until day 14 p.i., when they were sacrificed. Interestingly, one mouse on each of days 11 and 13 p.i. showed hindlimb paralysis. Mice passively transferred with 500μl of undiluted normal serum, succumbed by day 7 p.i. with 100% mortality, similar to untreated mice. These data indicate that passive transfer of HI serum both pre and post infection can abrogate encephalitis in the naïve mice in the i.p. model, but not in the i.n. model. Very high dose immune serum is required to extend the life of naïve mice in the i.n. model.

7.3.4. Effect of adoptively transferred hyper-immune splenocytes on survival

It was demonstrated that passive protection with HI serum was effective in the i.p. model and not in the i.n. model. Thus, the question arises as to whether these i.n. mice would be protected if adoptively transferred with splenocytes from HI mice. Therefore, naïve mice were adoptively transferred i.p. with $5x10^7$ splenocytes/mouse only in the i.n. model, as described in Materials and Methods, to determine whether passive protection occur via these cells in the i.n. model. Similar to the passive transfer of HI serum, adoptive transfer of immune splenocytes experiment was undertaken in B6.WT mice. Mice treated with HI or normal splenocytes or left untreated showed signs of clinical illness by day 6 p.i. and had all died by day 7 p.i. (Figure 7.7). Thus HI splenocytes were unable to protect mice inoculated by the i.n. route despite being given 24h before WNV inoculation.

Figure: 7.5 Survival of B6.WT mice passively transferred with hyper-immune or normal sera or left untreated and infected either i.p. or i.n. with WNV. Groups of 30 mice in each model, 10 mice/group were used in both i.p. and i.n. models. One group was treated with hyper-immune serum, one group was treated with normal serum and one group was left untreated in both models. Sera were diluted 1:3 and 200μl was injected i.p. 24h before infection in both models. All groups of mice were inoculated with $6x10^4$ pfu/mouse as decribed, and monitored for signs of illness 3 times/day over 14 days. The percent survival at each time point is shown. Figure A shows survival profiles of B6.WT mice passively transferred with sera and infected via the i.p. route. Figure B shows the survival profiles of of B6.WT mice passively transferred with sera and infected via the i.n. route.

A)

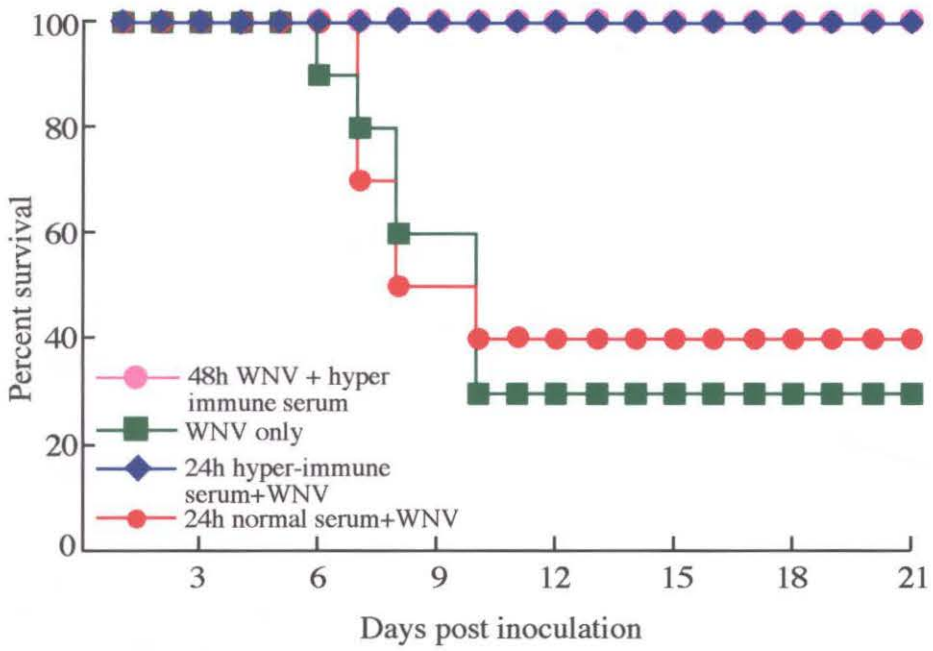

n = 10 mice/group

B)

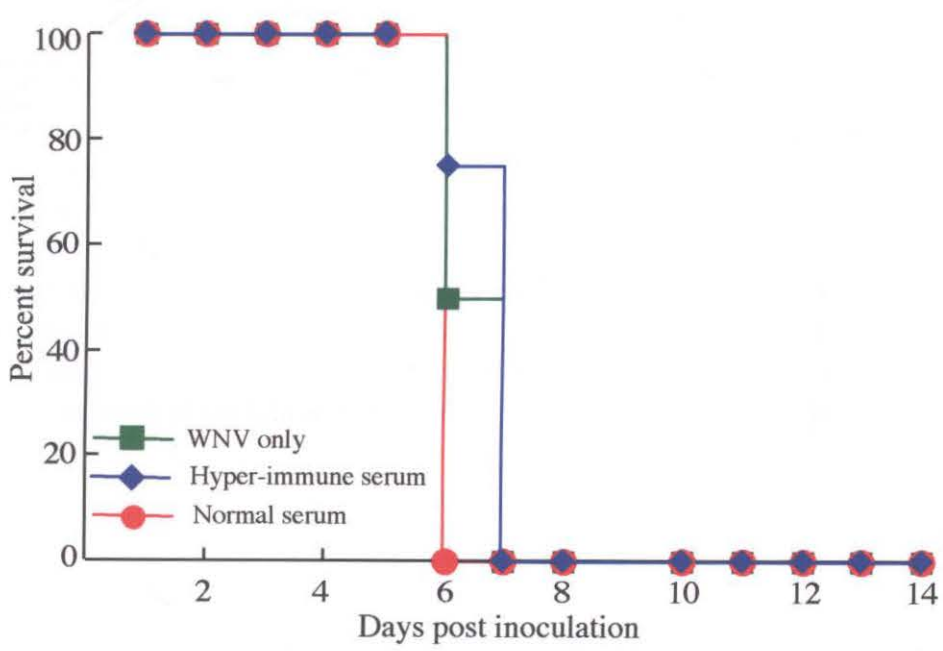

n = 10 mice/group

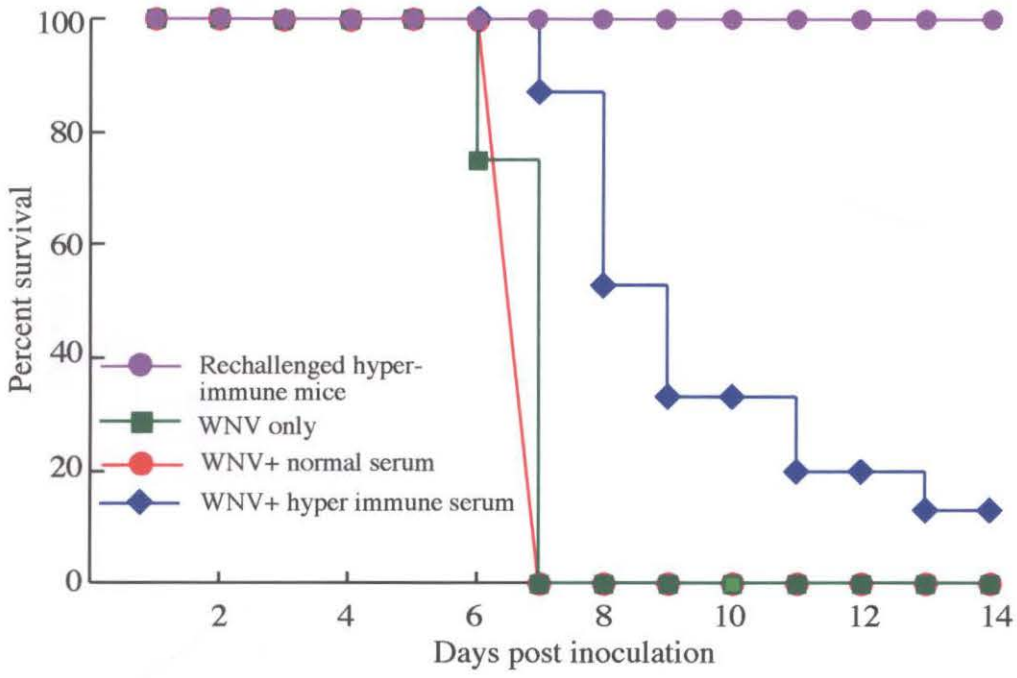

Figure: 7.6 Survival of B6.WT mice passively transferred with 500μl undiluted sera and infected i.n. with WNV. Groups of 35 naive mice were used. One group (n=15) was treated with hyper-immune serum, one group (n=10) was treated with normal serum and one group (n=10) was left untreated. Five hundred microlitres undiluted sera were passively transferred i.p. 24h before i.n. infection. All groups of mice were then inoculated i.n. with $6x10^4$ pfu/mouse as described in materials and methods. Groups of i.n. WNV-immune mice (n=8) were also rechallenged i.n. with 600-fold higher dose of WNV than the original dose, *i.e.*, $6x10^4$ pfu/mouse. They were monitored for signs of illness 3 times a day over 14 days. The percent survival at each timepoint is shown.

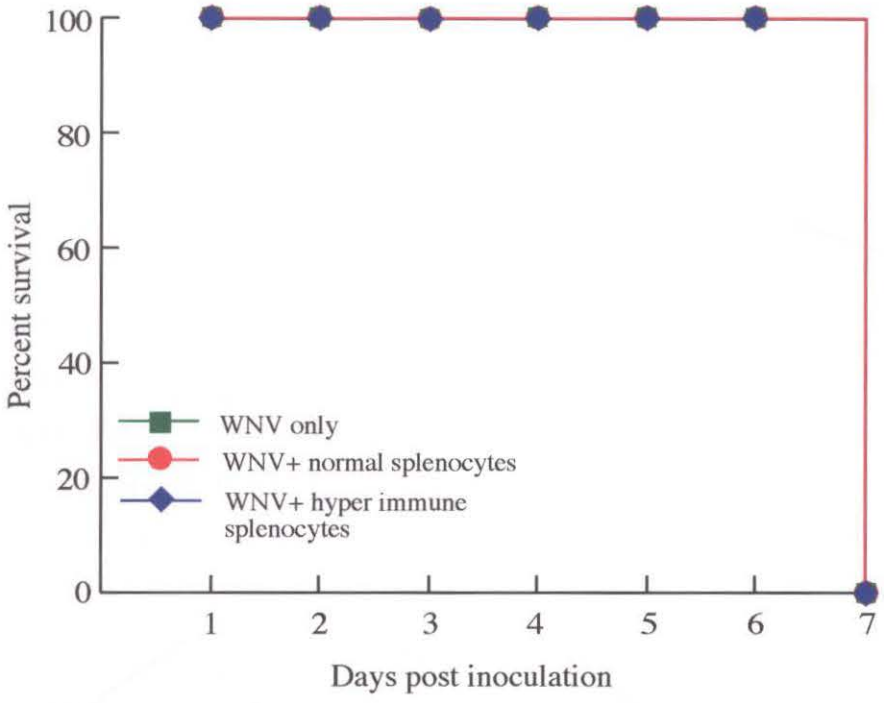

n = 10 mice/group

Figure: 7.7 Survival of B6.WT mice adoptively transferred with $5x10^7$ splenocytes/mouse and infected i.n. with WNV. Groups of 30 naive mice, 10 mice/group were used. One group was treated with hyper-immune splenocytes, one group was treated with normal splenocytes and one group was left untreated. Splenocytes were transferred 24h before infection and all groups of mice were then inoculated i.n. with $6x10^4$ pfu/mouse as described in materials and methods. They were monitored for signs of illness 3 times a day over 7 days. The percent survival at each timepoint is shown.

7.3.5. Effect of passively transferred sera on WNV antigen distribution in the CNS

Since none of the mice passively transferred with HI serum showed clinical illness and 100% survived in the i.p. model, the brains and spinal cords were analysed for WNV Ag on day 7 and 8 p.i. No WNV Ag was detected and the brain and spinal cords of these mice showed normal histology (data not shown). In contrast, in the i.n. model, all mice treated with low dose (200μl of 1:3 diluted) HI serum showed widespread neuronal infection at the time of death, on day 7 p.i, similar to that of normal serum-treated and untreated mice. Since high dose HI serum extended survival in the i.n. model and since a few mice were paralysed on day 11 and 13 p.i., it was necessary to see the pattern and extent of WNV Ag distribution in the brain and spinal cords of these mice. Mice passively transferred with a high dose of normal serum showed widespread neuronal infection in the OB (Figure 7.8 b), front cortex (Figure 7.8 a) and other parts of the brain by day 7 p.i., similar to untreated mice. Interestingly, no WNV Ag was detected in the OB of mice passively transferred with high dose HI serum on day 8 p.i. (Figure 7.8 c), but it was detected in a few neurones in the front cortex (Figure 7.8 d). No WNV Ag was detected in the OB on day 11 p.i. either (Figure 7.8 e), but infected neurones were observed in the cervical (Figure 7.8 f) and lumbar spinal cord on day 13 p.i. (Figure 7.8 h). At this time, also very few infected neurones were seen in the front cortex (Figure 7.8 g), compared to normal serum-treated mice (Figure 7.8 a). Histology showed high activation of microglia with formation of nodules throughout the brain. These data indicate that low dose HI serum is insufficient to abrogate direct infection via the olfactory neuroepithelium and suggest that mice died due to overwhelming neuronal infection. In contrast, high dose HI serum can extend survival.

Mice adoptively transferred with splenocytes showed very similar signs of clinical illness and mortality to that of normal splenocyte-transferred or untreated mice. Therefore, histopathology and WNV detection were not studied in these mice.

7.3.6. Survival after i.p. route of WNV inoculation in B6.μMT-/- mice

To further explore the role of Ab in WNV encephalitis, B6.μMT-/- mice were used in this study. In the i.n. model, although high dose HI serum extended survival it could not protect mice. Therefore, in B6.μMT-/- mice a survival study was performed using the i.p. route of

Figure: 7.8 Brain sections from B6.WT mice, passively transferred with 500μl undiluted hyper-immune or normal serum and WNV-infected, labelled with anti-WNV antibody in the i.n. model. Mice treated with normal serum showed extremely high neuronal infection in the front cortex (a) (solid arrows) and olfactory bulb (b) (solid arrows) at day 7 p.i. Mice pretreated with hyper-immune serum showed no detectable neuronal infection in the olfactory bulb (c) but very few infected neurones were observed in the front cortex (d) at day 8 p.i. Mice pretreated with hyper-immune serum also showed no detectable neuronal infection in the olfactory bulb at day 11 p.i (e) but WNV Ag was detected in the cervical spinal cord neurons at this timepoint (f) (solid arrows). On day 13 p.i. these mice showed very few infected neurones in the front cortex (g) (solid arrows). Infected neurones were also observed in the lumbar spinal cord (h) (solid arrows) at this timepoint. Scale bar = 100μm from a-e, g-h and 50μm f.

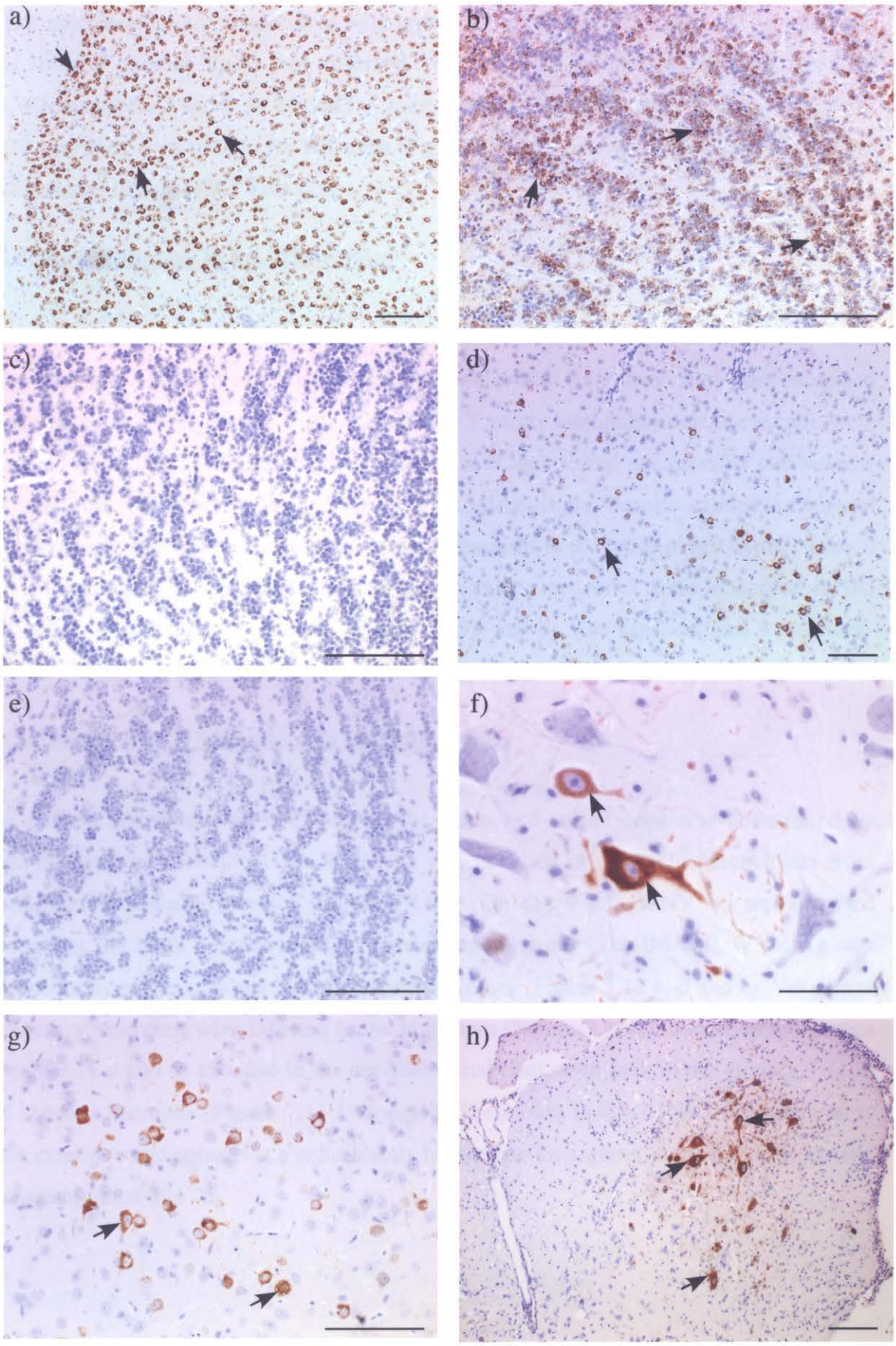
a)
b)
c)
d)
e)
f)
g)
h)

WNV inoculation, and compared to wild type mice. Like B6.WT, in B6.μMT-/- mice the first signs of clinical illness was observed from day 6 p.i. similar to those described for B6.WT in chapter 3 and 6. In B6.μMT-/- mice mortality occurred between day 6-9 p.i. with 100% mortality compared to B6.WT mice (Figure 7.9), suggesting that B6.μMT-/- mice are highly susceptible to WNV infection.

7.3.7. Histopathology in B6.μMT-/- mice

H and E staining was used to evaluate the histopathological changes in B6.μMT-/- mice mice (Figure 7.10). Since this is a preliminary study, tissues from these mice were examined at the time of death, on day 9 p.i. Like B6.WT mice, histopathological changes were observed in B6.μMT-/- mice, including infiltration of leukocytes, occasionally perivascular cuffs and microglial activation (Figure 7.10 a). Interestingly, despite extensive neuronal infection, very few infiltrating leukocytes were observed in the brain-parenchyma on day 9 p.i. Interestingly, unlike B6.WT, many degenerating neurones were observed in the pyramidal cells of the hippocampus (Figure 7.10 c and d). The hippocampus from mock-infected B6.μMT-/- mice showed normal histology (Figure 7.10 b).

7.3.8. Detection of WNV antigen in B6.μMT-/- mice

The pattern and extent of WNV Ag in the brain and spinal cord was determined by immunoperoxidase labelling. No WNV Ag was detected in the brain parenchyma from mock-infected B6.μMT-/- mice (Figure 7.11 a). On day 9 p.i., WNV Ag was detected throughout the brain parenchyma and cervical spinal cord. Like B6.WT, WNV Ag was confined only to the neuronal cytoplasm and processes (Figure 7.11 b, d and e). Very large numbers of neurones were infected in the brainstem (Figure 7.11 b), cortex, hippocampus (Figure 7.11 c and d) and also in the cervical spinal cord, with both motor (Figure 7.11 e) and sensory neurones (Figure 7.11 f) infected. These data indicate that CNS infection is more extensive and spreads at a significantly higher rate throughout the brain in the genetic absence of functional Ab.

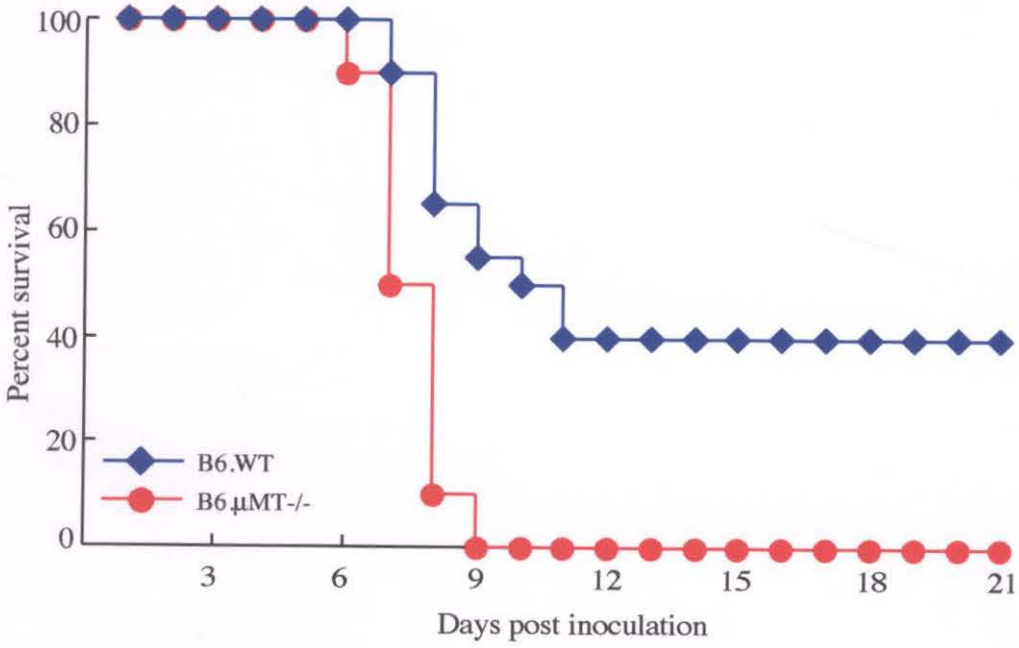

Figure: 7.9 Survival after i.p. inoculation of WNV in B6.WT and B6.μMT-/- mice. Groups of 20 mice from B6.WT and 15 mice from B6.μMT-/- mice were inoculated i.p with $6x10^4$ pfu/mouse. They were monitored for signs of illness 3 times a day over 21 days. The percent survival at each time point is shown. Mock-infected mice did not develop signs of illness in either group.

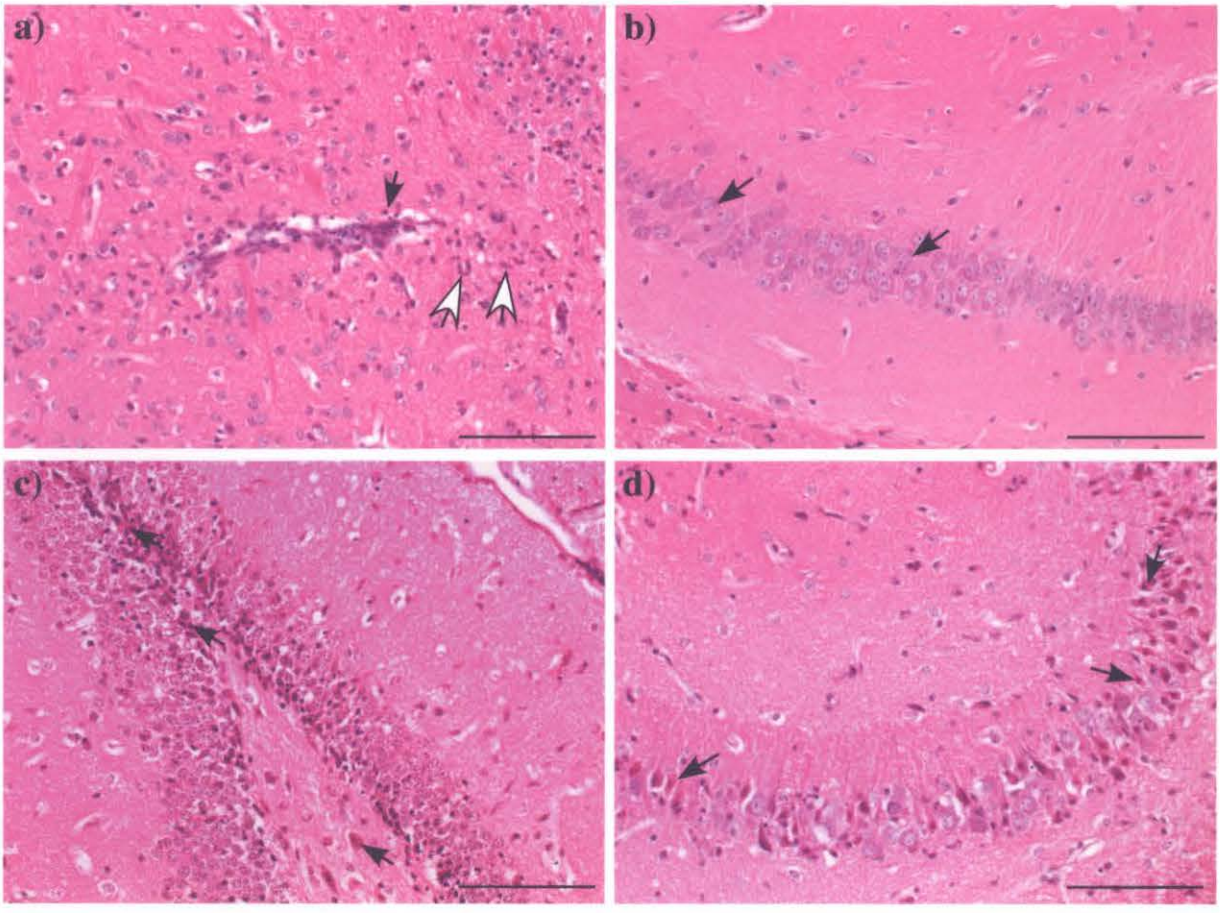

Figure: 7.10 H and E stained brain sections of mock-infected and WNV-infected B6.μMT-/- mice on day 9 p.i. Infected brain parenchyma showed infiltration of leukocytes with perivascular cuffing (a) (solid arrow), activation of microglia (a) (open arrows) and extensive neuronal degeneration in the hippocampus (c) and (d) (solid arrows). The hippocampus from mock-infected mice showed normal histology (b) (solid arrows). Scale bar = 100 μm.

Figure: 7.11 WNV-infected B6.μMT-/- mouse brain sections labelled with anti-WNV antibody on day 9 p.i. No WNV antigen was detected in the mock-infected brain parenchyma (a). On day 9 p.i., extensive neuronal infection was observed throughout the brain, including brainstem (b) (solid arrows), cortex (c) (solid arrows) and hippocampus (c) (open arrows). In the hippocampus, all neurones were infected (d) (solid arrows). At this timepoint, high numbers of infected motor neurones (e) (solid arrows) and sensory neurones (f) (solid arrows) were observed in the cervical spinal cord. Scale bar = 50μm a-b, d and e-f and 300μm c.

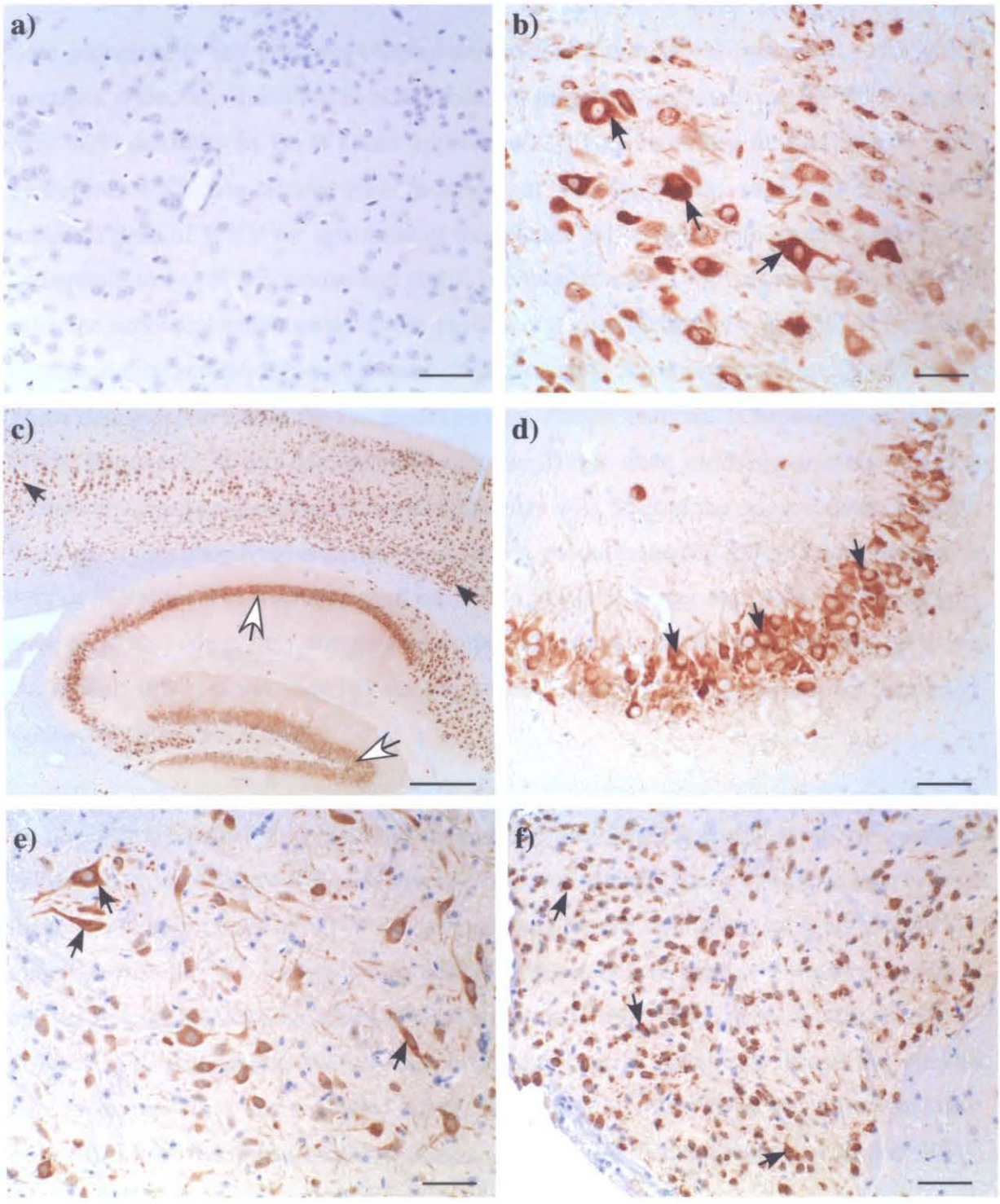
a)
b)
c)
d)
e)
f)

7.4. Discussion

Data presented in the previous chapter demonstrated that WNV was lethal, with 100% mortality when inoculated i.n. in both strains of mice, but the same dose of WNV caused only 60% mortality in B6.WT and approximately 17% mortality in B6.IFN-γ-/- mice. Therefore, WNV was titrated in both strains of mice in the i.n. model to determine a sublethal dose of WNV for this route of inoculation. Mice from both groups were highly susceptible to $6x10^4$ pfu/mouse and $6x10^3$ pfu/mouse, with 100% mortality, but showed extended survival when inoculated with $1x10^2$ pfu/mouse (Figure 7.1). Thus B6.WT showed 85% mortality and B6.IFN-γ-/- showed 65% mortality. Surviving mice appeared healthy These data indicate that in the i.n. model as well, disease outcome is dependent on dose of WNV. Previously, it was demonstrated (chapter 3) that mice surviving primary infection completely abrogate encephalitis upon rechallenge with 50-fold the original dose of WNV. Thus, surviving mice from either group in the i.n. model primarily infected with the lowest dose of WNV were also rechallenged i.n. with a 600-fold higher dose WNV. Interestingly, these mice also completely abrogate encephalitis. This data further confirms that, as in the i.p. model, IFN-γ is not required for the generation of primary or secondary immunity against WNV in the i.n. model.

To investigate whether the generation of secondary immunity is mediated via immune cells or Ab or both, naïve mice were adoptively transferred with HI serum or splenocytes in these models. The role of Ab in WNV encephalitis was further confirmed by using B6.μMT-/- mice compared to the corresponding wild type mice. Before passively transferring HI or normal sera the IgG titre and efficacy was determined using PRNT, as an *in vitro* test for the efficacy of neutralization. Twenty four hours after passive transfer of sera or splenocytes into naïve mice, they were infected either i.p. or i.n. with WNV at $6x10^4$ pfu/mouse. Mice were monitored for signs of clinical illness, survival and histopathology, as well as WNV Ag in the CNS.

It is clear that Ab plays an important role in controlling neurotropic viral infections. Most previous studies on neurotropic viral encephalitis is based on passive transfer of either monoclonal or polyclonal Ab. In HSV infection, passive transfer of HI serum protected mice from death and neurological diseases compared to control mice treated with normal

serum (McKendall *et al.* 1979). Experiments with flaviviruses also showed that passive transfer of immune Ab can protect mice from lethal infection (Kimura-Kuroda & Yasui 1988; Chiba *et al.* 1999; Kreil and Eible 1997). Antibody also plays an important role in alphavirus infection. SBV infection in mice is perhaps the most extensively studied model in the evaluation of the role of Ab in neurotropic viral infections. Genetic absence of either IFN-α/β or IFN-α/β receptor makes mice highly susceptible to a number of viral infections (Muller *et al.* 1994; Durbin *et al.* 2000). However, this susceptibility can be overcome by passive transfer of Ab. Thus passive transfer of monoclonal Ab was found to protect mice completely in the absence of IFN-α/β in SBV infection (Byrnes *et al.* 2000). Moreover, passive transfer of HI serum could also protect mice from SBV infection in the complete absence of T and B cells, as shown by Levine *et al.* (1991).

In the i.p. model of WNV encephalitis, mice passively transferred with HI serum 24h before infection were completely protected and appeared healthy until 14 days p.i., compared to mice passively transferred with normal serum or left untreated prior to WNV infection (Figure 7.6 A). Kimura-Kuroda & Yasui (1988) showed that passive administration of monoclonal Ab 24h before i.v. inoculation of JE virus increased protection, but the same Ab, if transferred 24h after infection, showed lower protection from lethal JE infection. In contrast, in TBE infection, passive transfer of Ab was effective at both 24h before and after peripheral infection, but not 48h after TBE infection (Chiba *et al.* 1999). Interestingly, in the i.p. model of WNV encephalitis, complete protection was observed even after passive transfer of HI serum 48h p.i. (Figure 7.5 A). The brain parenchyma of HI serum-treated mice showed normal histology and no WNV Ag was found on day 7 and 8 p.i. Moreover, these mice were completely protected upon rechallenge with a 50-fold more WNV than the original dose. It is not known whether this denotes the development of adaptive immunity, or whether the passively transferred Ab continued to be efficacious in these mice. Although Peiris & Porterfield (1979) showed Ab-dependent enhancement of infection in an *in vitro* culture system, this was not observed in WNV encephalitis.

WNV encephalitis in the i.p. model reflects immunopathology. Results from this chapter showed that passive transfer of HI serum 24h before and 48h after infection can completely abrogate IFN-γ-mediated immunopathology in the i.p. model. Similar results were also

found in LCMV infection (Wright & Buchmeier 1991). LCMV infection is a T-cell-mediated immunopathological disease (Zinkernagel 1992). Wright & Buchmeier (1991) showed that passive transfer of monoclonal Ab one or two days before infection completely protected mice from lethal LCMV immunopathological disease. In their model, LCMV was inoculated i.c. after passive transfer of Ab. They found both suppressed viral replication and a specific cytotoxic T-cell response in surviving mice.

Interestingly, unlike the i.p. model, in the i.n. model, mice passively transferred with the same dose of HI did not protect mice from disease. All mice treated with HI serum died by day 7 p.i., similar to normal serum-treated or untreated mice (Figure 7.5 B). Immunohistochemistry showed extremely high brain infection, similar to the normal serum-treated or untreated mice, suggesting that HI serum does not provide passive protection against the i.n. route of WNV inoculation. Dietzschold *et al.* (1992) have shown that passive transfer of monoclonal Ab protected rats against lethal rabies virus infection after i.n. inoculation. In control rats, rabies virus RNA was observed in the OB and front cortex after 6-12h p.i. respectively, but was not detected in Ab-treated mice even after 30 days p.i. HI serum can also passively protect mice against i.c. challenge (Chaturvedi *et al.* 1977; Byrnes *et al.* 2000; Wright & Buchmeier 1991).

It was speculated that in the i.n. model of WNV encephalitis, a higher dose of neutralizing Ab may be required to protect mice from lethal WNV infection. Therefore, a 750-fold higher dose of HI serum than the original neutralizing dose was transferred into naïve mice 24h before i.n. inoculation of WNV. Mice thus treated survived longer, compared to control mice treated with a 750-fold higher dose normal serum (Figure 7.6). However, only 13% of mice were able to survive until day 14 p.i. when they were sacrificed. Moreover, some of the surviving mice showed hindlimb paralysis, which was not previously observed in the i.n. model. More interestingly, on day 8 p.i. the brain parenchyma of moribund mice that had been treated with high dose HI serum showed very few infected neurones (Figure 7.8 d) in the front cortex. Surprisingly, none of the neurones in the OB and hippocampus showed detectable WNV infection, while mice treated with normal serum or left untreated showed extensive neuronal infection in the OB and front cortex at the time of death (Figure 7.8 a and b).

These data suggest that high dose HI serum-treated mice are not dying due to brain infection as in normal serum-treated or untreated mice, which died due to overwhelming brain infection. The mice that survived on day 11 and 13 p.i. showed infection of motor neurones in lumbar, thoracic and cervical spinal cord, but no detectable neuronal infection in the OB. Very few infected neurones were observed in the front cortex at day 13 p.i. (Figure 7.8). Highly activated microglia were observed throughout the brain, but not in the OB. Thus, entry of WNV via the olfactory route seems unlikely in these mice. These data indicate that passive transfer of high-dose HI serum extends survival in the i.n. model but suggests that it may also alter the route of WNV entry into the CNS. However, it is not clear how and why this route is altered in the presence of high dose Ab.

Since passive transfer of high-dose HI serum was unable to completely protect mice in the i.n. model, I speculated that effective immunity against WNV might occur via immune cells in the i.n. model. Therefore, mice were adoptively transferred with HI splenocytes $5x10^7$/mouse 24h before i.n. infection. Mice adoptively transferred with HI splenocytes showed the same disease outcome, with 100% mortality, by day 7 p.i. as that of normal splenocytes-treated and untreated mice (Figure 7.7). However, i.n. WNV-immune mice can abrogate encephalitis and death even with a 600-fold higher dose of WNV than the original dose. This data raises the question of whether the brain needs to be infected to become immune. Murali-Krishna and Manjunath (1996) have shown that adoptive transfer of JE-specific $CD8^+$ T cells when co-inoculated with JE virus via i.c. protected mice from lethal JE, but the same $CD8^+$ T cells were unable to protect mice when adoptively transferred via i.p. or i.v. in this model. Thus, adoptive transfer of splenocytes via i.c. before infection or at the time of i.n. infection could answer the question of whether these cells can abrogate encephalitis in the i.n. model. Unfortunately, HI splenocytes were not used as a positive control in the i.p. model. It is therefore possible that this experiment may not have worked for technical reasons. This will be addressed in future experiments in this laboratory.

Complete passive protection was observed in the i.p. model with HI Ab administered either before and after infection. Therefore, the role of Ab in the i.p. model was further investigated using B6.μMT-/- mice, compared to B6.WT mice to determine whether Ab is critically important in the normal immune response to WNV infection. As expected, it was

found that B6.μMT-/- mice were highly susceptible to WNV infection, with 100% mortality within 6-9 days p.i., compared to B6.WT (Figure 7.9). A similar result was found by Liu and Chambers (2001) in YF virus infection and by Beland *et al.* (1999) in HSV encephalomyelitis. On day 9 p.i., many neurones had degenerated in the hippocampus (Figure 7.10 c and d). At this timepoint, WNV Ag was observed throughout the brain parenchyma. Extremely high neuronal infection was observed both in the brain and spinal cord (Figure 7.11), suggesting that Ab plays an important role in restricting WNV spread in *in vivo*. This can be acquired either via passive transfer of HI serum or monoclonal Ab (Matthews *et al.* 2001; Levine *et al.* 1991; Dietzschold *et al.* 1992) or local production of Ab in the CNS (Tyor & Griffin 1993; Hatalski *et al.* 1998). However, depending on the route of infection, Ab may not be enough to control WNV infection of the CNS.

In conclusion, complete protection via passive transfer of HI serum was observed only in the i.p. model. In contrast, in the i.n. model, the same dose of HI serum as given to the naïve mice in the i.p. model, failed to protect mice from lethal WNV encephalitis. Extensive brain infection was observed in these mice, similar to the normal serum-treated or untreated mice. Very high dose HI serum was required to extend survival in the i.n. model, however, even this was still unable to protect the majority of mice, although a few survived, at least until day 14 p.i., when they were sacrificed. Some of the surviving mice in this model exihibited paralysis. In normal serum-treated mice, WNV used the olfactory route to enter the brain. But HI serum-treated moribund mice, on day 8 p.i. showed no infection of OB and very little neuronal infection in the front cortex. More interestingly, WNV Ag was detected in the spinal cords of surviving mice on day 11 and day 13 p.i. These data indicate that mortality, as well as disease profile, can be changed in the presence of high dose HI serum in the i.n. model. In the i.n. model, the adoptive transfer of HI splenocytes also completely failed to protect mice. B cell-deficient mice were highly susceptible to WNV infection. Extensive neuronal infection and extensive neuronal degeneration occurred in the absence of Ab. Taken together, these data show that Ab plays an important role in protecting mice from WNV infection. In the absence of functional Ab, the CNS is highly vulnerable to the uncontrolled spread of WNV infection, which leads to death.

Chapter-8

General Discussion

WNV encephalitis is one of the emerging mosquito-borne flaviviral diseases in the new world. Periodically, unusal epidemic outbreaks of WNV encephalitis occur in the world with high morbidity and mortality. Although WNV has been isolated since 1937 (Smithburn *et al.* 1940), little is known about the pathogenesis of encephalitis caused by this virus. Most of the previous work with flaviviruses has been done in neonatal or young mouse models. Encephalitis develops more readily and is more severe in young mice due to the immature immune system and less completely developed BBB. Therefore, an adult murine model was developed in this project to understand better the mechanisms of pathogenesis of WNV encephalitis in adult mice. The results reported in this thesis highlight the role of IFN-γ in survival and development of disease in WNV encephalitis acquired by peripheral routes. A plausible antiviral role for microglia was also observed in this study. In addition, the role of immune Ab in protecting mice against disease was clearly found to depend on the route of original infection. A summary of the pathogenesis of disease in i.p. and i.n. models is presented in figure 8.1 and 8.2, respectively.

8.1. Pathogenesis of WNV encephalitis after i.p. inoculation

8.1.1. WNV encephalitis is an immunopathological disease

IFN-γ is produced predominantly by T cells and NK cells (Harty 2000; Salazar-Mather *et al.* 2000; Christensen *et al.* 1999) and is one of the most important cytokines regulating immune and inflammatory events (Benveniste 1998; Boehm *et al.* 1997). It inhibits viral replication, either directly (Kohonen-Corish *et al.* 1990) or by activating other antiviral defences, including those mediated by CTL, NK cells and macrophages (Billiau 1996; Munoz-Fernandez & Fresno 1998). Thus, it plays an important role in the generation of immunity in a number of viral infections (Nansen *et al.* 1998; Huang *et al.* 1993; Bouley *et al.* 1995; Karupiah *et al.* 1990). Data presented in this thesis clearly demonstrate that IFN-γ is not required for survival or generation of immunity against WNV infection after i.p.

inoculation. On the contrary, genetic absence of IFN-γ significantly reduced mortality from WNV encephalitis (see figure 3.2). Therefore, this data indicates a role for IFN-γ in the generation of immune-mediated pathology or immunopathology leading to death from WNV encephalitis.

The incidence of flaviviral encephalitis remains a serious health problem in the tropical and subtropical areas of the world. These viruses predominantly infect neurones in the brain. They either directly kill or damage neurones (Despres *et al.* 1998; Hase *et al.* 1990) or infection is accompanied by a vigorous immune response within the CNS which in itself causes severe damage to the host (Andrews *et al.* 1999; Zinkernagel 1992). The presence of the BBB, which normally prevents entry of protein and limits entry of immune cells to that of activated T cells (Hickey *et al.* 1991), the low or absent expression of MHC molecules and the nonreplacable nature of neurones, make the CNS a unique organ system for the study of immunopathogenesis (Griffin *et al.* 1992). The mechanisms involved in causation of immunopathology in viral encephalitis include immune cytolysis, delayed-type hypersensitivity reactions, formation of immune complexes and autoimmune reactions. These result in lysis of infected cells, necrosis, demyelination, tissue destruction, haemorrhage and functional alteration of CNS resident cells, especially neurones (Lohler 1988).

Lymphocytic choriomeningitis has been extensively studied as an animal model of virus-induced immunopathological disease (Zinkernagel 1999). In this model, severe inflammation, mediated especially by MHC-I-restricted $CD8^+$ T cells, results in an acute neurological disease leading to death, which can be prevented by depletion of $CD8^+$ T cells (Doherty & Zinkernagel 1974). In contrast, in Borna disease, MHC-II restricted $CD4^+$ T cells cause neurological disease in the rat model. The adoptive transfer of the MHC-II restricted T cell line NM1, specific for Borna disease virus, can also result in a progressive meningoencephlomyelitis (Richt *et al.* 1989). Although pathology was associated with severe inflammation in these models, none could satisfactorily explain the exact cause of death. In LCMV infection, despite severe infiltration of T cells in meninges, ependyma and choroid plexus, only a low level of cell damage could be seen in these areas under both light and electron microscopy. This was not thought to be enough to explain the cause of death (reviewed by Lohler 1988). In addition to these areas, $CD8^+$ T cells were also detected in

the brainstem and cervical spinal cord in this model, but the absence of significant neuronal destruction or degeneration makes it hard to believe that CTL lysis is the cause of death in LCMV infection (reviewed by Lohler 1988). Besides cytolysis, $CD8^+$ T cells can also exert antiviral functions via secretion of IFN-γ (Harty *et al.* 2000; Klavinskis *et al.* 1989). Increasing evidence suggests that in the absence of IFN-γ, $CD8^+$ T cells can not clear virus, despite their potent CTL activity in LCMV infection (Bartholdy *et al.* 2000; Von Herrath *et al.* 1997). Furthermore, it has been reported that treatment of mice with sheep anti-IFN-γ protected mice from fatal LCMV infection, despite enhanced virus replication in the CNS (Leist *et al.* 1989). Therefore, it can be argued that generation of immunopathology by $CD8^+$ T cells in LCMV infection, as well as virus clearance, may be mediated via increased secretion of IFN-γ.

The disease-promoting role of IFN-γ emerged from work in MS in the 1980s, when IFN-γ was used as a therapeutic agent for MS. MS is a chronic inflammatory neurological disease of humans, characterized by infiltration of leukocytes into the CNS with localized myelin destruction and loss of oligodendrocytes and axons (Al-Omaishi *et al.* 1999). A small clinical trial using IFN-γ for treating MS patients showed a worsening of disease after administration of IFN-γ in these patients (Popko *et al.* 1997). This study opened the door to the further understanding of the role of IFN-γ in disease progression. Detection of increased numbers of IFN-γ-secreting T cells in the CSF of MS patients and IFN-γ in *postmortem* samples (Billiau 1996) further provided evidence for the involvement of IFN-γ in the progress of disease. Moreover, adoptive transfer of IFN-γ-secreting T cells isolated from animals affected by EAE, induced EAE in the adoptive host animals. In EAE also, increased numbers of IFN-γ-secreting T cells were observed in the CNS shortly before the onset of clinical signs. These signs could be inhibited by treatment with anti-IFN-γ Ab (Olsson 1995).

The role of IFN-γ in MS and EAE clearly suggests that IFN-γ can also play an immunopathological role in viral encephalitis. In the CNS, the source of IFN-γ seems almost exclusively to depend upon infiltrating T cells (Binder & Griffin 2001; Hammarberg *et al.* 2000; Finke *et al.* 1995; Cantin *et al.* 1995; Krakowski & Owens 1996), although CNS resident cells are also capable of producing IFN-γ upon stimulation (Mori *et al.* 2001;

Morris & Esiri 1998). Since T cells generally do not enter into the CNS due to the presence of the BBB, IFN-γ is generally not present in the normal CNS. However, during CNS infection and neurological disorders, increased numbers of these cells immigrate into the CNS and produce large amounts of IFN-γ there. In this manner CNS resident cells are exposed to the potent effect of IFN-γ. Moreover, IFN-γ plays a key role in leukocyte recruitment into the CNS (Liu & Chambers 2001; Baumgarth & Kelso 1996) by inducing several different chemokines (Simpson *et al.* 2000; McManus *et al.* 2000; Liu *et al.* 2001; Boehm *et al.* 1997). They are synthesized locally at sites of inflammation by different cell populations, including leukocytes, endothelial cells and CNS resident cells and may be located at or near the endothelial surface in association with other molecules to establish a concentration gradient. Leukocytes then transmigrate into the CNS in a concentration-dependent manner (Boehm *et al.* 1997).

The data presented in this thesis demonstrate that in WNV encephalitis significant numbers of leukocytes infiltrate into the brain parenchyma of wild type mice, compared to IFN-γ–deficient mice. Thus there was approximately 4-fold difference in the number of infiltrating leukocytes in the brain parenchyma on day 7 p.i. between the groups (see figure 3.10). This finding correlated with disease outcome in wild type mice. Significantly higher mortality occurred in wild type mice compared to IFN-γ-deficient mice (see figure 3.2), despite there being no significant difference in the number of neurones infected (see figure 3.9) or virus titres (see figure 3.8) in the brain between the strains. These data indicate that the cause of death in adult mice is not due to WNV by itself in this model. The paucity of significant neuronal death, despite high leukocyte infiltration in the brain parenchyma of wild type mice (see chapter 4), makes death mediated by $CD8^+$ T cells via cytolysis unlikely. Therefore, it seems likely that the cause of death in wild type mice was attributable to infiltrating T cells via increased secretion of IFN-γ. However, which subset of leukocytes is linked to this in immunopathogenesis is not yet clear.

Although chemokines play an important role in guiding leukocyte migration towards the site of inflammation, the process of transmigration is thought to begin with activation of endothelial cells. Endothelial cells are activated by proinflammatory cytokines leading to increased expression of CAM such as selectins and the immunoglobulin superfamily CAM

(Meager 1999; Imhof & Dunon 1995). Strong adhesion to the endothelial cells is required for extravasation of circulating leukocytes. Therefore, phenotypic alteration in the neurovascular endothelial cells with expression of CAM is required for extravasation. Selectins are involved in initial attachment and rolling of leukocytes along the vessel wall, whereas ICAM-1 and VCAM-1 provide firm adhesion by interacting with leukocyte integrins, LFA-1 and VLA-4, respectively. These integrins are constitutively expressed on the surface of leukocytes. Therefore, expression of ICAM-1 and VCAM-1 on the neurovascular endothelium is crucial for transmigration of leukocytes into the CNS parenchyma. These molecules are absent or expressed at low levels under normal conditions (Matyszak 1998). However, they are induced and upregulated during inflammation to recruit inflammatory leukocytes into the CNS. This initiates a cascade of inflammation in the CNS (Irani & Griffin 1996; Engelhardt *et al.* 1994; Lassmann 1997).

It has been shown that IFN-γ is responsible for induction of these molecules in both *in vivo* and *in vitro* culture systems (Deckert-Schluter et al 1999; Zielasek *et al.* 1993; Lee *et al.* 1999; Campbell *et al.* 1989). However, data presented in this thesis show that upregulation of ICAM-1 and VCAM-1 in WNV encephalitis is independent of IFN-γ. Besides IFN-γ, other cytokines, *eg.*, IL-1α/β, TNF and IL-4 can also induce upregulated expression of these molecules (Meager 1999; Shen *et al.* 1997; Mickelson *et al.* 1995; Wong & Dorovini-Zis 1992; Fabry *et al.* 1992; Masinovsky *et al.* 1990). It is likely that one or more of these cytokines is responsible for the induction of high levels of ICAM-1 and VCAM-1 in IFN-γ-deficient mice in WNV encephalitis.

It has been suggested that low levels of ICAM-1 and VCAM-1 expression are sufficient to recruit leukocytes into the CNS of IFN-γ-deficient mice (Deckert-Schluter et al 1999). Increased expression of these molecules increases the avidity of cell-cell interactions and subsequent migration (Bochner *et al.* 1991; Shimizu *et al.* 1991). However, data presented in this thesis show that despite extremely high expression of ICAM-1 and VCAM-1 in IFN-γ-deficient mice compared to wild type mice (see chapter 5), significantly lower numbers of leukocytes were observed to infiltrate into the brain in WNV encephalitis in IFN-γ-deficient mice (see chapter 3). Greater upregulation of these molecules was not sufficient in itself to enable the migration of large numbers of leukocytes into the brain parenchyma of IFN-γ-

deficient mice. This suggests that recruitment of greater numbers of inflammatory cells into the brain parenchyma may require IFN-γ-induced chemokines, in addition to increased ICAM-1 and VCAM-1 expression. The data also show that in addition to increased endothelial cell expression, increased levels of ICAM-1 was also observed on the microglia in the absence of IFN-γ. The actual role of ICAM-1 expression in glial cells has not been elucidated, however, it is assumed that they may involved in guiding infiltrating leukocytes into and through the CNS parenchyma (Merrill & Benveniste 1996). They are also involved in neuronal degeneration (Dallasta *et al.* 2000). However, the absence of neuronal degeneration in IFN-γ-deficient mice, despite high microglial ICAM-1 expression suggests there may be some other role for this molecule on microglia in WNV encephalitis. More detailed investigation is required to address these issues.

The mechanism by which IFN-γ exacerbates disease in MS and EAE is still unresolved. It is thought to be associated with demyelination occurring with the death of oligodendrocytes due to the cytotoxic effects of activating macrophage/microglia. This decreases demyelination and axonal necrosis in MS and EAE (Popko *et al.* 1997). IFN-γ is a potent inducer of IDO and NOS2 (Karupiah *et al.* 1993; Takikawa *et al.* 1990) and can contribute to immunopathology by inducing these molecules within the CNS (Maloney *et al.* 2000; Lane *et al.* 1999). For example, increased induction of IDO can significantly decrease the levels of tryptophan within the CNS, which is highly correlated with serotonin. Serotonin is a neurotransmitter; decreases in tryptophan levels can significantly alter CNS function and lead to death (Maloney *et al.* 2000). IDO expression was evaluated in this project to determine whether IFN-γ contributes to immunopathology via induction of IDO in the brain parenchyma. This study showed that expression of IDO was hardly detectable within the CNS in wild type mice (data not shown). This suggests that the immunopathological role of IFN-γ via the induction of IDO is unlikely in WNV encephalitis. Alternatively, NOS2 may be involved in the progression of disease via the production of reactive nitrogen species such as NO in WNV encephalitis. NOS2 associated with the progression of disease in many other neurotropic viral infections (Rose *et al.* 1998; Lane *et al.* 1999; Andrews *et al.* 1999). In these models, neutralization of NOS2 by aminoguanidine significantly reduced mortality and disease. Therefore, an experiment was set up to neutralize NOS2 using aminoguanidine in wild type mice. Aminoguanidine is a selective inhibitor of NOS2 (reviewed in Cross *et al.* 1994). This study showed that there was no difference in mortality between

aminoguanidine-treated and untreated animals (data not shown), suggesting that progression of disease by IFN-γ via induction of NOS2 is also unlikely. Due to the lack of significant IDO induction, neuronal death as well as negligible role of NOS2 in these mice, alteration in vital functions of neurones mediated by IFN-γ may be the only other alternative to explain the cause of such a fatal disease in WNV encephalitis. However, how IFN-γ may be involved in altering neuronal function or how it exerts its action in the CNS in WNV encephalitis is not resolved.

8.1.2. Is a clearance of WNV from brain mediated via microglia?

Mice deficient in IFN-γ exhibit increased neuronal infection in many neurotropic viral infections, suggesting a role for IFN-γ in termination of both acute and persistent infection in the CNS (Bartholdy *et al.* 2000; Christensen *et al.* 1999; Geiger *et al.* 1997; Lewandowski *et al.* 1998; Tishon *et al.* 1995). However, data presented in this thesis show that clearance of WNV from the CNS is independent of IFN-γ (see chapter 3). WNV was cleared from the brain parenchyma in the complete absence of IFN-γ, although a greater percentage of IFN-γ-deficient mice had neuronal infection compared to wild type mice (see figure 3.7). It is therefore possible that CNS resident cells, in particular astrocytes and microglia participate in controlling viral infection in the CNS in an IFN-γ-independent manner..

Microglia and astrocytes are important glial cells which provide physical and metabolic support, as well as protection of neurones from subtle changes in the CNS environment, thus helping to maintain neuronal function (Afifi & Bergman 1998). These glial cells also respond to various infectious and inflammatory stimuli by producing a range of different cytokines, chemokines, cytotoxic metabolites and growth factors, as well as upregulating or expressing *de novo* various immune receptor molecules. These molecules enable immune function in conjunction with the peripheral immune system within the CNS (Chao *et al.* 1994; Merrill *et al.* 1996; Brodie *et al.* 1997; Dallasta *et al.* 2000; Glabinski *et al.* 1999; Grzybicki *et al.* 1997; Benveniste 1992; Schijns *et al.* 1991; Persidsky *et al.* 1999; Sauder *et al.* 2000; Asensio *et al.* 1999). Thus, these cells are regarded as immunocompetent cells of the CNS, able themselves to mount immune responses.

Astrocyte activation, astrogliosis, has been demonstrated in many viral infections both *in vivo* and *in vitro* (Weissenbock *et al.* 2000; Schoneboom *et al.* 1999; Bi *et al.* 1995; Chen *et al.* 2000; Liu *et al.* 1989; Medana *et al.* 1996) and is thought to be mediated by IFN-γ (Balasingam *et al.* 1994; Yong *et al.* 1991). Data from this project show that in WNV encephalitis astrocytes were very rarely activated in either group of mice. Thus the presence or absence of IFN-γ neither induced astroglial activation nor reduced its activation (see chapter 4). These data indicate that astrocytes do not usually play a role in WNV encephalitis.

Although astrocytes act as immunocompetent cells of the CNS, immune defence within the CNS is predominantly provided by microglia (Cross & Woodroofe 2001; Mori *et al.* 2001; Chao *et al.* 1994). Therefore, microglia are seen as the first line of defence in the CNS in inflammation, infectious diseases, brain tumors, neurodegeneration, etc., (Kreutzberg 1996). Once activated, they can destroy invading microorganisms, remove cell debris, as well as enhance neuronal survival by secreting many different neurotrophic factors. They thus facilitate a return to normal tissue homeostasis (Kreutzberg 1996, Nakajima & Kohsaka 1998). Microglia in the normal adult brain display ramified morphology with small somata and numerous thin processes (Ling & Wong 1993) and in the resting state either do not express or express low levels of immune molecules (Streit *et al.* 1999; Raivich *et al.* 1999). Microglia are of monocyte origin and exhibit macrophage-like activity upon activation (Davis *et al.* 1994). Activation occurs in a graded fashion, as seen by the alteration of morphology from resting to activated and then reactive forms. Activated microglia have large cell bodies with shorter, stouter processes and are non-phagocytic, whereas reactive microglia no longer display any processes and exhibit a pleomorphic morphology, commonly including spherical and rod shapes. Reactive microglia are also known as amoeboid microglia and are phagocytic in nature (Raivich et al. 1999; Streit *et al.* 1999). Reactive microglia are involved in the formation of nodules which is a prominent feature of viral encephalitis (Dickson *et al.* 1991).

There are several schools of thought about microglial activation. One suggests that microglial activation is mediated by stressed neurones (Sudo *et al.* 1998). Another proposes their activation is mediated by IFN-γ (Grau *et al.* 1997; Meda *et al.* 1995; Sethna *et al.* 1991) or infiltrating leukocytes (Langford & Masiah 2001; Gehrmann *et al.* 1993, Aloisi *et*

al. 2000; Sedgwick *et al.* 1998; Bauer *et al.* 1995). Data from this project show that microglia were highly activated in both WNV-infected wild type and IFN-γ-deficient mice, displaying both activated and amoeboid morphology in both strains (see chapter 4). Thus, this study indicates that microglial activation can be independent of IFN-γ. The data presented in this thesis also show that infiltration of leukocytes was observed 48h before activation of microglia (Figure 4.4). It is possible therefore, that their activation may have been mediated by these infiltrating leukocytes. However, data from mice inoculated i.n. with WNV demonstrated that microglia were activated 48h before infiltration of leukocytes in the brain (see chapter 4 and 6), indicating that microglial activation is independent of infiltrating leukocytes in the CNS in WNV encephalitis. Indeed, it could be argued that in the i.p. model leukocyte infiltration delayed microglial activation, although it may enhance activation in other models (Aloisi *et al.* 2000).

The facial-nerve transection model shows that microglia activate in response to stressed neurones (Kreutzberg 1996). The data presented in this thesis show that microglia were activated within 24h of WNV Ag detection in the brain parenchyma only at or near the sites of demonstrable neuronal infection in both groups of mice in the i.p. model. The number of activated microglia subsequently increased showing various morphologies, as well as nodule formation. The numbers of activated microglia declined and their morphology returned to the resting ramified state after WNV Ag was undetectable in the brain parenchyma in both groups of mice (see chapter 4). Thus, these data strongly suggest that microglial activation was induced by infected neurones and that these cells may be involved in clearing WNV from neurones. The appearance of increased numbers of microglial nodules with little evidence of neuronal death (see chapter 4) also indicates that the presence of microglial nodules does not equate with neuronal death.

Recently, the antiviral capcity of microglia has been demonstrated in viral infection in an *in vitro* culture system (Cheeran *et al.* 2001). These microglia were found to produce antiviral cytokines like TNF, soon after CMV infection. These cells were able to control infection of astrocytes when co-cultured *in vitro*. In addition to this, microglia have also been shown to produce other potent antiviral cytokines like IFN-α and espress their receptors (Yamada *et al.* 1994; Akiyama *et al.* 1994; Yamada & Yamanaka 1995). These antiviral cytokines can dramatically reduce viral gene expression in the CNS (Akwa et al 1998; Carr *et al.* 1998;

Schijns *et al.* 1991). Although, a cytokine study was not done in this project, it can be postulated that such high numbers of activated microglia would produce one or more antiviral cytokines in WNV encephalitis and thus may help to clear WNV from the infected neurones. Besides the production of antiviral cytokines, activated microglia can upregulate *de novo* expression of FcR and CR3 receptors on their surface (Nakajima & Kohsaka 1998). Thus, they might be involved in controlling WNV in conjunction with antibody produced locally by infiltrating leukocytes in the brain via non-cytotoxic mechanisms. Further study of microglia in these systems will help us to understand better the role of microglia in controlling WNV in the CNS.

Data presented in this thesis show that more than 85% of surviving mice from both groups showed significantly high microglial activation in the absence of neuronal degeneration. Therefore, although microglia have been reported to be cytotoxic in the CNS (Banati *et al.* 1993), data from this thesis do not support such a role in WNV encephalitis. On the contrary, activated microglia may have a protective role. They can produce several different kinds of neurotrophic growth factors, including NGF, BDNF, basic fibroblast growth factor, thrombospondin, plasminogen, IL-6, IL-1, IL-1β, TGF-β and IL-3, etc,. These molecules are involved in survival, regulation and regeneration of neurones as well as remyelination (Soontornniyomkikj *et al.* 1998; Chamak *et al.* 1994; Mason *et al.* 2001; Hama *et al.* 1989; Kamegai *et al.* 1990; Frei *et al.* 1989; Giulian *et al.* 1994; Pratt & McPherson 1997; Elkabes *et al.* 1996; Mallat *et al.* 1989; Shimojo *et al.* 1991; Nakajima *et al.* 1992). A possible protective role for microglia is supported by the ischaemic lesion model in CSF-1-deficient mice. CSF-1 acts as a potent mitogen for microglia and its absence resulted in abnormal microglial activation, associated with increased neuronal susceptibility to ischaemia (Berezovskaya *et al.* 1995).

In the CNS, microglia represent the local APC (Shrikant 1996), although MHC-II is normally absent or expressed at low levels on these cells (Griffin *et al.* 1992). The induction of MHC-II is required to present Ag to $CD4^+$ T cells. Similar to MHC-II induction in peripheral cells, IFN-γ is also a potent inducer of MHC-II in microglia (Deckert-Schluter *et al.* 1999; Pazmany *et al.* 2000; Aloisi *et al.* 1998) and increased expression in microglia has been observed in many neurological disorders and encephalitic models (Bo *et al.* 1994; Song & Jia 1999; Schmitt *et al.* 1998; Morioka *et al.* 1992; Caplazi & Ehrensperger 1998;

Figure: 8.1 Kinetics of WNV antigen detection, microglial activation and leukocyte infiltration in the i.p. model in B6.WT mice. WNV antigen (open arrows) in the neurones was first detected in the brainstem parenchyma on day 6 p.i. (a) with infiltrating leukocytes (k) (open arrow). No microglial activation was observed at this timepoint (f). Microglial activation (open arrows) was detected within 24h of neuronal infection, *i.e.,* from day 7 p.i., with the formation of small nodules (solid arrows) (g). The number of infected neurones was increased (b) (open arrows) followed by increased leukocyte infiltration (l) (open arrows) at this timepoint. On day 11 p.i., very few infected neurones were detected (c) (open arrow) with significantly reduced leukocytes (m) (open arrows) (solid arrows show microglial nodules). At this timepoint microglia were still highly activated (h) (solid arrows). The morphology of activated microglia reverted almost to the ramified state (i) (open arrows) after WNV antigen was undetectable (d) in the brain parenchyma on day 15 p.i. Only the occasional leukocyte was detected at this timepoint (n), Some rod shaped microglia can be seen in H and E stained brain sections (n) (solid arrows). These stained faintly with GS-lectin (i). On day 30 p.i. activated microglia had completely reverted to the normal ramified state (j). At this timepoint no WNV antigen (e) and leucocytes (o) were detected. Scale bar = 40μm for all pictures.

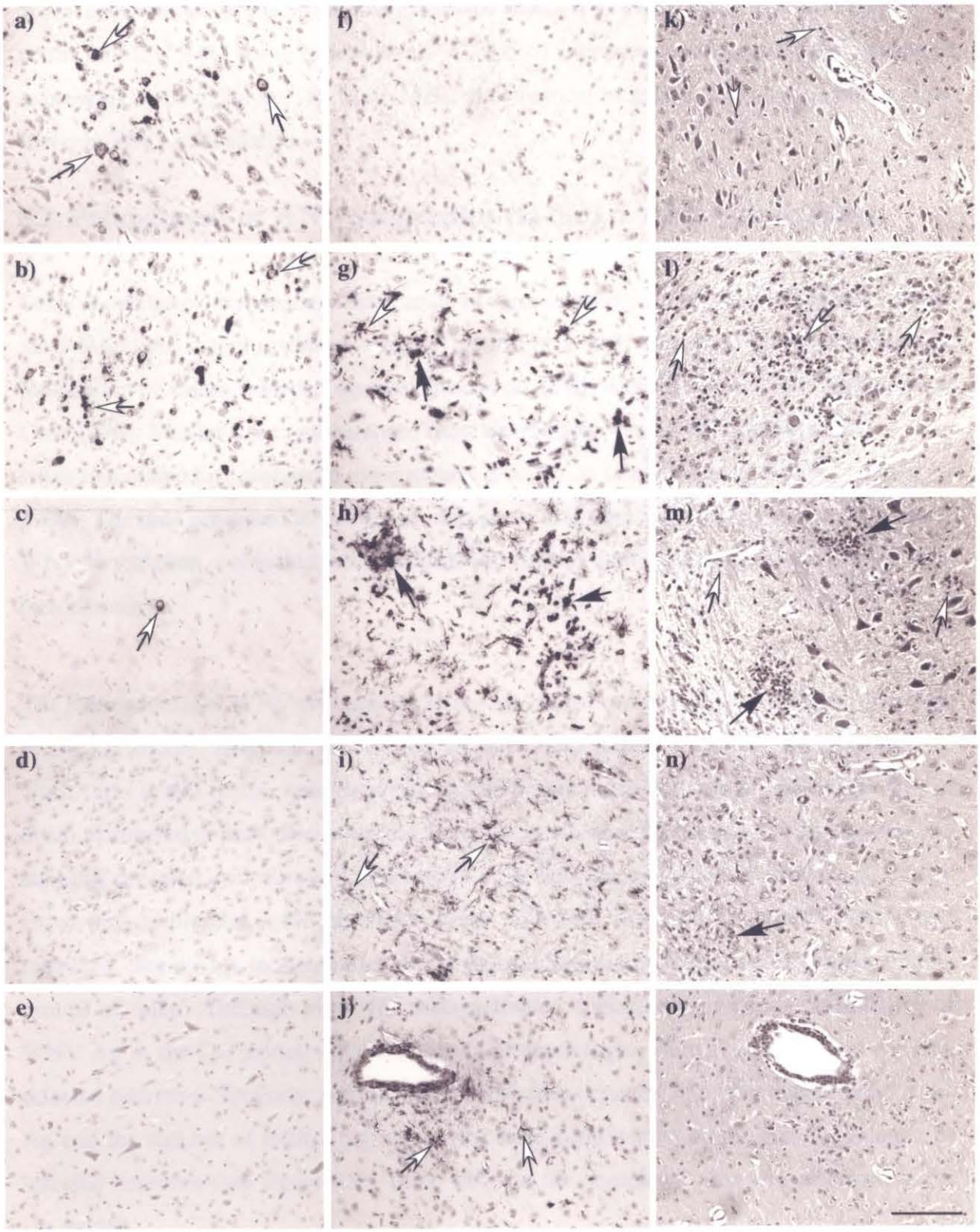
Anti-WNV stain
GS-lectin stain
H & E stain
a)
f)
k)
b)
g)
l)
c)
h)
m)
d)
i)
n)
e)
j)
o)

Gehrmann *et al.* 1993). Data presented in this thesis show that despite full activation in WNV encephalitis, not all microglia expressed MHC-II in either group and the presence or absence of IFN-γ did not influence levels of MHC-II expression or the numbers of microglia expressing it (see chapter 4). Thus MHC-II induction in microglia is not dependent on IFN-γ in WNV encephalitis.

8.2. Pathogenesis of WNV encephalitis via the i.n. route of inoculation

Disease outcome often depends upon route of virus inoculation into the host. In neurotropic viral infections i.c. inoculation usually results in a fatal outcome, whereas peripheral inoculation produces sublethal disease (Hase *et al.* 1990; Richards *et al.* 1981; Nathanson & Cole 1970). Similar to i.c. inoculation, most neurotropic viruses also produce fatal disease when inoculated i.n., compared to peripheral inoculation (Carbone *et al.* 1987; Thach *et al.* 2000). The data presented in this thesis also show that mice were highly susceptible to i.n. WNV inoculation, compared to i.p. inoculation in both wild type and IFN-γ-deficient mice (see chapter 6).

The pathogenesis of WNV encephalitis in the i.n. model was completely different from that of the i.p. model. After i.n. inoculation all mice died within 7 days p.i. (see figure 6.1). Virus titres in this model were nearly 5 log-fold higher in both groups of mice at the time of death, compared to peak titres detected in the i.p. model (see figure 6.2). Immunoperoxidase staining revealed widespread brain infection in both groups of mice in the i.n. model. However, despite far more extensive brain infection, than the i.p. model, WNV was restricted, like the i.p. model, only to the cytoplasm and major dendrites of neurones in both groups of mice. Although microglia were activated concurrently with the appearance of WNV Ag in the i.n. model, numbers of activated microglia were significantly fewer than infected neurones. Similarly, infiltration of leukocytes occurred 48h after detection of WNV Ag and the number of infiltrating leukocytes were significantly fewer than the number of infected neurones (see figure 6.9). Thus, this was the reverse of what was observed in the i.p. model.

In the i.n. route of inoculation, WNV replicated very quickly in the brain, presumably before the development of an effective peripheral immune response could control it. These

Figure: 8.2 Kinetics of WNV antigen detection and microglial activation in the i.n. model in B6.WT mice. WNV antigen was first detected in the outermost layer of olfactory bulb (OB) neurones on day 3 p.i. (a) (open arrows) with concurrent activation of microglia at the site of neuronal infection (e) (open arrows). The number of infected neurones increased on day 5 p.i. (b) (open arrows) with concommitantly increased microglial activation (f) (open arrows). At this timepoint, both WNV antigen and activated microglia were observed in other areas of the (OB). On day 6 p.i. the number of infected neurones increased significantly (c) (open arrows) followed by high microglial activation (g) (open arrows). At the time of death, on day 7 p.i, almost all neurones were infected in the OB (d) (open arrows) with massive microglial activation, predominantly of the phagocytic form (h) (open arrows). Scale bar = 200μm for all pictures.

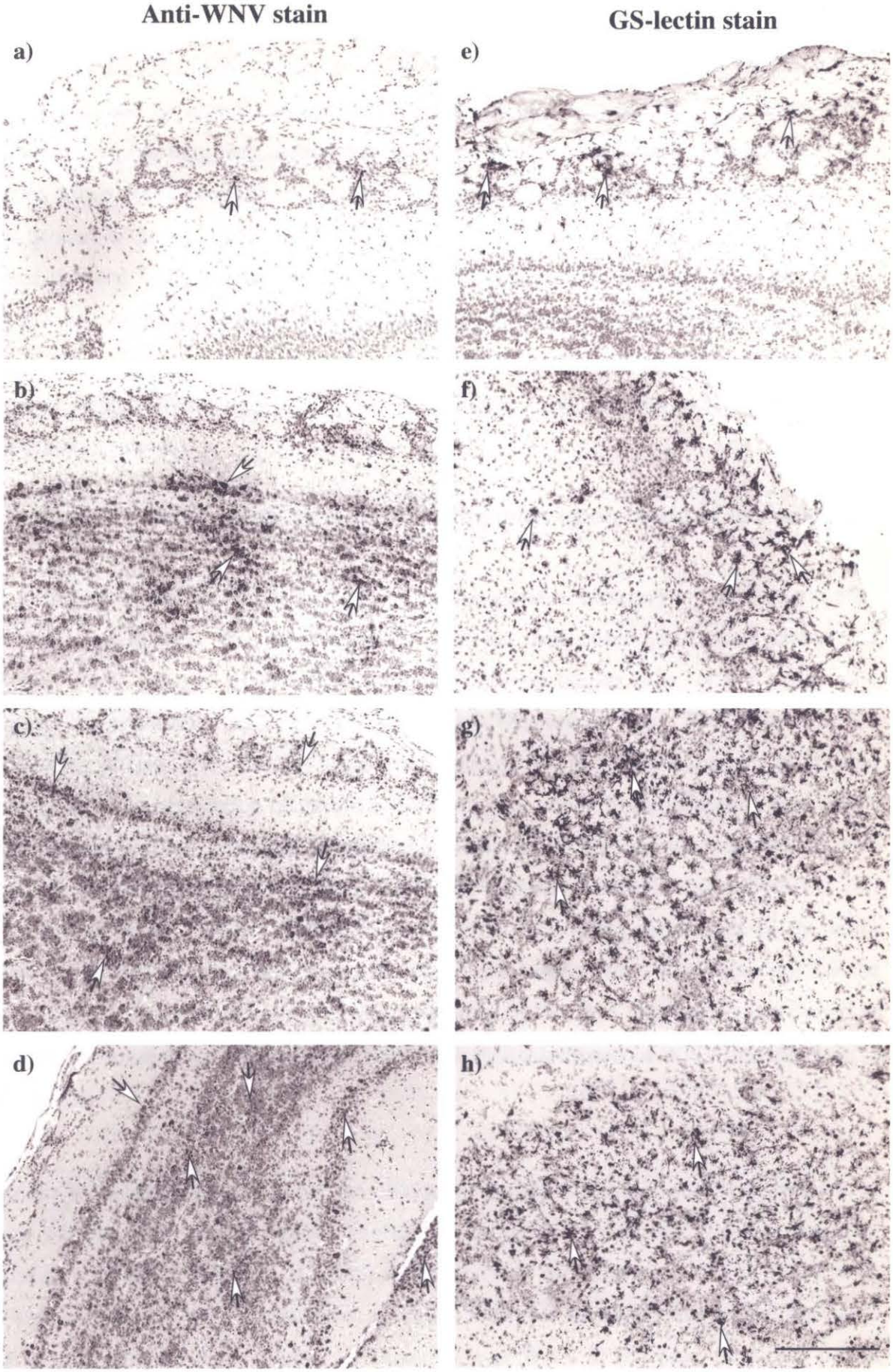
Anti-WNV stain
GS-lectin stain
a)
b)
c)
d)
e)
f)
g)
h)

data suggest that extensive neuronal infection causes death in both groups of mice and that, unlike the i.p. model, IFN-γ is not involved in the progression of disease in the i.n. model. In the absence of significant neuronal degeneration, despite extremely high WNV replication in the neurones, death may be associated with neuronal dysfunction in this model. Since 100% mortality occurred in the i.n. model with the chosen i.p. dose, WNV was titrated in the i.n. model to determine the sublethal dose in both strains of mice. It was found that the fatality was dose-dependent. Mortalities of 85% in B6.WT and 65% in B6.IFN-γ-/- mice occurred with 100 pfu/mouse (see figure 7.1). This data further confirmed that WNV is highly neurotropic in mice when inoculated i.n. The surviving mice in both groups, when rechallenged with a 600-fold higher dose than the original dose, were completely protected.

8.3. Portal of WNV entry into the CNS depends upon route of inoculation

Neurotropic viruses can invade the CNS by haematogenous, olfactory or neural routes after peripheral inoculation. The haematogenous route has been observed in many neurotropic viruses. These viruses either infect neurovascular endothelial cells, or are transported through the endothelial cells without replication (Wisniewski *et al.* 1983; Coffin & Lu 1957; Liou & Hsu 1998). Some viruses get access into the brain via diapedesis of infected leukocytes or by destruction of the BBB (Dallasta *et al.* 1999; Soilu-Hanninen *et al.* 1994; Johnson 1964). Data presented in this thesis show that WNV Ag was detected in brain neurones in the presence of an intact BBB and without neurovascular endothelial cell infection in the i.p. model. Similarly, none of the infiltrating leukocytes in the brain parenchyma was infected (see chapter 3). These data suggest that WNV does not use the haemtogenous route to invade CNS. Further studies by electron microscopy is required to exclude the possibility of neurovascular transendothelial transport of WNV into the brain in this model.

Besides the haematogenous route, the olfactory neuroepithelium is obviously a portal of entry into the CNS after peripheral inoculation in several neurotropic viruses, including some flaviviruses (Monath *et al.* 1983; Albrecht 1962; McMinn *et al.* 1996; Vogel *et al.* 1996; Charles *et al.* 1995; Reinacher *et al.* 1983). However, data from this project also show that the OB was not infected after i.p. inoculation of WNV at any time during the period

investigated. Therefore, WNV entry into the CNS via olfactory route seems unlikely (see chapter 3).

Some neurotropic viruses, like rabies, human poliovirus and Borna disease virus, use pheripheral nerves as a route of CNS invasion from the periphery (Tang *et al.* 1999; Murphy *et al.* 1973; Nathanson & Bodian 1961; Carbone *et al.* 1987). These viruses replicate within nerves and are moved through the host via axonal transport. Data presented in this thesis show that WNV Ag was first detectable in the spinal cord motor neurones 24h before it was detected in the brainstem (see figure 3.4 and 3.6). Since these data were derived from an adult mouse model, another experiment was set up using 3-week-old mice to confirm these results. Interestingly, this study also showed a similar pattern of WNV Ag detection to that observed in the adult model (see figure 3.5). Specimens from *postmortem* human cases also revealed WNV Ag in the brainstem and spinal cords (Shieh *et al.* 2000). These data strongly suggest that WNV infects the spinal cord via retrograde axonal transport along motor nerves supplied by infected striated muscle after i.p. inoculation, and then invade brain parenchyma via transneuronal pathways. This study also shows that there was no difference in the route of CNS invasion in both wild type and IFN-γ-deficient mice, indicating that IFN-γ does not alter the route of CNS invasion.

Similarly, neurotropic viruses can also invade the CNS by different routes after i.n. inoculation. In i.n. inoculation, viruses are introduced into the nasal cavity, which is innervated by both olfactory and trigeminal nerves (reviewed in Barnett & Perlman 1993). The receptor neurones of the neuroepithelium of the nasal cavity send axons to the brain where they first synapse with neurones of the OB. Many viruses use this route for brain invasion (Barnett & Perlman 1993; Plakhov *et al.* 1995; Charles *et al.* 1995). Some viruses use the trigeminal nerve. They infect the trigeminal ganglion initially, followed by anterograde transneuronal transfer to the spinal trigeminal nucleus (Perlman *et al.* 1989), with subsequent invasion of the rest of the brain. It has been also observed that some viruses use both olfactory and trigeminal routes (Esiri & Tomlinson 1984). In addition to these, viruses like pseudorabies use 3 different routes after i.n. inoculation to invade the CNS. These include the trigeminal, sympathetic and parasympathetic, but not olfactory routes to enter the brain (Babic *et al.* 1994). Data from this project show that WNV Ag was first detected only in the outermost layer of the OB (see figure 6.3 and 6.7) after i.n. inoculation

whereas no WNV Ag was detected in the cervical spinal cord and brainstem at this timepoint. After this WNV Ag was detected in other parts of the OB and brain proper, spreading in a rostral-to-caudal direction. Therefore these data strongly suggest that WNV uses the olfactory route to enter into the CNS after i.n. inoculation. Similar results have been found in other encephalitis models (Thach *et al.* 2000; Huneycutt *et al.* 1994; Barnett *et al.* 1993; Anderson *et al.* 1983). In conclusion, data presented in this thesis suggest that CNS involvement is influenced by the route of WNV inoculation and this determines the portal of entry into the CNS.

Although WNV uses the olfactory route as a portal of entry into the CNS in the i.n. model, this route can be altered. In the preliminary study reported here on passive transfer of high-dose HI serum 24h before i.n. infection resulted in a pattern of disease pathogenesis similar to the i.p. model (see chapter 7). Here, WNV Ag was not detected in the OB, although a few infected neurones were observed in the front cortex of moribund mice on day 8 p.i. Surviving mice on days 11 and 13 p.i. showed infection of motor neurones in the cervical and lumbar spinal cord, respectively. However, WNV Ag was not detected in the OB at this timepoint (see figure 7.8). Therefore, these data suggest that route of WNV entry into the CNS can be altered in the presence of high dose HI serum. However, how HI serum is involved is not known.

8.4. The role of antibody in WNV encephalitis induced by different routes of WNV inoculation

Although cell-mediated immunity makes a major contribution to controlling viral infections in the CNS (Binder & Kundig 1991; Binder & Griffin 2001; Christensen *et al.* 1999; Harty *et al.* 2000; Noske *et al.* 1998; Stohlman *et al.* 1998; Weidinger *et al.* 2000; Geiger *et al.* 1997), humoral immunity also plays an important role in neurotropic viral infections (Matthews *et al.* 2001; Wright & Buchmeier 1991; Griffin *et al.* 1997; Levine *et al.* 1991; Dietzschold *et al.* 1992; Kapoor *et al.* 1982). Circulating Ab, especially antiviral Ab, functions to terminate primary infection and reduce the level of viraemia. This reduces or prevents disease and acts as a basis for protection against viral reinfection. Ab can be acquired after primary infection or by passive administration of HI or monoclonal Ab. Circulating antiviral Ab includes both neutralizing and non-neutralizing Ab (Griffin *et al.*

1997). Neutralizing Ab plays an important role in controlling infectious virus spread, as well as clearing viral RNA from neurones (Levine *et al.* 1991; Dietzschold *et al.* 1992; McKendall *et al.* 1979; Byrnes *et al.* 2000). The role of Ab in neurotropic viral infection has been extensively studied using passive transfer of HI serum (Chiba *et al.* 1999; Kreil & Eibl 1997; Kimura-Kuroda & Yasui 1988; Wright & Buchmeier 1991).

In this project preliminary studies were undertaken to evaluate the role of Ab by using 2 approaches. These included passive transfer of HI serum in the i.p. and i.n. models and the use of μMT-/- mice. Mice surviving i.p. inoculation of WNV, when rechallenged with a 50-fold higher dose of WNV than the original dose showed no clinical or histopathological signs of encephalitis. Moreover, passive transfer of low-dose HI serum into naïve wild type mice 24h before or 48h after i.p. inoculation of WNV also resulted in the complete abrogation of encephalitis with 100% survival (see figure 7.6). These data indicate that passive transfer of HI serum can protect naive mice from IFN-γ-mediated immunopathological disease in WNV encephalitis. It has been similarly shown that passive transfer of monoclonal Ab one or two days before infection completely protected mice from lethal LCMV immunopathological disease (Wright & Buchmeier 1991).

Passive transfer of monoclonal Ab can inhibit rabies viral RNA after i.n. inoculation and thus protect rats completely from lethal rabies disease (Dietzschold *et al.* 1992). However, work presented here shows that passive transfer of the same dose of HI serum as that given in the i.p. model, into naïve mice before i.n. inoculation did not protect mice from lethal WNV encephalitis. Indeed, all mice died with extensive neuronal infection (see figure 7.5). Since it was possible that the amount of Ab given was not sufficient to protect from lethal WNV encephalitis in this model, a 750-fold higher dose of HI than the original was transferred passively into naïve mice 24h before i.n. infection. These mice survived longer compared to mice treated with low-dose HI serum, however only 13% mice survived until day 14 p.i. (see figure 7.6). Interestingly, mice surviving low-dose WNV i.n. inoculation, when rechallenged with a 600-fold higher dose of WNV than the original dose showed 100% survival. It has been suggested that adoptive transfer of immune splenic cells can protect naïve mice from lethal flaviviral encephalitis (Jacoby *et al.* 1980). Therefore, it was speculated that in the i.n. model, the protection may be mediated via T cells. Data presented in this thesis show that adoptive transfer of hyper-immune splenocytes, $5x10^7$ splenocytes

per mouse 24h before i.n. infection also completely failed to protect mice from lethal WNV encephalitis (see figure 7.7). These data raise the question that whether brain need to be pre-infected to become "immune" in the i.n. model. Further studies are required to address this question. In conclusion, data presented here indicate that the efficacy of passive protection depends upon the route of WNV inoculation.

Use of μMT-/- mice further emphasize the role of Ab in viral encephalitis. These mice are highly susceptible to neurotropic viral infections (Liu and Chambers 2001; Beland *et al.* 1999). The preliminary study in μMT-/- mice reported here also shows that these mice were highly susceptible to WNV infection, with 100% mortality by day 9 p.i., compared to wild type mice (see figure 7.9). This study showed an extremely high number of neurones to be infected throughout the brain parenchyma and cervical spinal cord at this timepoint, as well as extensive neuronal degeneration in the hippocampus (see figure 7.10 and 7.11). Therefore, Ab may play a role in WNV encephalitis by restricting WNV spread through the CNS, and by limiting the growth of virus in neurones, thereby protecting them from death. However, detailed studies are required to investigate this further.

8.5. Conclusions and further perspectives

The data presented in this study have demonstrated that IFN-γ is not important for survival in primary WNV infection or generation of secondary anti-WNV immunity. It does not play a crucial role in the clearance of WNV from the CNS. However, it is critically involved in disease progression in the i.p. model. The precise mechanism by which IFN-γ exerts its action in the CNS is not resolved. However, understanding these mechanisms may enable therapeutic approaches to treatment in the acute disease, since this model exhibits similar pathology to that observed in the human.

This thesis also shows that ICAM-1 and VCAM-1 upregulation is independent of IFN-γ. Extremely high expression of these adhesion molecules on neurovascular endothelium was unable to facilitate the infiltration of compensatory numbers of leukocytes into the brain. ICAM-1 was also expressed at high concentration on microglia in the absence of IFN-γ. However, the functional significance of such high levels of adhesion molecule expression on these cells in WNV encephalitis in the absence of IFN-γ is not clear.

This work shows that microglial activation is independent of IFN-γ. The activation and normalization of activated microglia directly correlated with the appearance and disappearance, respectively, of WNV Ag from the brain. Absence of significant neuronal apoptosis despite substantial high microglial activation and nodule formation suggest that these microglia may be involved directly or indirectly in the clearance of WNV from neurones. However, how this occurs is unknown. Further study, both *in vivo* and i*n vitro,* is required to understand the mechanisms by which microglia may be efectively antiviral in WNV encephalitis.

Antibody plays an important role in WNV encephalitis. In the absence of effective antiviral therapy for WNV infection, passive protection with Ab could play an important role in prophylactic prevention or in reduction of WNV infection following peripheral inoculation. However, the failure to protect mice after i.n. inoculation of WNV, even with passive transfer of high-dose of HI serum in the i.n. model indicates a more complex involvement of Ab in this disease than was previously thought. Moreover, adoptive transfer of HI splenocytes was also unable to protect mice from lethal WNV encephalitis in the i.n. model. More detailed investigation using passive transfer of high dose HI before and after infection and adoptive transfer of splenocytes and lymphocytes subsets via i.c. and other routes will be required to understand these complex mechanisms.

References

Aarli JA. 1983. The immune system and the nervous system. *J Neurol* 229: 137-54.

Abbas AK, Lichtman AH, Pober JS. 1997. *Cellular and Molecular Immunology.* (3rd edn). W. B. Saunders Company, Philadelphia.

Acarin L, Gonzalez B, Castellano B. 2000. Neuronal, astroglial and microglial cytokine expression after an excitotoxic lesion in the immature rat brain. *Eur J Neurosci* 12: 3505-20.

Adams JH, D.I. G, Anderson JR, *et al.* 1994. The central nervous system and its reactions to disease. In *An introduction to Neuropathology.* Churchill Livingstone, London. 29-48.

Adler H, Beland JL, Del-Pan NC, *et al.* 1999. In the absence of T cells, natural killer cells protect from mortality due to HSV-1 encephalitis. *J Neuroimmunol* 93: 208-13.

Afifi AK and Bergman RA. 1998. *Functional Neuroanatomy*: Mc Graw-Hill Health Profession Division.

Akbar AN, Salmon M, Janossy G. 1994. Role of bcl-2 and apoptosis in viral infections. *Int Arch Allergy Immunol* 105: 359-62.

Akiyama H, Ikeda K, Katoh M, *et al.* 1994. Expression of MRP14, 27E10, interferon-alpha and leukocyte common antigen by reactive microglia in postmortem human brain tissue. *J Neuroimmunol* 50: 195-201.

Akwa Y, Hassett DE, Eloranta ML, *et al.* 1998. Transgenic expression of IFN-alpha in the central nervous system of mice protects against lethal neurotropic viral infection but induces inflammation and neurodegeneration. *J Immunol* 161: 5016-26

Al-Omaishi J, Bashir R, Gendelman HE. 1999. The cellular immunology of multiple sclerosis. *J Leukoc Biol* 65: 444-52.

Albagalic CR. 1959. A case of West Nile myocarditis. *J Med Associ Isr* 57: 274-5.

Albelda SM and Buck CA. 1990. Integrins and other cell adhesion molecules. *FASEB J* 4: 2868-80.

Albrecht P. 1962. pathogenesis of experimental infection with tick borne encephalitis virus. In *Biology of Viruses of the Tick-Borne encephalitis complex*, ed. Libikova H. Acedemic press, New York. 247-54.

Albrecht P. 1968. Pathogenesis of neueotropic arbovirus infection. In *Current Topics in Microb Immunol*, ed. Arber w. Springer Company, New York. 43: 45-91.

Aleman N, Quiroga MI, Lopez-Pena M, *et al.* 2001. Induction and inhibition of apoptosis by pseudorabies virus in the trigeminal ganglion during acute infection of swine. *J Virol* 75: 469-79.

Alkhatib G, Combadiere C, Broder CC, *et al.* 1996. CC CKR5: a RANTES, MIP-1alpha, MIP-1beta receptor as a fusion cofactor for macrophage-tropic HIV-1. *Science* 272: 1955-8.

Aloisi F, Ria F, Penna G, *et al.* 1998. Microglia are more efficient than astrocytes in antigen processing and in Th1 but not Th2 cell activation. *J Immunol* 160: 4671-80.

Aloisi F, Serafini B, Adorini L. 2000. Glia-T cell dialogue. *J Neuroimmunol* 107: 111-7.

Andersen IH, Marker O, Thomsen AR. 1991. Breakdown of blood-brain barrier function in the murine lymphocytic choriomeningitis virus infection mediated by virus-specific CD8+ T cells. *J Neuroimmunol* 31: 155-63.

Anderson JR and Field HJ. 1983. The distribution of herpes simplex type 1 antigen in mouse central nervous system after different routes of inoculation. *J Neurol Sci* 60: 181-95.

Andjelkovic AV and Pachter JS. 1998. Central nervous system endothelium in neuroinflammatory, neuroinfectious, and neurodegenerative disease. *J Neurosci Res* 51: 423-30.

Andrews DM, Matthews VB, Sammels LM, *et al.* 1999. The severity of Murray Valley encephalitis in mice is linked to neutrophil infiltration and inducible nitric oxide synthase activity in the central nervous system. *J Virol* 73: 8781-90.

Argall KG, Armati PJ, King NJ, *et al.* 1991. The effects of West Nile virus on major histocompatibility complex class I and II molecule expression by Lewis rat Schwann cells in vitro. *J Neuroimmunol* 35: 273-84.

Asensio VC, Kincaid C, Campbell IL. 1999. Chemokines and the inflammatory response to viral infection in the central nervous system with a focus on lymphocytic choriomeningitis virus. *J Neurovirol* 5: 65-75.

Babic N, Mettenleiter TC, Ugolini G, *et al.* 1994. Propagation of pseudorabies virus in the nervous system of the mouse after intranasal inoculation. *Virology* 204: 616-25.

Bacon KB and Harrison JK. 2000. Chemokines and their receptors in neurobiology: perspectives in physiology and homeostasis. *J Neuroimmunol* 104: 92-7.

Balasingam V, Tejada-Berges T, Wright E, *et al.* 1994. Reactive astrogliosis in the neonatal mouse brain and its modulation by cytokines. *J Neurosci* 14: 846-56.

Balish E, Wagner RD, Vazquez-Torres A *et al.* 1998. Candidiasis in interferon-gamma knockout (IFN-gamma-/-) mice. *J Infect Dis* 178: 478-87.

Balkwill F. 1997. Cytokine amplification and inhibition of immune and inflammatory responses. *J Viral Hepat* 4 Suppl 2: 6-15.

Banati RB, Gehrmann J, Schubert P *et al.* 1993. Cytotoxicity of microglia. *Glia* 7: 111-8.

Banks WA, Kastin AJ, Broadwell RD. 1995. Passage of cytokines across the blood-brain barrier. *Neuroimmunomodulation* 2: 241-8.

Bao S, King NJ, Dos Remedios CG. 1992. Flavivirus induces MHC antigen on human myoblasts: a model of autoimmune myositis? *Muscle & Nerve* 15: 1271-7.

Barbic J, Leef MF, Burns DL, *et al.* 1997. Role of gamma interferon in natural clearance of Bordetella pertussis infection. *Infect Immun* 65: 4904-8.

Barnett EM, Cassell MD, Perlman S. 1993. Two neurotropic viruses, herpes simplex virus type 1 and mouse hepatitis virus, spread along different neural pathways from the main olfactory bulb. *Neuroscience* 57: 1007-25.

Barnett EM and Perlman S. 1993. The olfactory nerve and not the trigeminal nerve is the major site of CNS entry for mouse hepatitis virus, strain JHM. *Virology* 194: 185-91.

Baron S, Singh I, Chopra A, *et al.* 2000. Innate antiviral defenses in body fluids and tissues. *Antiviral Res* 48: 71-89.

Barr ML and Kiernan JA. 1983. *The human nervous system: an anatomical viewpoint.* Harper and Row, Philadelphia.

Barrett AD and Gould EA. 1986. Antibody-mediated early death in vivo after infection with yellow fever virus. *J Gen Virol* 67: 2539-42.

Barten DM and Ruddle NH. 1994. Vascular cell adhesion molecule-1 modulation by tumor necrosis factor in experimental allergic encephalomyelitis. *J Neuroimmunol* 51: 123-33.

Bartholdy C, Christensen JP, Wodarz D, *et al.* 2000. Persistent virus infection despite chronic cytotoxic T-lymphocyte activation in gamma interferon-deficient mice infected with lymphocytic choriomeningitis virus. *J Virol* 74: 10304-11.

Bauer J, Bradl M, Hickley WF, *et al.* 1998. T-cell apoptosis in inflammatory brain lesions: destruction of T cells does not depend on antigen recognition. *Am J Pathol* 153: 715-24.

Baumgarth N and Kelso A. 1996. In vivo blockade of gamma interferon affects the influenza virus-induced humoral and the local cellular immune response in lung tissue. *J Virol* 70: 4411-8.

Becher B, Prat A, Antel JP. 2000. Brain-immune connection: immuno-regulatory properties of CNS-resident cells. *Glia* 29: 293-304.

Beland JL, Sobel RA, Adler H, *et al.* 1999. B cell-deficient mice have increased susceptibility to HSV-1 encephalomyelitis and mortality. *J Neuroimmunol* 94: 122-6.

Ben-Nathan D, Huitinga I, Lustig S, *et al.* 1996. West Nile virus neuroinvasion and encephalitis induced by macrophage depletion in mice. *Arch Virol* 141: 459-69.

Benveniste EN. 1992. Inflammatory cytokines within the central nervous system: sources, function, and mechanism of action. *Am J Physiol* 263: C1-16.

Benveniste EN. 1998. Cytokine actions in the central nervous system. *Cytokine & Growth Factor Rev* 9: 259-75.

Berezovskaya O, Maysinger D, Fedoroff S. 1995. The hematopoietic cytokine, colony-stimulating factor 1, is also a growth factor in the CNS: congenital absence of CSF-1 in mice results in abnormal microglial response and increased neuron vulnerability to injury. *Int J Dev Neurosci* 13: 285-99.

Bernardes-Silva M, Anthony DC, Issekutz AC, *et al.* 2001. Recruitment of neutrophils across the blood-brain barrier: the role of E- and P-selectins. *J Cereb Blood Flow Metab* 21: 1115-24.

Bi Z, Barna M, Komatsu T, *et al.* 1995. Vesicular stomatitis virus infection of the central nervous system activates both innate and acquired immunity. *J Virol* 69: 6466-72.

Billiau A. 1996. Interferon-gamma: biology and role in pathogenesis. *Adv Immunol* 62: 61-130.

Binder D and Kundig TM. 1991. Antiviral protection by CD8+ versus CD4+ T cells. CD8+ T cells correlating with cytotoxic activity in vitro are more efficient in antivaccinia virus protection than CD4-dependent IL. *J Immunol* 146: 4301-7.

Binder GK and Griffin DE. 2001. Interferon-gamma-mediated site-specific clearance of alphavirus from CNS neurons. *Science* 293: 303-6.

Biron CA, Nguyen KB, Pien GC, *et al.* 1999. Natural killer cells in antiviral defense: function and regulation by innate cytokines. *Annu Rev Immunol* 17: 189-220.

Black PH. 1994. Immune system-central nervous system interactions: effect and immunomodulatory consequences of immune system mediators on the brain. *Antimicrob Agents Chemother* 38: 7-12.

Bo L, Mork S, Kong PA, *et al.* 1994. Detection of MHC class II-antigens on macrophages and microglia, but not on astrocytes and endothelia in active multiple sclerosis lesions. *J Neuroimmunol* 51: 135-46.

Bochner BS, Luscinskas FW, Gimbrone MA, *et al.* 1991. Adhesion of human basophils, eosinophils, and neutrophils to interleukin 1-activated human vascular endothelial cells: contributions of endothelial cell adhesion molecules. *J Exp Med* 173: 1553-7.

Boehm U, Klamp T, Groot M, *et al.* 1997. Cellular responses to interferon-gamma. *Annu Rev Immunol* 15: 749-95.

Boje KM and Arora PK. 1992. Microglial-produced nitric oxide and reactive nitrogen oxides mediate neuronal cell death. *Brain Res* 587: 250-6.

Bouley DM, Kanangat S, Wire W, *et al.* 1995. Characterization of herpes simplex virus type-1 infection and herpetic stromal keratitis development in IFN-gamma knockout mice. *J Immunol* 155: 3964-71.

Brankin B, Hart MN, Cosby SL *et al.* 1995. Adhesion molecule expression and lymphocyte adhesion to cerebral endothelium: effects of measles virus and herpes simplex 1 virus. *J Neuroimmunol* 56: 1-8.

Briese T, Glass WG, Lipkin WI. 2000. Detection of West Nile virus sequences in cerebrospinal fluid [letter]. *Lancet* 355: 1614-5.

Brodie C, Weizman N, Katzoff A, *et al.* 1997. Astrocyte activation by Sindbis virus: expression of GFAP, cytokines, and adhesion molecules. *Glia* 19: 275-85.

Brooks TJ and Phillpotts RJ. 1999. Interferon-alpha protects mice against lethal infection with St Louis encephalitis virus delivered by the aerosol and subcutaneous routes. *Antiviral Res* 41: 57-64.

Brosnan CF, Cannella B, Battistini L *et al.* 1995. Cytokine localization in multiple sclerosis lesions: correlation with adhesion molecule expression and reactive nitrogen species. *Neurology* 45: S16-21.

Buchanan AR. 1951. The interstitial tissue of the central nervous system. In *Functional Neuro-Anatomy*. Lea and Febiger, Philadelphia. 217-25.

Burkitt HG. 1993. Nervous Tissues. In *Wheater's Functional Histology- A text and colour atlas*, ed. Burkitt HG, Young B, Heath JW.Churchill Livingstone.

Byrnes AP, Durbin JE, Griffin DE. 2000. Control of Sindbis virus infection by antibody in interferon-deficient mice. *J Virol* 74: 3905-8.

Caceci T. 2002. Motor end plate. Information available from http://education.vetmed.vt.edu/Curriculum/VM8054/Labs/Lab10/Examples/exmtrplt.htm, INTERNET.

Calisher CH, Karabatsos N *et al.* 1989. Antigenic relationships between flaviviruses as determined by cross-neutralization tests with polyclonal antisera. *J Gen Virol* 70: 37-43.

Camenga DL, Nathanson N, Cole GA. 1974. Cyclophosphamide-potentiated West Nile viral encephalitis: relative influence of cellular and humoral factors. *J Infect Dis* 130: 634-41.

Campbell IL, Krucker T, Steffensen S, *et al.* 1999. Structural and functional neuropathology in transgenic mice with CNS expression of IFN-α. *Brain Res* 835: 46-61.

Cantin EM, Hinton DR, Chen J, 1995. Gamma interferon expression during acute and latent nervous system infection by herpes simplex virus type 1. *J Virol* 69: 4898-905.

Caplazi P and Ehrensperger F. 1998. Spontaneous Borna disease in sheep and horses: immunophenotyping of inflammatory cells and detection of MHC-I and MHC-II antigen expression in Borna encephalitis lesions. *Vet Immunol Immunopathol* 61: 203-20.

Carbone KM, Duchala CS, Griffin JW, 1987. Pathogenesis of Borna disease in rats: evidence that intra-axonal spread is the major route for virus dissemination and the determinant for disease incubation. *J Virol* 61: 3431-40.

Carlos TM and Harlan JM. 1994. Leukocyte-endothelial adhesion molecules. *Blood* 84: 2068-101.

Carpenter MB. 1991. Meninges and Cerebrospinal fluid. In *Core Text of Neuroanatomy* Williams and Wilkins, Baltimore, London. 1-21.

Carpenter MB. 1991. Olfactory pathways, hippocampal formation and the amygdala. In *Core Text of Neuroanatomy*: Williams and Wilkins, Baltimore, London.

Carpenter MB. 1991. Spinal cord: Gross anatomy and internal structure. In *Core Text of Neuroanatomy*. Williams and Wilkins, Baltimore, London. 57-75.

Carr DJ, Veress LA, Noisakran S, 1998. Astrocyte-targeted expression of IFN-alpha1 protects mice from acute ocular herpes simplex virus type 1 infection. *J Immunol* 161: 4859-65.

Castle E, Leidner U, Nowak T, *et al.* 1986. Primary structure of the West Nile flavivirus genome region coding for all nonstructural proteins. *Virology* 149: 10-26.

Castle E, Nowak T, Leidner U, *et al.* 1985. Sequence analysis of the viral core protein and the membrane-associated proteins V1 and NV2 of the flavivirus West Nile virus and of the genome sequence for these proteins. *Virology* 145: 227-36.

Ceausu E, Erscoiu S, Calistru P, *et al.* 1997. Clinical manifestations in the West Nile virus outbreak. *Rom J Virol* 48: 3-11.

Centre for Disease Control. 2000. Information on arboviral encephalitis. Information available from http://www.cdc.gov/ncidod/dvbid/arbor/arbdet.htm, INTERNET.

Chabot S, Williams G, Hamilton M. 1999. Mechanisms of IL-10 production in human microglia-T cell interaction. *J Immunol* 162: 6819-28.

Chamak B, Morandi V, Mallat M. 1994. Brain macrophages stimulate neurite growth and regeneration by secreting thrombospondin. *J Neurosci Res* 38: 221-33.

Chan WL, Javanovic T, Lukic ML. 1989. Infiltration of immune T cells in the brain of mice with herpes simplex virus-induced encephalitis. *J Neuroimmunol* 23: 195-201.

Chao CC, Gekker G, Hu S. 1994. Human microglial cell defense against Toxoplasma gondii. The role of cytokines. *J Immunol* 152: 1246-52.

Chao CC, Hu S, Peterson PK. 1995. Modulation of human microglial cell superoxide production by cytokines. *J Leukoc Biol* 58: 65-70.

Charles PC, Walters E, Margolis F. 1995. Mechanism of neuroinvasion of Venezuelan equine encephalitis virus in the mouse. *Virology* 208: 662-71.

Chaturvedi UC, Tandon P, Mathur A. 1977. Effect of immunosuppression on dengue virus infection in mice. *J Gen Virol* 36: 449-58.

Cheeran MC, Hu S, Yager SL *et al.* 2001. Cytomegalovirus induces cytokine and chemokine production differentially in microglia and astrocytes: antiviral implications. *J Neurovirol* 7: 135-47.

Chen CJ, Liao SL, Kuo MD *et al.* 2000. Astrocytic alteration induced by Japanese encephalitis virus infection. *Neuroreport* 11: 1933-7.

Chiba N, Osada M, Komoro K *et al.* 1999. Protection against tick-borne encephalitis virus isolated in Japan by active and passive immunization. *Vaccine* 17: 1532-9.

Choe W, Stoica G, Lynn W *et al.* 1998. Neurodegeneration induced by MoMuLV-ts1 and increased expression of Fas and TNF-alpha in the central nervous system. *Brain Res* 779: 1-8.

Christen S, Peterhans E, Stocker R. 1990. Antioxidant activities of some tryptophan metabolites: possible implication for inflammatory diseases. *Proc Natl Acad Sci U S A* 87: 2506-10.

Christensen JP, Bartholdy C, Wodarz D *et al.* 2001. Depletion of CD4+ T cells precipitates immunopathology in immunodeficient mice infected with a noncytocidal virus. *J Immunol* 166: 3384-91.

Christensen JP, Cardin RD, Branum KC *et al.* 1999. CD4(+) T cell-mediated control of a gamma-herpesvirus in B cell-deficient mice is mediated by IFN-gamma. *Proc Natl Acad Sci USA* 96: 5135-40.

Christian AY, Barna M, Bi Z *et al.* 1996. Host immune response to vesicular stomatitis virus infection of the central nervous system in C57BL/6 mice. *Viral Immunol* 9: 195-205.

Clark WM, Lauten JD, Lessov N *et al.* 1995. Time course of ICAM-1 expression and leukocyte subset infiltration in rat forebrain ischemia. *Mol Chem Neuropathol* 26: 213-30.

Coffin DL and Lu C.1957 Studies on canine distemper infection by means of fluorescein labeled antibody. II. Pathology of naturally occurring disease in dogs and antigenic nature of inclusion body. Virology. 3: 132-145.

Cross AH, Trotter JL, Lyons J. 2001. B cells and antibodies in CNS demyelinating disease. *J Neuroimmunol* 112: 1-14.

Cross AK and Woodroofe MN. 2001. Immunoregulation of microglial functional properties. *Microsc Res Tech* 54: 10-7.

Cserr HF and Knopf PM. 1992. Cervical lymphatics, the blood-brain barrier and the immunoreactivity of the brain: a new view. *Immunol Today* 13: 507-12.

Cua DJ, Hutchins B, LaFace DM *et al.* 2001. Central nervous system expression of IL-10 inhibits autoimmune encephalomyelitis. *J Immunol* 166: 602-8.

Cuadros MA and Navascues J. 1998. The origin and differentiation of microglial cells during development. *Prog Neurobiol* 56: 173-89

Czarniecki CW. 1993. The role of tumor necrosis factor in viral disease. *Antiviral Res* 22: 223-58.

Dallasta LM, Pisarov LA, Esplen JE *et al.* 1999. Blood-brain barrier tight junction disruption in human immunodeficiency virus-1 encephalitis. *Am J Pathol* 155: 1915-27.

Dallasta LM, Wang G, Bodnar RJ *et al.* 2000. Differential expression of intercellular adhesion molecule-1 and vascular cell adhesion molecule-1 in chronic murine retroviral encephalitis [In Process Citation]. *Neuropathol Appl Neurobiol* 26: 332-41.

Dalton DK, Pitts-Meek S, Keshav S *et al.* 1993. Multiple defects of immune cell function in mice with disrupted interferon-gamma genes. *Science* 259: 1739-42.

Davis EJ, Foster TD, Thomas WE. 1994. Cellular forms and functions of brain microglia. *Brain Res Bull* 34: 73-8.

de Boer AG and Breimer DD. 1998. Cytokines and blood-brain barrier permeability. *Prog Brain Res* 115: 425-51.

De Groot CJ and Woodroofe MN. 2001. The role of chemokines and chemokine receptors in CNS inflammation. *Prog Brain Res* 132: 533-44.

de Jong AL, Green DM, Trial JA *et al.* 1996. Focal effects of mononuclear leukocyte transendothelial migration: TNF-alpha production by migrating monocytes promotes subsequent migration of lymphocytes. *J Leukoc Biol* 60: 129-36.

De Leo JA and Yezierski RP. 2001. The role of neuroinflammation and neuroimmune activation in persistent pain. *Pain* 90: 1-6.

Deckert-Schluter M, Bluethmann H, Kaefer N *et al.* 1999. Interferon-gamma receptor-mediated but not tumor necrosis factor receptor type 1- or type 2-mediated signaling is crucial for the activation of cerebral blood vessel endothelial cells and microglia in murine Toxoplasma encephalitis. *Am J Pathol* 154: 1549-61.

DeLuca C, Kwon H., Lin R *et al.* 1999. NF-kB activation and HIV-1 induced apoptosis. *Cytokine & Growth Factor Rev* 10: 235-53.

Deng H, Liu R, Ellmeier W *et al.* 1996. Identification of a major co-receptor for primary isolates of HIV-1. *Nature* 381: 661-6.

Despres P, Frenkiel MP, Ceccaldi PE *et al.* 1998. Apoptosis in the mouse central nervous system in response to infection with mouse-neurovirulent dengue viruses. *J Virol* 72: 823-9.

Dickson DW, Mattiace LA, Kure K *et al.* 1991. Microglia in human disease, with an emphasis on acquired immune deficiency syndrome. *Lab Invest* 64: 135-56.

Dickson DW, Lee SC, Mattiace LA *et al.* 1993. Microglia and cytokines in neurological disease, with special reference to AIDS and Alzheimer's disease. *Glia* 7: 75-83.

Dietzschold B, Kao M, Zheng YM *et al.* 1992. Delineation of putative mechanisms involved in antibody-mediated clearance of rabies virus from the central nervous system. *Proc Natl Acad Sci U S A* 89: 7252-6.

Dobbie MS, Hurst RD, Klein NJ *et al.* 1999. Upregulation of intercellular adhesion molecule-1 expression on human endothelial cells by tumour necrosis factor-alpha in an in vitro model of the blood-brain barrier. *Brain Res* 830: 330-6.

Doherty PC and Zinkernagel RM. 1974. T-cell-mediated immunopathology in viral infections. *Transplant Rev* 19: 89-120.

Domachowske JB, Bonville CA, Dyer KD *et al.* 2000. Pulmonary eosinophilia and production of MIP-1alpha are prominent responses to infection with pneumonia virus of mice. *Cell Immunol* 200: 98-104.

Dong Y and Benveniste EN. 2001. Immune function of astrocytes. *Glia* 36: 180-90.

Dopp JM, Breneman SM, Olschowka JA. 1994. Expression of ICAM-1, VCAM-1, L-selectin, and leukosialin in the mouse central nervous system during the induction and remission stages of experimental allergic encephalomyelitis. *J Neuroimmunol* 54: 129-44.

Dorf ME, Berman MA, Tanabe S *et al.* 2000. Astrocytes express functional chemokine receptors. *J Neuroimmunol* 111: 109-21.

Douglas MW, Kesson AM, King NJ. 1994. CTL recognition of west Nile virus-infected fibroblasts is cell cycle dependent and is associated with virus-induced increases in class I MHC antigen expression. *Immunology* 82: 561-70.

Doukas J and Pober JS. 1990. IFN-gamma enhances endothelial activation induced by tumor necrosis factor but not IL-1. *J Immunol* 145: 1727-33.

Durbin JE, Fernandez-Sesma A, Lee CK *et al.* 2000. Type I IFN modulates innate and specific antiviral immunity. *J Immunol* 164: 4220-8.

Edwards KM, Davis JE, Browne KA. 1999. Anti-viral strategies of cytotoxic T lymphocytes are manifested through a variety of granule-bound pathways of apoptosis induction. *Immunol Cell Biol* 77: 76-89.

Eldadah AH and Nathanson N. 1967b. Pathogenesis of West Nile Virus encepahlitis in mice and rats. II. Virus multiplication, evolution of immunofluorescence, and development of histological lesions in the brain. *Am J Epidemiol* 86: 776-90.

Elkabes S, DiCicco-Bloom EM, Black IB. 1996. Brain microglia/macrophages express neurotrophins that selectively regulate microglial proliferation and function. *J Neurosci* 16: 2508-21.

Encephalitis Support Group. 2001. In Encephalitis Support Group, North Yorks. Available from http://glaxocentre.merseyside.org/, INTERNET.

Engelhardt B, Conley FK, Butcher EC. 1994. Cell adhesion molecules on vessels during inflammation in the mouse central nervous system. *J Neuroimmunol* 51: 199-208.

Eralinna JP, Soilu-Hanninen M, Roytta M *et al.* 1996. Blood-brain barrier breakdown and increased intercellular adhesion molecule (ICAM-1/CD54) expression after Semliki Forest (A7) virus infection facilitates the development of experimental allergic encephalomyelitis. *J Neuroimmunol* 66: 103-14.

Esiri MM and Tomlinson AH. 1984. Herpes simplex encephalitis. Immunohistological demonstration of spread of virus via olfactory and trigeminal pathways after infection of facial skin in mice. *J Neurol Sci* 64: 213-7.

Everett H and McFadden G. 1999. Apoptosis: an innate immune response to virus infection. *Trends Microbiol* 7: 160-5.

Fabry Z, Waldschmidt MM, Hendrickson D *et al.* 1992. Adhesion molecules on murine brain microvascular endothelial cells: expression and regulation of ICAM-1 and Lgp 55. *J Neuroimmunol* 36: 1-11.

Fehniger TA, Herbein G, Yu H *et al.* 1998. Natural killer cells from HIV-1+ patients produce C-C chemokines and inhibit HIV-1 infection. *J Immunol* 161: 6433-8.

Ferber IA, Brocke S, Taylor-Edwards C *et al.* 1996. Mice with a disrupted IFN-gamma gene are susceptible to the induction of experimental autoimmune encephalomyelitis (EAE). *J Immunol* 156: 5-7.

Finke D, Brinckmann UG, Ter Meulen V *et al.* 1995. Gamma interferon is a major mediator of antiviral defense in experimental measles virus-induced encephalitis. *J Virol* 69: 5469-74.

Fischer HG and Reichmann G. 2001. Brain dendritic cells and macrophages/microglia in central nervous system inflammation. *J Immunol* 166: 2717-26.

Flatau E, Kohn D, Daher O *et al.* 1981. West Nile fever encephalitis. *Isr J Med Sci* 17: 1057-9.

Flory E, Pfleiderer M, Stuhler A *et al.* 1993. Induction of protective immunity against coronavirus-induced encephalomyelitis: evidence for an important role of CD8+ T cells in vivo. *Eur J Immunol* 23: 1757-61.

Fontana A, Frei K, Bodmer S *et al.* 1987. Immune-mediated encephalitis: on the role of antigen-presenting cells in brain tissue. *Immunol Rev* 100: 185-201.

Frei K, Malipiero UV, Leist TP *et al.* 1989. On the cellular source and function of interleukin 6 produced in the central nervous system in viral diseases. *Eur J Immunol* 19: 689-94.

Fujii S, Akaike T, Maeda H. 1999. Role of nitric oxide in pathogenesis of herpes simplex virus encephalitis in rats. *Virology* 256: 203-12.

Gay D and Esiri M. 1991. Blood-brain barrier damage in acute multiple sclerosis plaques. An immunocytological study. *Brain* 114: 557-72.

Gebicke-Haerter PJ, Spleiss O, Ren LQ *et al.* 2001. Microglial chemokines and chemokine receptors. *Prog Brain Res* 132: 525-32.

Gehrmann J, Banati RB, Kreutzberg GW. 1993. Microglia in the immune surveillance of the brain: human microglia constitutively express HLA-DR molecules. *J Neuroimmunol* 48: 189-98.

Gehrmann J, Gold R, Linington C *et al.* 1993. Microglial involvement in experimental autoimmune inflammation of the central and peripheral nervous system. *Glia* 7: 50-9.

Geiger KD, Gurushanthaiah D, Howes EL *et al.* 1995. Cytokine-mediated survival from lethal herpes simplex virus infection: role of programmed neuronal death. *Proc Natl Acad Sci U S A* 92: 3411-5.

Geiger KD, Nash TC, Sawyer S *et al.* 1997. Interferon-gamma protects against herpes simplex virus type 1-mediated neuronal death. *Virology* 238: 189-97.

George S, Gourie-Devi M, Rao JA *et al.* 1984. Isolation of West Nile virus from the brains of children who had died of encephalitis. *Bull World Health Organ* 62: 879-82.

Georges A, Lesbordes J, Georges-Courbot M *et al.* 1987. Fatal hepatitis from West Nile virus. *Ann Inst Pasteur/Virology* 138: 237-44.

Gessani S and Belardelli F. 1998. IFN-gamma expression in macrophages and its possible biological significance. *Cytokine Growth Factor Rev* 9: 117-23.

Ghiasi H, Cai S, Perng GC *et al.* 2000. The role of natural killer cells in protection of mice against death and corneal scarring following ocular HSV-1 infection. *Antiviral Res* 45: 33-45.

Giulian D, Baker TJ, Shih LC *et al.* 1986. Interleukin 1 of the central nervous system is produced by ameboid microglia. *J Exp Med* 164: 594-604.

Giulian D and Ingeman JE. 1988. Colony-stimulating factors as promoters of ameboid microglia. *J Neurosci* 8: 4707-17.

Giulian D, Li J, Leara B *et al.* 1994. Phagocytic microglia release cytokines and cytotoxins that regulate the survival of astrocytes and neurons in culture. *Neurochem Int* 25: 227-33.

Glabinski AR, Krakowski M, Han Y. 1999. Chemokine expression in GKO mice (lacking interferon-gamma) with experimental autoimmune encephalomyelitis. *J Neurovirol* 5: 95-101.

Glimcher LH and Kara CJ. 1992. Sequences and factors: a guide to MHC class-II transcription. *Annu Rev Immunol* 10: 13-49.

Godiska R, Chantry D, Dietsch GN *et al.* 1995. Chemokine expression in murine experimental allergic encephalomyelitis. *J Neuroimmunol* 58: 167-76.

Gonzalez-Scarano F and Baltuch G. 1999. Microglia as mediators of inflammatory and degenerative diseases. *Annu Rev Neurosci* 22: 219-40.

Gould EA, Buckley A, Groeger BK *et al.* 1987. Immune enhancement of yellow fever virus neurovirulence for mice: studies of mechanisms involved. *J Gen Virol* 68: 3105-12.

Graeber MB. 1993. Microglia, macrophages and the blood-brain barrier. *Clin Neuropathol* 12: 296-7.

Graham MB, Dalton DK, Giltinan D *et al.* 1993. Response to Influenza infection in Mice with a targeted disruption in interferon gamma gene. *J Exp Med* 178: 1725-32.

Grau V, Herbst B, van der Meide PH *et al.* 1997. Activation of microglial and endothelial cells in the rat brain after treatment with interferon-gamma in vivo. *Glia* 19: 181-9.

Greenfield JG. 1997. Microglia. In *Greenfield's Neuropathology*, ed. David IG. and Peter LL. University Press, New York, Oxford.

Grieder FB and Vogel SN. 1999. Role of interferon and interferon regulatory factors in early protection against Venezuelan equine encephalitis virus infection. *Virology* 257: 106-18.

Griffin D, Levine B, Tyor W *et al.* 1997. The role of antibody in recovery from alphavirus encephalitis. *Immunol Rev* 159: 155-61.

Griffin DE and Hardwick JM. 1999. Perspective: virus infections and the death of neurons. *Trends Microbiol* 7: 155-60.

Griffin DE, Levine B, Tyor WR *et al.* 1994. Age-dependent susceptibility to fatal encephalitis: alphavirus infection of neurons. *Arch Virol Suppl* 9: 31-9.

Griffin DE, Levine B, Tyor WR *et al.* 1992. The immune response in viral encephalitis. *Semin Immunol* 4: 111-9.

Grzybicki DM, Kwack KB, Perlman S *et al.* 1997. Nitric oxide synthase type II expression by different cell types in MHV-JHM encephalitis suggests distinct roles for nitric oxide in acute versus persistent virus infection. *J Neuroimmunol* 73: 15-27.

Guidotti LG and Chisari FV. 2001. Noncytolytic control of viral infections by the innate and adaptive immune response. *Annu Rev Immunol* 19: 65-91.

Guidotti LG, McClary H, Loudis JM *et al.* 2000. Nitric oxide inhibits hepatitis B virus replication in the livers of transgenic mice. *J Exp Med* 191: 1247-52.

Gutierrez KM and Prober CG. 1998. Encephalitis. Identifying the specific cause is key to effective management. *Postgrad Med* 103: 123-5, 9-30, 40-3.

Halevy M, Akov Y, Ben-Nathan D *et al.* 1994. Loss of active neuroinvasiveness in attenuated strains of West Nile virus: pathogenicity in immunocompetent and SCID mice. *Arch Virol* 137: 355-70.

Halley S, Roffey P, Hansen P *et al.* 2000. Arboviruses pathogenic to humans in Australia. *Today's Life Sci* 12: 36-40.

Hama T, Miyamoto M, Tsukui H *et al.* 1989. Interleukin-6 as a neurotrophic factor for promoting the survival of cultured basal forebrain cholinergic neurons from postnatal rats. *Neurosci Lett* 104: 340-4.

Hammarberg H, Lidman O, Lundberg C *et al.* 2000. Neuroprotection by encephalomyelitis: rescue of mechanically injured neurons and neurotrophin production by CNS-infiltrating T and natural killer cells. *J Neurosci* 20: 5283-91.

Hartung HP, Michels M, Reiners K *et al.* 1993. Soluble ICAM-I serum levels in multiple sclerosis and viral encephalitis. *Neurology* 43: 2331-5.

Harty JT, Tvinnereim AR, White DW. 2000. CD8+ T cell effector mechanisms in resistance to infection. *Annu Rev Immunol* 18: 275-308.

Hase T, Dubois DR, Summers PL. 1990. Comparative study of mouse brains infected with Japanese encephalitis virus by intracerebral or intraperitoneal inoculation. *Int J Exp Pathol* 71: 857-69.

Hatalski CG, Hickey WF, Lipkin WI. 1998. Humoral immunity in the central nervous system of Lewis rats infected with Borna disease virus. *J Neuroimmunol* 90: 128-36.

Havenith CE, Askew D, Walker WS. 1998. Mouse resident microglia: isolation and characterization of immunoregulatory properties with naive CD4+ and CD8+ T-cells. *Glia* 22: 348-59.

Hemmer K, Fransen L, Vanderstichele H *et al.* 2001. An in vitro model for the study of microglia-induced neurodegeneration: involvement of nitric oxide and tumor necrosis factor-alpha. *Neurochem Int* 38: 557-65.

Herbein G and O'Brien WA. 2000. Tumor necrosis factor (TNF)-alpha and TNF receptors in viral pathogenesis. *Proc Soc Exp Biol Med* 223: 241-57.

Hery C, Sebire G, Peudenier S *et al.* 1995. Adhesion to human neurons and astrocytes of monocytes: the role of interaction of CR3 and ICAM-1 and modulation by cytokines. *J Neuroimmunol* 57: 101-9.

Heyes MP, Saito K, Jacobowitz D *et al.* 1992. Poliovirus induces indoleamine-2,3-dioxygenase and quinolinic acid synthesis in macaque brain. *FASEB J* 6: 2977-89.

Hickey WF, Hsu BL, Kimura H. 1991. T-lymphocyte entry into the central nervous system. *J Neurosci Res* 28: 254-60.

Hopkins SJ and Rothwell NJ. 1995. Cytokines and the nervous system I: Expression and recognition. *Trends Neurosci* 18: 83-8.

Howard AY and Hardy KJ. 1995. Role of Interferon gamma in Immune Cell regulation. *J Leuko Biol* 58: 373-81.

Hu S, Chao CC, Ehrlich LC *et al.* 1999. Inhibition of microglial cell RANTES production by IL-10 and TGF-beta. *J Leukoc Biol* 65: 815-21.

Huang S, Hendriks W, Althage A *et al.* 1993. Immune response in mice that lack the interferon-gamma receptor. *Science* 259: 1742-5.

Hubalek Z and Halouzka J. 1999. West Nile fever--a reemerging mosquito-borne viral disease in Europe. *Emerg Infect Dis* 5: 643-50.

Huneycutt BS, Plakhov IV, Shusterman Z *et al.* 1994. Distribution of vesicular stomatitis virus proteins in the brains of BALB/c mice following intranasal inoculation: an immunohistochemical analysis. *Brain Res* 635: 81-95.

Hurwitz AA, Berman JW, Lyman WD. 1994. The role of the blood-brain barrier in HIV infection of the central nervous system. *Adv Neuroimmunol* 4: 249-56.

Huynh HK and Dorovini-Zis K. 1993. Effects of interferon-gamma on primary cultures of human brain microvessel endothelial cells. *Am J Pathol* 142: 1265-78.

Imhof BA and Dunon D. 1995. Leukocyte migration and adhesion. *Adv Immunol* 58: 345-416.

Irani DN and Griffin DE. 1996. Regulation of lymphocyte homing into the brain during viral encephalitis at various stages of infection. *J Immunol* 156: 3850-7.

Issekutz TB, Stoltz JM, vd Meide P. 1988. Lymphocyte recruitment in delayed-type hypersensitivity. The role of IFN-gamma. *J Immunol* 140: 2989-93.

Iwasaki Y, Zhao JX, Yamamoto T *et al.* 1986. Immunohistochemical demonstration of viral antigens in Japanese encephalitis. *Acta Neuropathol (Berl)* 70: 79-81.

Jacoby RO, Bhatt PN, Schwartz A. 1980. Protection of mice from lethal flaviviral encephalitis by adoptive transfer of splenic cells from donors infected with live virus. *J Infect Dis* 141: 617-24.

Janeway CA, Travers P, Walport M *et al.* 2001. *Immunobiology: The immune system in health and disease*: Churchill Livingstone, New York, Tokyo.

Jiang Y, Salafranca MN, Adhikari S *et al.* 1998. Chemokine receptor expression in cultured glia and rat experimental allergic encephalomyelitis. *J Neuroimmunol* 86: 1-12.

Johnson LJ, Halliday GM, King NJ. 1996. Phenotypic changes in Langerhans' cells after infection with arboviruses: a role in the immune response to epidermally acquired viral infection? *J Virol* 70: 4761-6.

Johnson RT. 1964. The pathogenesis of Herpes Simplex virus encephalitis I. Pathways to the nervous system of suckling mice demonstrated by fluorescent antibody staining. *J Exp Med* 119: 343-56.

Johnson RT. 1982. *Viral infections of the nervous system*: Raven Press, New York.

Johnson RT. 1987. The pathogenesis of acute viral encephalitis and postinfectious encephalomyelitis. *J Infect Dis* 155: 359-64.

Johnson RT, Burke DS, Elwell M *et al.* 1985. Japanese encephalitis: immunocytochemical studies of viral antigen and inflammatory cells in fatal cases. *Ann Neurol* 18: 567-73.

Johnstone M, Gearing AJ, Miller KM. 1999. A central role for astrocytes in the inflammatory response to beta-amyloid; chemokines, cytokines and reactive oxygen species are produced. *J Neuroimmunol* 93: 182-93.

Kamegai M, Niijima K, Kunishita T *et al.* 1990. Interleukin 3 as a trophic factor for central cholinergic neurons in vitro and in vivo. *Neuron* 4: 429-36.

Kamimura S, Eguchi K, Yonezawa M *et al.* 1991. Localization and developmental change of indoleamine 2,3-dioxygenase activity in the human placenta. *Acta Med Okayama* 45: 135-9.

Kapoor AK, Nash AA, Wildy P. 1982. Pathogenesis of herpes simplex virus in B cell-suppressed mice: the relative roles of cell-mediated and humoral immunity. *J Gen Virol* 61: 127-31.

Karupiah G, Blanden RV, Ramshaw IA. 1990. Interferon gamma is involved in the recovery of athymic nude mice from recombinant vaccinia virus/interleukin 2 infection. *J Exp Med* 172: 1495-503.

Karupiah G, Chen JH, Nathan CF *et al.* 1998. Identification of nitric oxide synthase 2 as an innate resistance locus against ectromelia virus infection. *J Virol* 72: 7703-6.

Karupiah G, Hunt NH, King NJ *et al.* 2000. NADPH oxidase, Nramp1 and nitric oxide synthase 2 in the host antimicrobial response. *Rev Immunogenet* 2: 387-415.

Karupiah G, Xie QW, Buller RM *et al.* 1993. Inhibition of viral replication by interferon-gamma-induced nitric oxide synthase. *Science* 261: 1445-8.

Kato H and Walz W. 2000. The initiation of the microglial response. *Brain Pathol* 10: 137-43.

Katz G, Rannon L, Nili E *et al.* 1989. West Nile fever--occurrence in a new endemic site in the Negev. *Isr J Med Sci* 25: 39-41.

Kesson AM and King NJ. 2001. Transcriptional regulation of major histocompatibility complex class I by flavivirus West Nile is dependent on NF-kappaB activation. *J Infect Dis* 184: 947-54.

Kettle DS. 1995. Arboviruses. In *Medical and veterinary entomology*. CAB International, UK, Cambridge.

Kiefer R and Kreutzberg GW. 1990. Gamma interferon-like immunoreactivity in the rat nervous system. *Neuroscience* 37: 725-34.

Kimura T and Griffin DE. 2000. The role of CD8(+) T cells and major histocompatibility complex class I expression in the central nervous system of mice infected with neurovirulent Sindbis virus. *J Virol* 74: 6117-25.

Kimura-Kuroda J and Yasui K. 1988. Protection of mice against Japanese encephalitis virus by passive administration with monoclonal antibodies. *J Immunol* 141: 3606-10.

King NJ and Kesson AM. 1988. Interferon-independent increases in class I major histocompatibility complex antigen expression follow flavivirus infection. *J Gen Virol* 69: 2535-43.

King NJ, Maxwell LE, Kesson AM. 1989. Induction of class I major histocompatibility complex antigen expression by West Nile virus on gamma interferon-refractory early murine trophoblast cells. *Proc Nat Acad Sci USA* 86: 911-5.

King NJ, Mullbacher A, Tian L *et al.* 1993. West Nile virus infection induces susceptibility of in vitro outgrown murine blastocysts to specific lysis by paternally directed allo-immune and virus-immune cytotoxic T cells. *J Reprod Immunol* 23: 131-44.

Klavinskis LS, Geckeler R, Oldstone MB. 1989. Cytotoxic T lymphocyte control of acute lymphocytic choriomeningitis virus infection: interferon gamma, but not tumour necrosis factor alpha, displays antiviral activity in vivo. *J Gen Virol* 70: 3317-25.

Klein J. 1979. The major histocompatibility complex of the mouse. *Science* 203: 516-21.

Knoblach SM, Fan L, Faden AI. 1999. Early neuronal expression of tumor necrosis factor-alpha after experimental brain injury contributes to neurological impairment. *J Neuroimmunol* 95: 115-25.

Kohonen-Corish M, King NJ, Woodhams CE *et al.* 1990. Immunodeficient mice recover from infection with vaccinia virus expressing interferon-gamma. *Eur J Immunol* 20: 157-61.

Komatsu T, Bi Z, Reiss CS. 1996. Interferon-gamma induced type I nitric oxide synthase activity inhibits viral replication in neurons. *J Neuroimmunol* 68: 101-8.

Komatsu T, Ireland DD, Chen N *et al.* 1999. Neuronal expression of NOS-1 is required for host recovery from viral encephalitis. *Virology* 258: 389-95.

Krakowski M and Owens T. 1996. Interferon-gamma confers resistance to experimental allergic encephalomyelitis. *Eur J Immunol* 26: 1641-6.

Kreil TR and Eibl MM. 1995. Viral infection of macrophages profoundly alters requirements for induction of nitric oxide synthesis. *Virology* 212: 174-8.

Kreil TR and Eibl MM. 1997. Pre- and postexposure protection by passive immunoglobulin but no enhancement of infection with a flavivirus in a mouse model. *J Virol* 71: 2921-7.

Kreutzberg GW. 1996. Microglia: a sensor for pathological events in the CNS. *Trends Neurosci* 19: 312-8.

Kuby J. 1994. *Immunology*: W. H. Freeman and Company, New York.

Kundig TM, Hengartner H, Zinkernagel RM. 1993. T cell-dependent IFN-gamma exerts an antiviral effect in the central nervous system but not in peripheral solid organs. *J Immunol* 150: 2316-21.

Kundin WD, Liu C, Hysell P *et al.* 1962(a). Studies on West Nile virus infection by means of fluorescent antibodies I) Pathogenesis of west nile virus infection in experimentally inoculated suckling mice. *Archiv Fur Die Gesamte Virusforschung* 12: 514-29

Kurane I, Innis BL, Nimmannitya S *et al.* 1990. Human immune responses to dengue viruses. *Southeast Asian J Trop Med Public Health* 21: 658-62.

Kure K, Weidenheim KM, Lyman WD. 1990. Morphology and distribution of HIV-1 gp41-positive microglia in subacute AIDS encephalitis. Pattern of involvement resembling a multisystem degeneration. *Acta Neuropathol (Berl)* 80: 393-400.

Kyrkanides S, Olschowka JA, Williams JP *et al.* 1999. TNF alpha and IL-1beta mediate intercellular adhesion molecule-1 induction via microglia-astrocyte interaction in CNS radiation injury. *J Neuroimmunol* 95: 95-106.

Lachmann PJ and Davies A. 1997. Complement and immunity to viruses. *Immunol Rev* 159: 69-77.

Lane TE, Fox HS, Buchmeier MJ. 1999. Inhibition of nitric oxide synthase-2 reduces the severity of mouse hepatitis virus-induced demyelination: implications for NOS2/NO regulation of chemokine expression and inflammation. *J Neurovirol* 5: 48-54.

Lane TE, Liu MT, Chen BP *et al.* 2000. A central role for CD4(+) T cells and RANTES in virus-induced central nervous system inflammation and demyelination. *J Virol* 74: 1415-24.

Langford D and Masliah E. 2001. Crosstalk between components of the blood brain barrier and cells of the CNS in microglial activation in AIDS. *Brain Pathol* 11: 306-12.

Larrick JW and Wright SC. 1990. Cytotoxic mechanism of tumor necrosis factor-alpha. *FASEB J* 4: 3215-23.

Lassmann H. 1997. Basic mechanisms of brain inflammation. *J Neural Transm Suppl* 50: 183-90.

Lawson LJ, Perry VH, Dri P *et al.* 1990. Heterogeneity in the distribution and morphology of microglia in the normal adult mouse brain. *Neuroscience* 39: 151-70.

Ledeboer A, Breve JJ, Poole S *et al.* 2000. Interleukin-10, interleukin-4, and transforming growth factor-beta differentially regulate lipopolysaccharide-induced production of pro-inflammatory cytokines and nitric oxide in co-cultures of rat astroglial and microglial cells. *Glia* 30: 134-42.

Lee SJ and Benveniste EN. 1999. Adhesion molecule expression and regulation on cells of the central nervous system. *J Neuroimmunol* 98: 77-88.

Lee SJ, Park JY, Hou J *et al.* 1999. Transcriptional regulation of the intercellular adhesion molecule-1 gene by proinflammatory cytokines in human astrocytes. *Glia* 25: 21-32.

Lehrmann E, Kiefer R, Christensen T *et al.* 1998. Microglia and macrophages are major sources of locally produced transforming growth factor-beta1 after transient middle cerebral artery occlusion in rats. *Glia* 24: 437-48.

Leist TP, Eppler M, Zinkernagel RM. 1989. Enhanced virus replication and inhibition of lymphocytic choriomeningitis virus disease in anti-gamma interferon-treated mice. *J Virol* 63: 2813-9.

Letterio JJ. 2000. Murine models define the role of TGF-beta as a master regulator of immune cell function. *Cytokine Growth Factor Rev* 11: 81-7.

Levine B, Goldman JE, Jiang HH *et al.* 1996. Bc1-2 protects mice against fatal alphavirus encephalitis. *Proc Natl Acad Sci U S A* 93: 4810-5.

Levine B and Griffin DE. 1992. Persistence of viral RNA in mouse brains after recovery from acute alphavirus encephalitis. *J Virol* 66: 6429-35.

Levine B, Hardwick JM, Trapp BD *et al.* 1991. Antibody-mediated clearance of alphavirus infection from neurons. *Science* 254: 856-60.

Lewandowski G and Hobbs MV. 1998. Evidence for deficiencies in intracerebral cytokine production, adhesion molecule induction, and T cell recruitment in herpes simplex virus type-2 infected mice. *J Neuroimmunol* 81: 58-65.

Lewis J, Wesselingh SL, Griffin DE *et al.* 1996. Alphavirus-induced apoptosis in mouse brains correlates with neurovirulence. *J Virol* 70: 1828-35.

Ley K and Tedder TF. 1995. Leukocyte interactions with vascular endothelium. New insights into selectin-mediated attachment and rolling. *J Immunol* 155: 525-8.

Leyssen P, De Clercq E, Neyts J. 2000. Perspectives for the treatment of infections with Flaviviridae. *Clin Microbiol Rev* 13: 67-82.

Li H, Jerrells TR, Spitalny GL *et al.* 1987. Gamma interferon as a crucial host defense against Rickettsia conorii in vivo. *Infect Immun* 55: 1252-5.

Liao CL, Lin YL, Wang JJ *et al.* 1997. Effect of enforced expression of human bcl-2 on Japanese encephalitis virus-induced apoptosis in cultured cells. *J Virol* 71: 5963-71.

Ling EA and Wong WC. 1993. The origin and nature of ramified and amoeboid microglia: a historical review and current concepts. *Glia* 7: 9-18.

Linke AT, Antonopoulos M, Davies DH *et al.* 2000. Strain specific variation in cytokine regulated ICAM-1 expression by rat brain-endothelial cells. *J Neuroimmunol* 104: 10-4.

Liu MT, Armstrong D, Hamilton TA *et al.* 2001. Expression of Mig (Monokine Induced by Interferon-gamma) is important in T lymphocyte recruitment and host defense following viral infection of the central nervous system. *J Immunol* 166: 1790-5.

Liu MT, Chen BP, Oertel P *et al.* 2000. Cutting edge: the T cell chemoattractant IFN-inducible protein 10 is essential in host defense against viral-induced neurologic disease. *J Immunol* 165: 2327-30.

Liu T and Chambers TJ. 2001. Yellow Fever Virus Encephalitis: Properties of the Brain-Associated T-Cell Response during Virus Clearance in Normal and Gamma Interferon-Deficient Mice and Requirement for CD4(+) Lymphocytes. *J Virol* 75: 2107-18.

Liu Y, King N, Kesson A *et al.* 1989. Flavivirus infection up-regulates the expression of class I and class II major histocompatibility antigens on and enhances T cell recognition of astrocytes in vitro. *J Neuroimmunol* 21: 157-68.

Lobigs M, Blanden RV, Mullbacher A. 1996. Flavivirus-induced up-regulation of MHC class I antigens; implications for the induction of CD8+ T-cell-mediated autoimmunity. *Immunol Rev* 152: 5-19.

Lodge PA and Sriram S. 1996. Regulation of microglial activatioon by TGF-β, IL-10 and CSF-1. *J Leuko Biol* 60: 502-8.

Loughlin AJ, Woodroofe MN, Cuzner ML. 1993. Modulation of interferon-gamma-induced major histocompatibility complex class II and Fc receptor expression on isolated microglia by transforming growth factor-beta 1, interleukin-4, noradrenaline and glucocorticoids. *Immunology* 79: 125-30.

MacMicking J, Xie QW, Nathan C. 1997. Nitric oxide and macrophage function. *Annu Rev Immunol* 15: 323-50.

Maddox DE, Shibata S, Goldstein IJ. 1982. Stimulated macrophages express a new glycoprotein receptor reactive with Griffonia simplicifolia I-B4 isolectin. *Proc Natl Acad Sci U S A* 79: 166-70.

Magnus T, Chan A, Grauer O *et al.* 2001. Microglial phagocytosis of apoptotic inflammatory T cells leads to down-regulation of microglial immune activation. *J Immunol* 167: 5004-10.

Mallat M, Houlgatte R, Brachet P *et al.* 1989. Lipopolysaccharide-stimulated rat brain macrophages release NGF in vitro. *Dev Biol* 133: 309-11.

Maloney EM, St Claire Morgan O, Widner B *et al.* 2000. Central nervous system activation of the indoleamine-2,3-dioxygenase pathway in human T cell lymphotropic virus type I-associated myelopathy/tropical spastic paraparesis. *J Infect Dis* 181: 2037-40.

Mannick JB. 1995. The antiviral role of nitric oxide. *Res Immunol* 146: 693-7.

Marten NW, Stohlman SA, Bergmann CC. 2001. MHV infection of the CNS: mechanisms of immune-mediated control. *Viral Immunol* 14: 1-18.

Martin PM and O'Callaghan JP. 1995. A direct comparison of GFAP immunocytochemistry and GFAP concentration in various regions of ethanol-fixed rat and mouse brain. *J Neurosci Methods* 58: 181-92.

Masinovsky B, Urdal D, Gallatin WM. 1990. IL-4 acts synergistically with IL-1 beta to promote lymphocyte adhesion to microvascular endothelium by induction of vascular cell adhesion molecule-1. *J Immunol* 145: 2886-95.

Mason JL, Suzuki K, Chaplin DD *et al.* 2001. Interleukin-1beta promotes repair of the CNS. *J Neurosci* 21: 7046-52.

Matthews AE, Weiss SR, Shlomchik MJ *et al.* 2001. Antibody is required for clearance of infectious murine hepatitis virus a59 from the central nervous system, but not the liver. *J Immunol* 167: 5254-63.

Matyszak MK. 1998. Inflammation in the CNS: balance between immunological privilege and immune responses. *Prog Neurobiol* 56: 19-35.

Mauerhoff T, Pujol-Borrell R, Mirakian R *et al.* 1988. Differential expression and regulation of major histocompatibility complex (MHC) products in neural and glial cells of the human fetal brain. *J Neuroimmunol* 18: 271-89.

McGeer PL, Kawamata T, Walker DG *et al.* 1993. Microglia in degenerative neurological disease. *Glia* 7: 84-92.

McKendall RR, Klassen T, Baringer JR. 1979. Host defenses in herpes simplex infections of the nervous system: effect of antibody on disease and viral spread. *Infect Immun* 23: 305-11.

McManus CM, Brosnan CF, Berman JW. 1998. Cytokine induction of MIP-1 alpha and MIP-1 beta in human fetal microglia. *J Immunol* 160: 1449-55.

McManus CM, Liu JS, Hahn MT *et al.* 2000. Differential induction of chemokines in human microglia by type I and II interferons. *Glia* 29: 273-80.

McMinn PC, Dalgarno L, Weir RC. 1996. A comparison of the spread of Murray Valley encephalitis viruses of high or low neuroinvasiveness in the tissues of Swiss mice after peripheral inoculation. *Virology* 220: 414-23.

McQuaid S, McMahon J, Herron B *et al.* 1997. Apoptosis in measles virus-infected human central nervous system tissues. *Neuropathol Appl Neurobiol* 23: 218-24.

Meager A. 1999. Cytokine regulation of cellular adhesion molecule expression in inflammation. *Cytokine Growth Factor Rev* 10: 27-39.

Meda L, Cassatella MA, Szendrei GI *et al.* 1995. Activation of microglial cells by beta-amyloid protein and interferon-gamma. *Nature* 374: 647-50.

Medana IM, Chan-Ling T, Hunt NH. 1996. Redistribution and degeneration of retinal astrocytes in experimental murine cerebral malaria: relationship to disruption of the blood-retinal barrier. *Glia* 16: 51-64.

Medana IM, Chaudhri G, Chan-Ling T *et al.* 2001. Central nervous system in cerebral malaria: 'Innocent bystander' or active participant in the induction of immunopathology? *Immunol Cell Biol* 79: 101-20.

Medana IM, Gallimore A, Oxenius A *et al.* 2000. MHC class I-restricted killing of neurons by virus-specific CD8+ T lymphocytes is effected through the Fas/FasL, but not the perforin pathway. *Eur J Immunol* 30: 3623-33.

Medana IM, Hunt NH, Chaudhri G. 1997. Tumor necrosis factor-alpha expression in the brain during fatal murine cerebral malaria: evidence for production by microglia and astrocytes. *Am J Pathol* 150: 1473-86.

Merrill JE and Benveniste EN. 1996. Cytokines in inflammatory brain lesions: helpful and harmful. *Trends Neurosci* 19: 331-8.

Meucci O, Fatatis A, Simen AA *et al.* 2000. Expression of CX3CR1 chemokine receptors on neurons and their role in neuronal survival. *Proc Natl Acad Sci U S A* 97: 8075-80.

Mickelson JK, Kukielka G, Bravenec JS, Mainolfi E, Rothlein R, *et al.* 1995. Differential expression and release of CD54 induced by cytokines. *Hepatology* 22: 866-75.

Milligan GN, Bourne N, Dudley KL. 2001. Role of polymorphonuclear leukocytes in resolution of HSV-2 infection of the mouse vagina. *J Reprod Immunol* 49: 49-65.

Mitrasinovic OM, Perez GV, Zhao F. 2001. Overexpression of macrophage colony-stimulating factor receptor on microglial cells induces an inflammatory response. *J Biol Chem* 276: 30142-9.

Miyajima A, Kitamura T, Harada N *et al.* 1992. Cytokine receptors and signal transduction. *Annu Rev Immunol* 10: 295-331.

Mokhtarian F, Wesselingh SL, Choi S *et al.* 1996. Production and role of cytokines in the CNS of mice with acute viral encephalomyelitis. *J Neuroimmunol* 66: 11-22.

Molina-Holgado E, Vela JM, Arevalo-Martin A *et al.* 2001. LPS/IFN-gamma cytotoxicity in oligodendroglial cells: role of nitric oxide and protection by the anti-inflammatory cytokine IL-10. *Eur J Neurosci* 13: 493-502.

Momburg F, Koch N, Moller P *et al.* 1986. In vivo induction of H-2K/D antigens by recombinant interferon-gamma. *Eur J Immunol* 16: 551-7.

Monath TP. 1986. Pathobiology of the Flaviviruses. In *The Togaviridae and Flaviviridae*, ed. Schlesinger S and Schlesinger MJ. Plenum Press, New York and London.

Monath TP, Cropp CB, Harrison AK. 1983. Mode of entry of a neurotropic arbovirus into the central nervous system. Reinvestigation of an old controversy. *Lab Invest* 48: 399-410.

Monath TP and Heinz FX. 1996. Flavivirus. In *Fields Virology*, ed. Fields BN. Philadelphia Lipponcott-Raven Publishers. 961-1034.

Moore S and Thanos S. 1996. The concept of microglia in relation to central nervous system disease and regeneration. *Prog Neurobiol* 48: 441-60.

Morbidity and Mortality Weekly Report. Outbreak of West Nile like viral encephalitis-New York. 1999. October 1. *Morbidity and Mortality Weekly Report* 48: 845-9.

Mori I, Hossain MJ, Takeda K *et al.* 2001. Impaired microglial activation in the brain of IL-18-gene-disrupted mice after neurovirulent influenza A virus infection. *Virology* 287: 163-70.

Mori S, Sternberger NH, Herman MM *et al.* 1991. Leakage and neuronal uptake of serum protein in aged and Alzheimer brains. A postmortem phenomenon with antemortem etiology. *Lab Invest* 64: 345-51.

Morioka T, Kalehua AN, Streit WJ. 1992. Progressive expression of immunomolecules on microglial cells in rat dorsal hippocampus following transient forebrain ischemia. *Acta Neuropathol (Berl)* 83: 149-57.

Morris CS and Esiri MM. 1998. The expression of cytokines and their receptors in normal and mildly reactive human brain. *J Neuroimmunol* 92: 85-97.

Mosmann TR, Cherwinski H, Bond MW *et al.* 1986. Two types of murine helper T cell clone. I. Definition according to profiles of lymphokine activities and secreted proteins. *J Immunol* 136: 2348-57.

Mucke L and Eddleston M. 1993. Astrocytes in infectious and immune-mediated diseases of the central nervous system. *FASEB J* 7: 1226-32.

Mullbacher A and Blanden RV. 1979. The effect of virus-immune serum on anti-viral cytotoxic T-cells in vivo and in vitro. *J Gen Virol* 45: 73-80.

Muller U, Steinhoff U, Reis LF *et al.* 1994. Functional role of type I and type II interferons in antiviral defense. *Science* 264: 1918-21.

Munoz-Fernandez MA and Fresno M. 1998. The role of tumour necrosis factor, interleukin 6, interferon-gamma and inducible nitric oxide synthase in the development and pathology of the nervous system. *Prog Neurobiol* 56: 307-40.

Murali-Krishna K, Ravi V, Manjunath R. 1996. Protection of adult but not newborn mice against lethal intracerebral challenge with Japanese encephalitis virus by adoptively transferred virus-specific cytotoxic T lymphocytes: requirement for L3T4+ T cells. *J Gen Virol* 77: 705-14.

Murphy F, Bauer S, Harrison A *et al.* 1973. Comparative pathogenesis of rabies and rabies like viruses. *Lab Invest* 28: 261-75.

Nakajima K and Kohsaka S. 1998. Functional roles of microglia in the central nervous system. *Hum Cell* 11: 141-55.

Nakajima K, Tsuzaki N, Nagata K *et al.* 1992. Production and secretion of plasminogen in cultured rat brain microglia. *FEBS Lett* 308: 179-82.

Nansen A, Christensen JP, Ropke C *et al.* 1998. Role of interferon-gamma in the pathogenesis of LCMV-induced meningitis: unimpaired leucocyte recruitment, but deficient macrophage activation in interferon-gamma knock-out mice. *J Neuroimmunol* 86: 202-12.

Nansen A, Jensen T, Christensen *et al.* 1999. Compromised virus control and augmented perforin-mediated immunopathology in IFN-gamma-deficient mice infected with lymphocytic choriomeningitis virus. *J Immunol* 163: 6114-22.

Nathanson N and Bodian D. 1961. Experimental poliomyelitis following intramuscular virus infection. I. The effect of nural block on a neurotropic and pantropic strain. *Bull. Johns Hopk. Hosp* 108: 308-19.

Nathanson N and Cole GA. 1970. Immunosuppression and experimental virus infection of the nervous system. *Adv Virus Res* 16: 397-448.

Neumann H. 2001. Control of glial immune function by neurons. *Glia* 36: 191-9.

Neumann H, Schmidt H, Cavalie A *et al.* 1997. Major histocompatibility complex (MHC) class I gene expression in single neurons of the central nervous system: differential regulation by interferon (IFN)-gamma and tumor necrosis factor (TNF)-alpha. *J Exp Med* 185: 305-16.

Neumann H, Wekerle H. 1998. Neuronal control of the immune response in the central nervous system: Linking brain immunity to Neurodegeneration. *J Neuropathol Expt Neurol* 57: 1-9.

Nir Y, Beemer A, Goldwasser RA. 1965. West Nile Virus infection in mice following exposure to a viral aerosol. *Br J Exp Pathol* 46: 443-9.

Nohava K, Malipiero U, Frei K *et al.* 1992. Neurons and neuroblastoma as a source of macrophage colony-stimulating factor. *Eur J Immunol* 22: 2539-45.

Noske K, Bilzer T, Planz O *et al.* 1998. Virus-specific CD4+ T cells eliminate borna disease virus from the brain via induction of cytotoxic CD8+ T cells. *J Virol* 72: 4387-95.

Ochsenbein AF, Fehr T, Lutz C *et al.* 1999. Control of early viral and bacterial distribution and disease by natural antibodies. *Science* 286: 2156-9.

Ochsenbein AF, Pinschewer DD, Odermatt B *et al.* 1999. Protective T cell-independent antiviral antibody responses are dependent on complement. *J Exp Med* 190: 1165-74.

Ochsenbein AF and Zinkernagel RM. 2000. Natural antibodies and complement link innate and acquired immunity. *Immunol Today* 21: 624-30.

Ogra PL, Morag A, Tiku MT. 1975. Humoral Immune response. In *Viral immunology and immunopathology*, ed. Notkins AL. Academic Press, New York. 57-75.

Okuda Y, Sakoda S, Fujimura H *et al.* 1997. Nitric oxide via an inducible isoform of nitric oxide synthase is a possible factor to eliminate inflammatory cells from the central nervous system of mice with experimental allergic encephalomyelitis. *J Neuroimmunol* 73: 107-16.

Olsson T. 1995. Cytokine-producing cells in experimental autoimmune encephalomyelitis and multiple sclerosis. *Neurology* 45: S11-5.

Opal SM and DePalo VA. 2000. Anti-inflammatory cytokines. *Chest* 117: 1162-72.

Palma JP and Kim BS. 2001. Induction of selected chemokines in glial cells infected with Theiler's virus. *J Neuroimmunol* 117: 166-70.

Paresce DM, Ghosh RN, Maxfield FR. 1996. Microglial cells internalize aggregates of the Alzheimer's disease amyloid beta-protein via a scavenger receptor. *Neuron* 17: 553-65.

Parra B, Hinton DR, Marten NW *et al.* 1999. IFN-gamma isrequired for viral clearance from central nervous system oligodendroglia. *J Immunol* 162: 1641-7.

Pasparakis M, Alexopoulou L, Douni E *et al.* 1996. Tumour necrosis factors in immune regulation: everything that's interesting is...new! *Cytokine Growth Factor Rev* 7: 223-9.

Pasparakis M, Alexopoulou L, Episkopou V *et al.* 1996. Immune and inflammatory responses in TNF alpha-deficient mice: a critical requirement for TNF alpha in the formation of primary B cell follicles, follicular dendritic cell networks and germinal centers, and in the maturation of the humoral immune response. *J Exp Med* 184: 1397-411.

Patel AJ, Wickenden C, Jen A *et al.* 1996. Glial cell derived neurotrophic factors and Alzheimer's disease. *Neurodegeneration* 5: 489-96.

Pazmany T, Kosa JP, Tomasi TB *et al.* 2000. Effect of transforming growth factor-beta1 on microglial MHC-class II expression. *J Neuroimmunol* 103: 122-30.

Peiris JS and Porterfield JS. 1979. Antibody-mediated enhancement of Flavivirus replication in macrophage-like cell lines. *Nature* 282: 509-11.

Pender MP and Rist MJ. 2001. Apoptosis of inflammatory cells in immune control of the nervous system: Role of glia. *Glia* 36: 137-44.

Perelman A and Stern J. 1974. Acute pancreatitis in West Nile Fever. *Am J Trop Med Hyg* 23: 1150-2.

Perlman S, Evans G, Afifi A. 1990. Effect of olfactory bulb ablation on spread of a neurotropic coronavirus into the mouse brain. *J Exp Med* 172: 1127-32.

Perry VH and Gordon S. 1988. Macrophages and microglia in the nervous system. *Trends Neurosci* 11: 273-7.

Persidsky Y, Ghorpade A, Rasmussen J *et al.* 1999. Microglial and astrocyte chemokines regulate monocyte migration through the blood-brain barrier in human immunodeficiency virus-1 encephalitis. *Am J Pathol* 155: 1599-611.

Peterson PK, Hu S, Salak-Johnson J *et al.* 1997. Differential production of and migratory response to beta chemokines by human microglia and astrocytes. *J Infect Dis* 175: 478-81.

Petito CK and Cash KS. 1992. Blood-brain barrier abnormalities in the acquired immunodeficiency syndrome:Immunohistochemical localization of serum proteins in postmortem brain. *Ann Neurol* 32: 658-66.

Pimentel-Muinos FX, Munoz-Fernandez MA, Fresno M. 1994. Control of T lymphocyte activation and IL-2 receptor expression by endogenously secreted lymphokines. *J Immunol* 152: 5714-22.

Plakhov IV, Arlund EE, Aoki C *et al.* 1995. The earliest events in vesicular stomatitis virus infection of the murine olfactory neuroepithelium and entry of the central nervous system. *Virology* 209: 257-62.

Planz O, Ehl S, Furrer E *et al.* 1997. A critical role for neutralizing-antibody-producing B cells, CD4(+) T cells, and interferons in persistent and acute infections of mice with lymphocytic choriomeningitis virus: implications for adoptive immunotherapy of virus carriers. *Proc Natl Acad Sci U S A* 94: 6874-9.

Pogodina VV, Frolova MP, Malenko GV *et al.* 1983. Study on West Nile virus persistence in monkeys. *Arch Virol* 75: 71-86.

Popko B, Corbin JG, Baerwald KD *et al.*. 1997. The effects of interferon-gamma on the central nervous system. *Mol Neurobiol* 14: 19-35.

Pratt BM and McPherson JM. 1997. TGF-beta in the central nervous system: potential roles in ischemic injury and neurodegenerative diseases. *Cytokine Growth Factor Rev* 8: 267-92.

Prehn JH, Bindokas VP, Marcuccilli CJ *et al.* 1994. Regulation of neuronal Bcl2 protein expression and calcium homeostasis by transforming growth factor type beta confers wide-ranging protection on rat hippocampal neurons. *Proc Natl Acad Sci U S A* 91: 12599-603.

Prinz M and Hanisch UK. 1999. Murine microglial cells produce and respond to interleukin-18. *J Neurochem* 72: 2215-8.

Puche A. 2001. Olfactory Bulb. Anatomy and Neurobiology Faculty, School of Medicine, University of Maryland, Available from http://neurobiology.umaryland.edu/puche.htm, INTERNET.

Raine CS, Cannella B, Duijvestijn AM *et al.* 1990. Homing to central nervous system vasculature by antigen-specific lymphocytes. II. Lymphocyte/endothelial cell adhesion during the initial stages of autoimmune demyelination. *Lab Invest* 63: 476-89.

Raivich G, Bohatschek M, Kloss CU *et al.* 1999. Neuroglial activation repertoire in the injured brain: graded response, molecular mechanisms and cues to physiological function. *Brain Res Brain Res Rev* 30: 77-105.

Ramshaw IA, Ramsay AJ, Karupiah G *et al.* 1997. Cytokines and immunity to viral infections. *Immunol Rev* 159: 119-35.

Ransohoff RM, Glabinski A, Tani M. 1996. Chemokines in immune-mediated inflammation of the central nervous system. *Cytokine Growth Factor Rev* 7: 35-46.

Razvi ES and Welsh RM. 1995. Apoptosis in viral infections. *Adv Virus Res* 45: 1-60.

Reed LJ and Muench H. 1938. A simple method of estimating fifty percent endpoints. *The Am J Hyg* 27: 493-7.

Reinacher M, Bonin J, Narayan O *et al.* 1983. Pathogenesis of neurovirulent influenza A virus infection in mice. Route of entry of virus into brain determines infection of different populations of cells. *Lab Invest* 49: 686-92.

Reiss CS and Komatsu T. 1998. Does nitric oxide play a critical role in viral infections? *J Virol* 72: 4547-51.

Renno T, Krakowski M, Piccirillo C *et al.* 1995. TNF-a expression by resident microglia and infiltrating leucocytes in the central nervous system of mice with experimental allergic encephalomyelitis. *J Immunol* 154: 944-53

Rice CM. 1996. Flaviviridae: The viruses and their replication. In *Fields Virology*, ed. Fields B.N., Knipe D.M. ea Howley P.M. Philadelphia: Lippincott-Raven Publishers

Richards JT, Kern ER, Overall JC *et al.* 1981. Differences in neurovirulence among isolates of Herpes simplex virus types 1 and 2 in mice using four routes of infection. *J Infect Dis* 144: 464-71.

Rodriguez M, Pavelko K, Coffman RL. 1995. Gamma interferon is critical for resistance to Theiler's virus-induced demyelination. *J Virol* 69: 7286-90.

Roehrig J. 2001. West Nile Virus: The US Experience. Centre for disease control, available from http://www.cdc/gov/ncidod/dvbid/westnile/misc/slides/index.htm. INTERNET.

Rokutanda HK. 1969. Relationship between viremia and interferon production of Japanese encephalitis virus. *J Immunol* 102: 662-70.

Rollins BJ. 1997. Chemokines. *Blood* 90: 909-28.

Romagnani S. 1999. Th1/Th2 cells. *Inflamm Bowel Dis* 5: 285-94.

Romani L, Puccetti P, Bistoni F. 1997. Interleukin-12 in infectious diseases. *Clin Microbiol Rev* 10: 611-36.

Rose JW, Hill KE, Wada Y *et al.* 1998. Nitric oxide synthase inhibitor, aminoguanidine, reduces inflammation and demyelination produced by Theiler's virus infection. *J Neuroimmunol* 81: 82-9.

Rossol-Voth R, Rossol S, Schutt KH *et al.* 1991. In vivo protective effect of tumour necrosis factor alpha against experimental infection with herpes simplex virus type 1. *J Gen Virol* 72: 143-7.

Rothman AL, Kurane I, Lai CJ *et al.* 1993. Dengue virus protein recognition by virus-specific murine CD8+ cytotoxic T lymphocytes. *J Virol* 67: 801-6.

Rubbins JB and Pomeroy C. 1997. Role of gamma-interferon in the pathogenesis of bacteremic pneumococcal pneumonia. *Infect Immun* 65: 2975-7.

Rubin LL and Staddon JM. 1999. The cell biology of the blood-brain barrier. *Annu Rev Neurosci* 22: 11-28.

Ruby JC. 1997. Antiviral activity of gamma interferon. In *Gamma interferon in antiviral defence*. ed. G Karupiah. R.G. Lades Company, New York, Albany: 86-100.

Ruddle NH, Bergman CM, McGrath KM *et al.* 1990. An antibody to lymphotoxin and tumor necrosis factor prevents transfer of experimental allergic encephalomyelitis. *J Exp Med* 172: 1193-200.

Russell RC and Dwyer DE. 2000. Arboviruses associated with human disease in Australia. *Microbes Infect* 2: 1693-704.

Salazar-Mather TP, Hamilton TA, Biron CA. 2000. A chemokine-to-cytokine-to-chemokine cascade critical in antiviral defense. *J Clin Invest* 105: 985-93.

Sampson BA, Ambrosi C, Charlot A *et al.* 2000. The pathology of human West Nile Virus infection. *Hum Pathol* 31: 527-31.

Sanni LA, Thomas SR, Tattam BN *et al.* 1998. Dramatic changes in oxidative tryptophan metabolism along the kynurenine pathway in experimental cerebral and noncerebral malaria. *Am J Pathol* 152: 611-9.

Santamaria A, Galvan-Arzate S, Lisy V *et al.* 2001. Quinolinic acid induces oxidative stress in rat brain synaptosomes. *Neuroreport* 12: 871-4.

Sarawar SR, Cardin RD, Brooks JW *et al.* 1997. Gamma interferon is not essential for recovery from acute infection with murine gammaherpesvirus 68. *J Virol* 71: 3916-21.

Sasseville VG, Newman WA, Lackner AA *et al.* 1992. Elevated vascular cell adhesion molecule-1 in AIDS encephalitis induced by simian immunodeficiency virus. *Am J Pathol* 141: 1021-30.

Sauder C, Hallensleben W, Pagenstecher A *et al.* 2000. Chemokine gene expression in astrocytes of Borna disease virus-infected rats and mice in the absence of inflammation. *J Virol* 74: 9267-80.

Saura M, Zaragoza C, McMillan A *et al.* 1999. An antiviral mechanism of nitric oxide: inhibition of a viral protease. *Immunity* 10: 21-8.

Sawada M, Suzumura A, Hosoya H *et al.* 1999. Interleukin-10 inhibits both production of cytokines and expression of cytokine receptors in microglia. *J Neurochem* 72: 1466-71.

Saxena SK, Singh A, Mathur A. 2000. Antiviral effect of nitric oxide during Japanese encephalitis virus infection. *Int J Exp Pathol* 81: 165-72.

Schijns VE, Van dNR, Haagmans BL *et al.* 1991. Tumour necrosis factor-alpha, interferon-gamma and interferon-beta exert antiviral activity in nervous tissue cells. *J Gen Virol.* 72: 809-15

Schluesner HJ, Seid K, Kretzschmar J *et al.* 1996. Leucocyte chemotactic factor, a nature ligand to CD4+, is expressed by lymphocytes and microglial cells of the MS plaques. *J Neurosci Res* 15: 606-11.

Schmitt AB, Brook GA, Buss A et al 1998. Dynamics of microglial activation in the spinal cord after cerebral infarction are revealed by expression of MHC class II antigen. *Neuropathol Appl Neurobiol* 24: 167-76.

Schoneboom BA, Fultz MJ, Miller TH, McKinney LC, Grieder FB. 1999. Astrocytes as targets for Venezuelan equine encephalitis virus infection. *J Neurovirol* 5: 342-54.

Schonrock LM, Kuhlmann T, Adler S *et al.* 1998. Identification of glial cell proliferation in early multiple sclerosis lesions. *Neuropathol Appl Neurobiol* 24: 320-30.

Sedgwick JD, Ford AL, Foulcher E *et al.* 1998. Central nervous system microglial cell activation and proliferation follows direct interaction with tissue-infiltrating T cell blasts. *J Immunol* 160: 5320-30.

Sethi SK, Bianco A, Allen JT *et al.* 1997. Interferon-gamma (IFN-gamma) down-regulates the rhinovirus-induced expression of intercellular adhesion molecule-1 (ICAM-1) on human airway epithelial cells. *Clin Exp Immunol* 110: 362-9.

Sethna MP and Lampson LA. 1991. Immune modulation within the brain: recruitment of inflammatory cells and increased major histocompatibility antigen expression following intracerebral injection of interferon-gamma. *J Neuroimmunol* 34: 121-32.

Shen J, T-To SS, Schrieber L *et al.* 1997. Early E-selectin, VCAM-1, ICAM-1, and late major histocompatibility complex antigen induction on human endothelial cells by flavivirus and comodulation of adhesion molecule expression by immune cytokines. *J Virol* 71: 9323-32.

Shieh WJ, Guarner J, Layton M *et al.* 2000. The role of pathology in an investigation of an outbreak of West Nile encephalitis in New York, 1999. *Emerg Infect Dis* 6: 370-2.

Shimizu Y, Newman W, Gopal TV *et al.* 1991. Four molecular pathways of T cell adhesion to endothelial cells: roles of LFA-1, VCAM-1, and ELAM-1 and changes in pathway hierarchy under different activation conditions. *J Cell Biol* 113: 1203-12.

Shimojo M, Nakajima K, Takei N *et al.* 1991. Production of basic fibroblast growth factor in cultured rat brain microglia. *Neurosci Lett* 123: 229-31.

Shinya K, Shimada A, Otsuki K *et al.* 2000. Avian influenza virus intranasally inoculated infects the central nervous system of mice through the general visceral afferent nerve. *Arch Virol* 145: 187-95.

Shope RE and Meegan JM. 1993. Arbovirus. In *Viral Infections of Humans Epidemiology and control*, ed. Evans AS. and Kaslow RA. Plenum Medical Book Company, New York, London. 151-83.

Shrikant P and Benveniste EN. 1996. The central nervous system as an immunocompetent organ : role of glial cells in antigen presentation. *J Immunol* 157: 1819-22.

Siebert H, Sachse A, Kuziel WA *et al.* 2000. The chemokine recepto CCR2 is involved in macrophage recruitment to the injured peripheral nervous system. *J Neuroimmunol* 110: 117-85.

Simmons A and Nash AA. 1987. Effect of B cell suppression on primary infection and reinfection of mice with herpes simplex virus. *J Infect Dis* 155: 649-54.

Simpson JE, Newcombe J, Cuzner ML *et al.* 2000. Expression of the interferon-gamma-inducible chemokines IP-10 and Mig and their receptor, CXCR3, in multiple sclerosis lesions. *Neuropathol Appl Neurobiol* 26: 133-42.

Skulachev VP. 1998. Possible role of reactive oxygen species in antiviral defense. *Biochemistry (Mosc)* 63: 1438-40.

Smithburn KC, Hughes TP, Burke AW, J.H. aP. 1940. A neurotropic virus isolated from the blood of native Uganda. *Am J Trop Med* 20: 471-92.

Sobel RA, Mitchell ME, Fondren G. 1990. Intercellular adhesion molecule-1 (ICAM-1) in cellular immune reactions in the human central nervous system. *Am J Pathol* 136: 1309-16.

Soilu-Hanninen M, Eralinna JP, Hukkanen V *et al.* 1994. Semliki Forest virus infects mouse brain endothelial cells and causes blood-brain barrier damage. *J Virol* 68: 6291-8.

Song GY and Jia W. 1999. The heterogeneity in the immune response and efficiency of viral dissemination in brain infected with herpes simplex virus type 1 through peripheral or central route. *Acta Neuropathol (Berl)* 97: 649-56.

Soontornniyomkij V, Wang G, Pittman CA *et al.* 1998. Expression of brain-derived neurotrophic factor protein in activated microglia of human immunodeficiency virus type 1 encephalitis. *Neuropathol Appl Neurobiol* 24: 453-60.

Southan GJ and Szabo C. 1996. Selective pharmacological inhibition of distinct nitric oxide synthase isoforms. *Biochem Pharmacol* 51: 383-94.

Spellberg B and Edwards JE. 2001. Type 1/Type 2 immunity in infectious diseases. *Clin Infect Dis* 32: 76-102.

Springer TA. 1990. Adhesion receptors of the immune system. *Nature* 346: 425-34.
Srivastava S, Khanna N, Saxena SK *et al.* 1999. Degradation of Japanese encephalitis virus by neutrophils. *Int J Exp Pathol* 80: 17-24.

Stanimirovic D and Satoh K. 2000. Inflammatory mediators of cerebral endothelium: a role in ischemic brain inflammation. *Brain Pathol* 10: 113-26.

Steele KE, Linn MJ, Schoepp RJ *et al.* 2000. Pathology of fatal West Nile virus infections in native and exotic birds during the 1999 outbreak in New York City, New York. *Vet Pathol* 37: 208-24.

Stence N, Waite M, Dailey ME. 2001. Dynamics of microglial activation: a confocal time-lapse analysis in hippocampal slices. *Glia* 33: 256-66.

Stevens CF. 2001. Nervous System.: Discover Channel School, original content provided by World Book

Stohlman SA, Bergmann CC, Lin MT *et al.* 1998. CTL effector function within the central nervous system requires CD4+ T cells. *J Immunol* 160: 2896-904.

Stoll G and Jander S. 1999. The role of microglia and macrophages in the pathophysiology of the CNS. *Prog Neurobiol* 58: 233-47.

Streit WJ and Kreutzberg GW. 1987. Lectin binding by resting and reactive microglia. *J Neurocytol* 16: 249-60.

Streit WJ, Walter SA, Pennell NA. 1999. Reactive microgliosis. *Prog Neurobiol* 57: 563-81.

Sudo S, Tanaka J, Toku K *et al.* 1998. Neurons induce the activation of microglial cells in vitro. *Exp Neurol* 154: 499-510

Suzuki Y, Kang H, Parmley S *et al.* 2000. Induction of tumor necrosis factor-alpha and inducible nitric oxide synthase fails to prevent toxoplasmic encephalitis in the absence of interferon-gamma in genetically resistant BALB/c mice. *Microbes Infect* 2: 455-62.

Switzer RC, Olmos JD, Heimer L. 1985. Olfactory System. In *The Rat Nervous System*, ed. Paxinos G. Academic Press, Sydney, New York, London. 1-35.

Szczepanik AM, Funes S, Petko W *et al.* 2001. IL-4, IL-10 and IL-13 modulate A beta(1--42)-induced cytokine and chemokine production in primary murine microglia and a human monocyte cell line. *J Neuroimmunol* 113: 49-62.

Szilak I and Minamoto GY. 2000. West Nile viral encephalitis in an HIV-positive woman in New York. *N Engl J Med* 342: 59-60.

Taylor WP. and Marshall ID. 1975. Adaptation studies with Ross River virus: laboratory mice and cell cultures. J Gen Virol 28: 59-72.

Takikawa O, Habara-Ohkubo A, Yoshida R. 1990. IFN-gamma is the inducer of indoleamine 2,3-dioxygenase in allografted tumor cells undergoing rejection. *J Immunol* 145: 1246-50.

Tang Y, Rampin O, Giuliano F *et al.* 1999. Spinal and brain circuits to motoneurons of the bulbospongiosus muscle: retrograde transneuronal tracing with rabies virus. *J Comp Neurol* 414: 167-92.

Taoufik Y, de Goer de Herve MG, Giron-Michel J *et al.* 2001. Human microglial cells express a functional IL-12 receptor and produce IL-12 following IL-12 stimulation. *Eur J Immunol* 31: 3228-39.

Thach DC, Kimura T, Griffin DE. 2000. Differences between C57BL/6 and BALB/cBy mice in mortality and virus replication after intranasal infection with neuroadapted Sindbis virus. *J Virol* 74: 6156-61.

Thomas SM, Garrity LF, Brandt CR *et al.* 1993. IFN-gamma-mediated antimicrobial response. Indoleamine 2,3-dioxygenase-deficient mutant host cells no longer inhibit intracellular Chlamydia spp. or Toxoplasma growth. *J Immunol* 150: 5529-34.

Thomas SR, Mohr D, Stocker R. 1994. Nitric oxide inhibits indoleamine 2,3-dioxygenase activity in interferon-gamma primed mononuclear phagocytes. *J Biol Chem* 269: 14457-64.

Tilg H and Kaser A. 1999. Interferons and their role In inflammation. *Curr Pharm Des* 5: 771-85.

Tishon A, Lewicki H, Rall G *et al.* 1995. An essential role for type 1 interferon-gamma in terminating persistent viral infection. *Virology* 212: 244-50.

Tong N, Perry SW, Zhang Q *et al.* 2000. Neuronal fractalkine expression in HIV-1 encephalitis: roles for macrophage recruitment and neuroprotection in the central nervous system. *J Immunol* 164: 1333-9.

Topham DJ, Tripp RA, Doherty PC. 1997. CD8+ T cells clear influenza virus by perforin or Fas-dependent processes. *J Immunol* 159: 5197-200.

Tran EH, Prince EN, Owens T. 2000. IFN-gamma shapes immune invasion of the central nervous system via regulation of chemokines. *J Immunol* 164: 2759-68.

Tsai TF, Popovici F, Cernescu C *et al.* 1998. West Nile encephalitis epidemic in southeastern Romania. *Lancet* 352: 767-71.

Tsuru S, Fujisawa H, Taniguchi M *et al.* 1987. Mechanism of protection during the early phase of a generalized viral infection. II. Contribution of polymorphonuclear leukocytes to protection against intravenous infection with influenza virus. *J Gen Virol* 68: 419-24.

Tucker PC, Griffin DE, Choi S *et al.* 1996. Inhibition of nitric oxide synthesis increases mortality in Sindbis virus encephalitis. *J Virol* 70: 3972-7.

Tyor WR and Griffin DE. 1993. Virus specificity and isotype expression of intraparenchymal antibody-secreting cells during Sindbis virus encephalitis in mice. *J Neuroimmunol* 48: 37-44.

Utermohlen O, Dangel A, Tarnok A *et al.* 1996. Modulation by gamma interferon of antiviral cell-mediated immune responses in vivo. *J Virol* 70: 1521-6.

Van Strijp JA, Miltenburg LA, van der Tol ME *et al.* 1990. Degradation of herpes simplex virions by human polymorphonuclear leukocytes and monocytes. *J Gen Virol* 71: 1205-9.

Vogel P, Abplanalp D, Kell W *et al.* 1996. Venezuelan equine encephalitis in BALB/c mice: kinetic analysis of central nervous system infection following aerosol or subcutaneous inoculation. *Arch Pathol Lab Med* 120: 164-72.

Wagner S, Czub S, Greif M *et al.* 1999. Microglial/macrophage expression of interleukin 10 in human glioblastomas. *Int J Cancer* 82: 12-6.

Wang ZE, Reiner SL, Zheng S *et al.* 1994. CD4+ effector cells default to the Th2 pathway in interferon gamma-deficient mice infected with Leishmania major. *J Exp Med* 179: 1367-71.

Watanabe D, Adachi A, Tomita Y *et al.* 1999. The role of polymorphonuclear leukocyte infiltration in herpes simplex virus infection of murine skin. *Arch Dermatol Res* 291: 28-36.

Weener A, Martin S, Gutierrez-Ramos JC *et al.* 2001. Leukocyte recruitment and neuroglial activation during facial nerve regeneration in ICAM-1-deficient mice: effects of breeding strategy. *Cell Tissue Res* 305: 25-41.

Weidinger G, Czub S, Neumeister C *et al.* 2000. Role of CD4(+) and CD8(+) T cells in the prevention of measles virus-induced encephalitis in mice. *J Gen Virol* 81: 2707-13.

Weiner LP and Fleming JO. 1984. Viral infections of the nervous system. *Journl of Neurosurg* 61: 207-24.

Weissenbock H, Hornig M, Hickey WF *et al.* 2000. Microglial activation and neuronal apoptosis in Bornavirus infected neonatal Lewis rats. *Brain Pathol* 10: 260-72.

Welsh RM, Lin MY, Lohman BL *et al.* 1997. Alpha beta and gamma delta T-cell networks and their roles in natural resistance to viral infections. *Immunol Rev* 159: 79-93.

Whitton JL and Oldstone MB. 1996. Immune response to viruses. In *Fields Virology*, ed. Fields BN, Knipe DM, Howley PM *et al.* Lippincott-Raven Publishers,Philadelphia.

Willenborg DO, Fordham SA, Staykova MA *et al.* 1999. IFN-gamma is critical to the control of murine autoimmune encephalomyelitis and regulates both in the periphery and in the target tissue: a possible role for nitric oxide. *J Immunol* 163: 5278-86.

Willenborg DO, Simmons RD, Tamatani T *et al.* 1993. ICAM-1-dependent pathway is not critically involved in the inflammatory process of autoimmune encephalomyelitis or in cytokine-induced inflammation of the central nervous system. *J Neuroimmunol* 45: 147-54.

Williamson JS and Stohlman SA. 1990. Effective clearance of mouse hepatitis virus from the central nervous system requires both CD4+ and CD8+ T cells. *J Virol* 64: 4589-92.
Winkelhake JL. 1978. Immunoglobulin structure and effector functions. *Immunochemistry* 15: 695-714.

Wisniewski HM, Brown HR, Thormar H. 1983. Pathogenesis of viral encephalitis: demonstration of viral antigen(s) in the brain endothelium. *Acta Neuropathol (Berl)* 60: 107-12.

Wong D and Dorovini-Zis K. 1995. Expression of vascular cell adhesion molecule-1 (VCAM-1) by human brain microvessel endothelial cells in primary culture. *Microvasc Res* 49: 325-39.

Wright KE and Buchmeier MJ. 1991. Antiviral antibodies attenuate T-cell-mediated immunopathology following acute lymphocytic choriomeningitis virus infection. *J Virol* 65: 3001-6.

Yamada T, Horisberger MA, Kawaguchi N *et al.* 1994. Immunohistochemistry using antibodies to alpha-interferon and its induced protein, MxA, in Alzheimer's and Parkinson's disease brain tissues. *Neurosci Lett* 181: 61-4.

Yamada T and Yamanaka I. 1995. Microglial localization of alpha-interferon receptor in human brain tissues. *Neurosci Lett* 189: 73-6.

Yang AG, Bai X, Huang XF *et al.* 1997. Phenotypic knockout of HIV type 1 chemokine coreceptor CCR-5 by intrakines as potential therapeutic approach for HIV-1 infection. *Proc Natl Acad Sci U S A* 94: 11567-72.

Yong VW, Moumdjian R, Yong FP *et al.* 1991. Gamma-interferon promotes proliferation of adult human astrocytes in vitro and reactive gliosis in the adult mouse brain in vivo. *Proc Natl Acad Sci U S A* 88: 7016-20.

Yoshida R, Urade Y, Tokuda M *et al.* 1979. Induction of indoleamine 2,3-dioxygenase in mouse lung during virus infection. *Proc Natl Acad Sci U S A* 76: 4084-6.

Young HA and Hardy KJ. 1995. Role of interferon-gamma in immune cell regulation. *J Leukoc Biol* 58: 373-81.

Yu Z, Manickan E, Rouse BT. 1996. Role of interferon-gamma in immunity to herpes simplex virus. *J Leukoc Biol* 60: 528-32.

Zhao B and Schwartz JP. 1998. Involvement of cytokines in normal CNS development and neurological diseases: recent progress and perspectives. *J Neurosci Res* 52: 7-16.

Zhao ML, Kim MO, Morgello S *et al.* 2001. Expression of inducible nitric oxide synthase, interleukin-1 and caspase-1 in HIV-1 encephalitis. *J Neuroimmunol* 115: 182-91.

Zielasek J, Archelos JJ, Toyka KV *et al.* 1993. Expression of intercellular adhesion molecule-1 on rat microglial cells. *Neurosci Lett* 153: 136-9.

Zinkernagel RM. 1992. Virus-induced acquired immune suppression by cytotoxic T cell-mediated immunopathology. *Vet Microbiol* 33: 13-8.

Zisman B, Wheelock EF, Allison AC. 1971. Role of macrophages and antibody in resistance of mice against yellow fever virus. *J Immunol* 107: 236-43.

Appendix

A) Tris-buffer, pH 7.6

Tris (Tris hydroxymethyl aminomethane)	24.4g
Distilled water	1800ml
1N hydrochloric acid	74ml

Dissolve Tris in 1800ml distilled water. Add hydrochloric acid and adjust pH dilute to 7.6 with conc. HCL and make upto 2L.

To 2L of 0.1M Tris buffer add

Sodium chloride	17.54g
Tween 20	1ml

B) Citrate buffer, pH 6.0

Citric acid	2.1g
Distilled water	900ml

Dissolve citric acid in 900ml distilled water. Adjust pH to 6.0 with NaOH and make up to 1L.

C) Carbonate buffer pH 9.1

Sodium carbonate (Na_2CO_3)	5.72g
Sodium hydrogen carbonate ($NaHCO_3$)	15.12g
Distilled water	2L

Dissolve sodium salt in 1800 ml distilled water. Adjust pH to 9.1 with NaOH or HCl and make up to 2L.

D) RBC lysis buffer, pH 7.4

Ammonium chloride (NH_4Cl)	8.29g
Potassium hydrogen carbonate ($KHCO_3$)	1 g
Sodium Ethylenediaminetetraacetic acid (Na_2EDTA	37.2 mg
Distilled water	900ml

Dissolve above contents in 900 ml water and adjust pH to 7.4 with 1M HCl and make up to 1L. Filter sterilize through a 0.2μm filter and store at room temperature.